

University of Warwick institutional repository: <http://go.warwick.ac.uk/wrap>

**A Thesis Submitted for the Degree of PhD at the University of Warwick**

<http://go.warwick.ac.uk/wrap/35747>

This thesis is made available online and is protected by original copyright.

Please scroll down to view the document itself.

Please refer to the repository record for this item for information to help you to cite it. Our policy information is available from the repository home page.

**Behaviour of Ceramic Cutting  
Tools When Machining  
Superalloys**

by

Houshang Khamsehzadeh, H.N.D, P.G.D., M.Sc.

A Thesis submitted for the degree of  
Doctor of Philosophy  
in Engineering

Engineering Department, University of Warwick

May 1991



## DEDICATION

To the memory of my grand mother

NARGES KHAMSEHZADEH

to whom I am greatly indebted

## ACKNOWLEDGMENTS

The author wishes to thank:

Dr. J. Wallbank and Mr. I.R. Pashby for their supervision, specialised advice, guidance and encouragement during the course of this project.

Dr. A. Jawaid, Mr. J.F. Hill and Dr. E.O. Ezugwu for their invaluable advice and help.

Technical staff who have contributed to this work in particular Mr. M.A. Robinson, Mr. K. Cooper Mr. B. Bryden, Mrs. V. Käding and Mr. G. Canham.

Dr. A.R. Machado, a dear friend whose knowledge is greatly admired.

Rolls Royce Plc for providing the material for the tests and also Greenleaf Corporation, Kennametal UK and Sandvik Coromant for providing the relevant literature.

Finally my parents for their supportive role, patience, encouragement and dedication, and to whom I always remain grateful.

## ABSTRACT

The nickel-base superalloys Waspaloy, INCO 901 and INCO 718 have been machined with four different types of ceramic cutting tools. The cutting inserts were pure alumina (CC620), mixed alumina (CC650), composite ceramic (WG-300) and finally silicon nitride (Kyon 2000).

Tests in the form of turning were carried out, in dry and wet conditions, in order to study the behaviour of the above mentioned cutting tools when machining superalloys. The cutting speeds employed for these tests were 90, 150, 215 and 300 m/min with feed rates of 0.125 and 0.18 mm/rev together with depths of cut of 1 and 2.5 mm.

Machining in the presence of different atmospheres was also performed.

In the majority of cases depth of cut notching (DOCN) proved to be the domineering factor controlling tool lives under different cutting conditions. However, flank wear, nose notch and surface roughness were the other tool failure modes.

Attrition wear was predominant throughout the tests which was influenced by the cutting temperatures. The high temperatures also caused diffusion wear mechanisms to take effect.

## NOMENCLATURE

AFW	-	Average flank wear
MFW	-	Maximum flank wear
FW	-	Flank wear
SR	-	Surface roughness
Ch	-	Chipping
N	-	Notching
NN	-	Nose notch
DOCN	-	Depth of cut notch
CF	-	Catastrophic failure
EP	-	Excessive power
V	-	Cutting speed (m/min)
F	-	Feed rate (mm/rev)
DOC	-	Depth of cut (mm)

# CONTENT

Chapter 1.0	INTRODUCTION	1
Chapter 2.0	LITERATURE SURVEY	4
2.1	Historical Background	4
2.2	Terminology Used in Metal Cutting	6
2.3	Cutting Processes and Chip Formation	8
2.3.1	Discontinuous Chips	8
2.3.2	Segmented Chips	9
2.3.3	Continuous Chips without a Built-Up-Edge	10
2.3.4	Continuous Chips with a Built-Up-Edge	10
2.4	Forces In Metal Cutting	11
2.5	Heat Generated During Machining	12
2.6	Tool Failure Modes	15
2.6.1	Flank Wear	15
2.6.2	Wear on the Rake Face	16
2.6.3	Wear at the End of Depth of Cut	17
2.6.4	Failure by Fracture or Mechanical Damage	19
2.7	The Tool Wear Mechanisms	20
2.7.1	Abrasion Wear	21
2.7.2	Attrition Wear	21
2.7.3	Diffusion Wear	23
2.7.4	Plastic Deformation	24
2.7.5	Wear by Chemical Interaction	25
2.8	Tool Materials (excluding Ceramics)	26
2.8.1	Tool Material Requirements	26
2.8.2	Carbon Steel and Low/Medium Alloy Steel	27
2.8.3	High Speed Steel Tools	28
2.8.4	Cemented Carbide Tools	30
2.8.5	Ultra Hard Tool Materials	33
2.9	Ceramic Tool Materials	34
2.9.1	Introduction	34
2.9.2	Development of the Ceramic Tool Materials	35
2.9.3	Variation in the Based Matrix of Ceramics	37
2.9.4	Manufacturing Process	38
2.9.4.1	White Ceramics	38
2.9.4.2	Black Oxide Ceramics	39
2.9.4.3	Silicon Nitride Based Ceramics	40
2.9.4.4	Influence of the Additives and Alloying Elements	43
2.9.4.5	Wear of Ceramic Cutting Tools	47
2.10	Work material - Superalloys	49
2.10.1	Nickel-Base Superalloys	49
2.10.2	Grain Structure	52
2.10.3	Machining Characteristics of Nickel-Base Alloys	53

Chapter 3.0	EXPERIMENTAL TECHNIQUES	56
3.1	Introduction	56
3.2	Machining Operations	57
3.3	Cutting Conditions	58
3.4	Work Materials	58
3.5	Tool Materials and Geometries	58
3.6	Tool Life Criteria	59
3.7	Examination and Measurement of Worn Areas	60
3.8	Measurement of Surface Finish	60
3.9	Measurement of Cutting Forces	61
3.10	Quick Stop Technique	61
3.11	Preparation of Specimens	62
Chapter 4.0	EXPERIMENTAL RESULTS	64
4.1	Introduction	64
4.2	Machining of WASPALOY	64
4.2.1	Machining of WASPALOY with CC620 Ceramic Inserts	64
4.2.2	Machining of WASPALOY with CC650 Ceramic Inserts	66
4.2.3	Machining of WASPALOY with KYON 2000 Ceramic Inserts	69
4.2.4	Machining of WASPALOY WITH WG-300 Ceramic Inserts	72
4.3	Machining of INCO 901	76
4.3.1	Machining of INCO 901 with CC650 Ceramic Inserts	76
4.3.2	Machining of INCO 901 with KYON 2000 Ceramic Inserts	78
4.3.3	Machining of INCO 901 with WG-300 Ceramic Inserts	80
4.3.4	Comparative Tests	81
4.3.4.1	Machining with Round WG-300 Insert	81
4.4	Machining of INCO 718	82
4.4.1	Machining of INCO 718 with Kyon 2000 Ceramic Inserts	82
4.4.2	Machining of INCO 718 with WG-300 Ceramic Inserts	83
4.4.3	Comparative Tests	84
4.4.3.1	Machining with Round Ceramic Inserts	84
4.4.3.2	Machining with Rhomboid Ceramic Inserts	84
4.4.3.3	Machining in Presence of Different Gases	85
4.5	Statistical Analysis	86
Chapter 5.0	DISCUSSION	91
5.1	Introduction	91
5.2	Intoduction to Machining	91
5.3	Failure Modes	93
5.4	Tool Wear Mechanism	93
5.4.1	Attrition Wear	93
5.4.1.1	Effect of Tool Microstructure on Attrition Wear Rate with Waspaloy	96
5.4.1.2	Influence of Coolant on Attriton Wear with Waspaloy	99
5.4.1.3	Effect of Workpiece Material on Attrition Wear	100

5.4.1.4	Effect of Machining Parameters	102
5.4.1.4.1	Cutting Speed	102
5.4.1.4.2	Coolant	102
5.4.1.4.3	Feed Rate	104
5.4.1.4.4	Depth Of Cut	104
5.4.1.5	Overall wear rates	105
5.4.2	Abrasion Wear	106
5.4.3	Diffusion Wear	108
5.4.4	Depth Of Cut Notch (DOCN)	109
5.4.5	Nose Notch	112
5.4.6	Chipping (Flaking) and Catastrophic Failure	114
5.5	Influence of Various Gases on Tool Lives	115
5.6	Comparative Tests	117
5.6.1	Influence of Tool Geometries	117
5.6.2	Influence of Chamfer on the Work Material	117
5.7	Summary of Discussion	118
Chapter 6.0	CONCLUSIONS	120
Chapter 7.0	FUTURE WORK	122

## CHAPTER 1

### INTRODUCTION

History has shown that man has always been in search of new materials. The search possibly started in the stone age and has proceeded since then through the Bronze age and Iron ages into the Industrial revolution and continues today.

It was at the beginning of this century that the engineers, manufacturers and people involved in other industries realised the need for stronger and more corrosion resistant alloys than those of copper, iron and steels available at the time. This potential demand led to the discovery and development of austenitic stainless steel.

Later additions of small amounts of aluminium and titanium were found to significantly increase the creep resistance. This was the initiation point of the development of the superalloys.

Subsequently the development of the jet engine by the United States, Great Britain and Germany forced the metallurgist to work towards the improvement and/or development of tool materials in order to be able to withstand the demands imposed by the new materials.

Scarcity of Tungsten after the Second World War and the need for a stronger cutting tool, forced the metallurgist to provide the metalworking industry with an alternative to



tungsten carbide and HSS cutting tools. Around 1950 Alumina based Ceramic cutting tools were made available. In spite of their hot hardness, strength and chemical stability introduction and marketing of the cutting tool materials was not successful. The drawback was insufficient toughness and poor thermal properties.

Improvement of the ceramic cutting tool material started to show up in the early seventies [1]. One approach to this was the refinement of the microstructure of the material. Also addition of different additives improved the properties of the cutting tools remarkably. Subsequent development of the ceramic tools based on Silicon Nitride catered for the need for high speed machining. Furthermore ceramic cutting tool inserts were also reinforced by silicon carbide whiskers. These tools provided a higher fracture toughness and even higher cutting speeds were claimed.

The improvements and modifications of the ceramic cutting tools have certainly been noticeable throughout the metal cutting environment. Machining of non-ferrous metals, steels, cast iron [2] and nickel-based alloys [3] can be performed at high speeds and high feed rates.

Undoubtedly both the aircraft and automotive industries have benefited immensely from the implementation of the ceramic cutting tools, and dramatic gains in productivity, as much as 300% have been reported [4].

With all these improvements industry still stays reluctant to use ceramic cutting tool inserts. The unwillingness to use these cutting tools is due to their

unpredictability coupled with their brittleness

In 1985 it was reported [5] that in Japan, (one of the main ceramic tool consumers), sales of ceramic tools represented between 5 and 7% of all cutting tools purchased. This figure was even lower, at 2 to 3% in the United States. However, Whitefield [6] estimated that by the year 2000, the United States is expected to export \$2 billion worth of advanced ceramics.

Unpredictability of pure alumina cutting tools ("pure alumina", is usually referred to a tool with only a few percentage of additive/s) has been experienced under different cutting speeds when machining Waspaloy and unacceptably short tool lives were obtained [7]. Sialon tools have machined INCO 718 at a speed of 120 m/min, where previously carbide tools were used at 30 m/min. Metal removal rate was increased by 400% [8]. Also Billman et al [9] estimated a 73% saving, when machining Waspaloy with silicon carbide whisker reinforced alumina cutting tool insert instead of pure alumina.

Consequently considerable savings are potentially available from utilising the best ceramic tool for a particular application. Little data on performance and wear mechanisms has been reported in depth previously. The present work aims at understanding how the tools can best be utilised and analyses the reasons for failure.

## CHAPTER 2

### LITERATURE SURVEY

#### 2.1 Historical background

The existence of cutting tools is by no means new to mankind. Even in prehistoric periods stone was cut to produce knives, drills and weapons. And indeed Benjamin Franklin's comment that *man is a tool making animal* is noteworthy [10].

Flint was used some 2500 B.C. by Egyptian artisans for boring the inside of vases. The first lathe which was fairly primitive was possibly developed in the Bronze age in the Indus Valley [11]. The invention of the steam engine presented an opportunity for the first breakthrough for the metal cutting industry [12]. Carbon steel tools which were hardened and tempered by blacksmiths were used for machining of materials such as cast and wrought iron.

Due to a lack of cutting tool strength productivity remained low until the late nineteenth century when F.W.Taylor [13] found a link between heat treatment and tool performance for steel alloyed with the addition of tungsten(W). Further investigations resulted in the invention of High Speed Steel (HSS). Following this, Taylor discovered that the addition of a higher percentage of

tungsten to the newly developed tool material increased its resistance to temperatures as high as  $650^{\circ}\text{C}$ . Due to the improvements achieved with this discovery, this series of tool materials allowed the machining field to be revolutionised and higher speeds to be implemented when machining mild steel.

The search for a better tool material continued and around 1930 Germany introduced a new tool material to the market. It was based on tungsten carbide cemented with a soft binder and capable of turning mild steel at approximately 250 m/min.

During the Second World War scarcity of tungsten and a demand for higher productivity forced the developers to introduce ceramics. Pure alumina was the first ceramic cutting tool sintered at high temperature and suitable for machining grey cast iron. This tool material had a good reputation for its high abrasion resistance. However, inadequate fracture toughness and poor thermal shock resistance limited its performance in machining steels.

Thus the search for tougher ceramic tool materials continued resulting in the discovery of a range of grades. These new developments, enabled the people involved in machining to have a wider choice of tool material for a specific job particularly when a harder work material was involved.

In relation to the development and discovery of tool materials, Swinhart [14] suggests the followings:

1. A new tool material rarely replaces an old one; the old

tool material merely gives up part of its field of application to the new tool material.

2. As new tool materials are introduced, machine tool builders respond accordingly to take advantage of the new capabilities.
3. When a new class of workpiece material that is difficult to machine using existing tool materials assumes commercial importance, new tool materials will be developed to satisfy the new need.
4. Even the older tool materials, such as HSS, continue to undergo substantial improvements as new technology is brought to bear upon their constitution and processing.

## 2.2 Terminology USED in Metal Cutting

British Standard Association Publication [15] and the ISO [16], have laid down a set of standard terminology for the machining processes which have not yet been universally accepted. However, the following are terms most commonly used for a single point turning operation. The workpiece is held firmly in the chuck of a lathe and rotated at a speed of  $V$  for the processes of turning. The tool is held solidly in a tool post and moved at a fixed rate parallel to the axis of the bar, removing the unwanted material in layers which are known as chips (figure 1).

Single point turning terms usually refer to a series of tool materials with only one cutting part and one shank. Tool materials such as milling cutters which possess more than one cutting part are known as multi point tools.

*Cutting speed ( $V$ )*, is the rate at which the workpiece moves

across the cutting edge of the tool and is measured in metres per minute (m/min).

*Feed rate (F)*, is defined as the distance travelled by the tool for each revolution of the workpiece material and is calculated in millimetres per revolution (mm/rev).

*Depth of cut (DOC)*, is the thickness of the unwanted material removed from the bar in the radial direction and is expressed in millimetres (mm).

*Metal removal rate (MRR)*, is a parameter often used to determine the efficiency of a cutting operation; it is the product of cutting speed, feed rate and depth of cut.

*Rake face*, is the tool surface over which the chip flows during the machining processes (figure 2).

*Flank face*, is the surface of the tool over which the freshly cut surface of the workpiece passes.

*Primary cutting edge*, is the intersection of the flank with the rake face and forms the cutting edge.

*Secondary cutting edge*, is the remainder of the cutting edge which may not actually be engaged in the cutting process.

*Nose*, is the intersection of the primary and secondary cutting edges. In order to achieve higher strength at the cutting edge a radius is usually provided.

*Shear zones*, there are two major zones of shear when a chip forms. One is the primary shear zone which is the boundary between the unsheared work material and the chip. And the other is the secondary shear zone, also known as flow zone which, is the interface between the tool and the chip on the

rake face.

*Orthogonal cutting*, is the process where the major cutting edge only is used and the rake face of the tool is arranged to be positioned perpendicular to the direction of relative work-tool motion with  $0^\circ$  approach angle (figure 3). Turning of a tube is a typical example of this.

*Semi-orthogonal cutting*, is the method where the cutting operation takes place and the chip is generated by engagement of the major cutting edge as well as the nose radius and the minor cutting edge. Both the rake and approach angles are  $0^\circ$ . Turning a solid bar is a classic example of this process.

*Non-orthogonal cutting*, takes place for example when an approach angle is introduced on the major cutting edge, so that the cutting edge is inclined to the axis of rotation.

## **2.3 Cutting Processes and Chip Formation**

There are four different types of chip produced during the machining process:

1. discontinuous chips
2. segmented chips
3. continuous chips without a built-up-edge
4. continuous chips with a built-up edge.

### **2.3.1 Discontinuous Chips**

Discontinuous are usually formed when brittle material with a crack initiation phase like cast iron or bronze is cut. These chips are produced when materials cannot

withstand the large strains which occur in a very short space of time and hence the material fractures [17].

### 2.3.2 Segmented chips

Segmented chips may sometimes be termed *serrated chips* or *saw toothed chips*. Serrated chips which are continuous chips have periodic variations in thickness.

Adiabatic shear may take place when machining materials with poor thermal conductivity such as titanium alloys [18]. In this case the serrated type chip forms due to unstable adiabatic shear. Unlike discontinuous chips in which fracture is complete, the individual serrations are separated by a narrow band. The cutting process can be characterised by large shear strains which are confined to these narrow bands between segments with very little deformation within the segments.

Cook [19] has attributed vibration excitation to a varying shear stress on the shear plane. However, Sullivan et al [20] carried out a series of tests on EN58C austenitic stainless steels and with the results obtained concluded that the serrated chip formation is not due to the machine tool vibrations but is an inherent feature of the material[21]. It was also found that the strength of the material in the secondary zone was greater than that of the primary zone though no definite reason was given. It was further suggested that elimination of this type of chip formation could enhance the tool life by decreasing the wear rate.



### 2.3.3 Continuous Chips without a Built-Up-Edge

Formation of continuous chips without built-up-edge, also known as ribbon-like chips, may be generated when machining single phase materials or multi-phase alloys at high speeds and feed rates.

In the process of cutting, highly distorted crystals in the chip are sheared off from the parent material at the shear plane (line OD, figure 4). As the material slips along one plane, it work hardens and resists further distortion. The stresses build up on the next plane to bring about slip in the new material, and so on [22].

In the process of machining, as the tool advances against the work material a field of stress is generated at the primary deformation zone. Stress at this zone is at its maximum which causes shear of the work material as it passes through this area. For research purposes and ease of calculation many authors consider this zone as a plane called the "shear plane" [23,24]. However, other researchers continue to advocate the term "shear zone" [25,26].

### 2.3.4 Continuous Chips with a Build-Up-Edge

These types of chips can be obtained by machining two phase materials at low speeds. During machining the continuous chip removes any contaminant on the tool face. Subsequently, due to the high affinity of the chip and the newly exposed surface of the tool, a strong bond is formed and shear is transferred to a subsequent layer. In a process that involves work hardening and crack initiation/propagation the Build-Up-Edge (BUE) is formed.

The occurrence of the built-up-edge is influential on surface finish and can play an important role in tool wear [27].

## 2.4 Forces in Metal Cutting

Forces in machining are an important parameter. Knowledge and awareness of their behaviour is essential in the design and manufacture of machine tools to provide sufficient rigidity and eliminate vibration. Accurate measurement of the forces present in metal cutting will also help in the design of tool geometries.

The forces present during the cutting process can be resolved into three components which are shown in figure 5. The first component is the cutting force  $F_c$ , which is usually the largest force acting on the rake face in the direction of the cutting velocity. Second the feed force  $F_f$ , acting parallel to the direction of the tool feed and finally the radial force  $F_r$ , which tends to push the tool away in a radial direction.

In the field of metal cutting, the contact length between the tool and the chip plays an important role, and is related to the cutting forces. Trent [28] has shown that machining in the presence of oxygen may reduce the contact area between the tool and the chip leading to a considerable reduction in the cutting forces.

The maximum compressive stress acts on the cutting edge and reduces to zero when approaching the end of the contact zone [29]. Turning materials which produce discontinuous

chips tend to produce lower forces due to the shorter contact length. Increase in the feed rate will increase the contact length between the chip and the tool, resulting in higher force generation.

During machining of materials with high strength, large forces are required due to the high stresses on the shear plane which subsequently result in a large amount of heat generated in the cutting zone. With the increase in heat the yield strength of the tool material drops rapidly [17].

Another factor which influences the cutting forces is the rake angle. Selection of a tool with a larger rake angle will require lower forces but the increase in the rake angle will have the tendency to weaken the cutting edge thereby creating conditions for tool failure [30].

Cutting speed is another factor which influences the cutting forces. As the cutting speed increases the forces acting on the tool generally decrease [31] (figure 6).

## 2.5 Heat Generated during Machining

For the productivity of the machine tool, heat generated during metal cutting and the temperature rise at the cutting edge are of fundamental importance. At the beginning of this century Taylor [32] showed with the development of HSS tools that heat generated in metal cutting plays a vital role in controlling tool life. Before that cutting speed was limited to only a few m/min. Due to the higher temperature resistance of HSS tools, cutting speeds were increased to about 30m/min.

The phenomenon of tool wear depends very much on the

temperature [33], and the temperature generated at the cutting edge is a deciding factor for the control of the maximum possible rate of metal removal when machining materials like iron, steel and nickel alloys with high melting points [35].

According to the investigation by Braiden [34] heat is generated in three major zones which are as follows:

- (i) The primary shear zone, in which a great deal of deformation occurs
- (ii) The tool/chip interface (secondary shear zone)
- (iii) The flank face of the tool, where heat is generated by the interaction of the workpiece with the tool.

Boothroyd [36] has concluded that if the tool material is not perfectly sharp, (which is true in most practical cases) the latter part (iii), would always be present. He continues stating that, unless the tool material is severely worn, this heat source would be small and will be ignored.

Trent [35] has also stated that in metal cutting, heat is generated by work done in plastic deformation of the material in two regions: (i) intense strain at the shear plane, and (ii) extremely intense strain either at the top of the built-up edge or in the flow zone.

During machining the generation of heat in the chip occurs due to deformation on the primary shear plane. The temperature of the chips is not usually very high unless machining is performed at very high speeds, although experience has shown that when turning nickel-base superalloys at speeds of about 300 m/min red hot ribbon-like

chips are produced. Shaw et al [37] noticed from their experiments that a Waspaloy chip had red hot edges while the centre of the chip was cooler.

Figures 7 and 8 illustrate the distribution of the heat generated during machining [38,39]. The approximate values indicate that the majority of the heat is being taken away by the chips and only a small amount is conducted into the tool and the work material.

Since the early 1920's [18] many researchers [40,41,42] have tried to achieve a method for measuring the temperature generated in metal cutting which is precise, universal and easy to apply.

The tool/work thermocouple technique was initially implemented by Herbert [43] and other workers to determine the temperature generated on the face of the cutting tool. This method uses the fact that an e.m.f. is generated at the interface of two dissimilar metals when the temperature of the interface changes. The major drawback of this method is that it only records an average value of the chip temperature with no temperature distribution.

Wright and Trent [44] have developed a metallographic technique to measure cutting tool temperatures. According to this method, temperature distribution on the surfaces (usually sectioned) of carbon steel tools or HSS tools can be obtained. The accuracy involved with this method claims to be  $\pm 25^{\circ}\text{C}$ . The disadvantage with this method is that it can only be used within a certain range of temperature. For example for HSS the recognisable structural changes can only

be obtained between temperatures of 600 to 900°C and for carbon steel tools temperatures between 300 to 600°C [45]. An extension of this method to cemented carbide tools was provided by Dearnley [46]. Instead of cobalt, he used iron and iron-silicon bonded carbides as the binder element which enables the temperature to be determined based on different austenite transformation temperatures of each binder. The disadvantage of this technique is that such cemented carbide tools are not commercially available.

## 2.6 Tool Failure Modes

Wear is a very complex subject and plays an important role in metal cutting operations. Trent has described wear as removal of material from the tool which may be in the form of fragments not larger than a few microns or at an atomic level. Preferably a cutting tool insert must retain its original cutting edge shape and continue to cut.

### 2.6.1 Flank Wear

This type of wear takes place in a narrow band on the flank face just below the cutting edge (figure 2). Generally, flank wear is a major cause for the rejection of cutting tools. The deciding action for discarding the tools is a set of established and recognised criteria which clearly define the tool lives [15,16].

Figure 9 illustrates the increase in the flank wear in relation to time [47]. This increase is high at the beginning and subsequently tends to rise at a steady rate, up to a critical point (C in figure 9) where wear is

accelerated again leading to the unpredictable collapse of the tool.

Flank wear may develop by temperature dependent mechanisms and therefore the use of a coolant may help in prolonging tool life. Excessive flank wear can cause chatter and a poor finish on the machined surface [48].

#### 2.6.2 Wear on the Rake Face

Wear on the rake face of the tool is by the formation of a crater at the tool/chip contact area or by grooving at the extremes of the depth of cut. Crater wear usually takes place some distance away from the cutting edge [17]. There is usually a narrow region at the cutting edge which is not subjected to wear during machining and cratering occurs behind this region which experiences high stresses and temperatures. However, when machining high creep resistant materials such as nickel and titanium alloys the crater wear can be developed very close to the cutting edge in such a way that it may join the flank wear thereby weakening the cutting edge [49].

The maximum depth of crater wear usually takes place near the midpoint of the contact length where normally the maximum tool face temperature exists [18]. Trent [35] has also suggested that the tools are worn more rapidly as the interface temperature rises. However, Whitney et al [1] feel that this is a story of the past with regard to ceramics. They state that the new generation of the tool materials possess the capability to withstand high temperatures while

maintaining suitable strength and hardness thus the heat generated in the shear zone ahead of the tool can now be used to advantage. Temperatures as high as  $1200^{\circ}\text{C}$  have been reported by some researchers [50,51] when machining INCO 718 with ceramic cutting tools. Using whisker reinforced ceramic tools when high speed machining nickel-base superalloys, temperatures approximately  $1400^{\circ}\text{C}$  have been reported [1].

Apart from speed and feed which are influential parameters, rake angle, approach angle and depth of cut play important roles in the crater wear rate.

### 2.6.3 Wear at the End of Depth of Cut

End of depth of cut wear or notching is a major problem and tool life dominating when machining superalloys [7,52]. It has a "V" shape and Shaw [18] has reported the occurrence of this type of wear when machining high temperature alloys, very soft steel or other materials with a strong tendency to strain harden during chip formation.

Many researchers [53,54,55,56] have carried out a variety of tests to determine the cause of notch formation and they suggest the following:

1. Presence of a work-hardened layer on the previously cut surface.
2. Stress concentration due to the stress gradient at the free surface.
3. Formation of thermal cracks due to the steep temperature gradient at the free surface.
4. Presence of a burr at the edge of the freshly machined



surface.

5. Presence of an abrasive oxide layer on the previously cut surface
6. Fatigue of the tool material due to the fluctuation of force at the free surface which accompanies the small lateral motions of the edge of the chip.
7. Particles of the tool material left behind on the previously cut surface which act as small cutting tools to induce wear.
8. Flow of built-up edge material parallel to the cutting edge.

The final point however, is not always the case since the formation of the notch may take place at high speeds beyond the range of speed for built-up edge formation.

Tonshoff et al [57] have reported that notch wear is influenced by cutting geometry when machining steel with ceramic tools. He states that an approach angle of  $85^{\circ}$  (compared to  $45^{\circ}$ ) in conjunction with higher feed rates results in greater notch wear. According to their findings chips generated at the lower approach angle were characterised by regular segmentation and relatively small curvature. Irregularity in chip segmentation and greater curvature as well as evident tooth formation on one edge of the chip were products of the higher approach angle. Only this edge of the chip traverses where the notch wear occurs on the cutting tool.

Jawaid [58] has also found that an increase in feed rate was partially responsible for the increase in the rate

of wear. He also suggested that notching takes place under sliding conditions and disappears at cutting conditions where seizure takes place.

It has also been found that the presence of different atmospheres will influence the notch wear rate [58,59]. Presence of an oxygen rich atmosphere has minimised the rate of wear in comparison with the presence of other gases like air, argon and nitrogen when Nickel-base superalloys were machined with ceramic cutting inserts.

During machining of superalloys the rate of notch formation is very high. Increasing the depth of cut notch will increase the longitudinal force and subsequent wear provides favourable conditions for the tool material to fracture [60].

#### **2.6.4 Failure by Fracture or Mechanical Damage**

Sudden failure or loss of the tool material during machining is an unwanted mechanism and people involved in metal cutting try to eliminate this characteristic. There are several parameters which should be taken into consideration. Selection of the right tool material with the right geometry for a specific operation is very important.

Tool materials with high positive rake angles are prone to chipping due to the small included angle of the tool tip. Nose radius is another important parameter which influences the strength of the tool tip. Tools with larger nose radii are stronger and can produce a better surface finish but require larger forces for cutting.

Tool materials which possess high hardness tend to be brittle. This brittleness is a drawback particularly when intermittent cutting such as milling takes place and chipping occurs due to mechanical shock. During interrupted cutting the presence of thermal cracks due to thermal cycling can also be the initiation point for the generation of chipping and sudden failure.

Excessive wear such as crater wear or notching at the end of the depth of cut weaken the tool at the affected area/s which subsequently can be good initiation points for failure. To avoid this type of failure the standard allowable limits [15,16] should be exercised. Poor handling of the tool materials and improper setting can also be responsible for this type of failure.

## 2.7 The Tool Wear Mechanisms

Tool wear mechanisms have been studied by many of the leading researchers in the field of metal cutting [61,62,63]. The term wear, in relation to the tool material has been defined by Trent [64] as the process by which material is removed from the tool surface in the form of very small particles.

Detailed research into tool failure modes has shown that the most common wear mechanisms fall into the following categories:

- (1) Abrasion wear
- (2) Attrition wear
- (3) Diffusion wear
- (4) Plastic deformation

## (5) Wear by chemical interaction

### 2.7.1 Abrasion Wear

In metal cutting abrasion wear is caused when hard particles are carried on the underside of the chip moving over the face of the tool and these scrape away fragments of the tool material. These abrasive particles could be present in the work material or they can be the fragments of the built-up-edge [65], they could equally be particles of tool material itself [66]. However, only large hard particles increase the rate of wear by abrasion, hard particles of smaller sizes having little influence in this process.

Since the cutting tool is always harder than the work material it is unlikely to experience this type of wear. However, it has been reported that abrasion wear has been partially responsible for the wear of tool material when machining superalloys [67], a titanium alloy [68] and an alloy steel [66].

Blankenstein [69] has reported that the abrasive wear of carbide tools is partially caused by the high hardness of its own components. During machining, particles of the tool material are removed from the cutting edge and will be pushed down by the machined surface. Due to the high normal stresses acting between cutting tool and the workpiece a feature similar to grinding marks can be generated.

### 2.7.2 Attrition Wear

Attrition wear, also known as adhesive wear is a mechanism that changes the geometry of the tool by

mechanical detachment of the small particles which are formed between the chip and the tool.

Trent [64] states that temperature is not the major influential factor in the process of attrition wear but it is more related to the uneven flow of metal as it passes the cutting edge and the ability of the tool to withstand the tearing action resulting from uneven flow under conditions of seizure.

Jawaid [58] has shown that sialon tools wear through the loss of microscopic sized particles. Subsequently, aided by a quick stop technique, he was able to detect sialon particles on the under side of the chip. He further suggested that under irregular chip flow conditions the loss of a single particle could lead to the loss of a whole cutting edge.

It has been reported that the hardness of the cutting tool will not influence this type of wear [17]. However, grain size of the cutting tool is an important factor in the wear rate. Trent [70] has shown that, when machining at low cutting speeds carbide cutting tools with a fine grain size (i.e. 1 micron) are more resistant to attrition wear than those cutting inserts with a larger grain size (i.e. 3-5 microns). Kitagawa et al [71] reported that powder metallurgy high speed steel (PM-HSS) tools with smaller and more uniform grain size and microstructure are more resistant to attrition wear and are more capable of retaining a sharp cutting edge than the conventional high speed steel tools.

There are a number of parameters such as low speeds and feed rates, lack of rigidity in the machine tool, vibrations and the formation of a built-up-edge which will influence and promote wear. The presence of built-up-edge (BUE) during machining changes the macrogeometry of the tool edge and may accelerate wear rate by repeated removal and fresh formation [65]. However, if this BUE is stable it may protect the cutting edge, enhancing tool life as has been reported [72] when machining steel with WC-CO alloys.

### 2.7.3 Diffusion Wear

Diffusion wear occurs when atoms move from a region of high atomic concentration to one of low concentration [73]. Therefore factors such as the metallurgical relationship between the work material and the cutting tool as well as the temperature generated in the cutting zone [74], and the rate of flow of the work material very close to the surface of the tool [64] play important roles and influence the rate of wear.

During machining of steel with carbides atoms of the tool material are transported into the moving chip and this is predominantly controlled by the solubility of the carbide phase in the chip material [17]. It has been proposed that this is the major cause of crater wear at high speeds [75].

It has been agreed by many researchers that this type of wear normally produces a smooth surface unlike the surfaces which are produced under conditions of attrition wear.

Jawaid [58] has also detected diffusion wear when machining Inconel 901 using SYALON cutting tools. At the interface, a reaction caused by the titanium and/or chromium from the work material with nitrogen from the beta prime phase of the tool material the formation of nitrides.

Narutaki et al [76] reported that when machining steel diffusion of the Fe and Ni was observed above 1000°C on cermet tools. He added that at 1300°C a thick reaction zone containing Fe, Ni, Mo, W and Ti was generated near the tool surface and rapid diffusion of carbon took place from the cutting tool to the work material.

King [77] has reported that there is a slight reaction between titanium, zirconium and alumina at 1400°C, and therefore does not recommend that titanium should be machined with ceramic tools.

#### 2.7.4 Plastic Deformation

Plastic deformation is an indirect wear process changing the cutting edge geometry by the application of heat and pressure. This phenomenon occurs when cutting materials with poor machinability characteristics like superalloys and certain steels. Due to high stresses involved during machining of materials with high yield strength, plastic deformation of the tool materials, even at low speeds is possible.

Since it is estimated that about 10% of the heat generated during machining will be diverted into the cutting edge, a relatively low cutting speed may provide favourable conditions for the cutting tool material to deform

plastically. Trent [17] suggests that carbide cutting tools can tolerate limited plastic deformation (figure 10). This suggestion has also been supported with high speed steel tools when machining steel.

Cook [48] suggests that the tool materials become plastically deformed at critical cutting speeds with feed, depth of cut and the machining environment as well as the type of tool and the work material being important.

Moskowitz et al [78] supported this by machining steels having different hardnesses with various grades of carbide tools. Subsequently he reported that the variation in the workpiece hardness values affected the deformation characteristics of the tool material (figure 11).

#### 2.7.5 Wear by Chemical Interaction

Wear by chemical interaction is an important mechanism in determining the tool life. Bhattacharyya et al [79] suggested that the atmospheres present during machining are partially responsible for the notching at the end of depth of cut. Jawaid [58] has shown that the presence of an oxygen rich atmosphere in the vicinity of cutting zone has enabled Syalon tool material to exhibit a longer life than in the presence of nitrogen, when machining Inconel 901. It is further suggested that [80] the titanium and chromium within this material have a greater affinity for oxygen than for nitrogen. Therefore the presence of oxygen provokes these materials to form oxides and inhibits the formation of nitrides which subsequently prevents the erosion of beta



crystal in the syalon cutting tool resulting in reduced notch wear.

Childs et al [81] summarised their results after machining medium carbon steel with high speed steel cutting tools.

- a. In dry conditions a nitrogen atmosphere promotes strong adhesion, the formation of a stationary layer, little sliding and little wear.
- b. During machining in dry conditions with an oxygen rich atmosphere present, although there is much sliding there is low adhesion and little wear.
- c. However, when machining in water vapour adhesion is slightly reduced which prevents the formation of the stationary layer without promoting good lubrication between the adhered layer and the flank which subsequently promotes wear.

## 2.8 Tool Materials (Excluding Ceramics)

### 2.8.1 Tool Material Requirements

There are a variety of tool materials available for the purpose of machining operations. The tool selection for a specific process must be in accordance with the specification of the material to be cut and cutting conditions.

The perfect tool should in theory possess two basic qualities, sufficient strength and wear resistance for accuracy and efficiency during machining.

Trent [82] detailed tool material requirements as follows:

- a. High compressive, tensile and shear strength
- b. Adequate toughness to resist deformation and premature failure.
- c. High hardness and strength at elevated temperature
- d. Good thermal shock properties
- e. High resistance to thermal and impact stress
- f. Good chemical inertness

The variation of the tool costs (ranging from several pence to several pounds) is by no means an indication of the quality of the tool for a specific job. The cheapest tool material is not necessarily the most economical one nor is the most expensive tool the best. However, the best tool material is the one which will maximise the efficiency and accuracy at the lowest cost [83].

Conventionally, the main cutting tool materials used for machining operations fall into groups which are listed below. Each of these tool materials have their own specific properties and characteristics which are summarised in tables 1 & 2.

- 1. Carbon steel and low/medium alloy steel
- 2. High speed steels
- 3. Cemented carbides
- 4. Ceramics
- 5. Ultra hard materials

#### 2.8.2 Carbon Steel and Low/Medium Alloy Steel

Carbon tool steels were the earliest form of cutting tools employed in metal cutting at the beginning of the

Nineteenth century. These tools are made from plain carbon steels and obtain their hardness through heat treatment. The main elements are 0.8-1.3% C, 0.1-0.4% Si and 0.1-0.4% Mn. The application of these tools has now been limited to just hand held tools, but their quality has been improved by small additions of chromium and tungsten.

Carbon tool steels were replaced in the market by low/medium alloy steel for greater machining productivity in many applications. These tools are hardened using a similar method to that used for carbon steel tools. Their composition is also similar except molybdenum and chromium are added to improve their hardenability. However, this hardness can easily be lost if the temperature exceeds their tempering temperatures which are about 150-340°C (figure 12). These tools suffer from limited abrasion resistance due to a low volume fraction of a hard, refractory carbide phase present in the alloys and are of limited use due to their low hot hardness values being therefore unsuitable for high speed machining. They are mostly used for drills, taps, dies and reamers (table 3), where heat generation is relatively low.

### 2.8.3 High Speed Steel Tools

At the beginning of this century Taylor and White, invented and introduced a new tool material subsequently called High Speed Steel (HSS). They discovered that an alloy steel of the Mushet type (an alloy steel developed by Mushet in 1861) acquired an improved cutting capacity if the hardening temperature was raised higher than had previously

been considered correct. The improved heat treatment technique enabled them to have significant increases in metal removal rates and cutting speeds. At this time the "red hardness" or ability to resist softening at elevated temperatures was recognised. Subsequently a grade containing 18% tungsten (W), 4% chromium (Cr) and 1% vanadium (V) was established and it remained the standard all purpose HSS until World War II, when the molybdenum (Mo) type (M series) which were developed in the 30's, came into general use because of the scarcity of tungsten (W).

The tungsten grades or T series HSS contain 12-20% tungsten (W) with chromium (Cr), vanadium (V) and cobalt (Co) as major alloying elements. The molybdenum (Mo) grades or M series contain 3.5-10% molybdenum (Mo) with chromium (Cr), vanadium (V), tungsten (W) and cobalt (Co) as the other alloying elements.

High speed steel tools can be manufactured by casting or powder metallurgy. Improper processing of cast HSS products can lead to undesirable microstructural features, including carbide segregation, formation of large particles and non-uniform distribution of carbides in the matrix. However, powder metallurgy high speed steel tools will provide a uniform carbide distribution throughout the matrix. This uniform carbide has proven that this group of tool materials can perform better and have longer tool lives at higher speeds [84] than the conventional high speed steel.

It has been reported [85] that the life of high speed

steel tools can be increased by coating the surface of the tool materials with titanium nitride.

Komanduri et al [86] have listed the advantages in using the high speed steel tool materials;

1. Through hardenability
2. Higher hardness than carbon steel and low/medium alloy steels
3. High toughness
4. Ability to alter hardness appropriately by suitable heat treatment
5. Reasonable cost
6. Easy to obtain

And the drawbacks are;

1. Hardness falls at elevated temperature
2. Limited wear resistance
3. Limited chemical stability
4. Greater tendency for adhesion of the chip to the tool.

#### 2.8.4 Cemented Carbide Tools

It was in the early twentieth century that Germany introduced a new tool material to the market which could perform at higher cutting speeds than high speed steel tools when machining cast iron. This was fine tungsten carbide powder bonded with cobalt and this helped to raise the production rate several fold when machining cast iron. It was later discovered that this type of tool material would not give the same improvements when machining steels. This short tool life was due to severe crater wear on the rake

face of the tool. Subsequently it was discovered that high temperature chemical interactions between the tool and the chip were responsible for this wear pattern. Improvements were made by the addition of titanium and other carbides.

Tungsten carbide tools have a unique combination of properties which are different to high speed steel tools in many aspects. They are [17,87];

1. Much harder
2. Chemically more stable
3. Superior hot hardness
4. Generally lower toughness
5. Carbide is the predominant phase in cemented carbides thus the Young's modulus (E) of the cemented carbide is two to three times higher than that of high speed steel
6. Higher fabrication costs
7. Cutting speed can be increased three to six times those used with HSS
8. More expensive
9. Use strategic materials ( W, Co, Ta) more extensively.

The carbide tools fall into three major groups which are;

- a. Tungsten carbide (WC)- cobalt (Co)
  - b. Mixed carbides
  - c. Coated carbides
- 
- a. Tungsten Carbide (WC) - Cobalt (Co)

Tungsten carbide cobalt (WC-Co) grades are the original form of this group of tool materials and still commercially

available. This grade consist of fine particles of hard, abrasion resistant tungsten carbide (WC) bonded together with metallic cobalt (Co). The WC/Co ratio is very important in determining the hardness and toughness of the tool material, increasing the percentage of WC which increases the hardness.

Low coefficient of thermal expansion of tungsten carbide coupled with a high thermal conductivity produces an excellent thermal shock resistance. High machining performance and greater thermal conductivity of WC-Co make this tool material superior to HSS particularly when machining cast iron, non-ferrous and exotic materials at high cutting speeds.

#### b. Mixed Carbide

Titanium carbide (TiC), tantalum carbide (TaC), and niobium carbide (NbC) are alloyed with tungsten carbide before bonding with cobalt or nickel to form the mixed carbide grades (also known as steel cutting grades).

Addition of these carbides to WC-Co improves the hardness and compressive strength at high temperature [17]. Improved resistance to diffusion wear and developmental work on these materials has enabled them to perform successfully on a variety of cast grey iron as well as steel and its alloys , especially when superior surface finish is required [88].

#### c. Coated Carbide Tools

In this group of tool materials a substrate generally

consisting of tungsten carbide is coated with different layer/s (few micrometers thick) of titanium carbide, titanium nitride, titanium carbonitride and/or alumina. Chemical vapour deposition (CVD) processes are the predominant method for coating these inserts. It has been reported that TiN coating is superior to TiC in that TiN has a much lower tendency to crater [89]. The toughness of the coating and the tool having a rounded edge enables the tool materials to have higher resistant to chipping and notching [90]. The evolution of coated carbides has resulted in an increased metal removal rate and tool life when machining cast irons. However, these grades of tool materials because of their chemical affinity, are not recommended for the machining of nickel and titanium alloys [91].

#### 2.8.5 Ultra Hard Materials

Cubic Boron Nitride (CBN) and diamond are known as ultra hard materials because of their high hardness (table 1).

Diamond was successfully synthesised in 1954 and three years later, man-made diamond became commercially available. This was followed by the production of cubic boron nitride (CBN) in 1968 [92].

Diamond tools are excellent for machining non-ferrous metals such as aluminium alloys and copper alloys. Due to their high hardness, their tool lives can be about 20 times higher than carbide tools [93]. Cubic boron nitride (CBN) tools have slightly lower hardness than diamonds, and they



possess excellent heat transfer characteristics, even better than copper, which help to dissipate the heat from the cutting zone. They are capable of machining hard, ferrous base materials and nickel-based superalloys (for instance Inconel 718, Rene 91 and Waspaloy) [94,95]. In order to achieve this the cutting must be performed at high speed to generate enough heat in the shear zone to enable the chips to flow plastically. This degree of heat cannot be tolerated by diamond [96]. However, since coated carbides and ceramics cost only a fraction of CBN tools (about  $1/30^{\text{th}}$ ) [96,97], a more detailed economical study would be necessary for the correct selection of the tool material.

## 2.9 Ceramic Tool Materials

### 2.9.1 Introduction

Although ceramic tool materials were in use thousands of years ago it was not before the early twentieth century that they became important again. It was not long before industry realised that these tool materials lacked the necessary mechanical and thermal properties. During and after the Second World War the scarcity of tungsten, and later the development of stronger alloys, compelled the material scientists to improve the mechanical properties of ceramic cutting tools by varying the manufacturing routes and trying different additives.

The brittleness of these tool materials, coupled with insufficient rigidity and lack of power within the machine tool, hindered their application and usage during their early development. However, these problems have been

overcome by developing new advanced ceramics and high powered, rigid machines. With these new developments ceramic cutting tools effectively machined cast iron in the automotive industry and are also capable of machining nickel-base superalloys in the aerospace industry, where they are beginning to displace high speed steel and carbide cutting tools.

Ceramic tool materials are based on either alumina ( $\text{Al}_2\text{O}_3$ ) or silicon nitride ( $\text{Si}_3\text{N}_4$ ). Their high hardness which has been obtained at the expense of their lower toughness coupled with their current cost may limit their applicability [98].

In 1986 it was estimated [99] that the worldwide usage of ceramic cutting inserts was in the region of 75 million dollars which will be increased to 150 million dollars by the year 1995.

### 2.9.2 Development of Ceramic Tool Materials

Twentieth century development of Aluminium Oxide tooling started as early as 1905 and the patents were registered in 1912 in England and one year later in Germany [100]. These newly developed tool materials however, were not introduced into the market until the early 1930s [101]. They were not very successful because they were characteristically thought of as brittle cutting tools with low strength and low impact resistance.

During the Second World War the scarcity and high cost of tungsten, drew attention again to alumina cutting tools.

Subsequently in the middle of the 1940s hot pressed aluminium oxide was introduced into the market place. But this series of tools still suffered from poor physical properties. Subsequently in the late 1960s scientists and tool manufacturers successfully developed a new ceramic tool material with improved properties by the addition of various alloying components into the base matrix. The major additives were  $ZrO_2$ , TiC and TiN.

The newly developed alumina-based cutting tools with wider applications were in service prior to the development of SiAlON which took place in Japan and England [102] around 1970. The development and introduction of silicon nitride ( $Si_3N_4$ ) based ceramic cutting tools occurred at the beginning of the 1980s.

In 1985 tool manufacturers successfully developed silicon carbide whisker reinforced alumina ( $Al_2O_3+SiC_w$ ). This alumina-based cutting tool has advantages in terms of toughness and thermal conductivity in comparison to the other alumina based tools and has been used in the aerospace industry for rough machining of some superalloys.

The table below summarises the introduction dates of the ceramic cutting tool materials [100,102,103]:

<u>Material</u>	<u>Year</u>
$Al_2O_3$ (sintered) .....	1930-1931
$Al_2O_3$ (hot pressed) .....	1944-1945
$Al_2O_3$ +Additives (hot pressed) .....	1968-1970
$Si_3N_4$ .....	1970
SiAlON .....	1980
$Al_2O_3+SiC_w$ .....	1984-1986

Whitney et al [1] stated that since about 1970 ceramic tool materials have improved tremendously and have the capability of machining various types of steels, cast irons and nonferrous metals such as brass, bronze and superalloys at high speeds and feeds. These developments are mainly due to:

- a. Microstructures that have been refined by controlling and improving the manufacturing processes.
- b. Toughening mechanisms that have improved the fracture toughness of ceramic tools and reduced susceptibility to thermal shock.
- c. New ceramic compositions which have been developed for cutting tool applications, particularly in high speed machining.
- d. Surfaces that have been conditioned by the removal of cracks, irregularities and residual stresses.

### 2.9.3 Variation in the Base Matrix of Ceramics

Ceramic tool materials generally fall into two categories and they are either based on alumina, known as oxide ceramics or are based on silicon nitride, known as nitride ceramics. Oxide ceramic cutting tools can be divided into two groups and have been termed white oxide or black oxide. The recently developed silicon carbide whisker reinforced alumina however, lies in the latter group and will be dealt with individually.

The recently introduced [9] Silicon Carbide whisker reinforced alumina ( $\text{Al}_2\text{O}_3\text{-SiC}_w$ ) cutting tools exhibit a superior combination of wear and fracture resistance by

means of SiC whisker reinforcement of the  $\text{Al}_2\text{O}_3$ .

Silicon nitrides ( $\text{Si}_3\text{N}_4$ ) fall into two forms (alpha and beta silicon nitrides), with both having a hexagonal structure with slight variations in the lattice dimensions. The alpha silicon nitride have a higher aluminium content and lower yttria ( $\text{Y}_2\text{O}_3$ ) compared to the beta silicon nitride. The latter contains very little oxygen and is a well formed particulate crystal in contrast to the whiskers usually observed in the case of the alpha form [58].

#### 2.9.4 Manufacturing Process

Ceramic tool materials are manufactured by two processes which are very similar to those of powder metallurgy. These methods of manufacturing are traditionally called cold pressing and hot pressing processes.

##### 2.9.4.1 White Ceramics

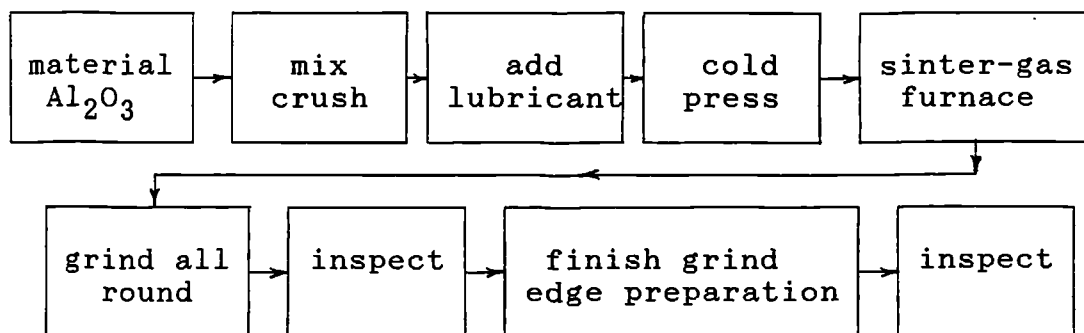
White ceramics are manufactured by cold pressing/sintering. The process starts with mixing and crushing the aluminium oxide and later a waxy temporary binder (which also acts as a lubricant during the manufacturing operations) is added. The mixed powder is then cold pressed with pressures of about  $35 \text{ kgf.mm}^{-2}$  (50,000 psi) to form the required insert shape. Subsequently the molded inserts are heated below the melting point to allow solid-state sintering to take place.

In order to achieve high quality microstructures (retain small grain size at high densities) sintering aids are employed [104].

The sintering temperature and the soaking time at a specified temperature will greatly influence the property of the finished product. The shrinkage in the alumina powder compact starts at temperatures above 1200°C, but it does not achieve a high density unless sintered at about 1700°C or above [77].

After sintering which will enable the product to obtain hardness, strength and thermal resistance, all round grinding takes place followed by inspection. If the products are to be cutting tool inserts final edge grinding and preparation followed by an inspection will end the process.

The figure below summarises the ceramic cold-press process [105].



#### 2.9.4.2 Black Oxide Ceramics

The process of hot pressing, which is conventionally used for manufacturing the black oxide ceramics, is very similar to that of cold pressing, the difference is that in this method the pressing process is carried out at sintering temperatures under the application of accurately controlled heat and pressure.

In the manufacture of hot pressed ceramic cutting tools, the aluminium oxide ( $\text{Al}_2\text{O}_3$ ) and titanium carbide ( $\text{TiC}$ ) are crushed and mixed and an organic binder added to provide internal lubrication between the powder particles, this is subsequently hot pressed. The controlled application of heat and pressure provide conditions for the mixture which is kept in an over sized graphite mould to undergo the repacking, plastic flow and grain rearrangement processes and allows for shrinkage to occur.

The addition of titanium carbide (up to about 30% wt) to the alumina matrix can be replaced by titanium carbonitride. This provides a uniform dispersion of very fine-grained carbonitride in a closely controlled aluminium oxide matrix [106]. Cutting tool inserts with these compositions exhibit higher compressive strength and abrasion resistance than the white ceramics.

The most recent alumina-based cutting tool materials, ( $\text{SiC}$  whisker reinforced  $\text{Al}_2\text{O}_3$ ), are also manufactured by hot pressing. Billman et al [9] reported that as much as 30-40 vol% single crystal silicon carbide whiskers are added to the fine equiaxed  $\text{Al}_2\text{O}_3$  together with densification aids such as  $\text{MgO}$  or  $\text{Y}_2\text{O}_3$ .

#### **2.9.4.3 Silicon Nitride Based Ceramics**

There are a variety of non oxide ceramic cutting tools based on silicon nitride readily available. In real terms silicon nitride cutting tool materials can be classified into two groups, namely silicon nitride and sialon tool materials.

Silicon nitrides have high strength and good resistance to thermal shock due to low thermal expansion, high thermal conductivity and high fracture toughness.

Silicon nitride ceramic tools can be manufactured containing different quantities of elements to cater for various requirements. One of these products is a composite consisting of 30% titanium carbide dispersed into the matrix phase to improve hardness and abrasion wear resistance.

SIALONS are another class of silicon nitride based cutting tools which are an alloy of silicon (Si), aluminium (Al), oxygen (O), and nitrogen (N). Their universally accepted name has been derived from these contributing elements.

SIALONS were developed in the early 1970's when it was realised that aluminium and oxygen could be substituted for silicon and nitrogen respectively. Liquid phase sintering process is used to manufacture Sialon tool materials. Silicon Nitride ( $\text{Si}_3\text{N}_4$ ), Alumina ( $\text{Al}_2\text{O}_3$ ), Aluminum Nitride, (AlN) and Yttria ( $\text{Y}_2\text{O}_3$ ) powders are mixed together. After drying they are pressed to form the required shape. Subsequently sintering takes place around  $1800^\circ\text{C}$ . During solidification yttria reacts with silicon nitride to form a silicate which is liquid at the sintering temperature [104]. Gradual cooling solidifies the liquid to a glassy phase, bonding together the fine grains of the beta silicon nitride crystals which are of the order of 1 micron.

These tool materials exhibit high fracture toughness, low coefficient of thermal expansion and high thermal



conductivity.

Another type of the nitride ceramic tool has silicon nitride as a base with additives of aluminium oxide  $\text{Al}_2\text{O}_3$ , yttria  $\text{Y}_2\text{O}_3$ , titanium carbide  $\text{TiC}$  and magnesium oxide  $\text{MgO}$  [60]. Most of these materials are manufactured by hot pressing or sintering.

Hot pressing is widely used for silicon nitride which produces virtually fully densified material [107], with additions of additives such as yttrium oxide and magnesium oxide in a nitrogen atmosphere. The densification process can be carried out either by hot pressing or hot isostatic pressing in nitrogen at temperatures from  $1700^\circ\text{C}$  to  $2000^\circ\text{C}$ . To achieve complete densification for the end product, Lumby [108] recommended alpha silicon nitride powder to be used as the starting material. The materials manufactured by the hot pressing process possess high density with very little porosity (which accounts for the higher strength) and mechanical properties which are superior to sintered silicon nitride. However, hot pressing is a very expensive and time consuming process and only fairly simple shapes can be manufactured.

In some of the mixed composite ceramic tool materials the sintering additives in conjunction with  $\text{SiO}_2$  form a glassy phase at the grain boundaries. The presence of the glassy phase has a detrimental effect on the high temperature properties of the  $\text{Si}_3\text{N}_4$ . Therefore the properties and the quality of the nitride tools are dependent on the type and amount of the sintering aid

employed.

#### 2.9.4.4 Influence of the Additives and Alloying Elements

##### a. Zirconium Oxide ( $\text{ZrO}_2$ zirconia) in White Ceramics

Oxide ceramic cutting tool materials contain tetragonal zirconia particles. These fine particles are dispersed in the alumina based matrix. When the load is applied, the tensile stress field surrounding the crack tip causes the tetragonal zirconia to transform to the stable monoclinic form [4]. This transformation together with the accompanying 3 to 5% volume expansion provides an increase in the fracture toughness and prevents crack propagation. Widia [10] reported that zirconia particles below a critical size remain in their tetragonal modification. These particles can be transformed by changes in external forces. This stress induced transformation also results in the desired strengthening of the matrix. Larger zirconia particles tend to form spontaneous microcracks during transformation which is undesirable.

Addition of zirconia will decrease the hardness of the composite (table 4) but increases the strength and the resistance of the cutting tool material to oxidation wear and plastic deformation during machining [100, 104].

The quantity of the zirconia used as an additive in the alumina base matrix can vary to suit the application. Some of the commercially available grades now contain up to 30% zirconia. Compositions containing low zirconia are more suitable for finish turning and grooving. However, cutting

inserts containing medium to high zirconia additions are more suitable for rough turning of grey cast iron, nodular cast iron and malleable cast iron hardened to 300 HB [109].

#### b. Titanium Carbide/Nitride (TiC/N) in Black Ceramics

Other additives which influence the mechanical and thermal properties of the ceramic cutting tool materials are titanium carbide and titanium nitride which can enhance thermal shock resistance and improve edge strength. As much as 25 to 40 volume % TiC is added to the alumina base matrix as a dispersed particulate phase [100]. The alloyed composite exhibits higher fracture toughness and higher hardness which is maintained at cutting temperatures. Additionally high hardness produces good abrasion wear resistance. Alumina-titanium carbide ceramic cutting inserts have high thermal conductivity and a low thermal expansion coefficient which strongly influences the thermal shock resistance.

These composites cover a wide range of applications and are suitable for turning hardened ferrous materials, finish turning of grey cast iron, and heat treated steels hardened to 64 HRC to very fine surface finishes and tolerances [109]. When machining softer steels chip control can be a problem [99].

#### c. Silicon Carbide Whiskers ( $\text{SiC}_w$ ) in Ceramic Tools

Silicon carbide whisker reinforced alumina ( $\text{Al}_2\text{O}_3 + \text{SiC}_w$ ) is a recent innovation. Alumina-SiC composite cutting tools usually contain 30-45% SiC whiskers [1]. Whiskers which are

single crystal silicon carbide are grown under carefully controlled conditions and are dispersed into the matrix. It has been reported [110] that one manufacturer uses whiskers that are about 0.02 micron in diameter and 1 micron long.

Contamination during the manufacturing process is one of the major problems which manufacturers have to overcome. And it has been reported that Krupp Widia of Germany has encountered such a problem and are reassessing the manufacturing process [111].

In addition to an increase in the fracture toughness of the brittle matrix, Smith [112] has reported that the thermal conductivity of this grade of cutting tool material has been increased by about forty percent resulting in a higher resistance to thermal shock and allows the use of flood coolant during machining.

As a result of enhanced thermo/mechanical properties, (shown in tables 5 and 6), produced by the addition of about 30% whiskers [109], silicon carbide whisker reinforced alumina cutting tools are used by the aircraft engine industry.

#### d. Additives in Silicon Nitride ( $\text{Si}_3\text{N}_4$ ) Ceramics

Silicon nitride inserts comprise a family of cutting tool materials with a variety of properties. Properties of each individual silicon nitride grade can be altered depending on composition and processing route. Bhattacharyya [113] reported that Lucas industries produced sialon cutting tool materials (which has a trade name of SYALON) the with following advantages over conventional

silicon nitrides:

- a. improved oxidation resistance
- b. improved corrosion resistance
- c. improved creep resistance
- d. improved abrasion resistance
- e. improved fabrication and sintering behaviour.

The introduction of sialon cutting tool materials facilitated a substantial increase in cutting speed by about ten fold, compared to cemented carbides e.g. when machining Inconel 901 [79].

The properties of sialon cutting tools are dependent on the type and quantity of sintering aid employed and the processing route followed during part fabrication.

Baldoni et al [100] have also reported that cutting inserts with  $\text{Si}_3\text{N}_4 + 2 \text{ wt\% Al}_2\text{O}_3 + 6 \text{ wt\% Y}_2\text{O}_3 + 30 \text{ wt\% HfC}$  have better performance and produce longer tool lives than cutting tools having a similar compositions but with TiC instead of HfC, this improvement is reportedly due to the solubility of HfC in iron being lower than that of TiC.

Addition of alumina to silicon nitride improves the chemical stability of the material significantly as well as the physical and mechanical properties (table 5). Increased thermal shock resistance is one of the main features of sialon cutting tools. This is due to a combination of the high thermal conductivity, high toughness and low thermal expansion coefficient.

Sialon cutting tool materials have a relatively high fracture toughness due to the interlocking nature of

elongated beta-Si<sub>3</sub>N<sub>4</sub>/sialon grains [114]. This high fracture toughness coupled with good thermal shock resistance exhibits a low susceptibility to fracture. This can be exploited advantageously in machining at high feed rates (figure 13) or in interrupted cutting.

Additionally Sialon cutting inserts are capable of machining even at elevated temperatures with very little decrease in the hardness (figure 14). Wertheim [115] has reported that the nickel-base alloys, Inconel 718 can be machined with silicon nitride cutting tools at cutting speeds almost 10 times faster than those conventional carbide tools for the same tool life.

The mechanical properties of silicon nitride ceramic cutting tool materials can be improved by reinforcing the nitride based matrix with silicon carbide whiskers [116,117].

#### 2.9.4.5 Wear of Ceramic Cutting Tools

Ceramic tool wear has been investigated by many researchers [118,119,9] and the mechanisms are classified into two categories namely mechanical wear and chemical wear.

Attrition and diffusion wear have been the cause of discarding sialon tools when machining cast iron [120]. Attrition wear which forms at slow cutting speeds shows loss of microscopic size particles. This slow speed however, can create favourable conditions for the formation of a built-up-edge and due to continuous formation and subsequent

removal of the built-up-edge attrition can occur. In the same test an increase in the speed to 310 m/min will raise the temperature which provides conditions for diffusion wear to be established and attrition to be suppressed.

Crater wear can form on the rake face of ceramic inserts. The occurrence of this type of wear does not usually limit tool life but can contribute to the chipping and fracture which limits tool life. Aucote et al [121] reported that the formation of crater wear when machining nickel-base alloys with sialon tools has been shown to take place by the generation of high temperatures within the affected area which softens the binder phase and undermines individual grains.

King [122] has reported plastic deformation within ceramic cutting tool inserts. This process takes place under high compressive stresses during machining. This causes the surface to crack, subsequently leading to fracture or chipping.

Venkatash [123] has machined mild steel and cast iron with oxide ceramics and has reported that aluminium oxide has no affinity for iron and therefore concluded that these inserts are chemically inert.

Narutaki et al [124] have reported that the life of ceramic tools in machining of Ca-Si deoxidised steel is shorter than that of normal carbon steel. He adds, CaO and SiO<sub>2</sub> react with ceramic tools and Ca and Si invade the ceramic tools by diffusion and soften the tool matrix. The reactivity of the Ca is reported to be more predominant than

Si and the distance of Ca invasion larger than that of Si.

Notching at the end of the depth of cut is a domineering wear mechanism when machining heat resistant steels, nickel and titanium alloys. Many researchers agree that this wear mechanism is formed by chemical interactions between the tool and the work material as well as being a mechanical wear [59,80].

The wear rates of ceramic cutting tool materials can be retarded by the application of a coating. It has been reported [60] that additional improvements in chemical wear resistance for silicon nitride based cutting tools have been achieved by coating the substrate with TiC or  $Al_2O_3$ .

A 1-2 micron alumina coating on silicon nitride tools can also possibly improve the friction properties in the contact zones and delay the diffusion and oxidation processes [125]. Godfrey [126] has also reported that the cutting edges can be protected by coating using titanium based grade with a nickel cobalt binder phase which has a higher oxidation resistance than the conventional grade.

## 2.10 Work Material - Superalloys

### 2.10.1 Nickel-Base Superalloys

superalloys fall into three groups:

1. nickel-base superalloys
2. cobalt-base superalloys
3. iron-base superalloys

Nickel-base superalloys are the most complex of the superalloys. A variety of these alloys are widely available in the market place.



Superalloys are constitutionally complex as shown in table 7. Addition of alloying elements like, Titanium (Ti), Aluminium (Al), Molybdenum (Mo), Cobalt (Co), Boron (B), Zirconium (Zr) and Carbon (C) have produced good mechanical properties. These properties render these alloys particularly suitable for service at 950°C and over for structural applications and 1200°C for non-load bearing components [127]. Superalloys have excellent strength which is maintained at elevated temperatures [128].

The alloying elements can be classified into three groups:

Group one:

This group contains nickel (as the main alloying element), cobalt, iron, chromium and molybdenum. These elements have a tendency to produce a face-centered cubic (FCC) austenite (gamma) matrix. The presence of molybdenum in solid solution will provide strength, and chromium will enhance the oxidation resistance. Cobalt decreases the solubility of elements which form precipitates.

Group two:

Elements in this group are titanium, aluminium and niobium. These elements are added to form the intermetallic face-centered cubic (FCC) gamma prime phase  $Ni_3X$  (X can be replaced by any of the elements stated in this group). Gamma prime is responsible for the useful high temperature properties of the superalloys. Hence this property depends on the aluminium and titanium content and particularly Al/Ti ratio [129]. Increasing Al/Ti ratio improves high

temperature properties [130,131]. It is important to achieve the right precipitation of gamma prime in the austenitic matrix during the heat treatment process as this strongly influences the properties. In alloys containing less than 0.1% carbon for instance INCONEL 901, INCONEL 718 and WASPALOY, precipitation is obtained by aging at a suitable temperature after solution annealing and rapid cooling to achieve a homogeneous solid solution.

Group three:

Elements in group three have a tendency to segregate to grain boundaries. These elements are boron, carbon and zirconium. They are usually added in small quantities in order to increase the creep rupture life of the alloys. Boron and carbon will be present in the austenitic matrix in form of borides and carbides respectively.

The presence of carbides in nickel-base superalloys is important and they play a major part in the mechanical behaviour of the alloys. Carbides have three main functions [130] which are:

- a. when properly formed at the grain boundaries, they strengthen the grain boundary and control grain boundary sliding
- b. precipitation of fine carbide in the matrix results strengthening
- c. control of some elements which could create phase instability during service.

The alloying composition and heat treatment will influence the type of carbides. The most common types are

MC,  $M_{23}C_6$  and  $M_6C$  (which M stands for one or more types of metal atoms).

The table below is a summary of the effect of the elements in nickel-base superalloys [130]:

<u>EFFECT*</u>	<u>ELEMENTS</u>
solid solution strengtheners .....	Co,Cr,Fe
Carbide form:	
MC .....	Ta,Ti,Mo,Nb
$M_7C_3$ .....	Cr
$M_{23}C_6$ .....	Cr,Mo
$M_6C$ .....	Mo
Carbonitrides .....	C,N
Forms gamma prime $Ni_3(Al,Ti)$ .....	Al,Ti
Raises solvus temperature .....	Co
Hardening precipitates and/or intermetallics	Al,Ti,Nb
Oxidation resistance .....	Al,Cr
Sulfidation resistance .....	Cr
Improves creep properties .....	B
Increases rupture strength .....	B**
Segregate to grain boundary .....	B,C,Zr

Note:

\* Not all these effect necessarily occur in a given alloy.

\*\* If present in large amounts, borides are formed.

### 2.10.2 Grain Structure

Microstructures of WASPALOY, INCO 901 and INCO 718 at different magnifications are shown in figures 15, 16 and 17 respectively. Variation in the grain size and grain structures can be observed.

Grain size is an important microstructural aspect within these materials. Materials with fine grains have superior room temperature properties such as hardness, tensile strength, yield strength, fatigue strength and

impact resistance. However, materials with coarser grain structures possess good creep properties and rupture strength at elevated temperatures (table 7).

One problem which exists with forged materials, in particular large disc forgings, is that the material is not uniformly worked. Subsequently some of the grains may grow to extreme sizes and provide a duplex structure similar to INCO 901 in figure 16a. The grain size will also influence the precipitation of carbides at the grain boundaries which are usually of the  $M_{23}C_6$  type. Initially the coarse grain will have less grain boundary surface area, therefore carbide precipitation will be more continuous and thicker (figure 15b) which impairs the properties [130]. To avoid this problem a uniform grain structure is desirable. Gadsby [132] has suggested that in the case of INCO 718, a short reheating before the final 20-33% reduction should result in a more uniform grain size.

### 2.10.3 Machining Characteristics of Nickel-base Alloys

As already mentioned nickel-base alloys contain aluminium, cobalt, molybdenum and a variety of other elements in different quantities. Addition of these elements enable the parent material to have high creep resistance and hot strength.

Due to these mechanical characteristics nickel-base alloys tend to be difficult to machine.

Nickel-base alloys have hardnesses in the range 250-500 HV and high toughness. According to Warburton [133] there are two basic problems associated with machining:

1. the inability of the tool material to perform cutting for a long time due to the work hardening.
2. the metallurgical damage to the workpiece due to the high cutting force which also gives rise to work hardening, surface tearing and distortion in finish machined parts caused by induced stresses.

However, these are not the only problems when machining nickel-base superalloys. The other difficulties with these alloys are:

1. ability to retain their high strength at elevated temperatures (figure 18 & 19 [134,50])
2. ability to develop high tool temperatures due to their low thermal conductivity
3. ability to react with cutting inserts at different rates in different atmospheres
4. ability to weld onto the surface of the cutting insert.

Distortion can be a severe problem when machining components of thin section. This cannot be rectified by subsequent heat treatment if dimensional and geometrical tolerances are to be maintained [135].

Kirk [136] has reported that, during machining of nickel-base alloys the tool/chip and tool/workpiece interface temperatures generated are in excess of 800°C with a high compressive stress of around 3450 MPa.

The pressures developed between the cutting tool and the workpiece during the machining process produce a stressed layer of deformed metal on the surface of the work

material. Many researchers have claimed that this work hardened layer is partially responsible for depth of cut notch formation on the cutting tools.

Microstructure is another parameter which affects the machinability of the nickel-base alloys. The presence of carbides produce an abrasive effect. Wrought alloys exhibit better machinability because of the uniform distribution of the carbides [136].

## EXPERIMENTAL TECHNIQUES

### 3.1 Introduction

The aim of this project was to investigate the machinability of nickel-base superalloys when using four different grades of ceramic cutting tools. The machining was confined to simple non-orthogonal turning.

A few prequalifying tests were carried out in-order to obtain the cutting conditions. The initial selection of the main variables (i.e. cutting speed, feed rate and depth of cut) was based on the literature and tool manufacturer recommendations. Using these cutting conditions, the obtained tool lives were generally not long. For this reason cutting operations were stopped after half a minute and/or one minute in-order to measure the wear on the tool by means of a travelling microscope. When the wear pattern on the tool had reached the rejection criteria, the cutting operation was stopped, and the tool was prepared for further detailed wear analysis. After each cut surface finish measurements of the freshly cut surface were taken using a portable stylus instrument (SURTRONIC 3). Samples of the chips produced were also collected.

The worn tool materials were later analysed at high

magnification by means of a Scanning Electron Microscopy (SEM). This process provided a condition to observe the wear area closely, study the wear pattern, and detect the presence of cracks which could later provide favourable conditions for fracture. Some of the cutting tools were sectioned, mounted, and polished. The wear was subsequently studied under the optical microscope and SEM to establish the wear mechanism and to formulate a pattern of tool failure under different cutting conditions.

The cutting was also tested in the presence of different atmospheres (air, oxygen, nitrogen and argon) to study their influence on the wear behaviour.

Tests were always repeated on occurrence of abnormal and unpredictable tool failure.

### 3.2 Machining Operations

Machining operations were carried out on Boehringer DM640 lathe. This lathe has a variable feed selector ranging from 0.05 to 1.8 mm/rev., and the speed selection ranging from 5 to 2500 rpm. Continuously variable motor current enables the desired speed selection within the machine's capability.

To avoid excessive damage on entry to the cut, a chamfer was machined on the outer edge of the work material using a spare cutting tool. This process provided a condition where the whole length of the cutting edge should be engaged simultaneously at the initiation of the cut.

Turning was performed in dry and wet conditions. The



coolant used was a general purpose mineral soluble oil hysol G, manufactured by Castrol with a concentration of 4%. The flow rate of the coolant was 3.75 lit/min.

### 3.3 Cutting Conditions

Single point turning tests were carried out at cutting speeds of 90, 150, 215 and 300 m/min with feed rates of 0.125 and 0.18 mm/rev and depths of cut of 1 and 2.5 mm.

After establishing the limiting wear factors, tests in various atmospheres were carried out in order to study the influence of Oxygen, Nitrogen and Argon on tool wear rates.

### 3.4 Work Materials

The nickel-base superalloys WASPALOY, INCO 901 and INCO 718 were used. The microstructures of these alloys are shown in figures 15, 16 and 17 respectively. The chemical compositions of these materials are given in table 7. This table also shows the hardness values which are measured by using a Vickers hardness machine under 30 Kg load.

The INCO 901 and INCO 718 materials were supplied in a bar form. WASPALOY was supplied in the form of a forged disc (figure 20). The materials were in the solution treated and aged condition.

### 3.5 Tool Materials and Geometries

Four different grades of ceramic indexable inserts of ISO designation SNGN 120416 having cutting edges with a chamfer of 0.20 mm x 20° were used. These inserts were 12.7 mm square, 4 mm thick with a nose radius of 1.6 mm supplied by different manufacturers (table below).

<u>grade</u>	<u>material</u>	<u>manufacturer</u>
CC620	$\text{Al}_2\text{O}_3+4\%\text{ZrO}_2$	Sandvik Coromant
CC650	$\text{Al}_2\text{O}_3+30\%\text{Ti(C,N)}$	Sandvik Coromant
Kyon 2000	$\text{Si}_3\text{N}_4+\text{Y}_2\text{O}_3$	Kennametal
WG-300	$\text{Al}_2\text{O}_3+<50\%\text{SiC}_w$	Greenleaf

For general machining tests these inserts were used in their as-received condition after inspection to ensure they were undamaged. Some properties of these inserts are presented in table 5.

For turning operations the inserts were mechanically clamped in a tool-holder to provide the following geometries:

Approach angle .....  $45^\circ$   
 Side rake angle .....  $-6^\circ$   
 Back rake angle .....  $0^\circ$   
 Clearance angle .....  $6^\circ$

### 3.6 Tool Life Criteria

The following tool life criteria were used:

1. The average flank wear land reaches 0.40 mm
2. The maximum flank wear land reaches 0.70 mm
3. The notch at the depth of cut or tool nose reaches 1 mm
4. The crater depth reaches 0.14 mm

5. The surface finish on the work material exceeds 5.00 micron (centre line average Ra)
6. Chipping (flaking) or premature failure occurs.

Prior to the machining operation the inserts were examined under the travelling microscope at x10 magnification to detect existence of any defects, such as, cracks, chipping, etc. The inserts were checked for the above mentioned criteria at predetermined intervals. Cutting was stopped and the tool discarded as and when premature failure or catastrophic fracture occurred.

### 3.7 Examination and Measurement of Worn Area

At the end of each predetermined machining time, the insert was removed for measurement and recording of the failure modes and wear rates. The average flank wear (AFW), maximum flank wear (MFW) and notch depth at both the nose and at the end of depth of cut were measured, using the travelling optical microscope.

### 3.8 Measurement of Surface Finish

A SURTRONIC 3 was used to measure the average surface roughness value (Ra). To achieve the maximum accuracy the instrument was calibrated prior to each measurement. Subsequently the moving stylus was positioned on the surface to be measured. Movement of the stylus was perpendicular to the feed marks. Each surface was measured three times and then the average value was calculated for further analysis. The mobility of this instrument eliminates the need for dismantling the work piece from the chuck of the lathe.

### 3.9 Measurement of Cutting Forces

A KISTLER piezo electric dynamometer was used to record the forces produced during machining. Design of this apparatus allows the three component forces in the directions of X, Y and Z to be measured. However, for the purpose of this work only the feed force and the cutting force were measured. A charge amplifier was connected between the dynamometer and a chart recorder enabling the signals to be recorded. The equipment was calibrated with the help of static loads before use.

### 3.10 Quick Stop Technique

The quick stop technique was used to investigate the chip formation. In order to accomplish this it is important to withdraw the cutting insert at very high speed while the turning operation is in progress. To achieve this action the quick stop device was used (figure 21). This device consists of a humane killer gun positioned above the tool holder which was supported by a notched shear pin. The gun consisted of a solid captive bolt which was projected at high speed when the gun was fired. The captive bolt struck against the tool holder, breaking the shear pin and the tool was accelerated very quickly away from the cutting position. Ample clearance was provided by the tool holder to avoid any contact between the work material and the insert. This process left a fragment of the chip attached to the work material. These fragments were later sawn off with a hacksaw and prepared for further analysis.

Many attempts were required to get a chip attached to the bar. Only after prolonged attempts at relatively slow speeds were satisfactory results were obtained.

### 3.11 Preparation of Specimens

Three groups of specimens were prepared for analysis, namely the work materials, the quick stop samples and the cutting tool inserts.

Small pieces of samples were taken from WASPALOY, INCO 901 and INCO 718 with a hacksaw. The samples were later mounted in a mould using a hand mounting press. The specimens were then ground using 200, 400, 600 and 1200 silicon grit sizes with water as lubricant. These samples were next polished to 6, 1 and 1/4 micron finish with diamond paste. The polished specimens were subsequently etched for 5 to 30 seconds with Glyceregia solution {1 part nitric acid ( $\text{HNO}_3$ ), 3 parts hydrochloric acid ( $\text{HCl}$ ), and 2 parts glycerol}. The etched specimens were examined under the microscope and photographs at various magnifications were taken.

The quick stop samples were mounted in epoxy resin. The top surface of the specimens was ground to a position half way along the depth of cut using silicon carbide paper of up to 1200 grit size. Subsequently the specimens were polished to a 1/4 micron finish. During the polishing process the samples were continuously measured by using a vernier to insure an accurate result. The samples were examined under the microscope and photographs at various magnifications were taken.

Specimens of the cutting inserts were prepared in two different ways. The first method was to examine the inserts in the SEM. The samples were initially ultrasonically cleaned in acetone and then mounted onto stubs by means of silver paint or an adhesive. The areas of no interest were coated with carbon paint to prevent charging and so produce better images of the worn areas. After drying the specimens were gold coated and then mounted in the SEM. The images were photographed at different magnifications.

Specimens used to study the wear mechanisms were prepared by mounting them in phenolic resin. Initially the specimens were ground with diamond impregnated discs followed by silicon carbide papers. In both cases water was used as lubricant. By using a micrometer care was taken not to exceed the targeted area. The polishing was carried out using a pad impregnated with diamond pastes of down to 1/4 micron finish using a lubricating liquid. The polished samples were then examined under the microscope and photographs at different magnifications were taken. Subsequently the specimens were prepared and studied in the SEM and images at high magnifications were taken.

## CHAPTER 4

# EXPERIMENTAL RESULTS

### 4.1 Introduction

Three different nickel-based superalloys, WASPALOY, INCO 901, and INCO 718 which were in the solution treated and aged condition were used. The ceramic cutting tool inserts employed for the turning operations were pure alumina (CC620), mixed ceramic (CC650), sialon (KYON 2000), and silicon carbide whisker reinforced ceramic (WG300). The microstructures of the cutting inserts are shown in figures 22, 23, 24 and 25 respectively. Figure 26 shows the fractured surface of a WG-300 tool.

### 4.2 MACHINING OF WASPALOY

#### 4.2.1 Machining of WASPALOY with CC620 ceramic inserts

Table 8 summarises the cutting conditions and the tool lives obtained for each individual test. Figures 27 and 28 present diagrammatically these results for depths of cut of 1 mm and 2.5 mm respectively and figures 27a and 28a the corresponding total volume of material removed. Only very short tool lives, as short as 20 seconds, were achieved throughout the machining test. In the majority of cases tool life has been limited by the depth of cut notching (DOCN) and occasionally by average flank wear, chipping and surface roughness. As shown in figure 29, notch at the DOC can

develop rapidly with practically no flank wear. Sudden failure of the cutting inserts - during some of the tests - has occurred, particularly at high cutting speeds and high depth of cut.

At a constant depth of cut of 1 mm and a constant feed rate of 0.18 mm/rev the notching seemed to be more severe at the higher cutting speeds when a coolant was present (figure 27). The trend in notch wear was changed when no coolant was used. The rate of wear started to decrease as the cutting speed increased and longer tool life was recorded at the speed of 215 m/min. As the speed increased to 300 m/min notch wear reduced the tool life to about 35 seconds. Reduction of the feed rate from 0.18 mm/rev to 0.125 mm/rev, in the presence of coolant, did not change the tool lives markedly. The only significant difference was in machining at a speed of 150 m/min. In this case the tool life increased from 0.7 minutes to 1.30 minutes. Repeating the same cutting conditions but without coolant, produced noticeably longer tool lives at higher cutting speeds. At the cutting speed of 215 and 300 m/min the tool lives were increased from 0.65 to 1.65 minutes and from 0.75 to 2 minutes respectively.

At the constant feed rate of 0.18 mm/rev and depth of cut of 2.5 mm (figure 28), notching was much more pronounced at the lower cutting speeds. The rate of DOC notching decreased as the cutting speed increased. The longest tool life was achieved at a speed of 300 m/min. Figures 30 to 32 show the formation of the microcracks running in different



to the cutting edge, when machining was performed in dry and wet conditions.

The bar-chart in figure 28 shows that machining under the same cutting conditions a slightly longer tool life was produced without coolants. Under this condition an increase in the cutting speed has promoted chipping.

Machining at a constant feed rate of 0.125 mm/rev (depth of cut of 2.5 mm) in the presence of coolant, produced moderate tool lives at speeds up to 215 m/min. At a speed of 300 m/min the tool life increased to about 1.3 minutes. Under dry condition, at a speed of 90 m/min, only a very short tool life was obtained and notching caused tool rejection. However, as the cutting speed increased longer tool lives were produced (figure 28). At a speed of 150 m/min the cutting insert was discarded due to excessive surface roughness. When machining under these conditions flank wear also prevailed (figure 33). Chipping (flaking) was the cause of rejecting the CC620 inserts at the higher speeds.

#### 4.2.2 Machining of WASPALOY with CC650 ceramic inserts

WASPALOY was machined at various cutting conditions and a summary of the results and tool lives obtained for each individual test is shown in table 9. Figures 34 and 35 show the performance and tool lives of the cutting inserts at constant depth of cuts of 1 mm and 2.5 mm respectively (figures 34a and 35a the correspondent total volume of metal removed). These figures clearly show that in the majority of

tests carried out the DOC notching has been a life limiting factor and the cause of discarding tools.

At a constant depth of cut of 1 mm the longest tool life achieved was at the lowest cutting speed with a feed rate of 0.18 mm/rev, in the presence of coolant (figure 34). As the speed increased the rate of notch wear accelerated. At the speed of 300 m/min, the notch value of 1.96 mm was recorded after 1 min of turning (figure 36). Machining under similar conditions but in the absence of coolant resulted in longer tool lives, in particular at the lowest speeds. Under these cutting conditions the insert was rejected due to excessive notching at the nose (figure 37). Increase in speed accelerated the end of DOC notch and subsequently resulted in shorter tool lives. Machining at a speed of 300 m/min produced notching both at the end of the DOC and at the nose of the insert (figure 38). Severe wear on the nose has been the cause of tool failure (figure 39).

Lowering the feed rate from 0.18 mm/rev to 0.125 mm/rev in the presence of coolant, reduced the tool lives slightly. The longest tool life was recorded at the lowest cutting speed and at the higher speeds notch wear was noticeably accelerated resulting in lower tool lives (figure 34).

Machining at a constant depth of 1 mm and a feed rate of 0.125 mm/rev in dry conditions produced somewhat different results than machining in wet conditions. In these series of tests the tool materials exhibited a high tendency to notching at low to moderate cutting speeds. Figure 40 shows the severe notching both at the nose and at the end of

DOC at the speed of 150 m/min. As the cutting speeds were increased to 215 and 300 m/min the inserts showed more resistance to notch wear. This can clearly be observed at the highest cutting speed when severe flank wear (figures 41 & 43) caused the insert to be rejected after 2 minutes of turning (figure 34).

Machining at a constant depth of cut of 2.5 mm resulted in slight variations in tool lives compared to depth of cut of 1 mm. At the higher feed rate the longest tool life was achieved at the lowest speed in the presence of coolant. The tool life decreased with increased cutting speed leaving end of DOC notch to be the life limiting factor (figure 35). Repeating the same tests in dry conditions resulted in tool life reduction. At the lowest speed the cutting insert was used for just over 1 minute and had to be discarded because of the high value of surface roughness. As the speed increased to 150 m/min end of DOC notching became the life limiting factor and became more pronounced with higher speeds. At the cutting speed of 300 m/min chipping of the insert restricted the test to 10 seconds.

End of DOCN dominated the tool lives again as the feed rate was lowered to 0.125 mm/rev and coolant was applied. However, notching was more pronounced on increasing the cutting speed from 90 to 150 m/min but fell as the speed was further increased to 215 and 300 m/min. When the coolant was cut off the shortest tool life was achieved at the lowest speed. Improvement was made in the tool life as the speed increased to 150 m/min but further increase in the cutting

speed accelerated the notching and shortened the tool life. At the highest cutting speed the operation was stopped due to higher power drawn from the lathe than the manufacturers recommendation. However, at this stage the cutting tool had not yet reached the rejection criteria.

#### 4.2.3 Machining of WASPALOY with KYON 2000 ceramic inserts

Table 10 shows the cutting conditions and the tool lives obtained for each individual test. Figures 44 and 45 represent these results diagrammatically and the cause of rejection of the Sialon cutting tool inserts when cutting WASPALOY at the constant depth of cuts of 1 mm and 2.5 mm respectively. The total volume of metal removed under these conditions is also shown in figures 44a and 45a.

Machining at the constant depth of cut of 1 mm has produced rather uniform results in comparison with the previous tests. The longest tool life has been achieved at the lowest cutting speed and by increasing the cutting speed the tool life has been reduced. At the lowest cutting speed the insert was rejected due to excessive notching after 4 minutes of machining when the feed rate was 0.18 mm/rev in the presence of coolant. Increase in cutting speed accelerated the DOCN resulting a shorter tool life. Severe end of DOC notching and also excessive flank wear were the causes of discarding the cutting tool insert at the highest cutting speed (figure 46). This accelerated wear together with previous results are shown in figure 47.

Machining under the same conditions but in the absence of coolant has followed the same tool life trend. Notching

has dominated the tool life throughout the test. Figure 48 shows the intensity of the notch wear at the lowest cutting speed. Machining under these conditions resulted the maximum tool life. Figure 49a shows the sectioned tool at the end of DOC notch when machining was carried out at the speed of 300 m/min. The enlarged views of this figure are presented in figures 49b and 49c showing the work material adhered to the flank of the sectioned insert.

Figure 44 shows that the longest tool life has been achieved when machining at the lowest speed with 1 mm depth of cut and a feed rate of 0.125 mm/rev in the presence of coolant. In this particular test the insert withstood 8 minutes of machining and eventually failed due to excessive DOC notching, figure 50. It is interesting to note the sudden increase of the notch wear (figure 51). Further increase in the cutting speed shortened the tool life. End of DOC notching is still present but has not been as extensive as maximum flank wear which has been the deciding factor for rejection of the cutting insert (figure 52). Further increase in the cutting speed to 215 m/min promoted the notch wear which was the life limiting factor. The flank wear formation (figure 53), under these cutting conditions shows how particles have been plucked out of the parent material with cracks running along the cutting edge. Further increase in the cutting speed to 300 m/min resulted in chipping on the rake face of the cutting tool which terminated its useful life.

Accelerated notching and subsequently shorter tool

lives were obtained when machining in dry conditions was carried out. Further increase in the cutting speed increased the rate of wear.

Figure 45 shows the results of machining at the constant depth of cut of 2.5 mm. At the lowest cutting speed the cutting insert was rejected after 2 minutes of machining due to end of DOC notching when the coolant was present. Figures 54 and 55 show the magnified views of DOC notch and the flank wear which has taken place under these machining conditions.

By increasing the speed to 150 m/min the insert survived machining for 5 minutes. Maximum flank wear and end of DOC notching have been partially responsible for discarding the insert (figure 56). Figure 57 shows the progression of the wear rate as the cutting time increases. Apart from the flank wear and notching, occurrence of the chipping on the rake face of the inserts has been unavoidable. This mechanism has shown itself very vigorously in the higher speeds (figure 45).

Repeating the tests under the same conditions but in the absence of coolant have produced slightly longer tool life at the lowest speed but the DOC notching was again the predominant factor in the tool life. At a speed of 150 m/min accelerated notch wear resulted in shorter tool lives (figure 58). Further increase in the cutting speed produces a large DOC notch (figure 59). However, the presence of the flank wear became more significant. Eventually flank wear became the life limiting factor at a speed of 300 m/min (fig

60).

Further tests were carried out at a constant depth of cut of 2.5 mm, with 0.125 mm/rev feed rate and flood coolant. Maximum tool life was achieved at the lowest cutting speed but subsequently the tool had to be rejected due to DOC notching. As the cutting speed increased the tool life decreased leaving notching as the life limiting factor at a speed of 150 m/min. At the higher cutting speeds occurrence of chipping on the rake face resulted in discarding the cutting tools.

Lower tool life was achieved at a speed of 90 m/min when the test was performed in dry conditions. After 3 min of machining the operation had to be stopped and the cutting insert was rejected due to severe notching. A further test at 150 m/min accelerated the notching which subsequently lowered the tool life (figure 45). The extent of flank wear increased and became the life limiting factor as the speed increased to 215 m/min. Chipping on the rake face of the cutting insert was apparent after 40 seconds of machining which led to rejection of the insert.

#### 4.2.4 Machining of Waspaloy with WG300 ceramic inserts

Table 11 summarises the cutting conditions and the tool lives achieved for each individual test. Figures 61 and 62 show diagrammatically these results when machining Waspaloy with WG300 cutting inserts at constant depths of cut of 1 and 2.5 mm respectively. The respective total volume of metal removed under the stated conditions is also shown in

figures 61a and 62a.

At the constant depth of cut of 1 mm flank wear as well as DOC notch have been the tool life limiting factors. Maximum tool life has been achieved at the lowest cutting speed at the feed rate of 0.18 mm/rev in the presence of coolant. The generated end of DOC notching and flank wear are shown in figure 63 but the former has not exceeded the criteria used for tool life. The enlarged view of the DOC notch and flank wear are shown in figures 64 and 65 respectively.

By increasing the cutting speed the tool life dropped sharply. At the speed of 150 m/min end of DOC notching became the life limiting factor but still the presence of the flank wear was apparent (figure 66). An enlarged view of the flank wear is shown in figure 67.

Increasing the speed to 215 m/min accelerated the end of DOC notching (figure 68) resulting in less than one minute of tool life (figure 61). Figures 69 to 70 are the views of the extent of the wear on the flank face of the cutting tool. Figure 71 is the magnified view of the latter figure showing the removed particles.

At a speed of 300 m/min both end of DOC notching and flank wear have been tool life limiting factors under the stated machining conditions (figure 72). Figure 73 shows the severity of the wear on the flank face of the WG300 insert. The magnified view of the notch wear is shown in figure 74.

At a cutting speed of 90 m/min notching was the life limiting factor after 4 minutes of machining in dry



conditions with a feed rate of 0.18 mm/rev and a constant depth of cut of 1 mm (figure 75). As the cutting speed increased to 150, 215 and 300 m/min the values of the flank wear accelerated (figure 76) and subsequently limited the tool lives in conjunction with notching. Figures 77a, b & c show the chips produced under the quick stop condition, when machining was performed at the speed of 150 m/min. These figures show the underneath, side and top of the chips respectively. The section through the quick-stop test is shown in figure 77d.

Machining performed in the presence of a coolant with a feed rate of 0.125 mm/rev resulted in a DOC notch after 2 minutes (figure 78). Figure 79 is the enlarged view of this area. As the speed increased to 150 m/min flank wear became the life limiting factor. The enlarged view of the flank wear (figure 80) shows cracks in the background running perpendicular to the cutting edge. Further increase in cutting speed accelerated the flank wear (figure 81) resulting in shorter tool lives (figure 61).

End of DOC notching dominated the tool lives throughout the tests when machining was carried out in dry conditions employing a constant depth of cut of 1 mm and a feed rate of 0.125 mm/rev (figure 82). Figure 83 shows the formation of the notching at the depth of cut after 2 minutes of machining. At a speed of 150 m/min flank wear became more apparent (figure 84) but this was not large enough to limit the life of the cutting insert. The rate of formation of the notch was accelerated even more as the speed was increased

to 215 and 300 m/min (figure 61).

Wet machining at a constant depth of cut of 2.5 mm and a feed rate of 0.18 mm/rev was performed. As in the previous tests flank wear restricted the life of the WG300 cutting inserts (figure 85). Maximum tool life was achieved at a speed of 90 m/min (figure 62). By increasing the speed the flank wear accelerated and reduced the tool life. Figure 86 shows the generated DOC notching - at the end of 3 minutes of machining - which is almost the same depth as the flank wear. Figure 87 shows a crack running parallel to the cutting edge. Tool lives reduced as the cutting speeds were increased to 215 and 300 m/min causing the flank wear to develop more rapidly (figure 85).

Notching at the nose dominated the tool life at the cutting speed of 90 m/min when machining was performed in dry condition. Flank wear and DOC notching were accelerated as the cutting speed was increased to 150 m/min. Figure 88 is the magnified view of the DOC notch area emphasising a crack running perpendicular to the cutting edge. As the cutting speeds were increased to 215 and 300 m/min formation of flank wear became more prominent (figures 89 & 90), and therefore reduction in tool life.

At a speed of 90 m/min flank wear still dominated the tool life when machining was performed at the lower feed rate of 0.125 mm/rev in the presence of coolant. Increase in the cutting speed showed DOC notching to develop more rapidly and exceeded the criteria after 2 minutes at speed of 150 m/min, and 1 minute at speed of 215 m/min. At the

highest cutting speed the operation had to be abandoned after 42 seconds of machining due to chipping on the insert.

DOC notching (figure 91) and flank wear (figure 92) dominated the tool lives, when machining was carried out in dry conditions. The maximum tool life was achieved at the lowest cutting speed. The recorded notch depth at this speed was 1.93 mm. By increasing the speed the notch wear accelerated (figure 93) and resulted in discarding the cutting insert after 2 minutes of machining (figure 62). DOC notching of 2 mm (figures 94 & 95) was recorded after 3 minutes of machining at the speed 215 m/min. Figure 96 shows that both notching and flank wear were generated after 2 minutes of machining at the speed of 300 m/min. Figure 97 is the magnified view of the severe flank wear.

#### 4.3 Machining of INCO 901

##### 4.3.1 Machining of INCO 901 with CC650 Ceramic inserts

Table 12 summarises the cutting conditions and the tool lives obtained for each test. Figures 98 and 99 show diagrammatically the results obtained for a depth of cut of 1 mm and 2.5 mm respectively. Total volume of metal removed under these conditions is shown in figures 98a and 99a.

At a constant depth of cut of 1 mm end of DOC notching has almost dominated the tool life throughout the machining. Turning at a feed rate of 0.18 mm/rev in the presence of coolant generated severe DOC notching after 3 minutes of machining when the lowest cutting speed was applied. The notch wear increased when the cutting speed was increased to 150 m/min (figure 100). As the cutting speed increased to

215 and 300 m/min flank wear prevailed and was the tool life deciding factor (figure 101).

End of DOC notching was more apparent when machining was carried out in dry conditions and the tool life was generally lower than when the test was carried out in presence of coolant. Machining at the lowest speed generated the shortest tool life. As the speed was increased to 150 and 215 m/min the tool life was increased. At the speed of 300 m/min however, the life was reduced (figure 98).

DOC notching dominated the tool lives throughout the machining in both dry and wet conditions at the lower feed rate of 0.125 mm/rev (figures 102 & 103). Machining in the presence of coolants showed longer tool lives than in dry cutting. However, the performance was opposite when higher cutting speeds were applied (figure 98).

Figure 99 shows the tool lives achieved when machining was performed at a constant depth of cut of 2.5 mm. When cutting at a constant feed rate of 0.18 mm/rev in the presence of coolants, DOC notch dominated the tool lives throughout machining. Dry machining, however, improved the tool lives when moderate to high cutting speeds were applied.

Occurrence of catastrophic failures and chipping of the cutting inserts were prominent when wet machining was carried out at a lower feed rate of 0.125 mm/rev. at the cutting speeds of 150 m/min and higher. Performance of the same tests in dry conditions eliminated the chipping and allowed the cutting inserts to exhibit longer tool lives

(figure 99).

#### 4.3.2 Machining of INCO 901 with KYON 2000 Ceramic Insert

Table 13 summarises the cutting conditions and the tool lives obtained for each individual test. Figures 104 and 105 show the machining performance at a constant depth of cut of 1 mm and 2.5 mm. The calculated total volume of metal removed under these conditions is shown in figures 104a and 105a.

Longest tool life was achieved at a speed of 90 m/min when wet machining at a constant depth of cut of 1 mm and a feed rate of 0.18 mm/rev. DOC notching which dominated the tool life at this speed accelerated rapidly and subsequently resulted in shorter tool life at the speeds of 150 and 215 m/min. At the highest cutting speed flank wear started to prevail and exceeded the criteria. Machining in dry conditions accelerated the formation of the flank wear. This wear pattern however, started slowly at the lowest cutting speed and had a higher rate of growth with increased speed (figure 106) and hence reduced tool life. The same pattern of tool life was achieved when machining was performed at a feed rate of 0.125 mm/rev in the presence of flood coolant. When machining was performed in dry conditions nose notch dominated the tool life at a speed of 90 m/min. An increase in the cutting speed resulted in a longer tool life, and flank wear accelerated rapidly dominating the tool life as the speed was increased to 215 and 300 m/min.

When wet machining at a higher depth of cut of 2.5 mm and at a feed rate of 0.18 mm/rev the longest tool life was achieved at the lowest cutting speed (figure 105). As the speed increased tool life decreased leaving notching and flank wear as the life limiting factors at speeds of 150 m/min and higher. Machining in dry conditions accelerated the wear on the tool throughout the cutting speed range and forced the cutting insert to be discarded after 1 minute of machining under all conditions. Figure 107 shows the formation of a crack after only 10 seconds of machining at a speed of 150 m/min. The generated crack at a speed of 300 m/min is shown in figure 108. Relative cutting forces under these cutting conditions are shown in figures 109. Figures 110a and 110b show samples of the chips obtained under the stated machining condition at the speeds of 150 m/min and 300 m/min respectively. Wet machining at a lower feed rate of 0.125 mm/rev improved the tool life only at the lowest cutting speed. Notching was the dominant factor under these conditions. As the speed increased notching increased and exceeded the failure criteria after 1 minute of machining. Very little improvement was made when machining was performed in dry conditions. A tool life up to 2 minutes was recorded at the speeds of 90 and 150 m/min. DOC notching was the tool life limiting factor at these speeds but flank wear formed at a higher rate at the higher speed. Figure 111 shows the wear pattern and a crack running along the cutting edge after only 10 seconds of machining at a speed of 150 m/min.

#### 4.3.3 Machining of INCO 901 with WG-300 Ceramic Inserts

INCO 901 work material was machined with a WG-300 tool. Table 14 summarises these results. Figures 112 and 113 present diagrammatically these results for a depth of cut of 1 mm and 2.5 mm respectively. Figures 112a and 113a represent the total volume of material removed under these conditions.

When machining was performed at a constant depth of cut of 1 mm unpredictability of the tool life was apparent.

The longest tool life was achieved at the lowest cutting speed when wet machining was performed at a feed rate of 0.18 mm/rev. Notching dominated the tool life at the speed of 90 and 150 m/min but flank wear was more domineering at the higher cutting speeds. Dry machining however, did not improve the tool life. At a speed of 90 m/min flank wear dominated the tool life and its presence was apparent at higher speeds (figures 114 & 115). As the cutting speed increased to 150 m/min and higher, more chipping on the rake face occurred and caused the tool to be discarded. Figure 116 show the quick stop tests carried out at a speed of 150 m/min. Figure 117 shows the formation of the side flow on the edge of the work material at this speed.

Machining at a lower feed rate of 0.125 mm/rev did not improve the tool lives. Cutting tools were capable of machining for maximum of 2 minutes in wet conditions and 1 minute in dry conditions. Notching, flank wear and chipping were the life limiting factors. A sectioned quick stop test

when machining wet at a speed of 90 m/min is shown in figure 118. Figure 119 shows the formation of a crack on the flank face when dry machining was performed at the 300 m/min.

Machining at a constant depth of cut of 2.5 mm produced a more predictable tool life. When chipping on the rake face did not occur flank wear dominated the tool life. Figure 113 shows that maximum tool life was achieved when wet machining at a feed rate of 0.18 mm/rev and a speed of 90 m/min. As the speed was increased the flank wear rate accelerated reducing tool lives. Figures 120, 121a and 121b show the intensity of the flank wear when machining was carried out under dry conditions. Chips generated at speeds of 150 and 300 m/min are shown in figures 122a and 122b respectively.

Figure 123 shows the formation of flank wear at various cutting speeds when wet machining at a lower feed rate of 0.125 mm/rev. Figure 124 shows the formation of the notch and the flank wear at the speed of 300 m/min. Figure 125 shows the cutting forces produced when dry machining was performed at a constant depth of cut of 2.5 mm at different speeds and feeds.

#### **4.3.4 Comparative Test**

##### **4.3.4.1 Machining with Round WG-300 Insert**

A round WG-300 insert was used to machine INCO 901 to evaluate the influence of the tool geometry. Machining was carried out in both wet and dry conditions at a constant speed of 215 m/min, feed rate of 0.125 mm/rev and depth of cut of 1 mm.



Excessive notching and flank wear forced the round WG-300 insert to be rejected after 5 minutes of machining in the presence of flood coolant. Compared to previous tests, a significant difference in tool life was recorded when a square insert was used to machine under the same cutting conditions (figure 126).

DOC notching and flank wear were more pronounced when machining was performed in dry conditions. The intensity of the wear and the subsequent generated poor surface finish reduced the tool life to 1.5 minute. This, however, is still higher than similar test carried out with square inserts.

#### 4.4 Machining of INCO 718

Due to restricted availability of the work material only limited tests were carried out.

##### 4.4.1 Machining of INCO 718 with KYON 2000 ceramic inserts

Table 15 summarises the cutting conditions and the tool lives obtained for each individual test. Figures 127 and 128 show diagrammatically these results for a constant depth of cut of 1 mm and 2.5 mm respectively. The total volume of material removed under these conditions is shown in figures 127a and 128a.

Machining at the lower feed rate of 0.125 mm/rev has produced the longest tool lives. An increase in the cutting speed accelerated the wear rate resulting in a shorter tool life. Chipping occurred when machining was performed at a speed of 215 m/min and higher when both feed rates were applied (figure 127). Severe wear on the flank face of the

insert was generated when machining was carried out at a speed of 90 m/min and a feed rate of 0.18 mm/rev. Machining under these conditions generated poor surface finish and occasionally severe pick-up was observed.

The wear rate accelerated as machining was performed at a constant depth of cut of 2.5 mm and chipping occurred more frequently (figure 128). Figure 129 shows the DOC notching when machining was performed at the lowest cutting speed with a feed rate of 0.125 mm/rev.

#### 4.4.2 Machining of INCO 718 with WG-300 ceramic inserts

Table 16 summarises the cutting conditions and the tool lives obtained for each test. Machining performance at a constant feed rate of 0.18 mm/rev in the presence of flood coolants is shown in figure 130. The respective total volume of metal removed is exhibited in figure 130a. DOC notching has dominated the tool life at all cutting speeds when machining was performed at a constant depth of cut of 1 mm. Longer tool lives were experienced when the depth of cut was increased to 2.5 mm. Generated forces under these conditions are shown in figure 131. Flank wear was the life limiting factor under the stated machining conditions at a speed of 150 m/min (figure 132). Notching became more apparent at speeds of 215 and 300 m/min.

Figure 133 shows the tool life of a WG-300 insert when machining took place at different speeds and at a constant depth of cut of 2.5 mm and a feed rate of 0.18 mm/rev. The total volume of metal removed under these conditions is shown in figure 133a.

Machining in dry conditions produced the longest tool life at a speed of 150 m/min. Notching was the life limiting factor and it accelerated with increase in speed. Further increases in speed promoted flank wear, exceeding the criteria after 1 minute of machining. Higher tool lives, particularly at the highest speed were achieved when wet machining was carried out under similar cutting conditions. Figures 134 to 136 show the progress of the average and maximum flank wear and notching respectively. Gradual deterioration of the machined surface is shown in figure 137.

Figure 138 shows the quick stop sample when machining was performed at a speed of 90 m/min, 0.18 mm/rev feed and a constant depth of cut of 2.5 mm.

#### **4.4.3 Comparative tests**

##### **4.4.3.1 Machining with round ceramic insert**

A round insert was used to machine INCO 718 to compare the results with square insert (figure 139). Machining was performed in dry and wet conditions at a constant speed of 215 m/min, feed rate of 0.125 mm/rev and 1 mm depth of cut. A significant tool life was achieved when a round WG-300 cutting tool was used to machine the work material in the presence of coolant. Machining in dry conditions did not, however, exhibit a longer life than the square tool.

##### **4.4.3.2 Machining with rhomboid ceramic inserts**

###### **a. Influence of different angles:**

Rhomboid WG-300 cutting inserts with  $80^{\circ}$  and  $35^{\circ}$  angles

were used to machine INCO 718. Machining was carried out at the speed of 215 m/min at a constant depth of cut of 1 mm and 0.125 mm/rev feed rate. Longer tool life was achieved when 80° rhomboid cutting tool was used, with DOC notching being the life limiting factor in both cases. Subsequently these results were compared with the results obtained from two other WG-300 tools having different geometries and were tested under identical machining conditions (figure 140). This figure shows that longest tool life was obtained by using round inserts followed by square inserts and finally rhomboids.

b. Influence of workpiece chamfer on the tool life:

In-order to determine the influence of the sharp edge and chamfer on tool life two separate tests were carried out. Initially the test was carried out on chamfered work material. Figure 141 shows that a longer tool life was achieved under this condition than the test carried out on not chamfered material. End of DOC notching has been the life limiting factor in both cases.

**4.4.3.3 Machining in the presence of different gases**

Inco 718 was machined in the presence of four different gases. Four minutes cutting was performed at the speed of 215 m/min, depth of cut of 2.5 mm and 0.18 mm/rev feed. Gases used for the test were Nitrogen, Oxygen, Argon and the results were compared with the test carried out in atmosphere (i.e. dry machining). The summary of the results is shown in figure 142. This figure shows that machining in

the presence of Argon-rich atmosphere has accelerated the rate of notch formation. Notching was generated at slower rates when machining took place in the presence of Nitrogen, Air and Oxygen gases respectively.

Figure 143 shows the actual tool life of the WG-300 insert when machining in the presence of different gases. Machining in the presence of Oxygen has produced the longest tool life. However, the cutting insert did not reach the notch wear criteria under these cutting conditions and further machining could have taken place (figure 142).

Figure 144 shows the wear rate of end of DOC notching when machining took place in dry conditions and also in the presence of Oxygen. Machining was performed at the speed of 150 m/min, 2.5 mm depth of cut and 0.18 mm/rev feed rate. The graph shows that the presence of Oxygen provided a favourable condition to retard the notch wear which previously has been aggressive when machining was performed in dry conditions (i.e. in the presence of air). The notch generated after 10 seconds of machining in the presence of Nitrogen, Argon, Air and Oxygen is shown in figures 145 to 148 respectively.

#### 4.5 Statistical Analysis

The results of the tool life trials show that the performance of all of the alloys tested was subject to considerable variation. Typically, the standard deviation on tool life was of the order of 0.7 (minutes) which implies that each result was subject to an uncertainty of +/- 1.5 to +/- 2.0. This is very high given that the mean tool lives

obtained are of the order of 1 to 2 minutes.

Such a degree of uncertainty means that identifying the most effective variables influencing tool life can only be achieved by statistical techniques. Therefore various combinations of tool material and work-piece material were studied under a variety of cutting conditions, the method of analysis used was multiple regression.

To use this method each individual parameter was treated as a variable and these were:

- C1 = Depth of cut (mm)
- C2 = Feed rate (mm/rev)
- C3 = Coolant used (Yes=1, No=0)
- C4 = Speed (m/min)
- C5 = Tool life (min)

The following is an example of input data which are extracted from table 8 to derive a tool life equation when machining Waspaloy with CC620 tools;

<u>DOC</u>	<u>FEED</u>	<u>COOLANT</u>	<u>SPEED</u>	<u>TOOL LIFE</u>
1	0.18	1	90	0.90
1	0.18	1	150	0.70
1	0.18	1	215	0.35
1	0.18	1	300	0.85
.	.	.	.	.
.	.	.	.	.
.	.	.	.	.
2.5	0.125	0	90	0.45
2.5	0.125	0	150	1.05
2.5	0.125	0	215	1.80
2.5	0.125	0	300	1.00

Derived regression equation from these results is:

$$C5 = 1.29 - 0.0396 C1 - 3.69 C2 - 0.259 C3 + 0.00202 C4$$

predictor	coef.	stdev	t-ratio	p	p-1
constant	1.2889	0.4062	3.17	0.004	0.996
C1	-0.03958	0.08160	-0.49	0.632	0.368
C2	-3.693	2.225	-1.66	0.109	0.891
C3	-0.2594	0.1224	-2.12	0.043	0.957
C4	0.0020191	0.0007849	2.59	0.016	0.984

From the calculations;

Standard deviation = 0.3462 and Mean square = 0.1198

It should be remembered that p-1 is the confidence limit and only values above 95% (i.e. 0.95) are regarded as significant. Therefore according to the selected confidence limit, under these machining conditions, C3 and C4 (i.e. coolant and speed) are the most influential variables.

Following are the calculations showing the derived equations by using the relative data (obtained from the tool lives in tables 9-15) under different machining conditions.

#### Machining of Waspaloy with CC650 tools

The obtained regression equation is:

$$C5 = 0.872 - 0.066C1 + 4.45C2 - 0.22C3 + 0.00197C4$$

from the calculation;

Standard deviation = 0.6269 & Mean square = 0.3930  
and the confidence limit (p-1) for the following parameters are:

$$C1 = 0.34, \quad C2 = 0.721, \quad C3 = 0.67 \quad \text{and} \quad C4 = 0.84$$

Therefore No Significant variables are identified.

#### Machining of Waspaloy with Kyon 2000 tools

The obtained regression equation is:

$$C5 = 5.76 - 0.467C1 - 4.33C2 + 0.881C3 - 0.0128C4$$

From the calculations:

standard deviation = 1.195 & Mean square = 1.428

and the confidence limit (p-1) for the following parameters are:

$C1 = 0.891$ ,  $C2 = 0.422$ ,  $C3 = 0.953$  and  $C4 = 0.9996$

Therefore  $C3$  and  $C4$  are the most influential variables.

#### Machining of Waspaloy with WG-300

The regression equation is;

$C5 = 1.86 + 0.117C1 + 8.99C2 + 0.056C3 - 0.00766C4$

From the calculations;

Standard deviation = 0.7753 & Mean square = 0.6011

and the confidence limits are:

$C1 = 0.374$ ,  $C2 = 0.898$ ,  $C3 = 0.169$  and  $C4 = 0.999$

Therefore the  $C4$  is the most effective variable.

#### Machining of INCO 901 with CC650

The regression equation is;

$C5 = 3.41 - 0.245C1 - 10.03C2 - 0.079C3 + 0.00134C4$

From the calculations;

Standard deviation = 0.7119 & Mean square = 0.5068

and the confidence limits are:

$C1 = 0.844$ ,  $C2 = 0.963$ ,  $C3 = 0.245$  &  $C4 = 0.586$

Therefore the  $C2$  is the most effective variable.

#### Machining of INCO 901 with Kyon 2000

The regression equation is;

$C5 = 2.61 - 0.107C1 - 2.69C2 + 0.039C3 - 0.00434C4$

From the calculations;



Standard deviation = 0.4786 & Mean square = 0.2291  
and the confidence limits are:

$$C1 = 0.649, C2 = 0.611, C3 = 0.182 \text{ \& } C4 = 0.999$$

Therefore the C4 is the most effective variable.

#### Machining of INCO 901 with WG-300

The regression equation is;

$$C5 = 0.586 - 0.168C1 + 11.0C2 + 0.447C3 - 0.00395C4$$

From the calculations;

$$\text{Standard deviation} = 0.3282 \text{ \& } \text{Mean square} = 0.1077$$

and the confidence limits are:

$$C1 = 0.942, C2 = 0.999, C3 = 0.998 \text{ \& } C4 = 0.999$$

Therefore the C2, C3 and C4 are the most effective variables.

#### Machining of INCO 178 with Kyon 2000

Since machining of INCO 718 was carried out in dry condition only, the C3 variable will therefore be eliminated from the calculations. Subsequently the regression equation is;

$$C5 = - 0.654 + 0.0802C1 + 2.69C2 + 0.00458C4$$

From the calculations;

$$\text{Standard deviation} = 0.2654 \text{ \& } \text{Mean square} = 0.07044$$

and the confidence limits are:

$$C1 = 0.618, C2 = 0.714 \text{ \& } C4 = 0.999$$

Therefore the C4 is the most effective variables.

Subsequently from these statistical analysis the most influential variables were identified which are shown in table 17.

## DISCUSSION

### 5.1 Introduction

From the collected machining data the failure modes and wear mechanisms of the cutting tools were investigated. An attempt is made to formulate a pattern to explain the tool lives and their behaviour.

### 5.2 Introduction to Machining

In machining nickel-base alloys, cutting tool materials undergo severe thermal and mechanical changes. The applied stresses and temperatures generated at, and close to, the cutting edge greatly influence the wear rate and hence the material removal rate.

The applied stresses on the cutting tool are usually divided into two types. The compressive stress (possibly in the region of  $1500 \text{ N/mm}^2$ ) acting normal to the rake face and the shear stress which is parallel to the rake face of the cutting tool acting in the direction of the chip flow. The cutting insert is acting as a cantilever, and the compressive stress is at its maximum at the cutting edge and decreases continuously to zero (where the chip separates from the tool). There is an ambiguity as to whether the increase in the cutting speed will increase the applied

stresses, however, there is no doubt that the temperature is speed related.

Heat is normally generated in the shear plane and the flow zone. The majority of the generated heat will be carried away by the moving chip (figure 8). The temperatures in the cutting tool insert, which may exceed  $1000^{\circ}\text{C}$  at the cutting edge (figure 19) [50], are dictated by heat generated in the flow zone which results from seizure at the interface. The heat generated and the temperature achieved are dependent on the property of the material being machined. When machining nickel-base alloys the region of high temperature will be situated close to the cutting edge.

The increase in the cutting speed will increase the cutting tool temperature which subsequently reduces its yield strength. The presence of a greater compressive stress (at high speed) than the yield strength of the cutting tool can result in catastrophic failure.

Generation of high temperatures at the cutting edge will impose a rapid temperature fluctuation when cutting is interrupted or the machining is conducted in the presence of a coolant. The intermittent contact of the coolant may penetrate to the flank face of the tool and reduce the subsequent temperatures. Introduction of the coolant to the surface in question will induce rapid temperature changes. Due to the presence of high cutting temperatures and cyclic penetration of the coolant, the region near the cutting edge will undergo fluctuating stresses resulting from the temperature fluctuations. Potential thermal damage can

therefore be minimised by selecting a tool with a low coefficient of thermal expansion. Additionally, high thermal conductivity of the cutting insert will help the cutting insert to decrease local temperatures, through better conduction of the heat.

### **5.3 Failure Modes**

Analysis of the results obtained from machining of nickel-base alloys have shown that end of depth of cut notch has been the life limiting factor in the majority of cases. Flank wear, nose notch, chipping and catastrophic failure have been the other factors affecting some of the tool lives. There was also another wear regime which was present on the honed area (interception of the flank face and the rake face), but it was never severe enough to dominate the tool life.

Tool materials failing due to notching and/or flank wear usually showed surfaces where small and large fragments of material were removed and the presence of cracks in many instances were apparent.

### **5.4 Tool Wear Mechanism**

#### **5.4.1 Attrition Wear**

Attrition is the removal of individual or aggregates of grains of tool material by the work material which subsequently leaves a rough area. This type of wear has been reported by many researchers [80, 121] when machining with ceramic tools.

During the machining operation the irregular flow of

the material over the cutting edge of the tool may wear surfaces resulting in breaking away the small fragments of the tool. Subsequently the removed fragments can be carried away by movement of the chip or the work surface. The grain size of the tool material plays an important role in the wear rate. Material with a smaller grain size will have a higher attrition wear resistance than material with larger grain sizes.

Fatigue induced by the serrated chip may also promote the rate of attrition wear. When machining nickel-base alloys with the specified cutting speeds (i.e. 90 m/min to 300 m/min) the chip is in the serrated form. A simple calculation shows that during machining Waspaloy at 150 m/min and a feed rate of 0.18 mm/rev the frequency of the serration in the chip (1 every 100 micron, figure 77b) is about 15 to 20 thousand per second. High frequency of the serration results in fluctuation of the stresses (and possibly temperatures) during machining which will generate mechanical fatigue processes. The presence of fatigue during the machining operation can initiate a crack and/or propagate the generated crack further.

Formation of cracks generated by thermal and mechanical fatigue is dependent on the behaviour of the crystals in the ceramic tool. These crystals which have a random orientation are interlocking with one another. The atoms of each crystal are regularly spaced with respect to each other. The crystals are separated by boundaries which are a few atoms thick and do not conform to any pattern. Normally they act

as barriers to the movement of dislocations. However, at elevated temperatures the interatomic distances increase by thermal vibration. Subsequently the bond strength decreases and the grain boundary becomes weaker. Also due to the random orientation of the crystals, the fluctuating stresses will cause some of the crystals to distort mechanically in particular directions more than adjacent crystals.

The generation of the serrated chip and intermittent cooling during machining will induce cyclic stresses on the tool. Subsequently these stresses will be transferred to the crystals in the matrix. At high temperatures the cyclic stresses induce cracks along grain boundaries (figure 30). It is proposed that this fluctuating stress system promotes attrition wear by the formation of cracks on grain boundaries. The cracks generated by fatigue may then propagate. This will subsequently promote removal of the particles (either individual grains or aggregates).

It is suggested that, since during machining the applied stresses remain almost the same and as the generated chip will be serrated from the beginning, cracks may initiate in the first few seconds of machining and propagate further with time. Formation of a void (figure 67) due to removal of a particle can also act as a stress concentration point [77] and further machining can generate further cracks by mechanical wedging. The generated cracks may join up so that the edge crumbles away (figure 53) or chipping takes place, in severe cases catastrophic failure may occur.

#### 5.4.1.1 Effect of Tool Microstructure on Attrition Wear Rate With Waspaloy

Deterioration of the tool material due to attrition wear (figures 50, 70 & 78) is mainly induced by grain boundary failure. In addition to high temperatures that lower the strength of the grain boundary, this wear mechanism can be heavily influenced by the alloying element/s (additives) in the tool material. Attrition wear is also a function of the cracks induced by thermal and mechanical fatigue. Any reduction in the formation of the crack will reduce the rate of attrition wear.

During machining the high temperature will be expected to increase the toughness of the cutting tool. Pure alumina cutting tools (CC620), have a relatively uniform microstructure. Only a low percentage of Zirconia, ensures that this cutting tool has little triaxial stress associated with differential expansion of second phase particles. An increase in overall temperature therefore may induce higher toughness and resistance to crack propagation at the higher cutting speeds which in turn should reduce the attrition wear rate. This is supported by the statistical analysis showing that increases in the cutting speed have resulted in longer tool lives (table 17).

The presence of TiC in the mixed oxide alumina cutting insert (CC650) increases the thermal conductivity of the tool (table 5). This thermal property is important since the heat generated during machining will increase the temperature at the cutting edge. Figure 19 shows the

temperature generated when machining INCO 718 at different speeds [50]. By considering the tensile properties of INCO 718, INCO 901 and Waspaloy (figure 18) we can assume that the temperature generated when machining these alloys will be of a similar magnitude. Therefore within the cutting speed range of 90 m/min to 300 m/min the generated cutting temperature will be about 900°C to 1200°C. A tool with a higher thermal conductivity will therefore allow the temperature to penetrate deeper into the tool which subsequently reduces the thermal gradient and hence the thermal stresses. This minimising of thermal stress apparently makes the tool behave tougher. Control of these thermal effects can therefore suppress attrition. However, differential expansion between the titanium carbide/nitride and alumina will contribute to a localised stress around the second phase. It appears from table 17 that there has been no response to attrition wear with increase in the cutting speed, probably because a balance between the alumina toughening at high temperature and the effect of the second phase act opposite to each other.

The composite ceramic ( $\text{Al}_2\text{O}_3 + \text{SiC}_w$ ) cutting insert, WG-300, is toughened by the addition of the silicon carbide whiskers to the matrix. Taking thermal and mechanical properties into consideration, silicon carbide whiskers have somewhat different properties to the alumina (table 4, 5, & 6). Low thermal expansion coefficient of silicon carbide (about  $4 \times 10^{-6}/^\circ\text{C}$  at 1000°C) in comparison to alumina (about  $8 \times 10^{-6}/^\circ\text{C}$  at 1000°C) will allow the alumina to expand twice



as much as the SiC during the machining operation. Thermal expansion will thus induce large localised stresses around the silicon carbide whiskers which are additive to the mechanical and thermal fatigue loads. Increase in the cutting temperature due to increase in the cutting speed will cause these stresses to increase and thus make the matrix more susceptible to cracking (figures 68 & 69).

Due to the presence of the silicon carbide whiskers within the matrix of the tool, a high fracture toughness (table 5 & 6) is achieved by crack deflection by the whiskers. The whiskers also form an interlocking mechanism within the matrix (figure 26). Therefore dislodgement of individual alumina particles from the matrix due to presence of this mechanism will be difficult. However, the percentage of fibres in the matrix (fibre volume,  $V_f$ ) and aspect ratio ( $L/D$ ) of the whiskers is important [118]. They can greatly influence the performance of the cutting tool by removal of the particles due to improper interlocking mechanisms. This interlocking action and crack propagation along the silicon carbide whisker is likely to lead to large attrition particles as whole fibres fail (figures 86 & 87).

Despite the good thermal properties of Sialon cutting tool materials (table 5) unexpectedly short tool lives are shown at high temperatures. Kyon 2000 tool is a two phase material consisting of a sialon nitride crystal and an intergranular glassy phase. The latter phase has a room temperature strength of 1000 MPa but as the temperature rises, particularly above 1000°C, it softens [102]. As

mentioned earlier at the lowest cutting speed of 90 m/min generated temperatures around the cutting edge will be of this order. Increases in the cutting speed raises the cutting temperature which can soften the glassy phase and reduce the bonding of the  $\beta$  prime phase leading to easy removal (figure 53). Higher cutting temperatures will increase the rate of softening and subsequently result in the loss of more grains and in shorter tool lives (figure 44). In order to reduce tool temperature and to achieve longer tool lives it is beneficial to perform machining in wet conditions, whenever feasible.

#### 5.4.1.2 Influence of Coolant on Attrition Wear with Waspaloy

Statistical analysis of the results has shown that the coolant has been the most influential parameter in determining the tool lives, after cutting speed.

Penetration of the coolant to the areas where the temperature is at its highest is impossible. The presence of a seizure zone at the tool-chip contact area will not allow a coolant to penetrate. During some of the tests at high cutting speeds it was noticed that the chip leaves the cutting tool in very small segments. This in itself can help the coolant to penetrate to areas which are inaccessible while machining at slow speeds. The application of the coolant may both reduce the overall temperature of the cutting area and contribute to the cyclic temperatures induced by the generated chip.

The coolant may intermittently penetrate to the flank

face of the tool and induce rapid temperature changes. Due to the presence of high cutting temperatures and cyclic penetration of the coolant to the surface in question, the cutting tool will be under continuous expansion and contraction. A tool material with a good thermal conductivity and a low coefficient of thermal expansion will therefore minimise thermal damage. However, application of the coolant during machining can have different effects on different materials. Presence of flood coolant on top of the rake face during machining of Waspaloy with CC620 cutting insert was detrimental to tool life whereas wet machining enhanced the tool life of the Kyon 2000 (table 17). The deficiency in thermal shock resistance of the pure alumina will contribute to the micro cracking. Figure 31 shows evidence of crack formation when machining Waspaloy at 215 m/min with CC620 tools. These cracks which are perpendicular to the cutting edge are typical of thermal cracks on cutting tools [77].

When machining Waspaloy with Kyon 2000 tool the glassy phase of the matrix will start to soften above 1000°C. The application of the coolant will reduce the overall temperature of the cutting area. This in turn will retard the removal of the  $\beta$  prime grains and hence longer tool lives will be achieved.

#### 5.4.1.3 Effect of Workpiece Material on Attrition Wear

Analysis of the results obtained from the machining tests has show that the cutting tool inserts behaved differently when machining different materials. This

variation was heavily influenced by the characteristics and chemical compositions of the workpiece material. The high temperature properties of Waspaloy, INCO 901 and INCO 718 play an important role. Percentages of Al and Ti which form gamma prime have a major influence on the high temperature properties.

Formation of carbides play an important part in the high temperature strengthening effects. Waspaloy has potentially the highest percentage of carbon followed by INCO 901 and INCO 718 (table 7) however, the specification allows for wide variation in any material. Formation of the carbides in these alloys is based on chromium, titanium, molybdenum, tungsten, iron and niobium.

These structures encourage the alloys to retain high levels of tensile and shear strength at high temperatures which occur during the machining operation.

At approximately 900°C to 1000°C (the estimated temperatures during machining) creep properties are apparently different for the three materials with Waspaloy, having the lowest creep rate INCO 901 and INCO 718 having higher creep rates [134].

Tensile properties (i.e. measured at higher strain rates than the creep properties) show the materials to have similar strength levels (figure 18). With even higher strain rates observed in machining (about  $10^4$ ) and the wide chemical specifications in the materials, temperatures generated when cutting cannot be predicted. Even the order of materials in terms of maximum temperature cannot be

predicted.

The force levels detected when machining these materials indicate that they are more influenced by the tool materials than the work materials (figures 109, 125 & 131) and again this makes it difficult to predict which material requires greater energy expenditure during machining.

Even though temperature estimation is not possible tool lives are considerably different for the various materials. One major effect which could cause this would be a change in cutting temperatures which is influenced by the cutting speed (figure 19), but other factors cannot be ignored.

#### 5.4.1.4 Effect of Machining parameters

##### 5.4.1.4.1 Cutting Speed

With Waspaloy only the CC620 tool showed an increase in tool life with increase in speed. However, as CC620 showed an overall tool life less than Kyon 2000 and WG-300, testing on INCO 901 and INCO 718 was not carried out. The other tool materials Kyon 2000 and WG-300 showed a decreased tool life with INCO 901 and INCO 718 consistent with the behaviour when machining Waspaloy (the effects previously commented on as being related to mechanical and thermal cycling).

##### 5.4.1.4.2 Coolant

According to statistical analysis (table 17) coolant has no effect on the Kyon 2000 when machining INCO 901 and INCO 718. A reduction in temperature with Waspaloy was significant and was associated with softening of the glassy phase. This appears to be less significant on INCO 901 and

INCO 718 suggesting lower temperatures may occur with these materials. Thus the glassy phase being relatively stronger prior to addition of coolant and attrition wear then proceeding by mechanical action.

With WG-300 an increase tool life with coolant on INCO 901 is apparent and not significant on Waspaloy by the statistical method used. This increase may be associated with the lower temperatures reducing the thermal stresses due to differential expansion between the silicon carbide and alumina (table 4).

Application of a coolant may reduce the cutting temperatures and it has been shown that generally reduction in temperatures has promoted the tool lives. It is suggested that the presence of a coolant may reduce the process of fatigue which is induced by irregular contact of the hot chip on the cutting tool. This therefore will reduce the generated cracks and also removal of the particles and hence a higher tool life will be achieved.

Figures 112 and 113 show the occurrence of chipping (i.e. large aggregates of grains removed together) which has been the life limiting factor in the majority of cases when machining was performed in dry conditions. Formation of the segmented chips will allow the coolant to have good access to the tool. This will in turn induce overall temperature field reduction and minimise the temperature fluctuation. Any reduction in the overall stress will therefore lower the rate of chipping and can give enough time for other types of wear to be developed and dominate the tool life.

#### 5.4.1.4.3 Feed rate

No effect was observed with Waspaloy but with INCO 901 a decreased tool life with CC650 and increased tool life with WG-300 was observed.

With CC650 a balance occurs as the temperature increases between toughening the alumina matrix and increasing localised thermal stress due to titanium carbide particles (see section 5.4.1.1). WG-300 tool material has larger particles and a higher volume fraction of the second phase. Also due to the presence of the whiskers within the matrix of WG-300 tools, an interlocking mechanism will be generated which holds the fractured matrix together (figure 26). This will therefore enable the WG-300 to resist higher overall loads due to higher feed rates. The higher feed rates are likely to generate higher temperatures, the alumina matrix could toughen sufficiently to reduce crack formation/growth hence giving longer tool lives at higher feeds.

In the case of CC650 the overall increase in load with feed may be sufficient to overcome the toughening of the alumina without the silicon carbide whiskers mechanically bonding it together thus reducing the tool life. The silicon carbide whiskers are therefore acting as a "load sharing" mechanism.

#### 5.4.1.4.4 Depth Of Cut

According to statistical analysis variation in the depth of cut during machining has not been influential on

tool lives.

Figure 131 shows that any increase in the depth of cut will proportionally increase the cutting forces. Therefore according to stress equation any increase in the area will proportionally increase the load by the same factor leaving the applied stress on the cutting tool unchanged. This same argument can also apply to the effect of the feed rate. However, it is well known that feed rate increases also cause temperature rises which is not normally significant with depth of cut increases.

#### 5.4.1.5 Overall Wear Rates

Failure due to attrition wear has been the major wear mechanism leading to discarding the cutting tool inserts. However, the presence of other types of wear mechanisms were apparent when machining nickel-base alloys. Occurrence of attrition wear is apparent on the flank face (figure 80), depth of cut notch (figure 129) and also on the honed area (figure 53) leaving a rough surface. Attrition wear has taken place at different rates according to cutting conditions and the material used. In the majority of cases the wear has been generated and increased with an increase in the temperature which is a product of the cutting speed.

General wear trends show that the formation of wear has been slow at low cutting speeds. Increase in the cutting speed accelerated the wear rate (figure 85).

WG-300 and Kyon 2000 have generally worn out at a slower rate and exhibited longer tool lives (figure 61 & 44



respectively) than the other cutting tools (figures 27 & 34). However, the latter tool outperformed the former when machining Waspaloy and the reverse was true when machining INCO 718 (figures 133 & 128). Reduction in tool life of the Kyon 2000 when machining INCO 718, and also change in its failure mechanism (figures 127 & 128), is probably due to generation of insufficient temperature to satisfy the toughening mechanism of the Sialon cutting tool which has resulted in chipping. Occurrence of chipping on rake face, particularly when dry machining at the higher cutting speed was predominant (figures 127 & 128). Under these conditions the wear did not have enough time to be developed to dominate the tool life.

However, when machining INCO 718, the presence of fibres in the matrix of the WG-300 cutting insert has enabled this tool to withstand the chipping due to the interlocking mechanism and long tool lives have been achieved (figure 130).

#### 5.4.2 Abrasion Wear

Abrasion wear is another type of wear mechanism which has been identified as deteriorating the cutting tool inserts. It is suggested that removal of the tool material particles may be due to attrition wear. These particles are either dragged along in the direction of the chip flow or the generated freshly cut surface subsequently abrading the surface in contact (i.e. flank face).

Generation of abrasion wear is also probable from the materials which contain hard carbide particles. Presence of

the carbides with a high hardness may have an abrading impression and scoring action. Apart from the high hardness, carbides usually possess high melting temperatures which can play an important part in controlling this type of wear mechanism. During machining operations the high temperatures generated in the cutting area will increase the ductility of the material. Higher melting temperature of the carbides enable them to soften at a slower rate than the parent material. Therefore under machining conditions the material with a higher melting point can have higher hardness even though the room temperature hardness may be the same.

Alumina has a hardness of 2000-3000 Knoop with an approximate melting temperature of  $2000^{\circ}\text{C}$  (table 4). Addition of the  $\text{TiC}$  with hardness of 1800-3200 Knoop and the melting temperature of  $3100^{\circ}\text{C}$ , or  $\text{SiC}$  with a hardness of 2100-3000 Knoop and the melting temperature of the  $2300$ - $2500^{\circ}\text{C}$  to the matrix will improve its properties. During machining the generated temperature which may be in the order of  $900^{\circ}\text{C}$  to  $1000^{\circ}\text{C}$  will soften the cutting tool insert and hence removal of the carbides which at this stage are harder than the parent material and can abrade the surface in question.

Figure 43 is evidence of the flank wear due to abrasion when machining Waspaloy with a CC650 tool. The figure shows that particles of the cutting tool have been taken out of the cutting edge. The free particles which were then trapped between the work material and the cutting tool were subsequently pushed down the flank face abrading this area.

Scoring action at the bottom of the SEM photo shown in figure 67 is indicating that the silicon carbide fibres may have been dragged down the flank face of the WG-300 cutting insert.

Figure 33 also shows the generated abrasion wear on the flank face of the CC620 cutting tool when machining Waspaloy. This figure indicates that the scoring mark has started half way down the flank face of the tool being too wide to be caused by individual Zirconia particles. It is suggested that during the machining operation the cutting edge will be damaged and particles will be dislodged in large aggregates, these will then be pushed down the flank face, abrading this area until the material is disengaged with the cutting insert. It was reported [101] that abrasion wear was found to be the domineering tool wear mechanism when machining cast iron with ceramic tools.

Even though evidence exists for abrasion the mechanism is usually not one controlling tool life.

#### 5.4.3 Diffusion Wear

Apart from attrition wear and abrasion wear another type of wear mechanism resulting in a smooth surface (figure 67) was observed. However, it was never severe enough to be a life limiting factor and control the tool lives. This type of wear process which usually took place on the rake face and honed area of the cutting insert is characteristic of the inter diffusion of atoms between the tool material and the chip. Diffusion wear mechanism is a temperature

dependant process. Machining at high speeds will generate high temperatures which may accelerate the diffusion process around the tool-chip interface. The wear rate is determined by the chemical composition of both tool and the work material.

Bhattacharyya et al [80] reported a two way diffusion mechanism when machining was carried out on INCO 901 with SIALON tools. Their finding was that the titanium, chromium, nickel and iron from the work material reacted with aluminium, silicon, and yttrium from the tool material. They added that Ti and Cr can have an stronger effect than Ni and Fe. These elements diffuse into the glassy phase of the tool matrix and lower its strength causing removal of the  $\beta$  prime crystals by attrition.

Presence of the iron in the workpiece material can have a major effect on the tool wear mechanism particularly if it is present in large volumes (table 7). As mentioned earlier this element reacts with the oxygen to form FeO. The oxide reacts with the alumina [62] or  $\beta$  prime in  $\text{Si}_3\text{N}_4$  (i.e. Kyon 2000) to form an unstable glass-like composite "spinel", which has a low melting point. Subsequently this reaction (along with the above mentioned) would weaken the area in contact and accelerate attrition-diffusion wear. This may be a reason why Kyon 2000 has shown longer tool lives when machining Waspaloy (with the minimal percentage of iron, table 7) than INCO 718 (with about 18.5% iron) and INCO 901 (with about 35% iron).

#### 5.4.4 Depth of Cut Notching (DOCN)

Notching at the depth of cut has been an important factor in limiting the life of ceramic cutting tools used for the tests. Notches were generated with very irregularly worn surfaces and different shapes (figures 46, 66 & 78) which often exhibited large fracture cracks (figure 87).

Investigation into the cause of the end of depth of cut notching has been undertaken by many researchers and many different theories exist. The possible ways in which notching occurs can be separated into two processes. The chip-workpiece separation process occurs with extensive lateral plastic flow of workpiece material at the edge of the shear zone. This first causes side flow to form a burr and second, side flow on the chip (figure 117) which causes chip spread both of which occur cyclically.

During machining the segmented chip (figure 77d) which is ragged on one side (figure 77c) will separate from the work material at temperatures around 900°C or higher. During separation the ragged edge of the chip will be intermittently in contact with the tool. The presence of high temperatures and forces in this area will generate a fatigue loading on the tool and the subsequent movement of the chip can complete the removal process after fracture is initiated. Shaw et al [37] when machining Waspaloy reported that the chip had glowing edges and a darker centre. He concluded that the edge of the chip which is not constrained receives a greater specific energy input than the centre. This was not observed in the present set of results. Shaw concluded that this induced large welds and heavy pullout of

the tool material at the edges but the present work does not support this mechanism as welding was also not observed.

Due to the presence of high stress generated from the cutting action, a work-hardened layer is subsequently squeezed out forming a burr at the edge of the workpiece, with a temperature similar to that of the chip (figure 117).

During the polishing process of the quick stop sample it was noticed that the formation of the burr due to the side flow effect occurred cyclically. Hardness test of the burr area did reveal a variation in relation to the parent work material. An increase of approximately 20 to 30% was recorded.

The presence of the burr at the edge of the workpiece is thought to have both thermal and mechanical effects generating extra fatigue forces locally on the cutting tool. Figure 30 shows microcracks running across the DOC notch area of CC620 cutting tool when machining Waspaloy at the cutting speed of 90 m/min. Resistance of the cutting insert to formation of the notch depends on the level of thermal-mechanical stress developed and the ability of the material to deal with that stress without microfracture by fatigue.

Figure 42 shows the adhered work material on the notched area after machining at a speed of 300 m/min. The material might subsequently either have been removed, which will then take out the particles of the cutting insert, or will be pushed down, and abrade the flank face of the tool. Similar effects were noticed when machining Waspaloy with Kyon 2000 (figure 54). Figure 49a shows a metallographic

section of the end of depth of cut notch area. White areas on the edge of the tool are the work material bonded to the tool. Higher magnification of the sectioned area is presented in figures 49b and 49c. This confirms that attrition wear takes place on the DOC notch area which is the subsequent result of an uneven flow pattern. Unlike the generation of the flank wear (figure 52) which takes place at a steady rate, the process of seizure and removal takes place at a faster rate as the worn area becomes more effected (figure 51).

High thermal conductivity coupled with low thermal expansion of Kyon 2000 has enabled this tool to outperform both CC620 and CC650 cutting inserts when machining Waspaloy. High tool life performance of the Sialon cutting insert is due to formation of DOC notch at a lower rate. Higher toughness has enabled this tool to resist the removal process of the particles. Baker [60] has also reported that since Kyon 2000 has a greater toughness than the conventional ceramic tools notching was generated at a slower rate when machining nickel-base alloy.

Figure 64 shows Waspaloy adhered to the DOC notch area of the WG-300 tool. During detachment of these patches the adhered material will be dislodged and pulled away. Figure 65 shows the after effect of this process. This SEM photomicrograph also emphasises the formation of the attrition wear in the centre of the photo.

#### 5.4.5 Nose Notch

Severe wear at the nose of the cutting tool (figure 39) has occasionally dominated the tool life (figure 34). This type of wear has been more pronounced when machining was carried out in the absence of a coolant.

When machining the tip of the cutting insert is always buried in the work material. Under these conditions the accessibility of the tool nose to air is very limited. Therefore chemical reaction with the atmosphere is unlikely.

It is suggested that this type of wear is due to a mechanical process and is resultant of the severe mechanical shock which is applied during the first few seconds of machining. This is supported by the fact that nose notching appeared infrequently and could rarely be reproduced. For this reason the tool materials with high resistance to mechanical shock will have a higher resistance to notch wear.

However, there is another possibility for generation of this type of wear. During the machining operation two processes take place

- a. the tool is being pushed out in the opposite direction to the depth of cut due to the forces present.
- b. by progression of cutting, the tip of the tool wears out subsequently leaving a larger diameter on the workpiece than when it started.

Therefore if the cutting is to be resumed where it was left at the end of last cutting operation, the tool material should penetrate inside the work material in order to



proceed with the true depth of cut rather than touching it. This in-going process rapidly wears out the tip of the cutting insert leaving a severe nose notch.

Formation of the nose notch may influence the quality of the surface roughness [84] by channelling the metal downwards resulting in extended feed marks.

#### 5.4.6 Chipping (Flaking) and Catastrophic Failure

Occurrence of catastrophic failure was influenced by the stress developed during machining and the toughness properties of the cutting tool. The high temperatures generated during turning [50] also promoted the development of uneven stress regions on the cutting tool due to varying microstructure which will increase the stress on the ceramic bond. Alumina cutting tools were more susceptible to this type of failure due to their low toughness. Addition of TiC will however, promote the apparent toughness of the cutting tool by increasing thermal conductivity and reduce the possibility of the fracture. However, occurrence of catastrophic failure of CC650 when wet machining INCO 901 at the speeds of 150 m/min and higher has been inevitable (figure 99).

Elimination of catastrophic failure of the WG-300 tools has been attributed to the addition of the silicon carbide fibres to the matrix which will reinforce the tool and act as crack arrestors. The whisker reinforcement has also improved the toughness of WG-300 tool. The interlocking of the fibres delays the separation of the cracked areas (figure 90). Failure may still occur by the gradual pullout

of the fibres from the matrix.

Apart from the thermal and mechanical properties, the severe wear of the flank face can weaken the cutting insert and later stress raiser and crack initiation points will be developed. Elimination of the clearance angle can also result in a heat source thereby increasing the temperature at the tool nose hence promoting the failure rate.

Machining of INCO 718 with Kyon 2000 at the speed of 215 m/min and higher resulted in chipping after only 1 minute of machining (figures 127 & 128), but catastrophic failure did not occur and it is well known that toughness of these materials is appreciably higher than the alumina ceramics combined with a uniform structure which leads to low localised thermal stresses.

### 5.5 Influence of Various Gases on Tool lives

INCO 718 was machined with WG-300 tools in the presence of various active and inert atmospheres. These tests were carried out in order to establish whether there are any chemical interactions between the tool and the work material, and the atmosphere which could influence the wear rate.

Machining was carried out at a constant depth of cut of 2.5 mm and 0.18 mm/rev feed rate at cutting speeds of 150 and 215 m/min in the presence of oxygen, nitrogen and argon. Subsequently the results were compared to those machined under identical conditions. Figures 145 to 148 show the formation of the notch in the presence of different

atmospheres after 10 seconds of machining.

Alumina is chemically very stable. The incorporation of silicon carbide, an intrinsically less stable compound, would be expected to lower the chemical inertness of WG-300 tool. Due to this reason it is therefore suggested that SiC may be involved in reactions with the atmospheres and work materials.

During the machining operation the cutting insert will generate a freshly cut surface. This newly cut surface is highly reactive and may chemically combine with atmospheres rapidly. When machining in air oxygen is readily available, this will rapidly form an oxide on the new surface. This is known as gettering [62]. A deoxidised surface may enhance the diffusion-attrition wear process as this can result in a surface which is very susceptible to bonding. Machining in the presence of an oxygen rich atmosphere will provide enough oxygen to suppress potential bonding. Silicon carbide has a higher affinity towards oxygen and may become oxidised. These two processes will hinder notch formation by lowering forces locally and longer tool lives will be achieved (figure 143). Increase in tool life of SIALON when machining INCO 901 in the presence of oxygen rich atmosphere is also reported by Jawaaid [58]. He stated that the great affinity of the Ti and Cr to oxygen has enabled them to form oxides which subsequently has prevented the erosion of the  $\beta$  prime crystals.

Severe notching and short tool lives were observed (figures 142 & 143) when machining was carried out in the

presence of argon and nitrogen rich atmospheres. These high rates of notching can be attributed to the absence of oxygen from the vicinity of cut and consequently higher bonding forces leading to easier "pullout".

## 5.6 Comparative Tests

### 5.6.1 Influence of Tool Geometries

In order to find out the effect of the tool geometries on tool life, four different types of WG-300 cutting inserts with various geometries were selected to machine INCO 718. Figure 140 shows how the tool lives have been affected by these cutting tools.

It was already established that the generation of the notch is greatly influenced by the formation of the chip and the chip flow is affected by the tool geometry.

Implementation of these cutting inserts will introduce different approach angles, according to their geometries. For instance comparing rhomboid cutting inserts with  $35^\circ$  nose angle with square inserts which have a  $90^\circ$  nose angle. The approach angle of the former cutting insert will be  $72.5^\circ$  in comparison with latter which will be  $45^\circ$ . Any variation within the approach angle will subsequently change the chip flow. It is therefore suggested that an increase in the approach angle which increases the curvature of the generated chip subsequently influences segmentation at the edge. This will affect the fatigue loading at the depth of cut hence influence tool life.

### 5.6.2 Influence of Chamfer on the Work Material

In order to evaluate the effect of a sharp corner of the work material on the cutting insert during engagement with the workpiece, machining was performed without a chamfer. Figure 141 shows the effect of this test. The tool life achieved under this cutting condition is almost half as long as the performed test with a chamfer.

Short tool life obtained when machining is performed in the absence of a chamfer, is thought to be due to the initial engagement. As soon as the cutting tool is introduced to the work material, the sharp corner may abrade and damage the area in contact. The damaged point of contact which is the weakest point on the cutting edge coincides with the end of depth of cut line and can promote the wear rate. This supports the work on nose notch formation and indicates that damage during engagement may be one of the major effects seen in industrial conditions.

## 5.7 Summary of Discussion

The wear of the ceramic cutting tools used in this thesis has shown that the rates and type of wear is significantly influenced by the following effects

1. Chip formation, this produces a variable load and possibly a variable temperature field across the tool with a frequency of 15 to 20 thousand cycles/sec. This is potentially capable of causing failure by fatigue.
2. Additions of coolant can locally affect temperatures, increasing temperature gradients (and hence thermal stresses) but also contributing to fatigue by producing variable thermal stress due to intermittent contact.

3. The microstructures of the tools have significant effect on the response to these effects. Alumina based tools appeared to suffer from grain boundary failure. This could be related to the mismatch of orientation across the boundary producing a localised stress on the grain boundary as each crystal responds differently to the applied stresses.
4. Additions to alumina contribute to these localised fatigue processes by producing localised stress around individual second phase particles. This effect will depend on the type, size and shape of the microstructural phase.
5. With silicon nitride based material temperatures are probably high enough to soften the 'binder' phase at the extremes of the cutting conditions encouraging grain removal. At less severe cutting conditions the high thermal conductivity, good toughness and uniform microstructure enables the tools to last in excess of those based on alumina with additives.
6. Other effects which are probably significant include interdiffusion between tool and workpiece and relative strength at high temperature of the workpieces. It is not clear from the results how significant these effects are.

## CONCLUSIONS

The machining of Nickel-base superalloys with various ceramic tools under the stated conditions resulted in the following conclusions:

1. Notching at the depth of cut (DOC) has been the life limiting factor in the majority of cases. Flank wear, nose notch, surface roughness and chipping were the other influential failure mechanisms.
2. The following wear mechanisms were detected
  - a. attrition
  - b. diffusion
  - c. abrasion
3. Generation of the segmented chip (about 15 to 20 thousand cycles per second) produced cyclic fatigue loading which subsequently induced cracks.
4. The Kyon 2000 and WG-300 cutting inserts showed increased tool lives when machining wet. This was more apparent when machining INCO 718 with the latter insert at the higher depth of cut of 2.5 mm. Under these conditions flank wear became dominant and DOC notching was formed at a slower rate.

5. From the economical point of view the best machining conditions resulted in the highest volume of metal removed. The range of work materials and tool materials and conditions for this optimum are:

<u>work</u> <u>Material</u>	<u>tool</u> <u>Material</u>	<u>Speed</u> <u>(m/min)</u>	<u>Feed</u> <u>(mm/rev)</u>	<u>DOC</u> <u>(mm)</u>	<u>Coolant</u> <u>Used</u>
Waspaloy	Kyon 2000	150	0.18	2.5	Yes
INCO 901	CC650	300	0.18	2.5	No
INCO 718	WG-300	300	0.18	2.5	Yes

6. Machining of INCO 718 with WG-300 in the presence of different atmospheres produced a significant effect on the notch wear rate. Notching decreased in the presence of oxygen and became more severe in the presence of argon.
7. Unlike hardness, alloying elements of the workpiece materials play an important role in controlling tool lives.
8. According to statistical analysis, cutting speed is the major influential parameter, controlling tool lives, followed by the coolant and finally the feed rate.
9. Comparative testing has shown that the tool geometry plays an important role in tool life. An increase in the approach angle increased the rate of notch formation and hence reduced tool life. Longer tool life was achieved when the approach angle was reduced.



## FUTURE WORK

According to the results the author has obtained and analysed, the following future work is recommended:

### 1. Micro Examination and X-ray Analysis

From all the data in these tests, it is clear that the temperature developed during machining plays an important role in controlling tool lives and wear mechanisms. The presence of elevated temperatures during machining (usually above  $1000^{\circ}\text{C}$ ) will enhance the rate of chemical interactions between the work and the tool materials particularly when a diffusion wear mechanism is operating. In addition to that, the high weldability of the work material will enhance the adhesion process. Micro examination and X-ray analysis will facilitate the investigation of the rate and intensity of interactions between elements from the work material and the cutting tool.

### 2. Role of Coolant

It has been shown that the presence of the coolant has improved tool lives in many instances. Mainly, this has been due to reduction in the cutting temperatures during the

machining operation. Apart from this major influential factor the coolant may be beneficial in other ways:

- a. to control the chip direction
- b. to act as a lubricant
- c. to be used as a carrier to transfer substances and/or elements which can be beneficial to tool life (e.g. Oxygen)

In view of the results when cutting in gaseous environments this latter phenomenon in particular should be investigated further.

### 3. Role of Tool Edge Micro-geometry on Wear Mechanism

From the results obtained it is apparent that tool geometry is a parameter which can influence the tool wear. This is thought to be due to variation in the geometry of the generated chip. Design of the edge micro-geometry of the cutting inserts may be undertaken to optimise the tool life. The effect of edge geometry on the shape, raggedness and possibly the segmentation of the chip should be investigated.

When machining INCO 901 with Syalon cutting inserts Jawaid [58] reported that the cutting tool with  $0.2\text{mm} \times 10^\circ$  chamfer outperformed the cutting tool having  $0.2\text{mm} \times 20^\circ$  chamfer. Subsequently he suggested that the increase in tool lives may have been due to:

- a. smaller angle allowing the chip to flow more freely and evenly
- b. lower stresses at the edge

Additionally variation in the tool geometry can affect the cutting forces which will influence the cutting temperature which has been shown to be detrimental in tool lives.

#### 4. Composition Modification

Analysis of the results has shown different tool lives when machining superalloys. This variation has partially been attributed to the microstructures of the cutting inserts. It has been reported that the volume fraction, aspect ratio, the size and alloying elements of the cutting tool materials have been dominating factors. It is important for tool manufacturers to achieve a high cutting performance and satisfactory tool lives by selecting the right tool compositions with an appropriate ratio. The results in this thesis can be used as a basis for the further development of tools.

## REFERENCES

- [1] Whitney E.D., Vaidyanathan P.N., " Engineering Ceramics for High Speed Machining", Proc. of a Conf., Feb 1987, p. 77-82.
- [2] Wallbank J., Ezugwu E., "Wear of Ceramic Tools When Machining Cast Iron", Adv. Mat. & Manuf. Process, 3(3), 1988, p.447-468.
- [3] Bhattacharyya S.K., Pashby I.R., Ezugwu E., Khamsehzadeh H., " Machining of INCO 718 & INCO 901 Superalloys with SiC Whisker Reinforced Al<sub>2</sub>O<sub>3</sub> Composite Ceramic Tools", Proc. Of the 6th Inter. Conf. on Prod. Eng., Osaka, 1987, p.176-181.
- [4] Whitney E.D., "Modern Ceramic Cutting Tool Materials", Powder Metallurgy International, V.15, 4, 1983, p.201-205.
- [5] Drodza T.J., "Ceramic Tools Find New Applications", Manuf. Eng., May 1985, p.34-39.
- [6] Whitfield G., "Advance ceramics At Front of Materials Technology", Cutting Tool Eng., Dec. 1988, p.40-42.
- [7] Pashby I.R., Khamsehzadeh H., "The Machining of Waspaloy With Various Ceramic Tools", First Intrna. Conf. on The Behaviour of Mat. in Eng., 8-10 Nov. 1988, p.6.1-6.5.
- [8] Vigneau J., Boulanger J.J., "Behaviour of Ceramic Tools During the Machining of Nickel Base Alloys", Annuals of CIRP, 1982, p.35-39.
- [9] Billman E.R., Mehrotra P.K., Shuster A.F., Beeghly C.W., "Machining with Al<sub>2</sub>O<sub>3</sub>-SiC-Whisker Cutting Tools", Ceramic Bulletin, Vol.67, No.6, 1988, p.1016-1019.
- [10] Barraclough, K.C., "From Flint to Laser", A cutting edge for 1990, Ins. of Metals, 19-21 Sep. 1989, p.1-7.
- [11] Singer, Holmyard & Hall, "A History of Technology", Clarendon press, Oxford, 1958.
- [12] Rolt, L.T.C., "Tools for the job", Bastford, 1965.
- [13] Taylor F.W., "Art of Metal Cutting", Trans ASME 28, 31, (1907).
- [14] Swinhart H.J., "Cutting Tool Material Selection", ASTME, 1968.
- [15] British Standard Institution publication No 5623, 1979.
- [16] International Standards Office Publication No3685, 1977.
- [17] Trent E.M., "Metal cutting", Butterworths, London, II edn., 1984.
- [18] Shaw M.C., "Metal Cutting Principals", Clarendon Press, Oxford, 1984.
- [19] Cook N.H., "Chip formation in machining titanium", proc. Symp. on Machining and Grinding Titanium, MA, March 31, 1953.
- [20] Sullivan K.F., et al, "Metallurgical appraisal of instabilities arising in machining", Metals Technology, 5, 1978, p.181.
- [21] Manyindo B.M., et al, "Modeling the Catastrophic Shear Type of Chip when Machining Stainless Steel", Proc.

- Inst. Mech. Engrs., 1986, Vol 200 No C5, p. 349-358.
- [22] Doyle L.E., "Manufacturing Processes and Materials for Engineers", II edi., 1969.
  - [23] Ernst H., et al, "Chip Formation Friction and finish", Cincinnati Milling Machine Co. Cincinnati, Ohio, 1948.
  - [24] Merchant M.E., "Mechanics of Metal Cutting Process", J. of App. Phy., Vol. 16, 1945, p. 267.
  - [25] Nakayama K., "Studies on the Mechanism of Metal Cutting" Bull. of Fac.Eng., Yokohama National Uni., Japan, Vol.7, 1958, p. 1-26.
  - [26] Christopherson D.G., et al, "Orthogonal Cutting of a Work-Hardening Material", Eng., Vol.186,1958,p.113-116.
  - [27] Wallbank J., "Structure of Built-Up-Edge Formed in Metal Cutting", Metals Tech., April 1979, p. 145-153.
  - [28] Trent E.M., Powder Met., 12, 24, 1969, p. 568.
  - [29] Trent E.M., "Metal Cutting and Tribology of Seizure: I Seizure in Metal Cutting", Wear, 128, 1988, P. 29-45.
  - [30] Rowe G.W., et al, Trans ASME, 89B, 1969, p. 530.
  - [31] Williams J.E., et al, Metallurgia, 81(1945), 3, 51, 89.
  - [32] Taylor F.W., "The Temperature on a Turning Tool" Trans ASME, 28, 31, (1907).
  - [33] Bickel E., ASME, Sep. 9-12, 1963, p. 89-94.
  - [34] Braiden P.M., "Thermal Conditions in Metalcutting", ISI preprint 126, 1970.
  - [35] Trent E.M., "Metal Cutting and Tribology of Seizure:III Temperatures in Metal Cutting", Wear, 128,1988,p.65-81.
  - [36] Boothroyd G., "Fundamentals of Metal Machining", Arnold, 1965.
  - [37] Shaw, M.C., Thurman, A.L. & Ahlgren, H.J., "A Plasticity Problem Improving Plain Strain and Plain Stress Simultaneously: Groove Formation in the Machining of High Temperature Alloys" J. Eng. Ind. Trans. ASME. p.142.
  - [38] Vieregge G., Zerspanung der Eisenwerkstoffe verlage Stahlasen, Dusseldorf, 1959.
  - [39] SECO Handbook on Fundamentals of Metal Cutting.
  - [40] Dearnley P.A., "New technique for determining Temp. distribution in cemented carbide turning tools", Metals Technology, Vol. 10,June 1983, p. 205-214.
  - [41] Write P.K., Trent E.M., J.I.S.I., May 1979, p. 371.
  - [42] Shore H., "Thermoelectric Measurement of Cutting Tool Temperatures", J. Washington Academy of Science", Vol.15, 1925, p. 85-88.
  - [43] Herbert E.G., Proc. Instn. Mech. Engrs., 1, 1926, 289.
  - [44] Write P.K., Trent E.M., "Metallographic methods of Determining Temp. Gradients in Cutting Tools", J.I.S.I., London, 211, 1973, p.364-368.
  - [45] Trent E.M., "Requirement for Tool Material for Cutting Metals", Int. Conf., London, 3-4 March, 1977, p. 1-16.
  - [46] Dearnley P.A., "New Technique for Determining Temperature Distribution in Cemented Carbide Cutting Tools", Metals Tech., June 1983, Vol.10, p. 205-214.
  - [47] Boothroyd G., "Fundamentals of Metal Machining and Machine Tools", McGraw-Hill, 1981, P. 111.
  - [48] Cook N.H., "Tool Wear and Tool Life", J. of Eng. for Ind., Nov. 1973, p. 931.

- [49] Richard N., Aspinwall D., "Use of Ceramic Tools for Machining Nickel Based Alloys", Int. J. Mach. Tools Manuf. V.29, No.4, 1989, p.575-588.
- [50] Jean Francois Huet, Kramer B. M., "The Wear of Ceramic tools", North American Manu. Res. Conf., May 24-25 1982, p. 297-304.
- [51] Kramer B.M., "On Tool Materials for High Speed Machining" ASME, Vol.12, 1984, p. 127-140.
- [52] Machado A. R., " Machining of Ti6Al4V and INCO 901 with a High Pressure Coolant System", Ph.D. Thesis, Warwick University, England, Aug. 1990.
- [53] Albercht P., Microtecnic, 10, 45, 1956.
- [54] Moltrecht K.E.H., "Tool Failure When Turning Nickel Base High Temperature Alloys", ASTME, V. 64(2) April 1964, p. 1-31.
- [55] Solaja V., Wear, 2, 40, 1958.
- [56] Lambert H.J., CIRP Annals, Proc. Int. Inst. Prod. Eng. Res., 10, 246, 1962.
- [57] Tönshoff H.K., Bartsch S., "Wear Mechanisms of Ceramic Cutting Tools", Ceramic Bul., Vol.67, No.6, 1988, p.1020-1025.
- [58] Jawaid A., PhD Thesis, 1982.
- [59] Paper Under publication
- [60] Baker R.D., "Kyon 2000: A New World of High Speeds and Performance" The Carbide and Tool Journal, May/June 1982, P. 10-18.
- [61] Trent E.M., "Metal Cutting and the Tribology of Seizure, II Movement of Work Material over the Tool in Metal Cutting", Wear, 128, (1988), p.47-64.
- [62] King A.G., "Ceramic Tool Wear", ASME, No. 63, prod. 11, (1963), p.1-11.
- [63] Obitz H., Konig W., "Basic Research on the Wear of HSS Cutting Tools", BISRA-ISI Conf., (April 1970), p.1-9.
- [64] Trent E.M., "Metallurgical Consideration In Machining From The Point Of View Of The Tool-I", ASME, Sep. 9-12 (1963), p. 161-167.
- [65] Svahn O., "Wear Of Cutting Tools and Tool Life", ASME, Sep. 9-12 (1963), p.120-129.
- [66] Heydari F., M.Sc. Thesis, 1985.
- [67] Focke A.E., "Wear of Superhard Materials When Cutting Superalloys", Wear 46, (1978), p. 65.
- [68] Dearnley P.A., Grearson A.N., "Evaluation of Principal Wear Mechanisms of Cemented Carbides and Ceramics used for Machining Titanium Alloy IMI 318", Mat. Sci. and Tech., Jan. 1986, 2, p. 47-58.
- [69] Blankenstein B., "Wear Mechanisms of Carbide Cutting Tools", SME, 1971, p. 1-11.
- [70] Trent E. M., " Wear Processes which control the life of the Cemented Carbide Cutting Tools", BISRA-ISI Conf. Scarborough, 14-16 April 1970, p.10-15.
- [71] Kitagawa R., Kahng C.H., "Wear Mechanism Of the PM-High Speed Steel Tools", SME, 1984, p. 271-277.
- [72] Trent E.M., "Three Wear Processes with Control Performance of Cemented Carbide Cutting Tools" SME, 1971, p. 1-15.
- [73] Ramaswami R., " A Study of Some Aspects of Wear During

- Machining Processes", *Wear of Materials*, 1979, p.470.
- [74] Wright P.K., "The Machining of Stainless Steels and Manganese Steel", *Inst. Of Eng.*, 74/3, 1974, p. 197-204.
  - [75] Wright P.K., Bagchi A., Horne J.G., "Identification of the Dominant Wear Mechanism in Specific Tool-Work Systems", *ASM*, 1980, p. 7-23.
  - [76] Narutaki N., Yamane Y., "Cutting Performance of Cermet Tools", *ASM*, 1980, p. 319- 333.
  - [77] King A.G., Wheildon W.M., "Ceramics in Machining processes", *Academic Press*, London 1966.
  - [78] Moskowitz D., Stauffer D.J., Lenz E., " Machining Tests For Two Modes of Carbide Tool Failure: Chipping/Breakage and Plastic Deformation", *Proc. on Hard Material Tool Technology*, June 1976, p. 79-92.
  - [79] Bhattacharyya S.K., Jawaid A., Lewis M.H., Wallbank J., "Wear Mechanisms of Syalon Ceramic Tools when Machining Nickel-Based Superalloys", *Metal Tech.*, Dec. 1983, Vol. 10, p.482-489.
  - [80] Bhattacharyya S.K., Jawaid A., "Tool Life and Wear Mechanism of Syalon Ceramic Tools when Machining Nickel Based Materials", *Conf. Proc.*, 1984, p.203-208.
  - [81] Childs T.H.C., Smith A.B., "Effects of Atmosphere on Flank Wear of High Speed Steel Tools used to turn Medium Carbon Steel in Built-up edge Condition", *Metal Tech.*, July 1982, Vol. 9, p.292-196.
  - [82] Trent E.M., "New Tool Materials and Cutting Techniques" *INT. Conf.*, March 1977.
  - [83] Shaw M.C., paper in "Cutting Tool Material Selection", book edited by Swinehart H.J., *SATME*, 1968.
  - [84] Khamsehzaheh H., *MSc. Thesis*, 1985.
  - [85] Hoyle G., *High Speed Steels*, Butterworth, 1988.
  - [86] Komanduri R., Desai J.D., "Tool Material for Machining" part 1, *The Carbide and Tool Journal*, Sep.-Oct. 1983.
  - [87] Komanduri R., "Tool Materials For Machining, part two of three part series", *The Carbide and Tool Jour.*, Sep.- Oct. 1983.
  - [88] Mayer J.E., Moskowitz D., Humenik M., "Titanium Carbide Cutting Tools: Development and performance", *BISRA-ISI Conf.*, Scarborough, 14-16 April 1970, p.112-121.
  - [89] Kiffer R., Reither N., Fister D., "New Developments in the field of Cemented-Carbide and Ceramic Cutting Tools", p.158-162.
  - [90] Wick C., "Coated Carbide Tools Enhance Performance", *Manu. Eng.*, March 1987, p. 45-50.
  - [91] Wright P.K., Trent E.M., *Metal Tech. I.*, 1974, p.13.
  - [92] Coleman J.R., "Taming Tough Turning", *Tooling and Production*, Aug. 1983, p. 19-32.
  - [93] Krauskopf B., "Diamond Turning: Reflecting demand for Precision", *Manuf. Eng.*, May 1984, p. 90-94.
  - [94] Iida T., "Cutting Tool For New Materials", *Manuf. Eng. and Marketing*, May 1986, p. 60-65.
  - [95] Herzog D.E., "Now: Turn Hardened Steels and Tough Superalloys as easily as Mild Steels", *Manuf. Eng.* Oct. 1975, V.75, Pt.4, p. 29-31.
  - [96] Komanduri R., Desai J.D., " Tool Materials for Machining" part three of three part series, *The Carbide*

- and Tool Journal, Jan.-Feb. 1984, p. 3-11.
- [97] Brookes K.J.A., "Hard and Super Hard Tools are a cut Above the rest", Metal Cutting Prod., Oct. 1986, p.92-104.
  - [98] Barraclough K.C., "From Flint to Laser", Autum Meeting of the Institute of Metals, Sep. 1989, p. 1-7.
  - [99] North B., "Ceramic Cutting Tools", Carbide and Tool Jour., Sep./Oct. 1986, p. 23-28.
  - [100] Baldoni J.G., Buljan S., "Ceramics for Machining", Ceramics Bulletin, Vol. 67, No. 2, 1988, p. 381-387.
  - [101] Sarin V.K., Buljan S.T., "Advance Silicon Nitride Base Ceramic for Cutting Tools", SME paper, MR83-189, 1983 p.9-13.
  - [102] Jack K.H., "Silicon Nitride, Sialon, and Related Ceramics, Proc. of a Soc. Somp., April 1986, p.259-279.
  - [103] Sarin V.K., Buljan S.T., "Advance Silicon Nitride Ceramic for Cutting Tools", SME paper, MR 83-189, 1983, P.9-13.
  - [104] Ezugwu E.O., Wallbank J., "Manufacture and Properties of Ceramic Cutting Tools: a review", Materials Science and Technology, Nov. 1987, V. 3, p.881-887.
  - [105] Funabashi T., "High Metal Removal Rates with Ceramics", Carbide and Tool Jour., May/June 1985, p.22-27.
  - [106] Krupp Widia-Techn. Information, "Advanced Machine Tool Call for Advanced Cutting Materials", Tool Eng., 1986, p.1-13.
  - [107] Metals Handbook, Ninth Edi., Vol. 7, 1984, p. 514.
  - [108] Lumby R.J., Coe R.F., "The Influence of Some Process Variables on the Mechanical Properties of Hot-pressed Silicon Nitride", Proc. Br. Ceramic Soc., 1970, 15, p.91-101.
  - [109] Gruss W.W., "Ceramic Tools Improves Cutting Performance" Ceramic Bull., V.67, 6, 1988, p.993-996.
  - [110] Drozda T.J., "Ceramic Tools Find New Applications" Manuf. Eng., May 1985, P.34-39.
  - [111] Personal communication with Krupp Widia.
  - [112] Smith K., "Ceramic Composites Offer Speed, Feed Gains", Machine and Tool Blue Book, Jan 1986, p.71-72.
  - [113] Bhattacharyya S.K., "The Super Ceramic", Production Eng., Feb.1981, p.31-33.
  - [114] North B., "Substitution of Ceramic for Conventional Cutting Tools", Materials and Society, Vol. 8, No. 2, 1984, p.257-270.
  - [115] Wertheim R., "Improved Tool Life with Silicon Nitride", Machine and Tool Blue Book, Jan. 1986, p. 66-68.
  - [116] Krupp Widia, Technical Information, "Advanced Machine Tools call for Advanced Cutting Materials", Tool Eng., HTV 78.521, p. 1-14.
  - [117] Whithney E., Vaidyanathan P.N., "Microstructural Engineering of Ceramic Cutting Tools", Ceramic Bulletin, Vol. 67, No. 6, 1988, p.1010-1014.
  - [118] Vigneau J., Bordel P., Leonard A., "Influence of the Microstructure of the Composite Ceramic Tools on their Performance when Machining Nickel Alloys", CIRP, Jan



- 1987, p.13-16.
- [119] Whitney E.D., "Ceramic Cutting Tools", Powder Metal Inter., 6, 2, 1974, p. 73-76.
  - [120] Bhattacharyya S.K., Jawaid A, Lewis M.H., "Behaviour of Syalon Ceramic Cutting Tools When Machining Cast Iron", 12th North American Manu. Research Conf. Proc., 1984, p. 265-270.
  - [121] Aucote J., Foster S.R., "performance of Sialon Cutting Tools when Machining Nickel-Base Superalloys", Mat. Science and Tech., July 1986, No.2, P.700-708.
  - [122] King A.G., "Ceramic Tool Wear", ASME, No.63, 11, 1963, p.2-11.
  - [123] Venkatesh V.C. "Tool Wear Investigations On Some Cutting Tool Materials" Wear of Materials, Conf. Book, 1979, p.501-508.
  - [124] Narutaki N., Murakoshi A., "Effect of Small Quantity Inclusion in Steel on the Wear of Ceramic Tools", Bull. Japan. Soc. of Prec. Eng., Vol. 11, No.3, Sep. 1977, p.121-126.
  - [125] Friedrich I., "Flexible Production with Ceramics", Prod. Eng., May 1987, p.18-19.
  - [126] Godfrey A., "Getting a Grip on Cutting Tools", by Bergstrom R.P., Manuf. Eng., Jan.1986, p. 55-59.
  - [127] Kalpakjian S., "Manufacturing Processes for Engineering Materials", Addison-Wesley Publication, 1984.
  - [128] Bever M.B., "Encyclopaedia of Materials Science and Engineering", Vol. 4, 1986, P.3182.
  - [129] Bradley E.F., Source book on Materials for Elevated Temperature applications, ASME, 1979, p.250.
  - [130] Voort F.V., James H.M., Metal hand book, 9th edition, "Metallography and Microstructure, Wrought Heat Resistant alloys", ASME, 1985.
  - [131] Barker J., Dunn E., Woodyatt L., "1400 F Ultra High Strength Alloy Development Program", Tech. Report AFML-TR-65-278, I, Aug. 1965.
  - [132] Gadsby D.M., "Forging and Solution Treating Alloy 718", Metals Progress, V.90, Pt6, 1966, p.87.
  - [133] Warburton P., "Problems of Machining Nickel-Base Alloys" Iron and Steel Institute, Special Report 94, London 1967, p.161-162.
  - [134] Sims C.T., et al, "Superalloys II", Oct. 1986.
  - [135] Kirk D.C., "New Tool Materials and Cutting Techniques" Inter. Conf., London, 3-4 March 1977, p.1-26.
  - [136] Kirk D.C., "Cutting Aerospace Materials", Tool and dies for Industry, Proc. Conf., 1976/77, p.1-22.

PROPERTY	HIGH SPEED STEELS	CAST ALLOYS	CEMENTED CARBIDES		CERAMICS	CUBIC BORON NITRIDE	DIAMOND
			WC	TC			
Hardness	83-86 HRA	82-84 HRA 46-62 HRC	90-95 HRA 1800-2400 HK	91-93 HRA 1800-3200 HK	91-95 HRA 2000-3000 HK	4000-6000 HK	7000-8000 HK
Compressive strength psi $\times 10^3$ MPa	600-650 4100-4500	220-335 1500-2300	600-850 4100-5850	450-580 3100-3850	400-650 2750-4500	1000 6900	1000 6900
Transverse rupture strength psi $\times 10^3$ MPa	350-700 2400-4800	200-300 1380-2050	150-375 1050-2600	200-275 1380-1900	50-135 345-950	105 700	200 1350
Impact strength in lb J	12-70 1.35-8	3-11 0.34-1.25	3-12 0.34-1.35	7-11 0.79-1.24	<1 <0.1	— —	— —
Modulus of elasticity psi $\times 10^4$ GPa	30 200	—	75-100 520-690	45-65 310-450	45-60 310-410	125 860	120-150 820-1050
Density g/cm <sup>3</sup> lb/in <sup>3</sup>	8.6 0.31	8-8.7 0.29-0.31	10-15 0.36-0.54	5.5-5.8 0.2-0.22	4-4.6 0.14-0.16	3.48 0.13	3.5 0.13
Volume of hard phase, %	7-15	10-20	70-90	—	100	95	95
Melting or decomposition temperature °F °C	2370 1300	—	2550 1400	2550 1400	3600 2000	2400 1300	1300 700
Thermal conductivity, W/m. °C	—	—	42-125	17	29	13	—
Coefficient of thermal expansion, $\times 10^{-6}/^{\circ}\text{C}$	12	—	4-6.5	7.5-9	6-7.5	4.8	—

Table 1: Cutting tool materials [127]

	CARBON AND LOW/MEDIUM ALLOY STEELS	HIGH SPEED STEELS	CAST COBALT ALLOYS	CEMENTED CARBIDES	COATED CARBIDES	CERAMICS	POLYCRYSTALLINE CUBIC BORON NITRIDE	DIAMOND
Hot hardness			increasing					
Toughness	←	←	increasing					
Impact strength	←	←	increasing					
Wear resistance			increasing					
Chipping resistance	←	←	increasing					
Cutting speed			increasing					
Depth of cut	light to medium	light to heavy	light to heavy	light to heavy	light to heavy	light to heavy	light to heavy	very light for single crystal diamond
Finish obtainable	rough	rough	rough	good	good	very good	very good	excellent
Method of processing	wrought	wrought, cast, HIP* sintering	cast and HIP sintering	good cold pressing and sintering	CVD†	cold pressing and sintering or HIP sintering	high pressure- high tempera- ture sintering	high pressure- high tempera- ture sintering
Fabrication	machining and grinding	machining and grinding	grinding	grinding		grinding	grinding and polishing	grinding and polishing
Thermal shock resistance	←	←	←	increasing				
Tool material cost			increasing					

\* Hot isostatic pressing  
† Chemical vapor deposition

Table 2: Characteristics of tool materials [86]

TOOL MATERIALS	MACHINING OPERATION AND (CUTTING SPEED RANGE)	MODES OF TOOL WEAR OR FAILURE	LIMITATIONS
Carbon steels	Tapping, drilling, reaming (low speed)	Buildup, plastic deformation, abrasive wear, microchipping	Low hot hardness, limited hardenability, and limited wear resistance
Low/medium alloy steels	Tapping, drilling, reaming (low speed)	Buildup, plastic deformation, abrasive wear, microchipping	Low hot hardness, limited hardenability, and limited wear resistance
High-speed steels	Turning, drilling, milling, broaching (medium speed)	Flank wear, crater wear	Low hot hardness, limited hardenability, and limited wear resistance
Cemented carbides	Turning, drilling, milling, broaching (medium speed)	Flank wear, crater wear	Cannot use at low speed due to cold welding of chips and microchipping
Coated carbides	Turning (medium to high speed)	Flank wear, crater wear	Cannot use at low speed due to cold welding of chips and microchipping
Ceramics	Turning (high speed to very high speed)	Depth-of-cut line notching, microchipping, gross fracture	Low strength, low thermomechanical fatigue strength
Cubic boron nitride	Turning, milling (medium to high speed)	Depth-of-cut line notching, chipping, oxidation, graphitization	Low strength, low chemical stability at higher temperature
Diamond	Turning, milling (high to very high speed)	Chipping, oxidation, graphitization	Low strength, low chemical stability at higher temperature

Table 3: Operating characteristics of cutting tools [96]

MAT. PROP.	Al2O3	SiC	ZrO2	MgO	WC	TiC	TiN	TaC	VC	NbC	SiALON	ZrC
APPROXIMATE MELTING TEMP (deg.C)	2050	2300- 2500	2500- 2600	2620	2775	3100	—	3675	2620	—	1750- 1900	—
COEF. OF THERM EXP ( $\times 10^{-6}$ /deg C)	8.2	4.0	0.96	1.3	3.84	7.74	9.35	6.29	7.2	6.65	3.3	6.73
THERM COND (W/M deg K)	—	46	—	—	—	41.8	5.85	—	39.5	18.41	9.0	33.47
KNOOP HARDNESS	2000- 3000	2100- 3000	1000	500	1800- 2400	1800- 3200	2000	—	2100- 2800	—	—	2100

Table 4: Mechanical and thermal properties of some of the materials

Material	Three-point Bend-Strength (MPa)	Young's Modulus (GPa)	Hardness <sup>+</sup> (GPa)	Toughness <sup>-</sup> K <sub>IC</sub> (MPa <sup>1/2</sup> )	Abrasive <sup>*</sup> Wear ---	Thermal <sup>†</sup> Exp. Coeff. (K <sup>-1</sup> x 10 <sup>6</sup> )	Thermal <sup>‡</sup> Cond. (Wm <sup>-1</sup> K <sup>-1</sup> )
Al <sub>2</sub> O <sub>3</sub>	700	400	17.2	4.3	1.00	8.0	10.5
Al <sub>2</sub> O <sub>3</sub> -ZrO <sub>2</sub>	---	390*	16.5	6.5	1.18	8.5*	8.0*
Al <sub>2</sub> O <sub>3</sub> -TiC	910	420	20.0	4.5	1.22	8.5	13.0
Al <sub>2</sub> O <sub>3</sub> -SiC <sub>w</sub>	---	420*	18.8	6.8	1.37	6.4	15.0*
Si <sub>3</sub> N <sub>4</sub> /Sialon I	760	300	15.6	6.5	1.34	3.1	9.7
Si <sub>3</sub> N <sub>4</sub> /Sialon II	---	300	14.6	6.5	1.21	3.1	17.2
C2 Carbide	2080	610	17.6	8.5	1.03	5.1	72.7
C5 Carbide	2170	510	14.9	10.8	1.06	6.7	45.4

<sup>\*</sup> Estimated Value  
<sup>+</sup> Vickers, 18 kg load  
<sup>-</sup> Indentation (1) or Short Rod (2)  
<sup>\*</sup> K<sub>IC</sub> 0.5-0.8 MPa<sup>1/2</sup> (E = Young's Modulus, H = Hardness)  
<sup>†</sup> Range 25 - 870 C  
<sup>‡</sup> 500 C Value

Table 5: Physical & mechanical properties of cutting tools [114]

<b>MICROSTRUCTURE</b>	2 Phase Polycrystalline > 50% Alumina < 50% Silicon Carbide Whiskers
<b>DENSITY</b>	= 3.74 g/cc
<b>MELTING POINT</b>	2040 °C (3,700 F.)
<b>HARDNESS</b>	≥ 94.4 RA
<b>MODULUS OF RIGIDITY</b> (4 POINT BEND)	(T.R.S.) = 100,000 ± 6,000 P.S.I.
<b>YOUNG'S MODULUS (E)</b>	= 57 x 10 <sup>6</sup> P.S.I.
<b>MODULUS OF RIGIDITY (G)</b>	= 23 x 10 <sup>6</sup> P.S.I.
<b>POISSON'S RATIO (M)</b> $M = \frac{E}{2G} - 1$	= .23
<b>WIEBULL MODULUS</b>	13 (Determines the predictability of failure at given level of stress. The higher the number, the lower the probability of failure.) e.g
<b>Cold Press AL<sub>2</sub>O<sub>3</sub></b>	= 3.0
<b>Hot Press Composite</b>	= 4.5
<b>SIALON</b>	= 5.0
<b>C2 Carbide</b>	= 20.0
<b>WG-300</b>	= 13.0
<b>FRACTURE TOUGHNESS</b> (Measures resistance of crack growth from stress.)	
<b>Cemented Carbide</b>	= 13.0
<b>Hot Pressed Composite</b>	= 3.8
<b>WG-300</b>	= 8.0

Table 6: Physical properties of WG-300 cutting tool [1]

COMP.		C	Mn	Si	Cr	Ni	Co	Mo	Nb	Fe	Ti	Al	B	Zr	H	T.C.
ALLOY																
WASPALLOY	*	0.08	—	—	19.5	Bal	13.5	4.3	—	—	3.0	1.3	0.006	0.06	453	894
	#	0.38	—	—	21.3	56.3	13.1	2.5	—	—	3.6	2.8	0.031	0.04		
INCO 901	*	0.05	0.10	0.10	12.5	42.5	—	5.7	—	Bal	2.8	0.2	0.015	—	407	826
	#	0.24	0.11	0.21	14.0	78.0	—	3.5	—	—	3.4	0.4	0.08	—		
INCO 718	*	0.04	0.20	0.30	18.6	Bal	—	3.1	5.0	18.5	0.9	0.4	—	—	504	802
	#	0.19	0.21	0.62	20.6	52.2	—	1.9	3.1	19.2	1.1	0.9	—	—		

H = Vickers Hardness

T.C. = Temp. Capability (temp. for 100 h life at 14 kgf/mm<sup>2</sup>)

\* weight Percent

# Atomic Percent

Table 7: Nominal composition (wt/o) of WASPALOY, INCO 901 & INCO 718 [129]

CUTTING CONDITIONS			CUTTING SPEED (m/min)			
DEPTH OF CUT mm	FEED mm/rev	COOLANT USED	90	150	215	300
1	0.18	YES	0.9	0.7	0.35	0.85
1	0.18	NO	0.75	1.0	1.45	0.65
1	0.125	YES	0.55	1.3	0.65	0.75
1	0.125	NO	0.8	0.65	1.65	2.0
2.5	0.18	YES	0.35	0.65	0.65	1.25
2.5	0.18	NO	0.65	1.0	0.7	1.0
2.5	0.125	YES	0.8	0.75	0.65	1.3
2.5	0.125	NO	0.45	1.05	1.8	1.0

Table 8: Tool life obtained (min) when machining Waspaloy with CC620 tool

CUTTING CONDITIONS			CUTTING SPEED (m/min)			
DEPTH OF CUT mm	FEED mm/rev	COOLANT USED	90	150	215	300
1	0.18	YES	1.45	0.6	0.75	0.5
1	0.18	NO	3.15	0.8	1.6	0.8
1	0.125	YES	1.2	0.3	0.45	0.5
1	0.125	NO	0.5	0.45	1.0	2.0
2.5	0.18	YES	2.2	1.4	0.5	0.5
2.5	0.18	NO	1.1	0.95	0.75	0.17
2.5	0.125	YES	0.7	0.3	0.9	1.25
2.5	0.125	NO	0.5	1.45	0.8	1.0

Table 9: Tool life obtained (min) when machining Waspaloy with CC650 tool

CUTTING CONDITIONS			CUTTING SPEED (m/min)			
DEPTH OF CUT mm	FEED mm/rev	COOLANT USED	90	150	215	300
1	0.18	YES	3.5	3.2	2.6	1.5
1	0.18	NO	3.7	2.25	1.75	1.7
1	0.125	YES	7.1	6.7	1.4	1.0
1	0.125	NO	2.1	1.75	1.5	0.8
2.5	0.18	YES	1.8	4.5	0.66	0.33
2.5	0.18	NO	2.7	1.7	1.5	1.65
2.5	0.125	YES	5.0	2.7	1.5	0.5
2.5	0.125	NO	2.25	2.0	1.8	0.75

Table 10: Tool life obtained (min) when machining Waspaloy with Kyon 2000

CUTTING CONDITIONS			CUTTING SPEED (m/min)			
DEPTH OF CUT mm	FEED mm/rev	COOLANT USED	90	150	215	300
1	0.18	YES	3.8	1.1	0.8	1.2
1	0.18	NO	3.45	2.7	2.7	1.55
1	0.125	YES	1.45	2.8	2.2	1.77
1	0.125	NO	1.8	1.9	1.1	0.6
2.5	0.18	YES	4.8	2.9	2.4	1.8
2.5	0.18	NO	1.98	2.4	1.95	0.75
2.5	0.125	YES	2.9	1.35	0.8	0.7
2.5	0.125	NO	3.2	1.95	2.25	1.6

Table 11: Tool life obtained (min) when machining Waspaloy with WG-300

CUTTING CONDITIONS			CUTTING SPEED (m/min)			
DEPTH OF CUT mm	FEED mm/rev	COOLANT USED	90	150	215	300
1	0.18	YES	2.75	1.3	2.7	1.85
1	0.18	NO	0.7	0.9	2.05	1.2
1	0.125	YES	3.1	2.45	1.5	1.05
1	0.125	NO	1.95	1.9	2.45	1.7
2.5	0.18	YES	0.7	0.7	0.4	0.8
2.5	0.18	NO	0.85	1.25	2.1	1.95
2.5	0.125	YES	0.6	2.0	2.03	2.05
2.5	0.125	NO	0.9	2.3	2.25	2.8

Table 12: Tool life obtained (min) when machining INCO 901 with CC650

CUTTING CONDITIONS			CUTTING SPEED (m/min)			
DEPTH OF CUT mm	FEED mm/rev	COOLANT USED	90	150	215	300
1	0.18	YES	1.65	0.8	0.85	0.9
1	0.18	NO	2.2	1.4	1.0	0.75
1	0.125	YES	2.5	1.45	0.95	0.9
1	0.125	NO	0.85	2.5	1.2	0.75
2.5	0.18	YES	2.6	0.76	1.0	0.92
2.5	0.18	NO	0.7	0.95	0.8	0.9
2.5	0.125	YES	2.0	1.0	0.6	0.8
2.5	0.125	NO	1.7	1.45	0.95	0.95

Table 13: Tool life obtained (min) when machining INCO 901 with Kyon2000

CUTTING CONDITIONS			CUTTING SPEED (m/min)			
DEPTH OF CUT mm	FEED mm/rev	COOLANT USED	90	150	215	300
1	0.18	YES	2.7	2.1	2.3	1.85
1	0.18	NO	2.0	2.0	2.0	1.0
1	0.125	YES	1.7	1.4	0.8	1.65
1	0.125	NO	1.0	0.96	0.9	0.75
2.5	0.18	YES	1.95	1.92	1.55	0.8
2.5	0.18	NO	2.0	1.75	1.0	1.0
2.5	0.125	YES	2.3	1.75	1.3	0.6
2.5	0.125	NO	1.0	0.95	0.8	0.4

Table 14: Tool life obtained (min) when machining INCO 901 with WG-300



CUTTING CONDITIONS			CUTTING SPEED (m/min)			
DEPTH OF CUT mm	FEED mm/rev	COOLANT USED	90	150	215	300
1	0.18	YES	2.75			
1	0.18	NO	2.75	1.8	1.0	1.0
1	0.125	YES				
1	0.125	NO	3.4	2.5	1.0	0.5
2.5	0.18	YES				
2.5	0.18	NO	2.3	3.0	1.0	1.0
2.5	0.125	YES				
2.5	0.125	NO	2.25	2.75	1.0	1.0

Table 15: Tool life obtained (min) when machining INCO 718 with Kyon 2000

CUTTING CONDITIONS			CUTTING SPEED (m/min)			
DEPTH OF CUT mm	FEED mm/rev	COOLANT USED	90	150	215	300
1	0.18	YES		4.8	3.25	3.5
1	0.18	NO				
1	0.125	YES			3.9	
1	0.125	NO			3.1	
2.5	0.18	YES		6.3	3.6	4.5
2.5	0.18	NO		6.1	3.2	0.9
2.5	0.125	YES				
2.5	0.125	NO				

Table 16: Tool life obtained (min) when machining INCO 718 with WG-300

PARAMETERS		DEPTH OF CUT (mm)	FEED RATE (mm/rev)		COOLANT USED		CUTTING SPEED (m/min)	
WORK MATERIAL	TOOL MATERIAL		LOW	HIGH	NO	YES	LOW	HIGH
WASPALLOY	CC620				↑	↓		↑
	CC650							
	Kyon 2000					↑		↓
	WG-300							↓
INCO 901	CC650			↓				
	Kyon 2000							↓
	WG-300			↑		↑		↓
INCO 718	Kyon 2000							↓

↑ Increase tool life

↓ Decrease tool life

Table 17: Summary of the results obtained by statistical analysis

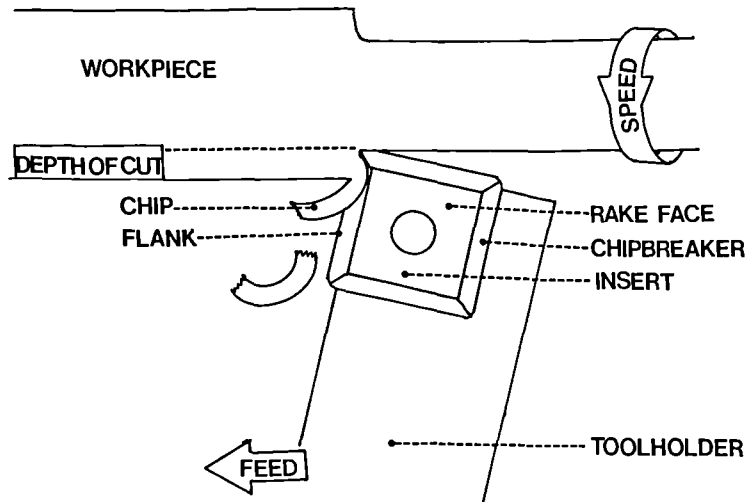


Figure 1: Illustration of turning process

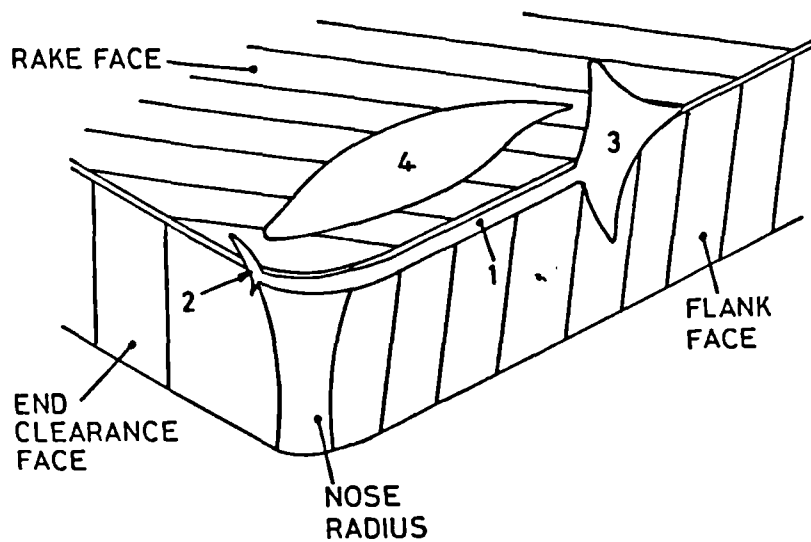


Figure 2: Geometry of a single point turning tool

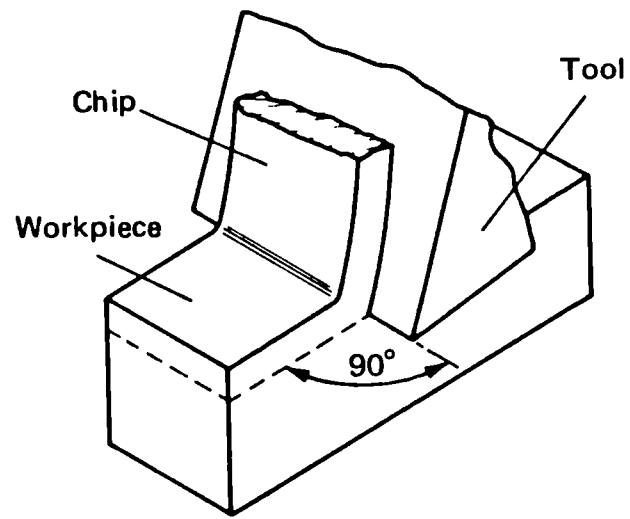


Figure 3: Orthogonal cutting

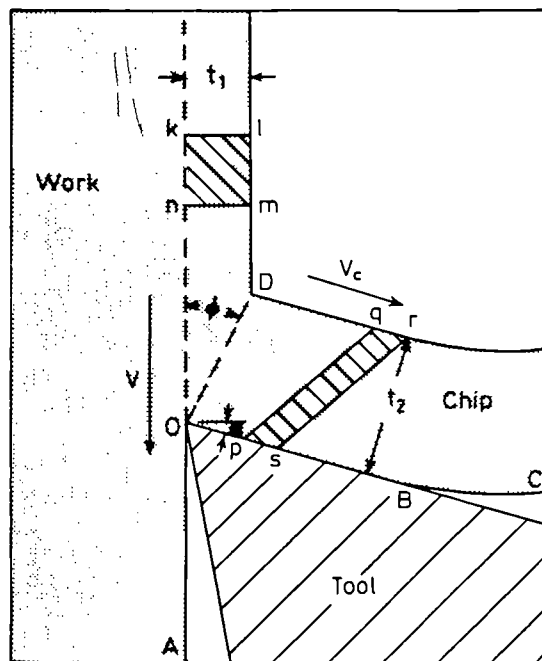


Figure 4: Metal cutting diagram [17]

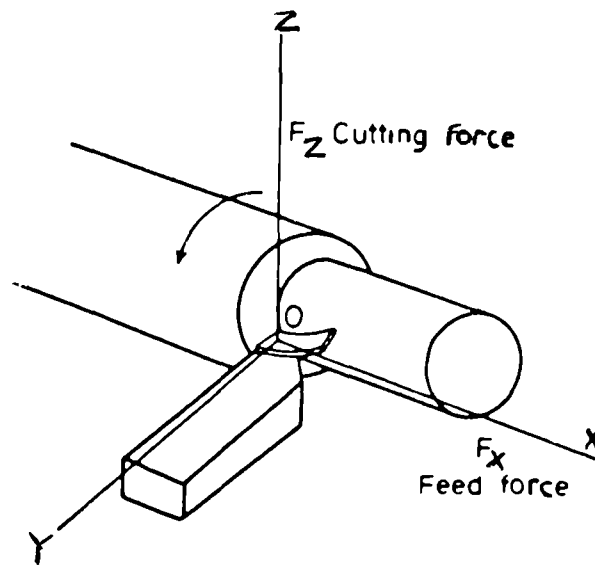


Figure 5: Three component forces acting on the cutting tool

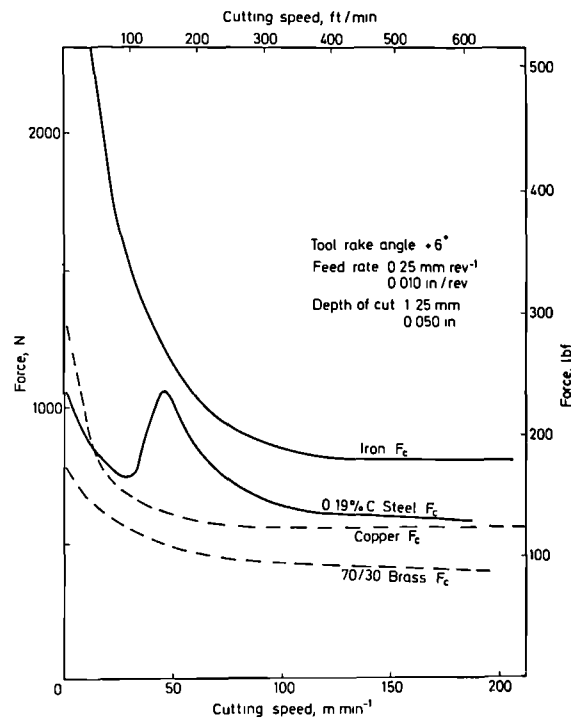


Figure 6: Cutting forces vs. speed [17]

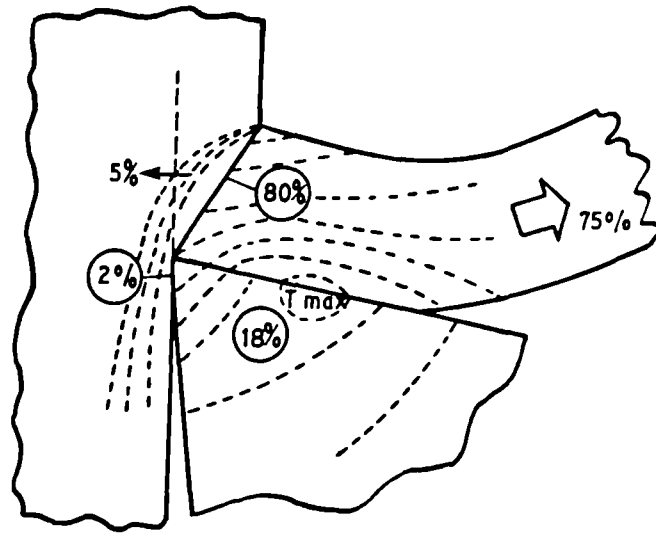


Figure 7: Presentation of generation and dissipation of heat in metal cutting [38]

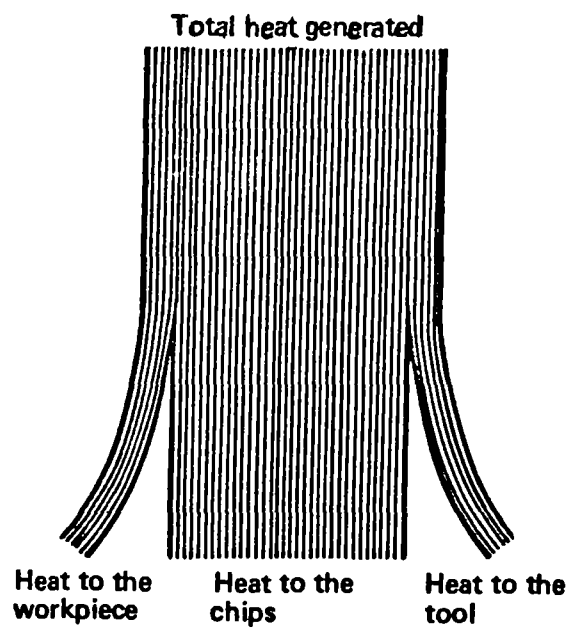


Figure 8: Heat dissipation in metal cutting

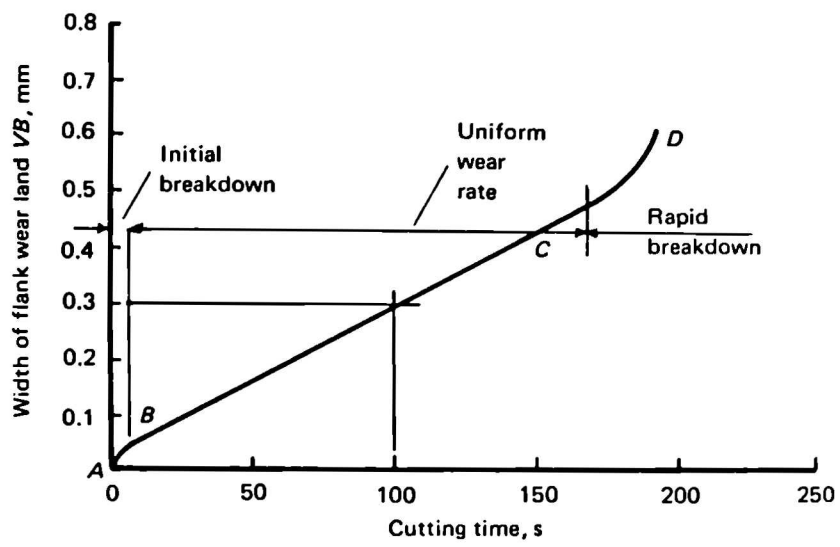


Figure 9: Development of flank wear with time [47]

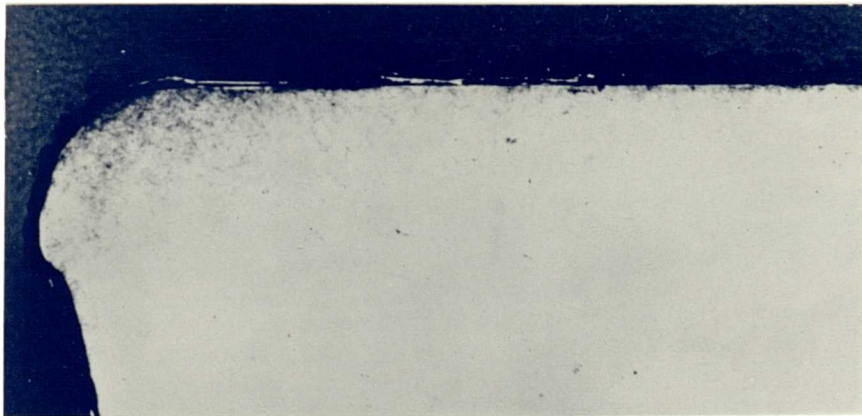


Figure 10: Indication of plastic deformation [17]

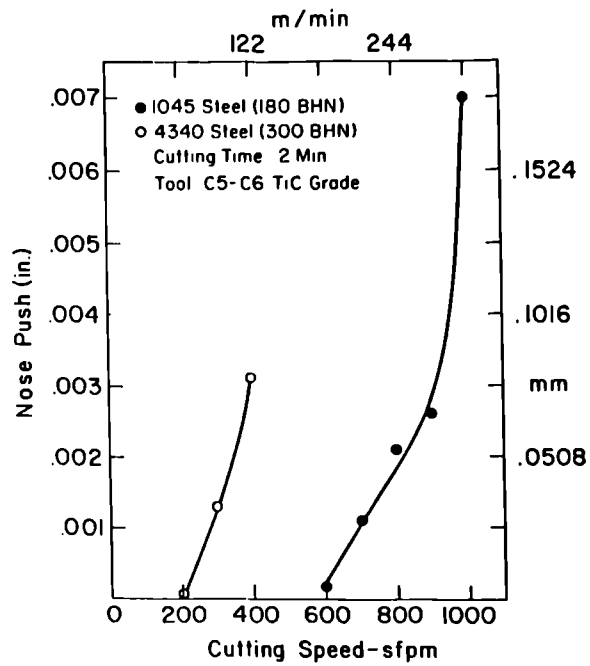


Figure 11: Nose deformation vs. cutting speed [78]

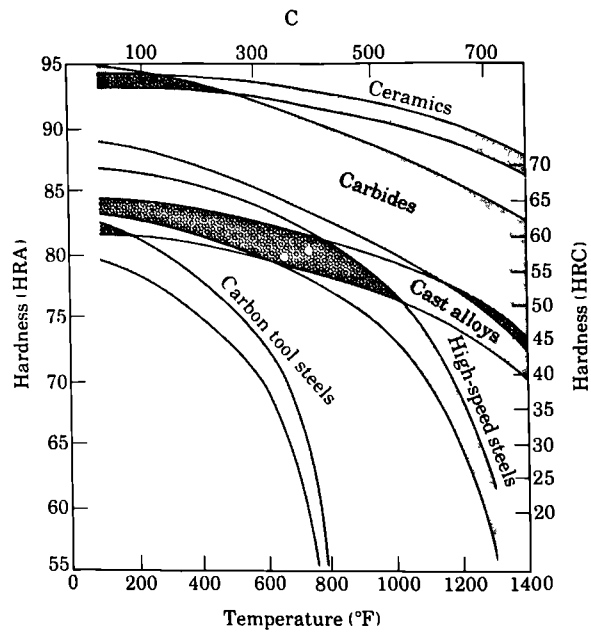


Figure 12: Hardness of various tool materials as a function of temperature [14]



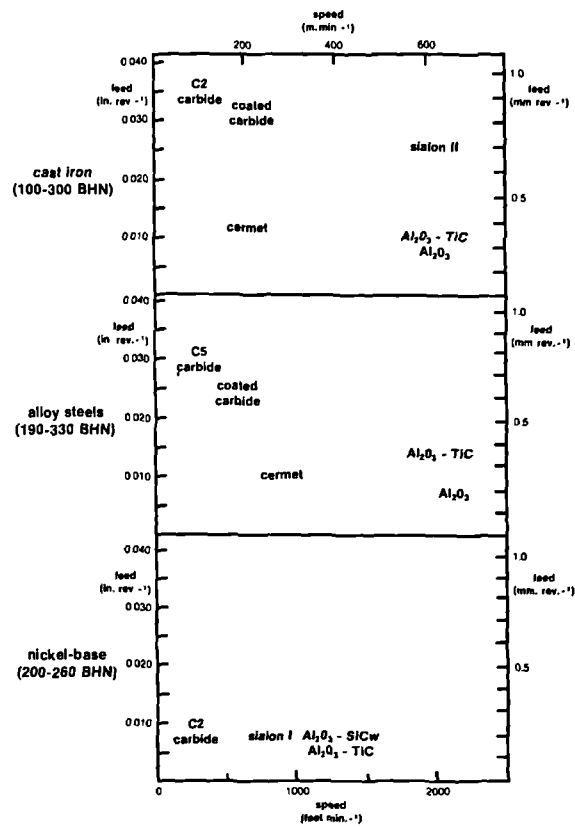


Figure 13: Approximate application ranges [99]

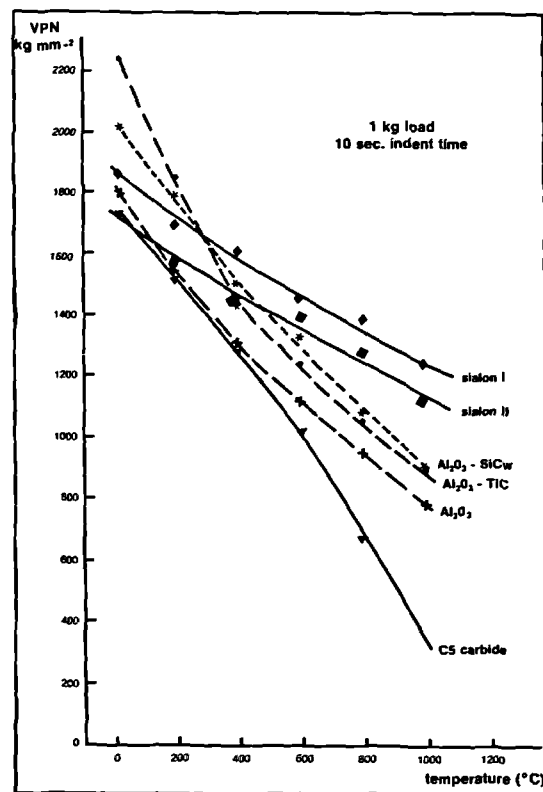
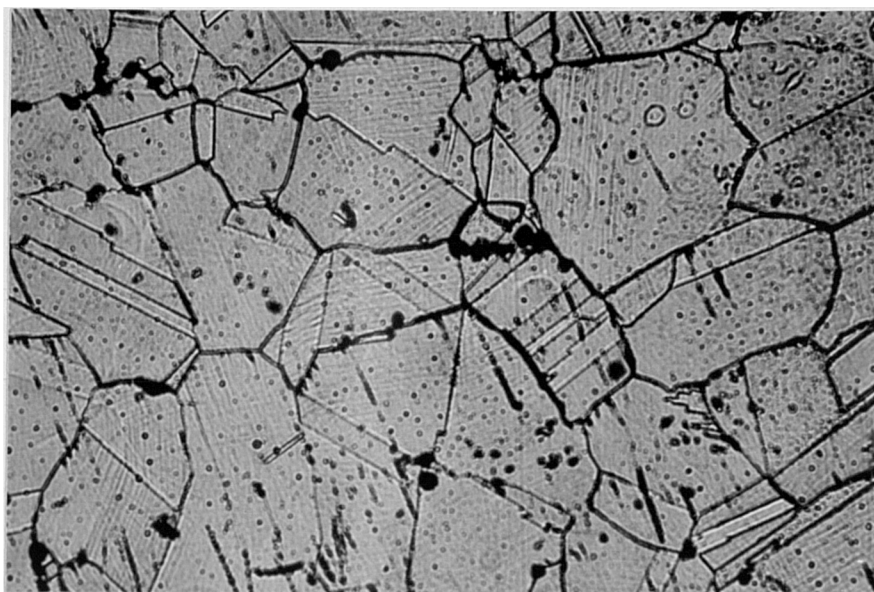
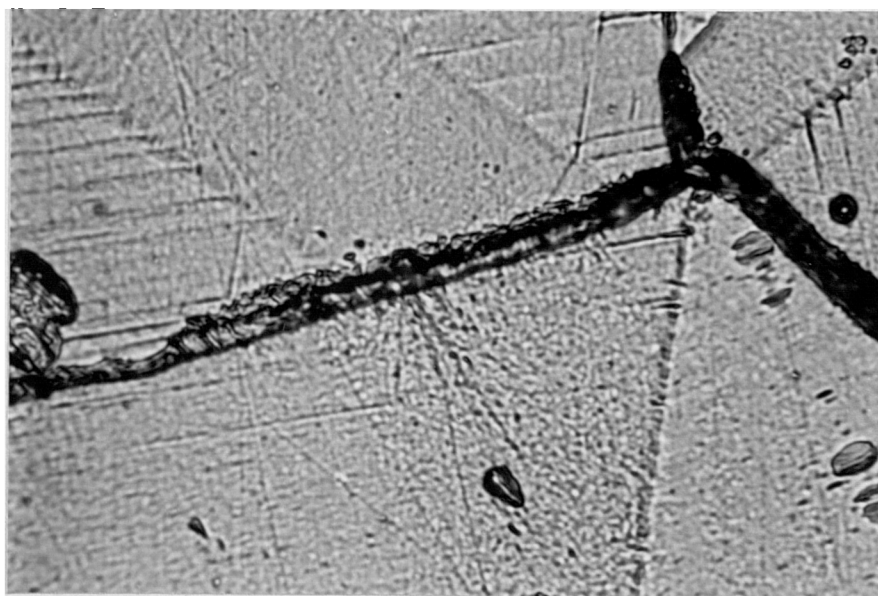


Figure 14: Vickers hardness vs. temperature [114]

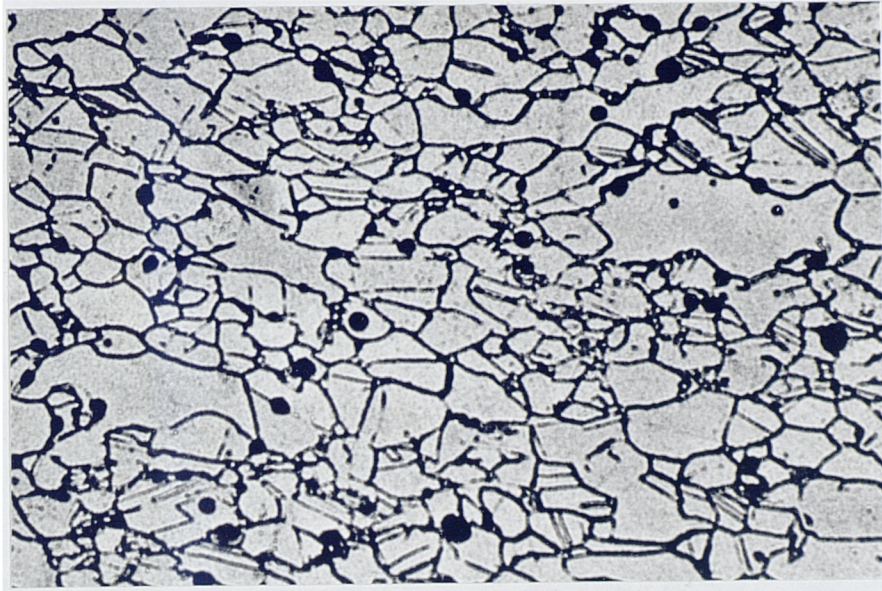


a. (x150)

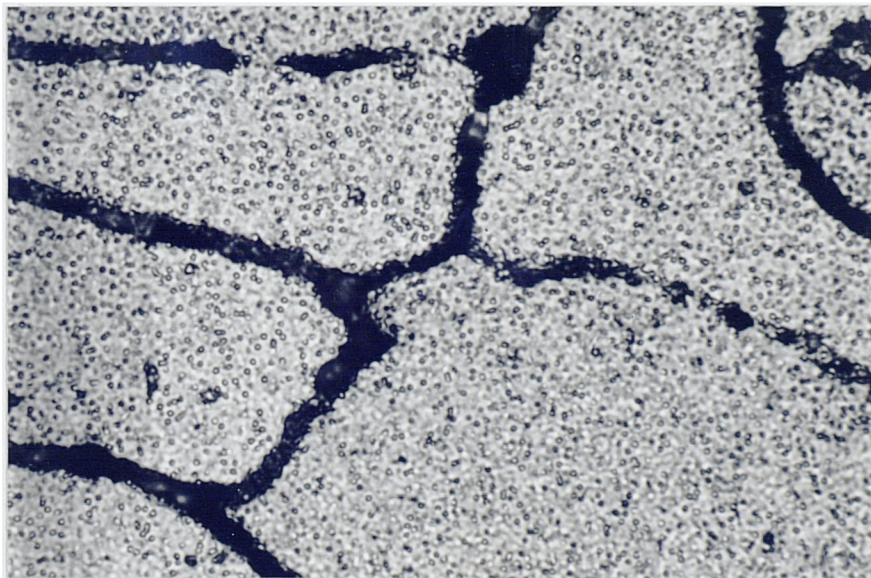


b. (x1500)

Figure 15: Microstructure of WAsPALOY



a. (x150)

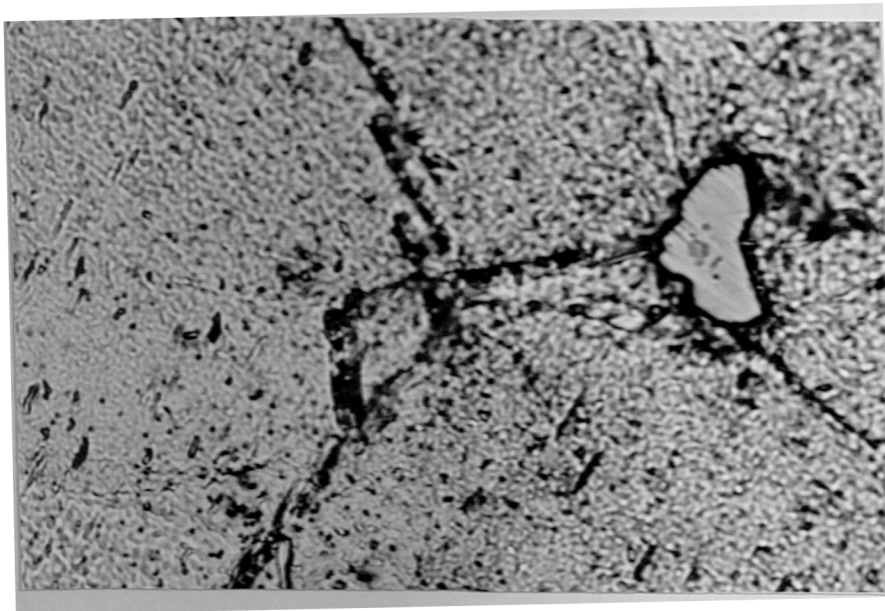


b. (x1500)

Figure 16: Microstructure of INCO 901



a. (x150)



b. (x1500)

Figure 17: Microstructure of INCO 718

VARIATION OF TENSILE PROPERTIES WITH  
TEMPERATURE FOR NICKEL-BASE ALLOYS

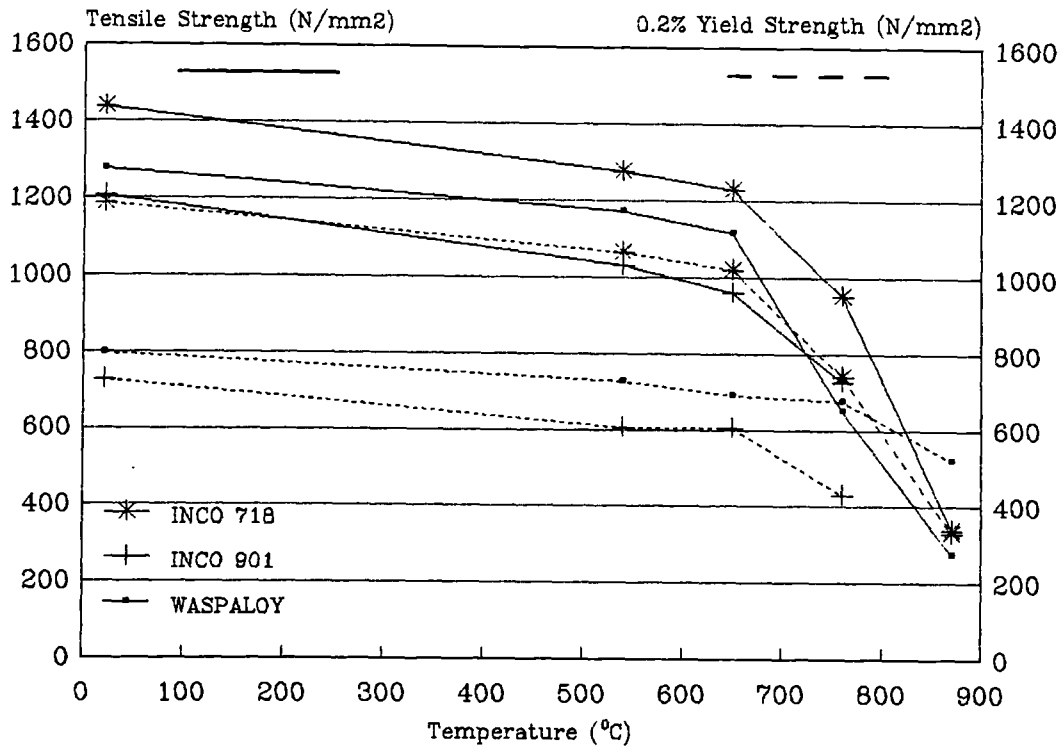


Figure 18 [134]

INFLUENCE OF INCO 718 ON CUTTING TEMP.  
WHEN MACHINING WITH CERAMIC COMPOSITE  
 $f=0.1\text{mm/rev}$ ,  $\text{DOC}=1\text{mm}$ , soluble oil coolant

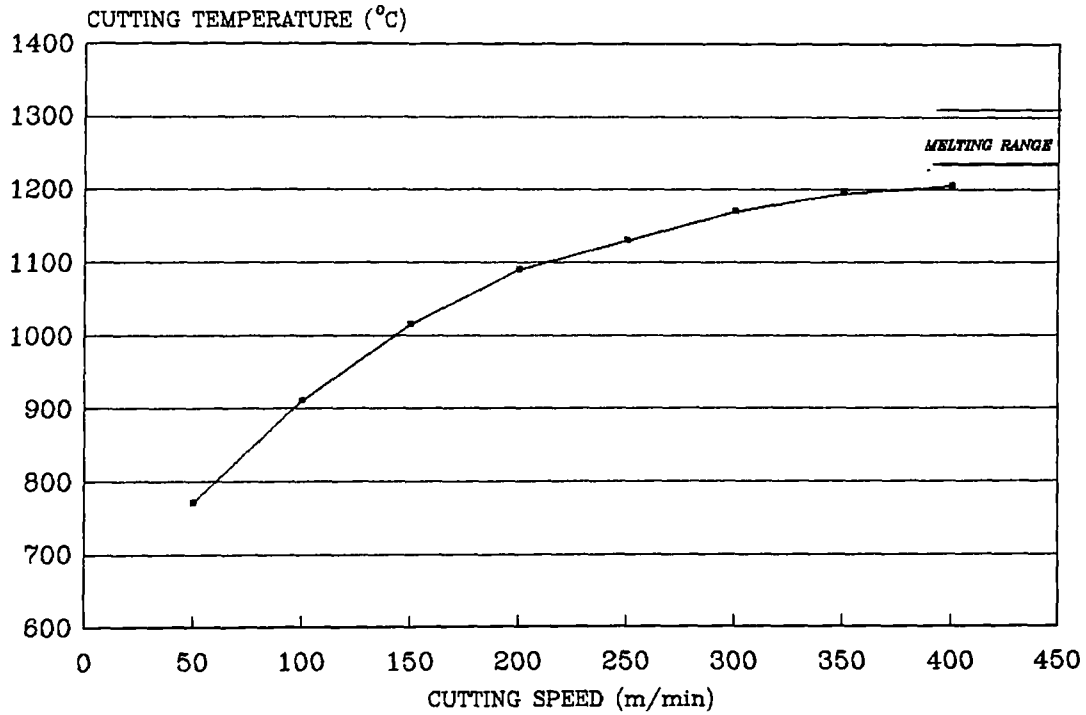


Figure 19 [50]

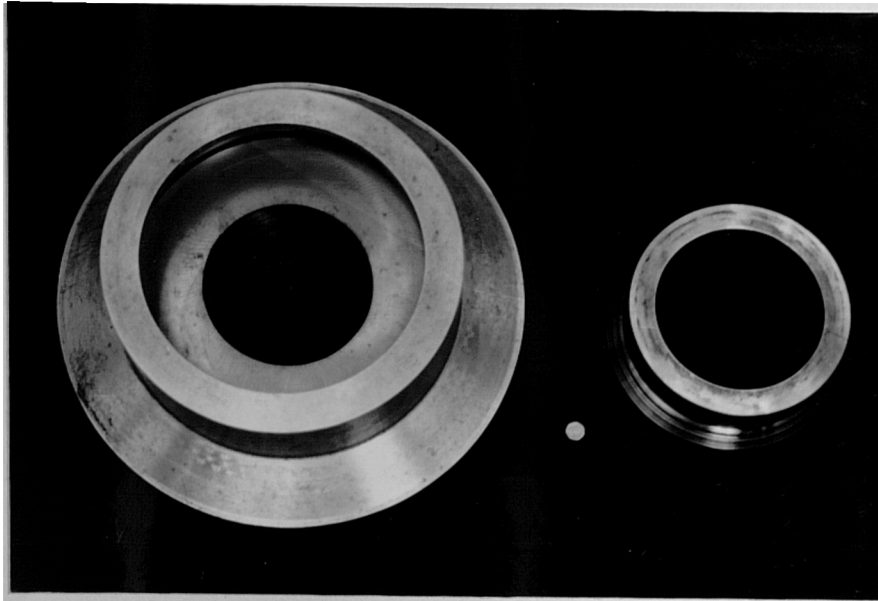


Figure 20: Waspaloy used for machining test

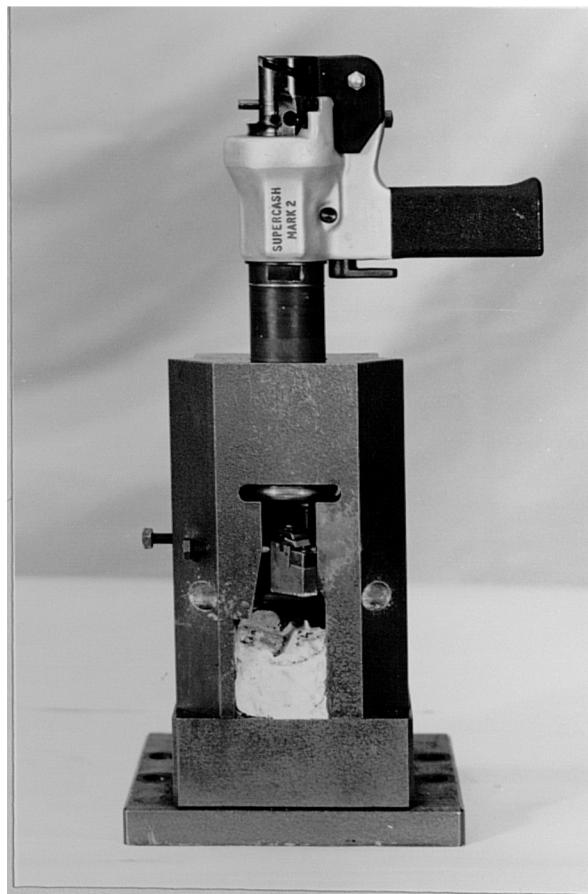


Figure 21: Quick-stop device



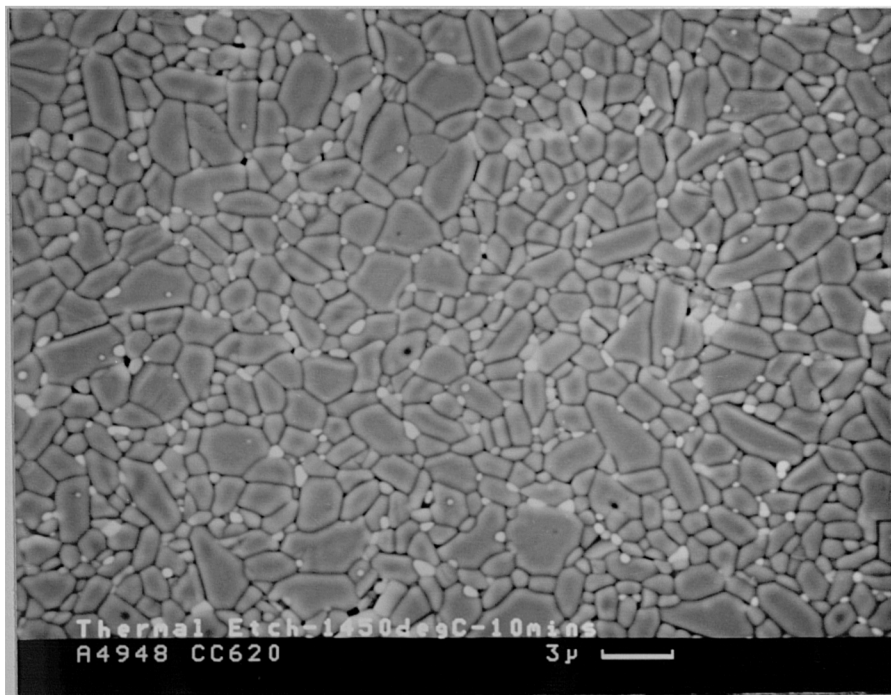


Figure 22: Microstructure of CC620 [courtesy of Sandvik]

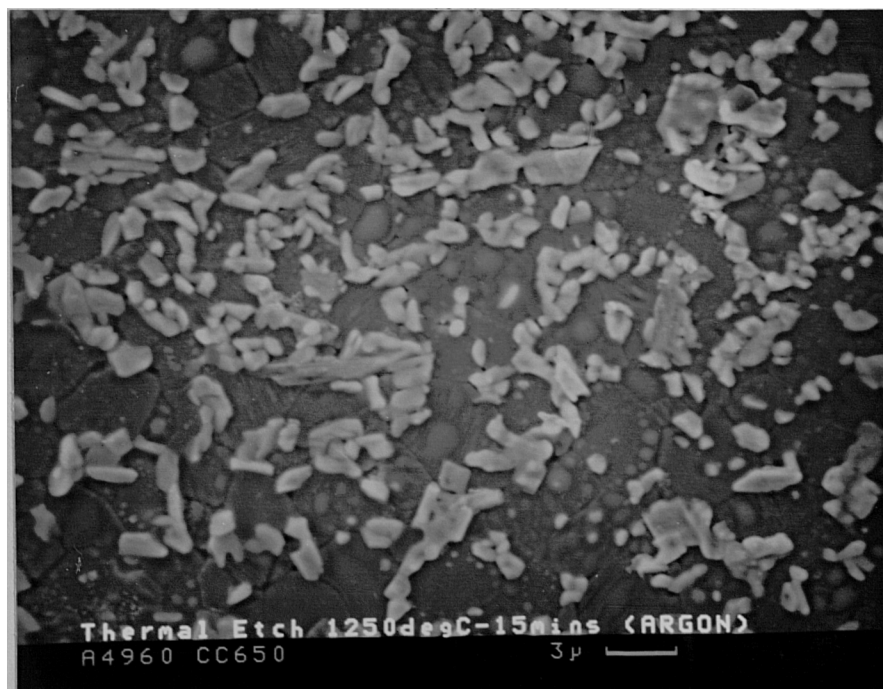


Figure 23: Microstructure of CC650 [courtesy of Sandvik]

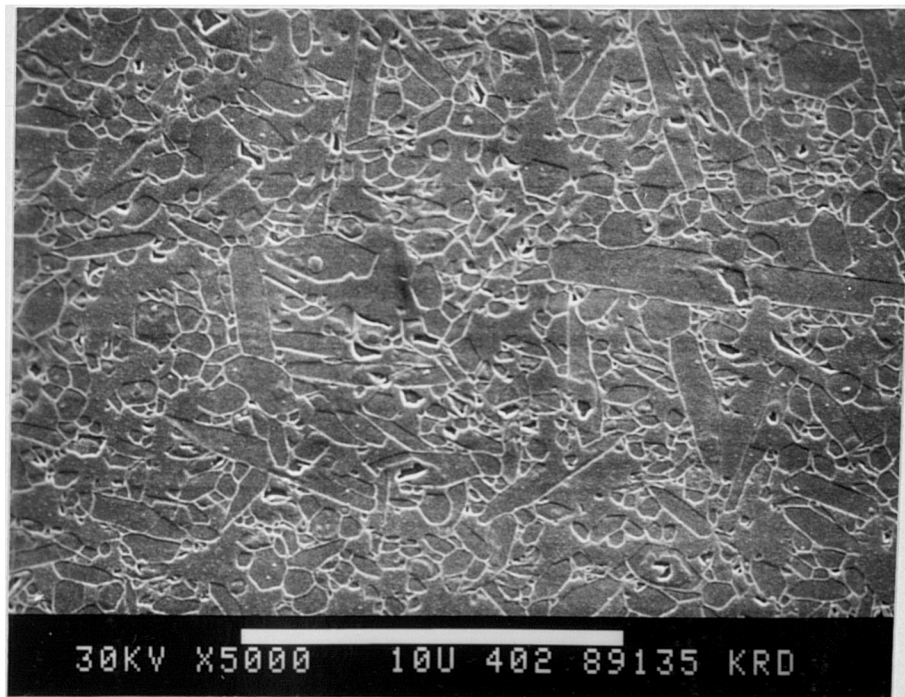


Figure 24: Microstructure of Kyon 2000 [courtesy of Kennametal]



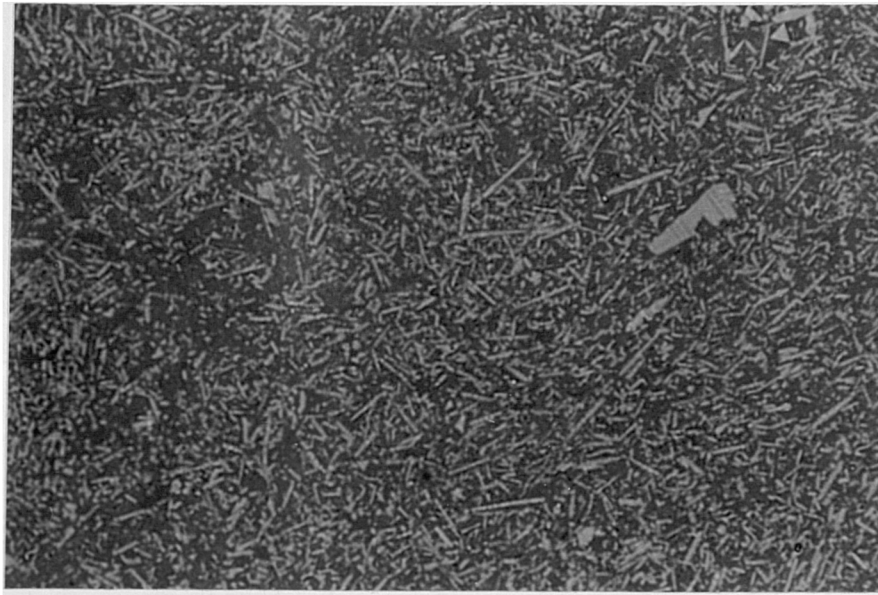


Figure 25: Microstructure of WG-300 (x680)



Figure 26: Fracture surface of WG-300

MACHINING OF WSPALOY WITH OC620  
DOC = 1mm

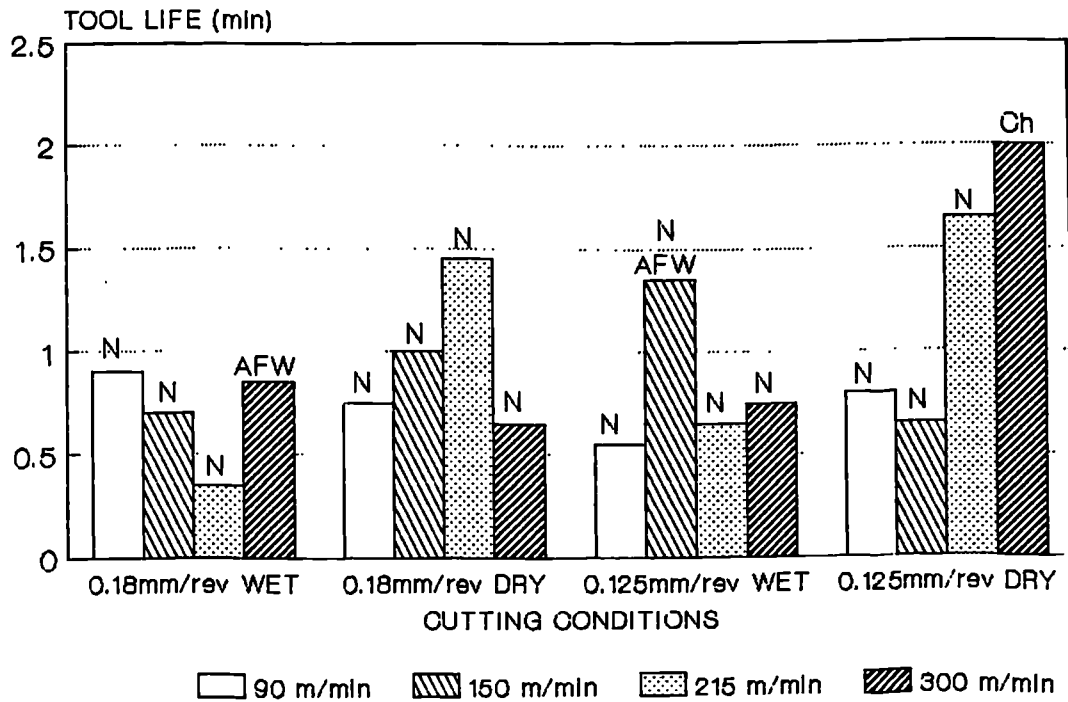


Figure 27

MACHINING OF WSPALOY WITH OC620  
DOC = 1mm

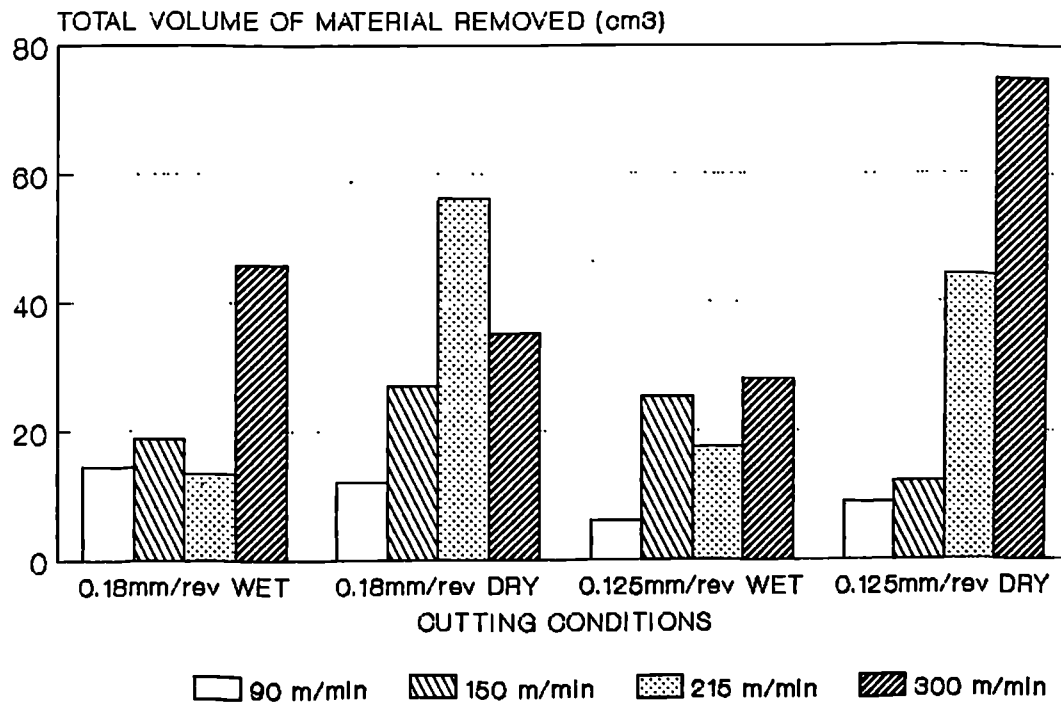


Figure 27a

MACHINING OF WASPALOY WITH OC620  
DOC = 2.5mm

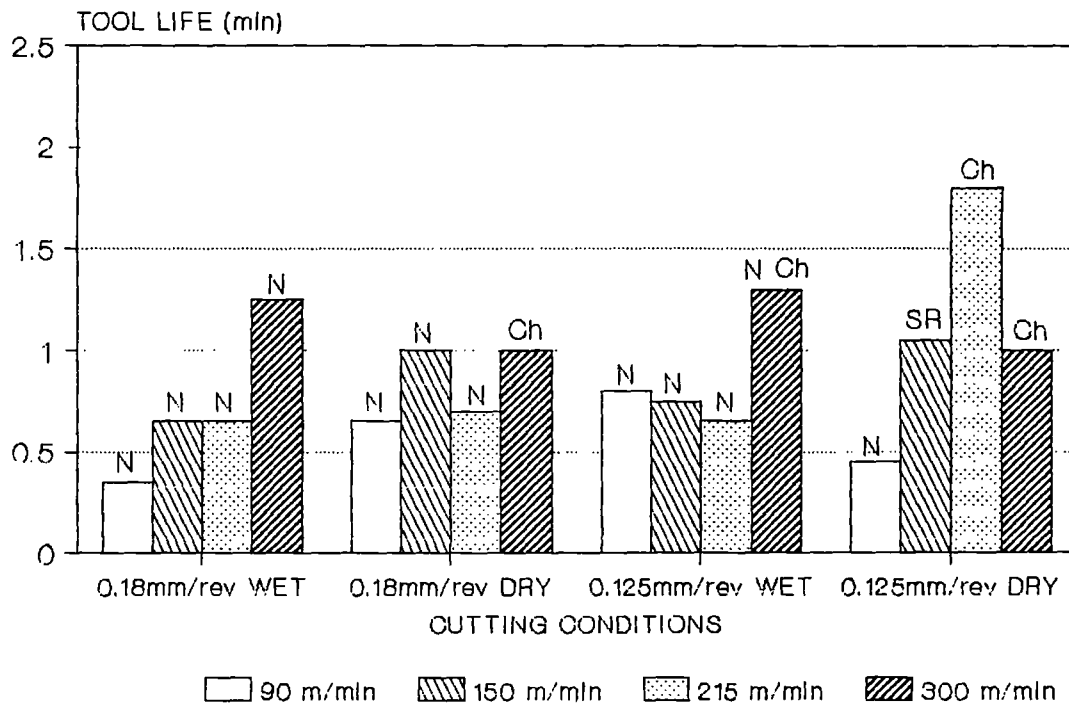


Figure 28

MACHINING OF WASPALOY WITH OC620  
DOC = 2.5mm

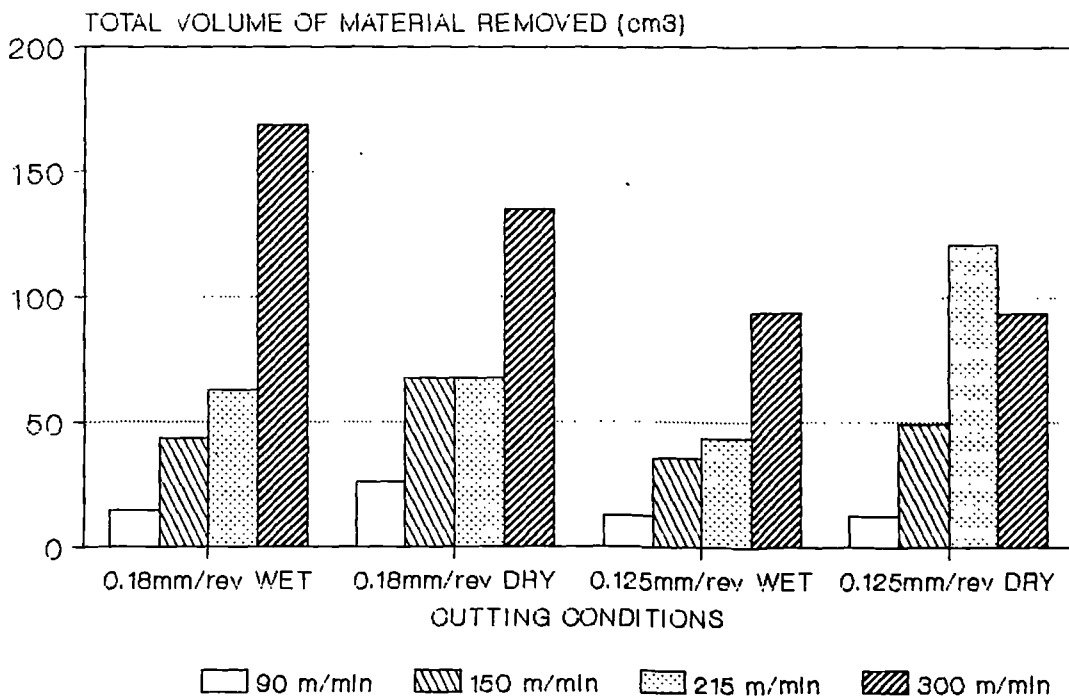


Figure 28a

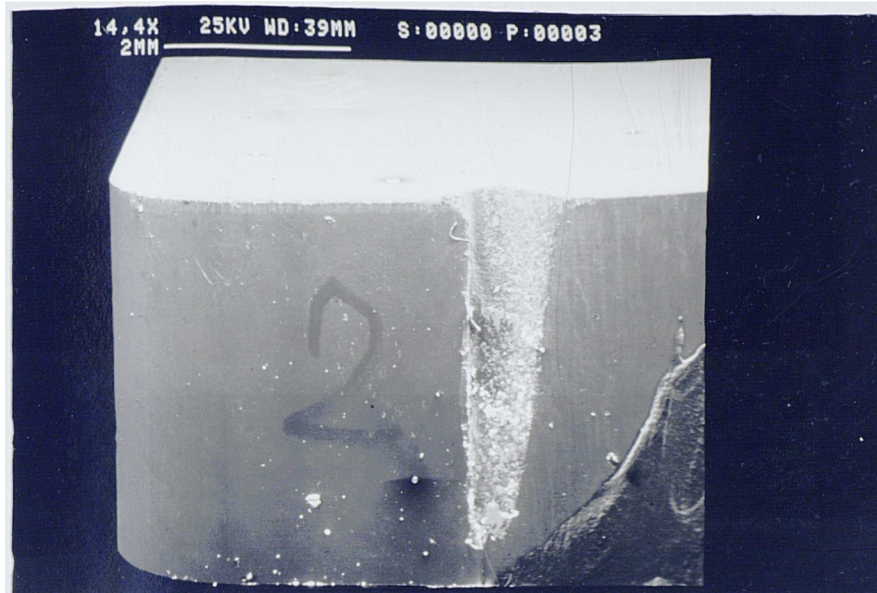


Figure 29: Severe DOC notch on the flank face of CC620 tool used in the dry machining of Waspaloy (V=150m/min, F=0.125mm/rev, DOC=2.5mm)

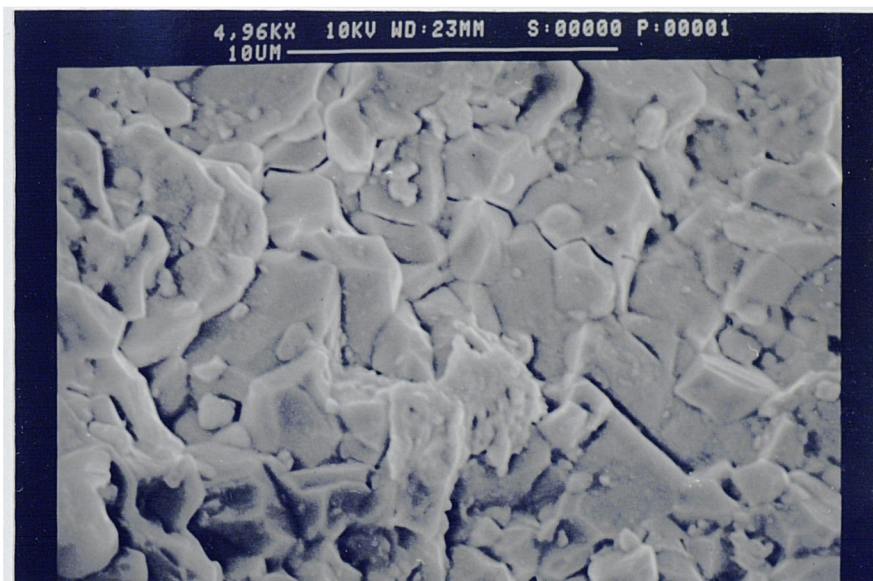


Figure 30: Formation of microcracks on the flank face of CC620 tool when used in dry machining of Waspaloy (V=90m/min, F=0.18mm/rev, DOC=2.5mm)



Figure 31: Formation of cracks running perpendicular to the cutting edge of CC620 tool when used in wet machining of Waspaloy, ( $V=215\text{m/min}$ ,  $F=0.18\text{mm/rev}$ ,  $\text{DOC}=2.5\text{mm}$ )



Figure 32: Formation of cracks running parallel to the cutting edge of CC620 tool used in wet machining of Waspaloy ( $V=300\text{m/min}$ ,  $F=0.18\text{mm/rev}$ ,  $\text{DOC}=2.5\text{mm}$ )

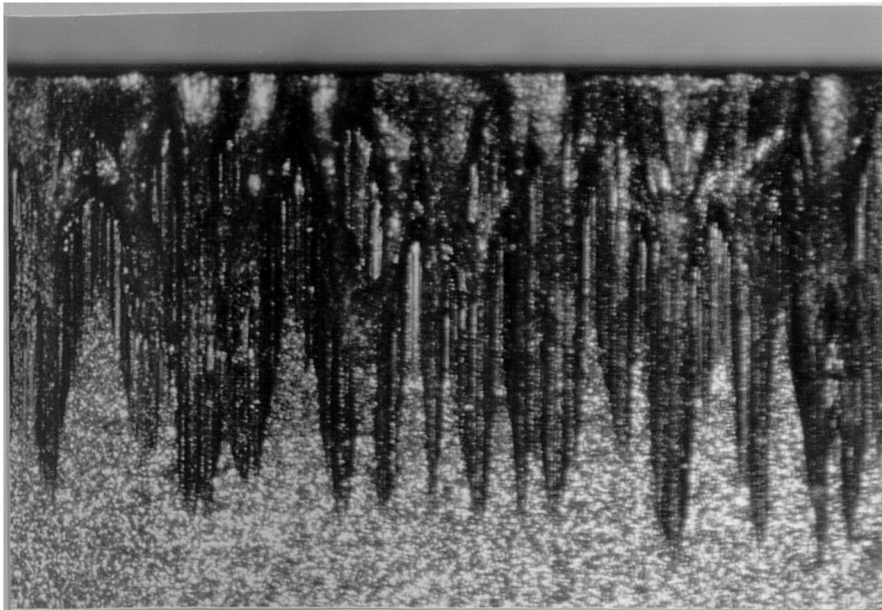


Figure 33: View of the flank face of CC620 tool x90 when used in dry machining of Waspaloy  $V=150\text{ m min}$ ,  $F=0.125\text{ mm/rev}$ ,  $\text{DOC}=2.5\text{ mm}$

MACHINING OF WAPALLOY WITH CO650  
DOC = 1mm

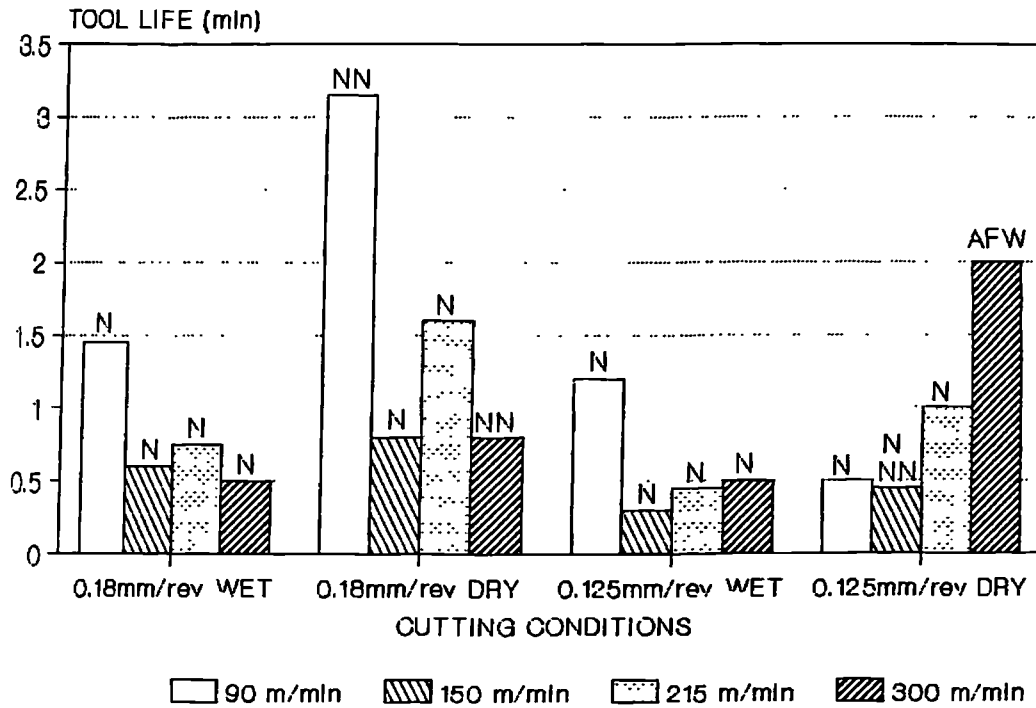


Figure 34

MACHINING OF WAPALLOY WITH CO650  
DOC = 1mm

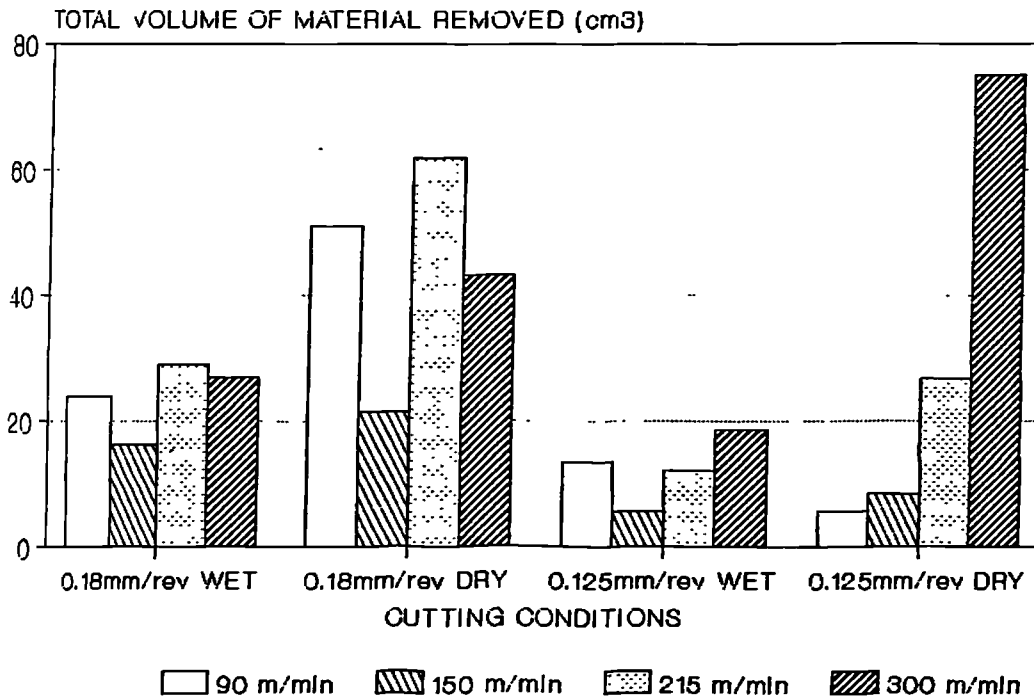


Figure 34a

MACHINING OF WASPALLOY WITH CC650  
DOC = 2.5mm

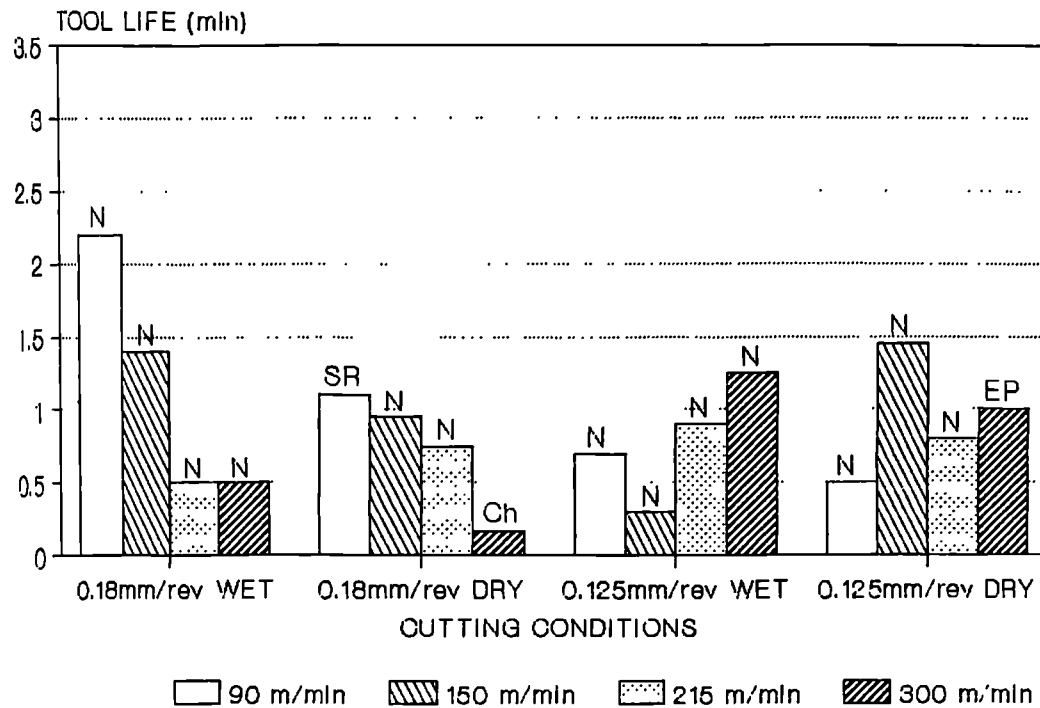


Figure 35

MACHINING OF WASPALLOY WITH CC650  
DOC = 2.5mm

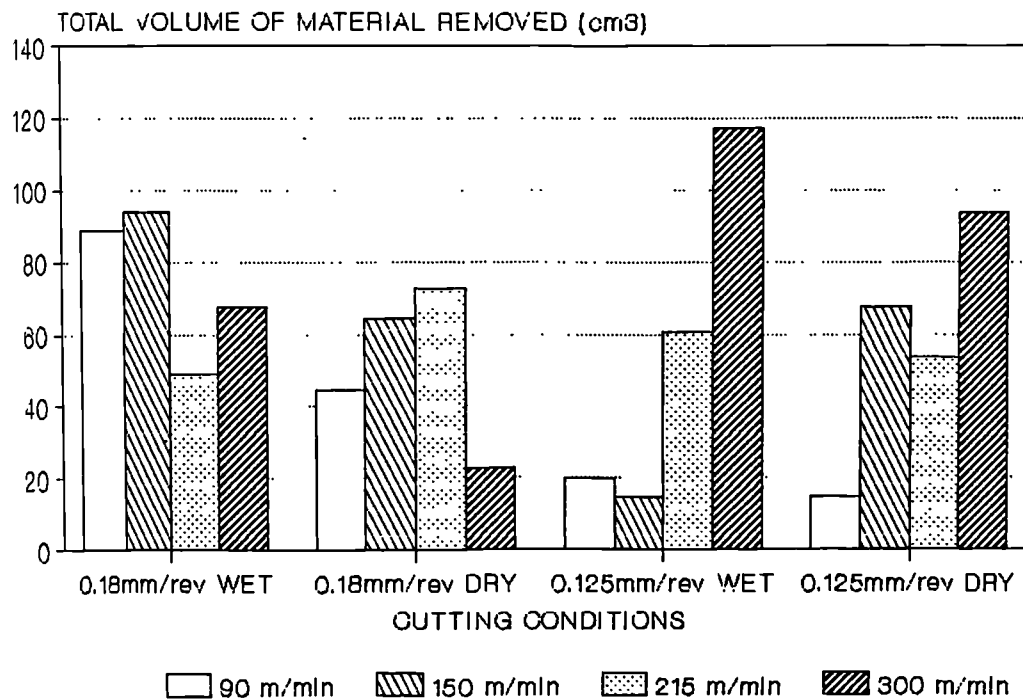


Figure 35a



MACHINING OF WASPALOY WITH CC650  
DOC=1mm, F=0.18mm, WET

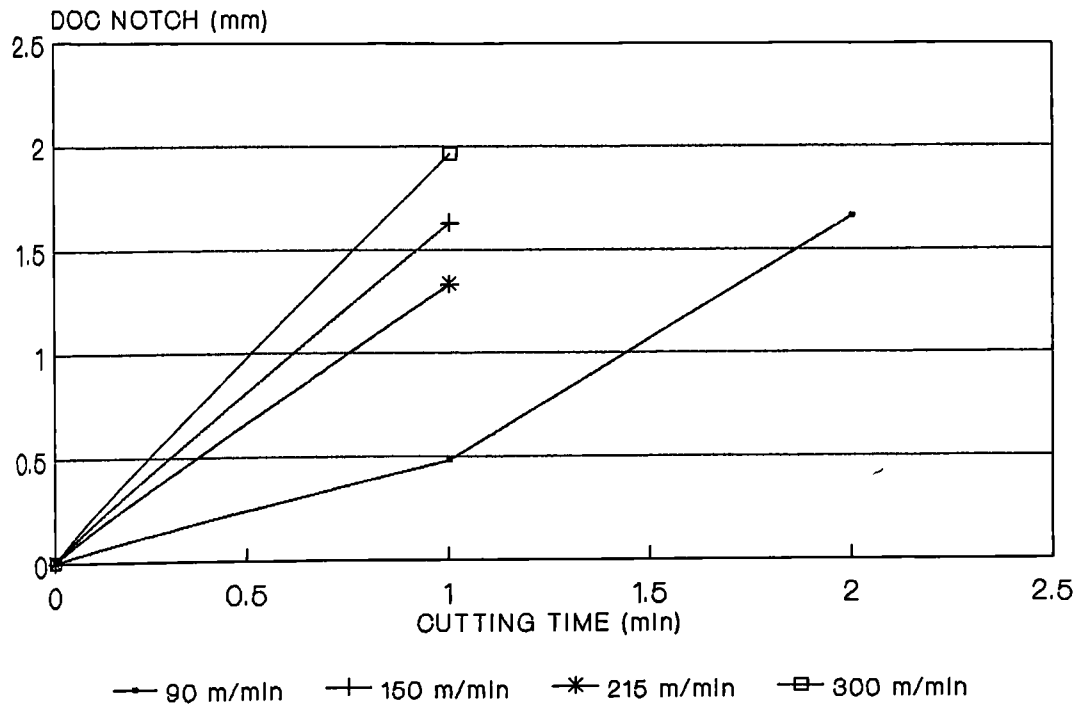


Figure 36

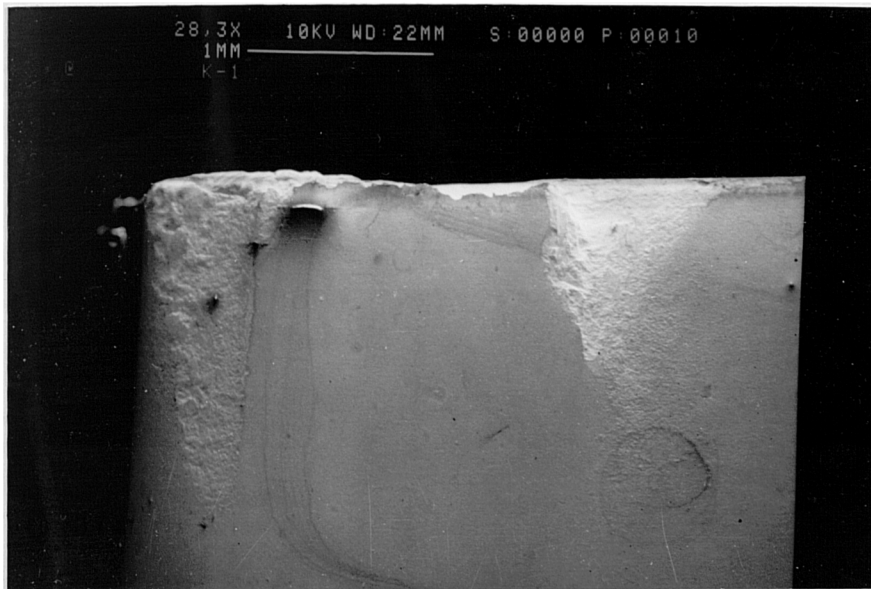


Figure 37: Formation of nose notch when using CC650 tool to machine Waspaloy in the presence of a coolant (V=300m/min, F=0.18mm/rev, DOC=1mm)

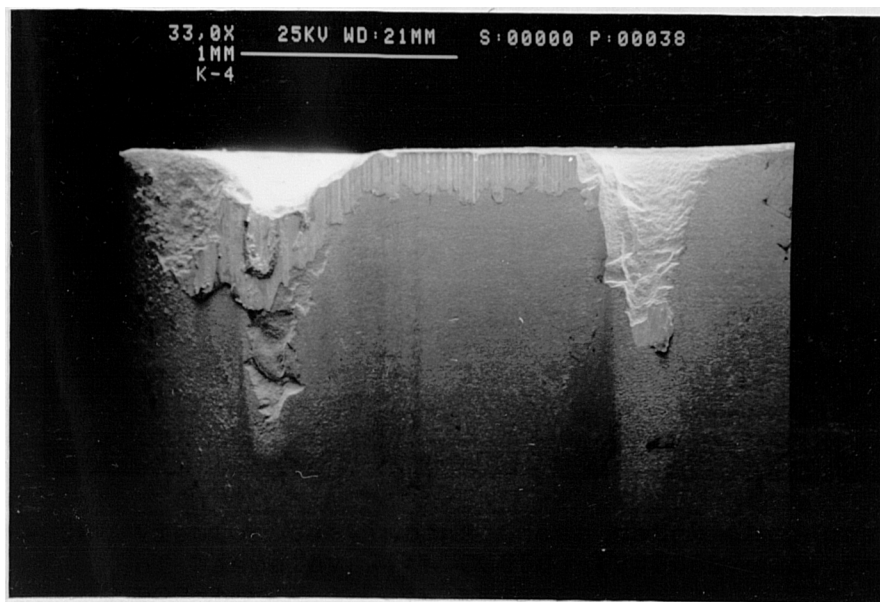


Figure 38: View of the intense nose notch when dry machining of Waspaloy with CC650 ( $V=300\text{m/min}$ ,  $F=0.18\text{mm/rev}$   $\text{DOC}=1\text{mm}$ )



Figure 39: Magnified view of the nose notch (figure above)

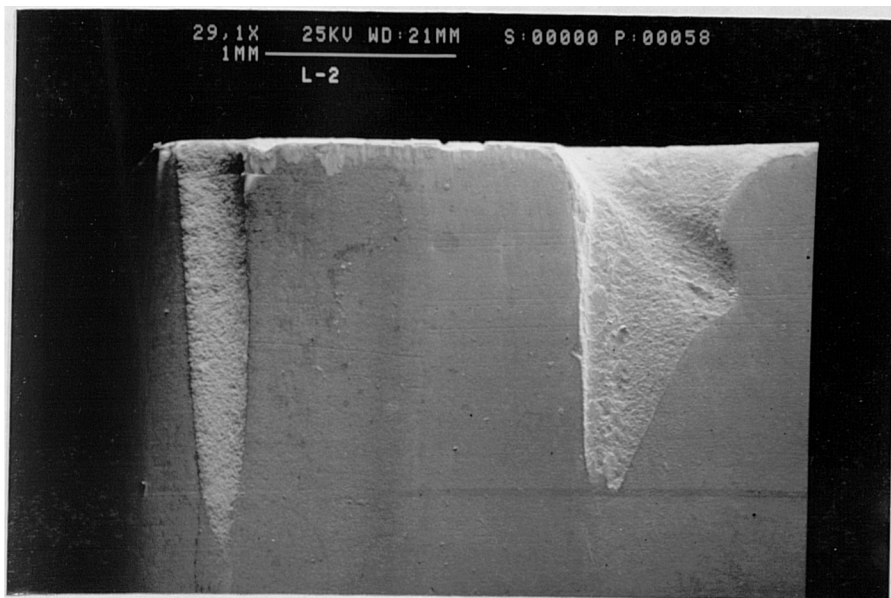


Figure 40: Generation of severe notching at the nose and at the end of DOC on CC650 tool when machining Waspaloy ( $V=150\text{m/min}$ ,  $F=0.125\text{mm/rev}$ ,  $\text{DOC}=1\text{mm}$ )



Figure 41: Wear on CC650 tool used for dry machining of Waspaloy ( $V=300\text{m/min}$ ,  $F=0.125\text{mm/rev}$ ,  $\text{DOC}=1\text{mm}$ )



Figure 42: Magnified view the above photo showing the adhered work material on the DOC notch area

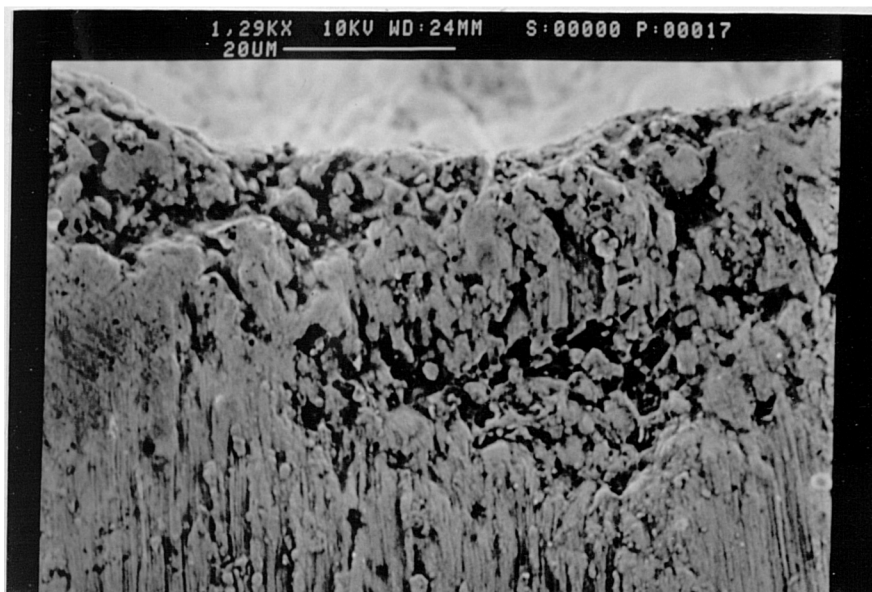


Figure 43: Wear on the CC650 tool used for dry machining of Waspaloy showing loss of particles ( $V=215\text{m/min}$ ,  $F=0.18\text{mm/rev}$ ,  $\text{DOC}=2.5\text{mm}$ )

MACHINING OF WASPALOY WITH KYON 2000  
DOC = 1mm

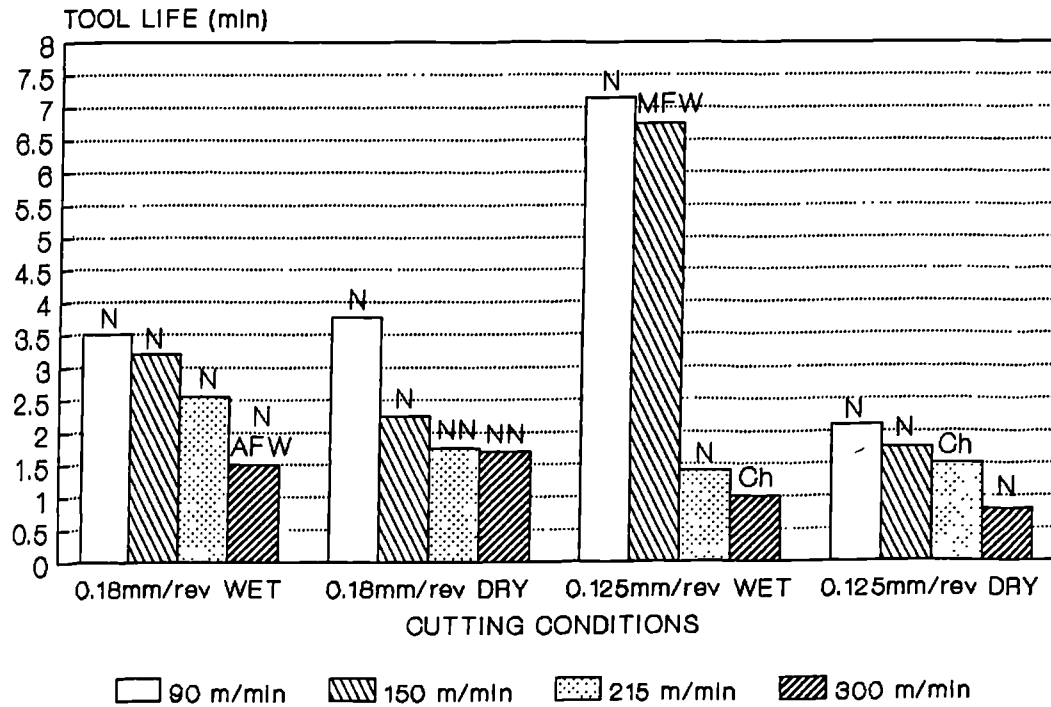


Figure 44

MACHINING OF WASPALOY WITH KYON 2000  
DOC = 1mm

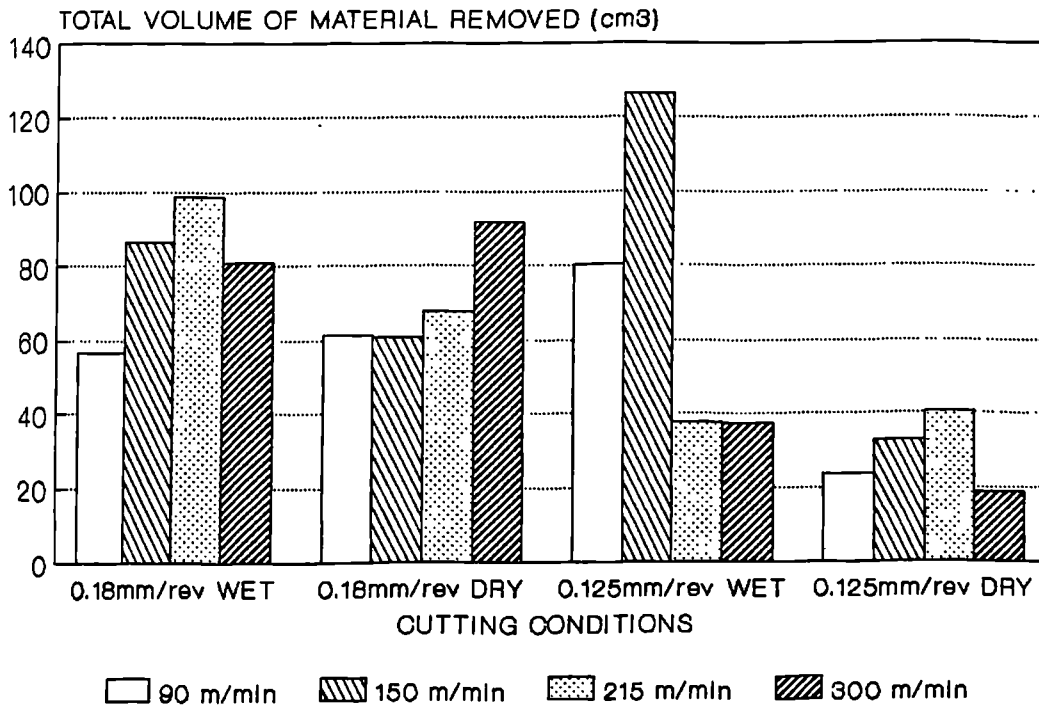


Figure 44a

MACHINING OF WASPALOY WITH KYON 2000  
DOC = 2.5mm

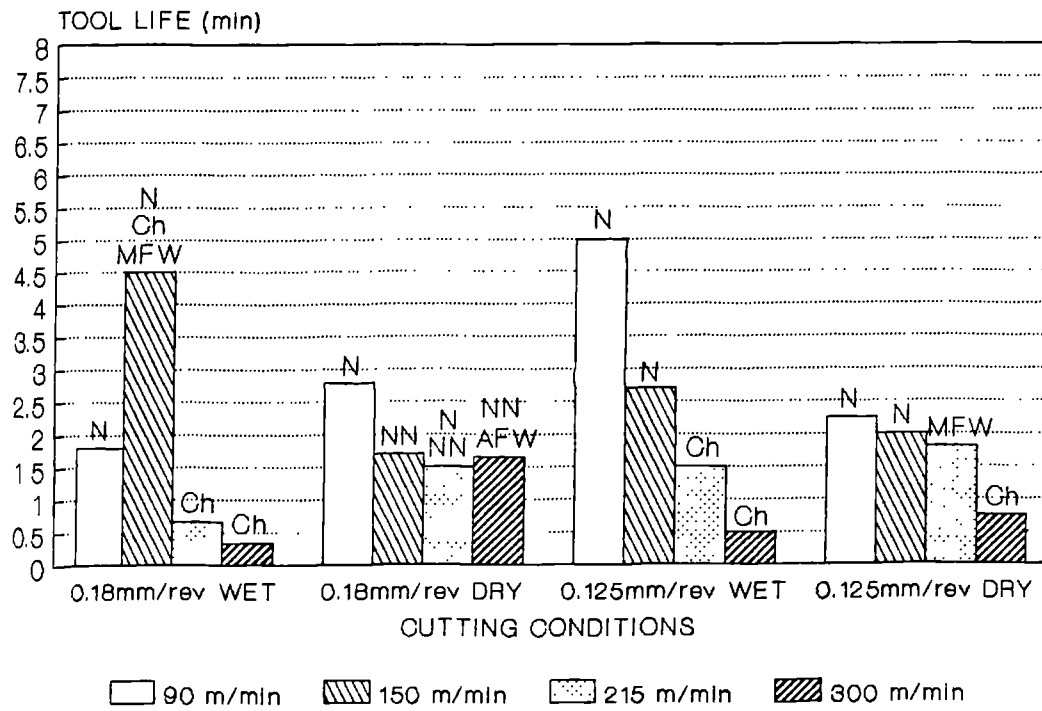


Figure 45

MACHINING OF WASPALOY WITH KYON 2000  
DOC = 2.5 mm

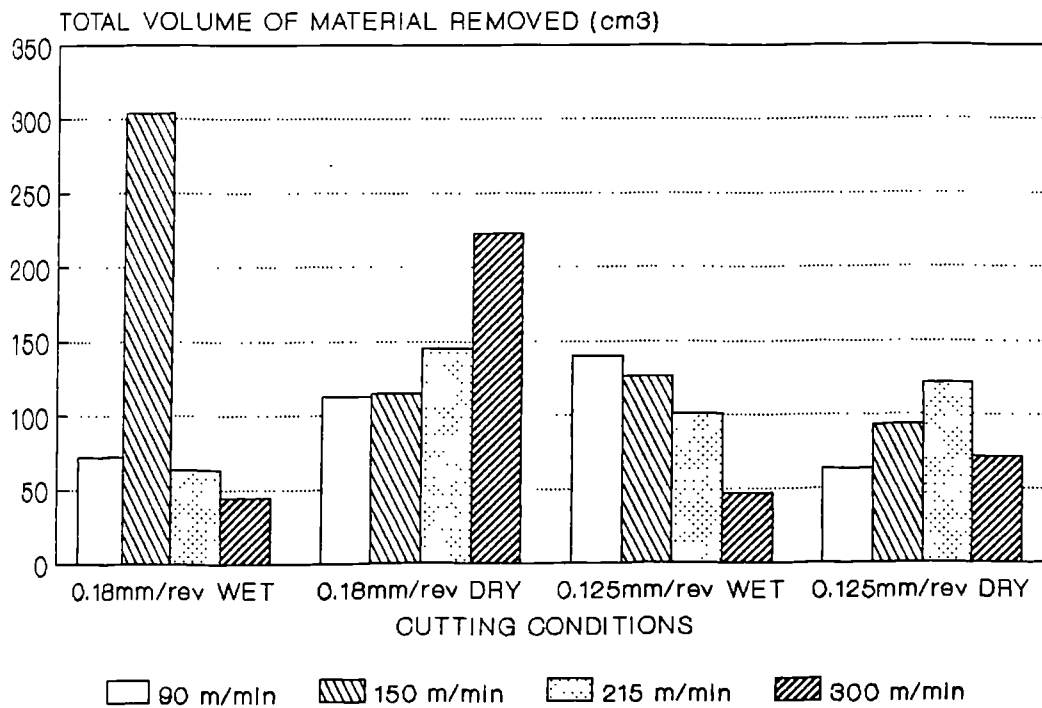


Figure 45a

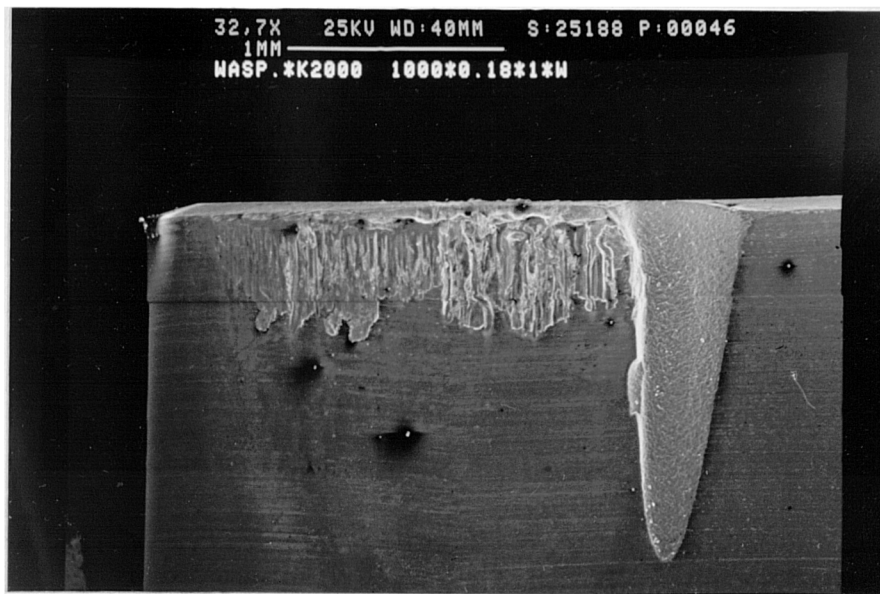


Figure 46: Wear of the flank face of Kyon 2000 tool used for wet machining of Waspaloy ( $V=300\text{m/min}$ ,  $\text{DOC}=1\text{mm}$ ,  $F=0.18\text{mm/rev}$ )

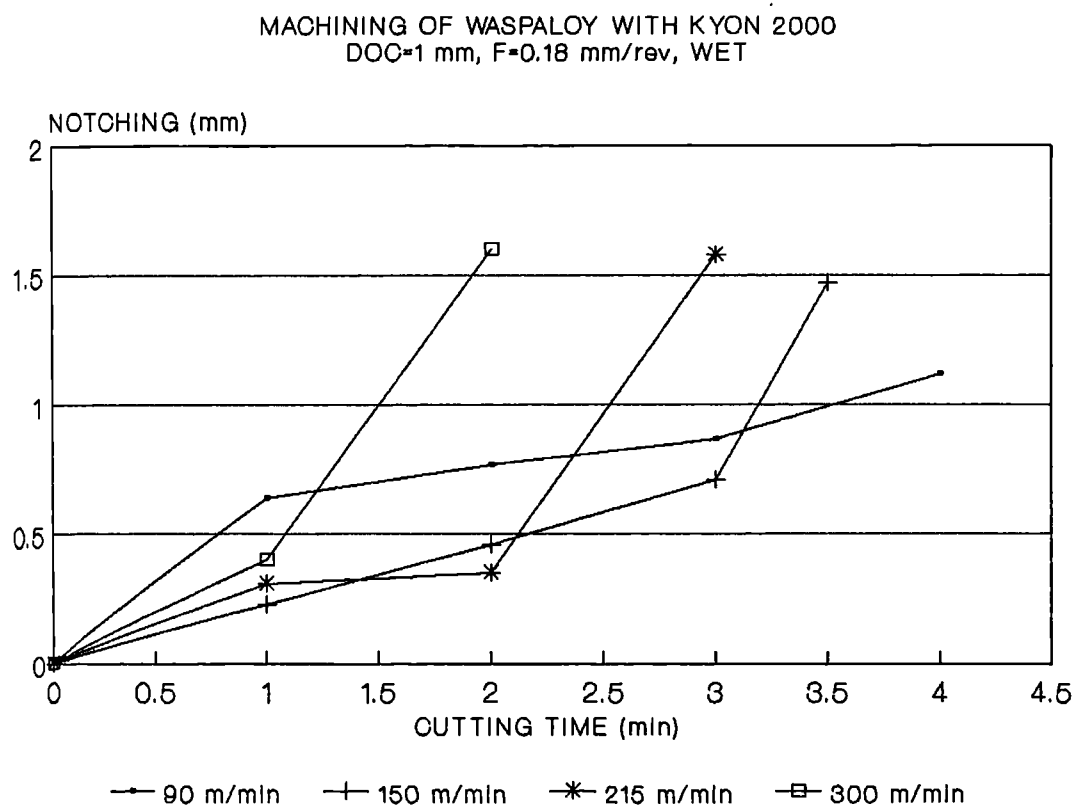


Figure 47



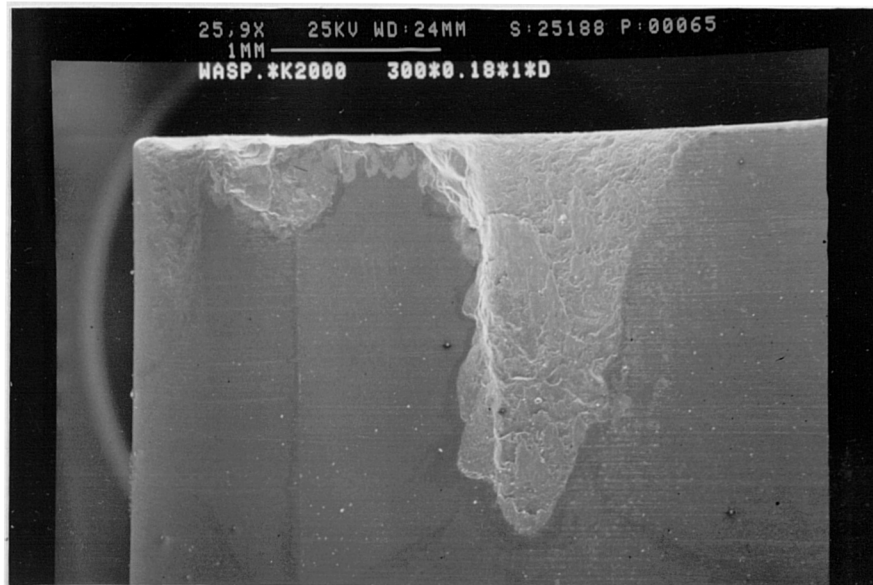


Figure 48: Formation of severe DOCN when dry machining of Waspaloy with CC650 cutting tool ( $V=90\text{m/min}$ ,  $F=0.18\text{mm/rev}$ ,  $\text{DOC}=1\text{mm}$ )

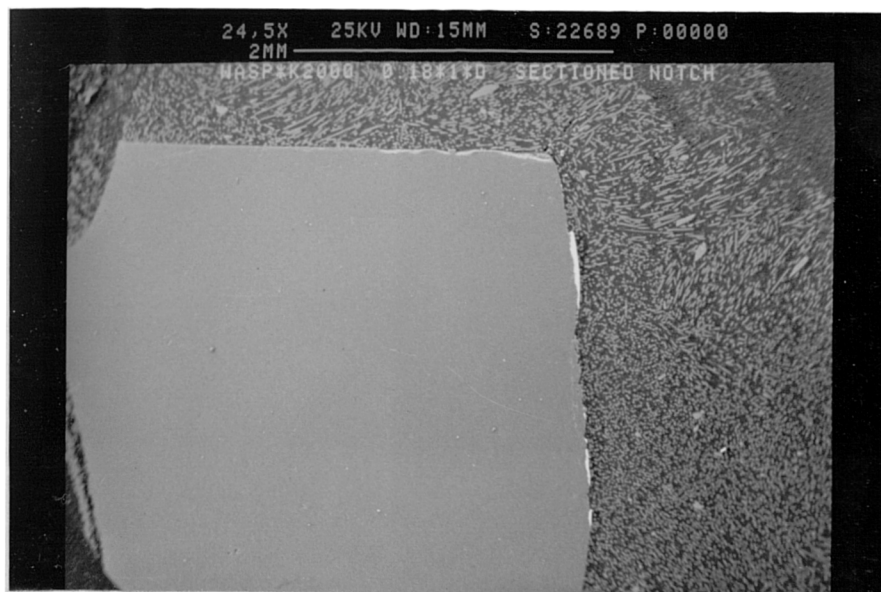


Figure 49a: A cross section at the DOC notch of Kyon 2000 tool showing the adhered Waspaloy (white patches) ( $V=300\text{m/min}$ ,  $F=0.18\text{mm/rev}$ ,  $\text{DOC}=1\text{mm}$ , Dry)

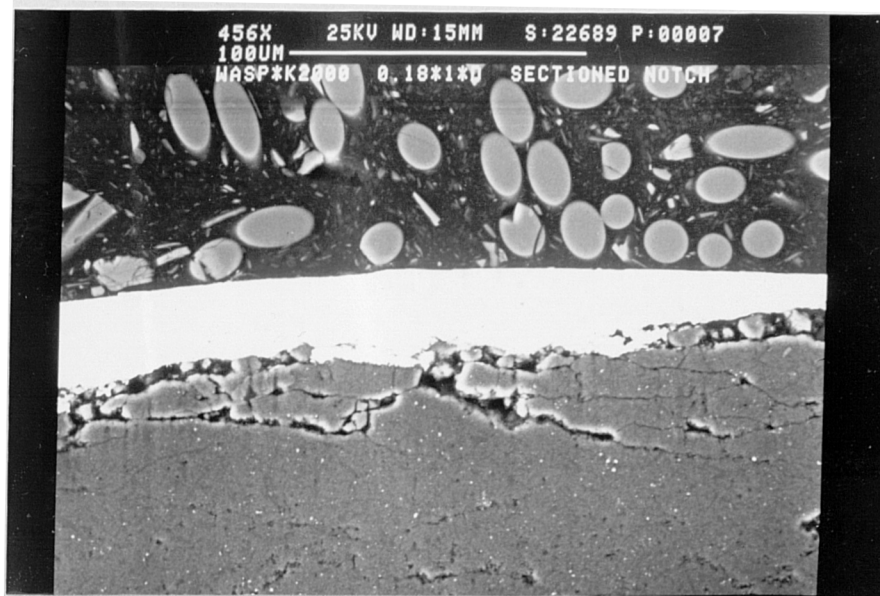


Figure 49b: A higher magnification of figure 49a

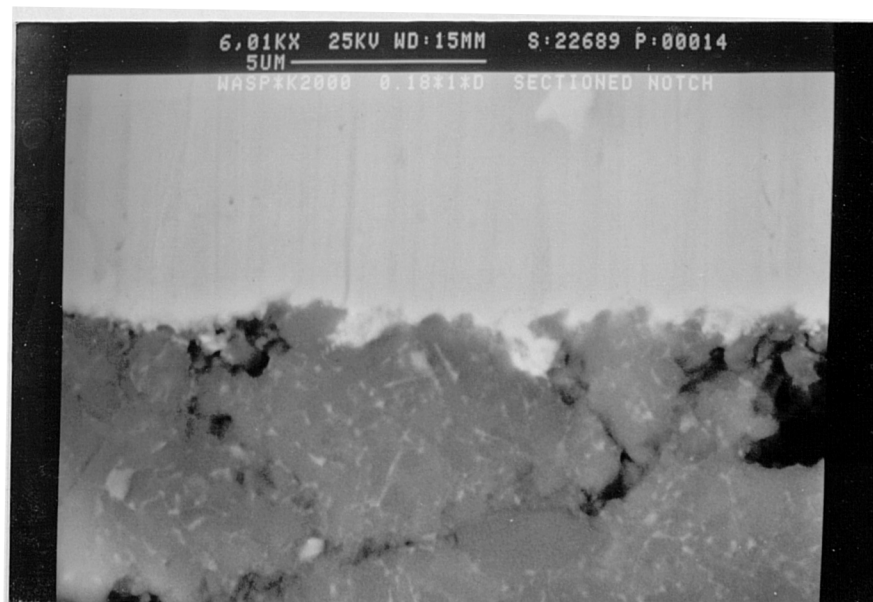


Figure 49c: Magnified view of the interface of the tool and the workpiece layer

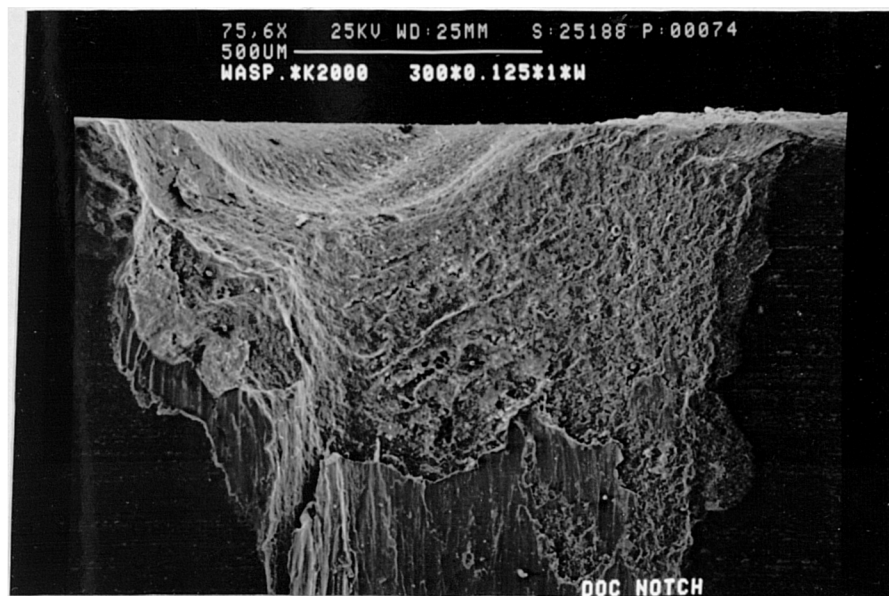


Figure 50: Generated DOC notch after 8 minutes wet machining of Waspaloy with Kyon 2000 ( $V=90\text{m/min}$ ,  $\text{DOC}=1\text{mm}$ ,  $F=0.125\text{mm/rev}$ )

MACHINING OF WASPALOY WITH KYON 2000  
V=90m/min, F=0.125mm/rev, DOC=1mm, WET

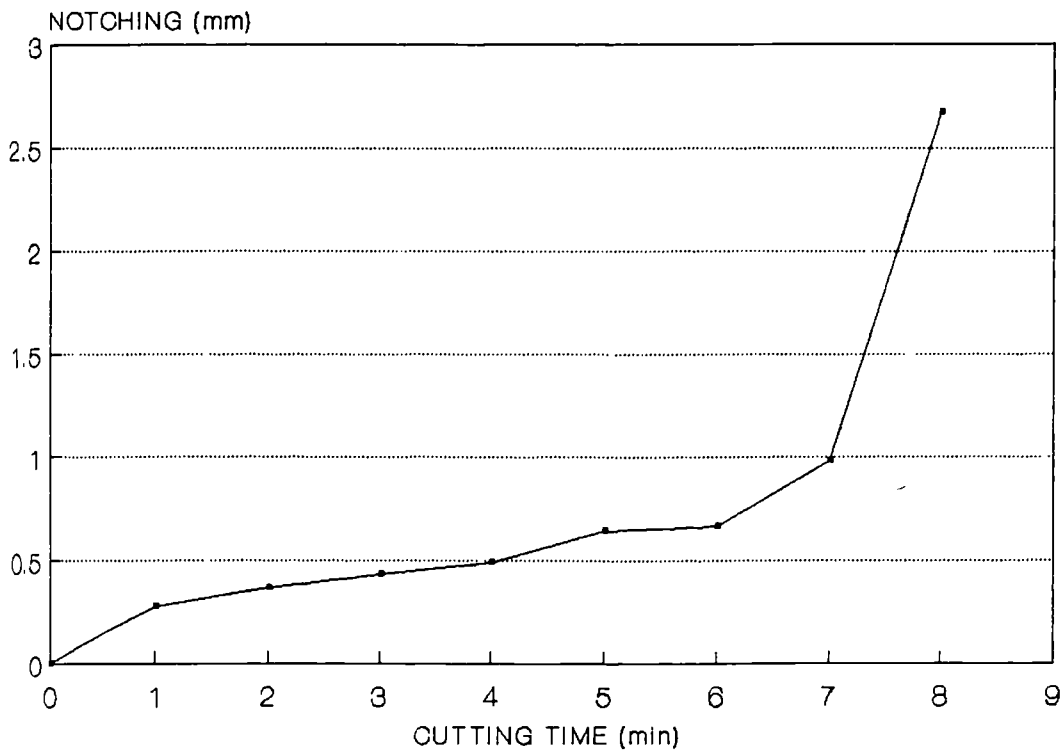


Figure 51

MACHINING OF WASPALOY WITH KYON 2000  
V=150m/min, F=0.125mm/rev, DOC=1mm, WET

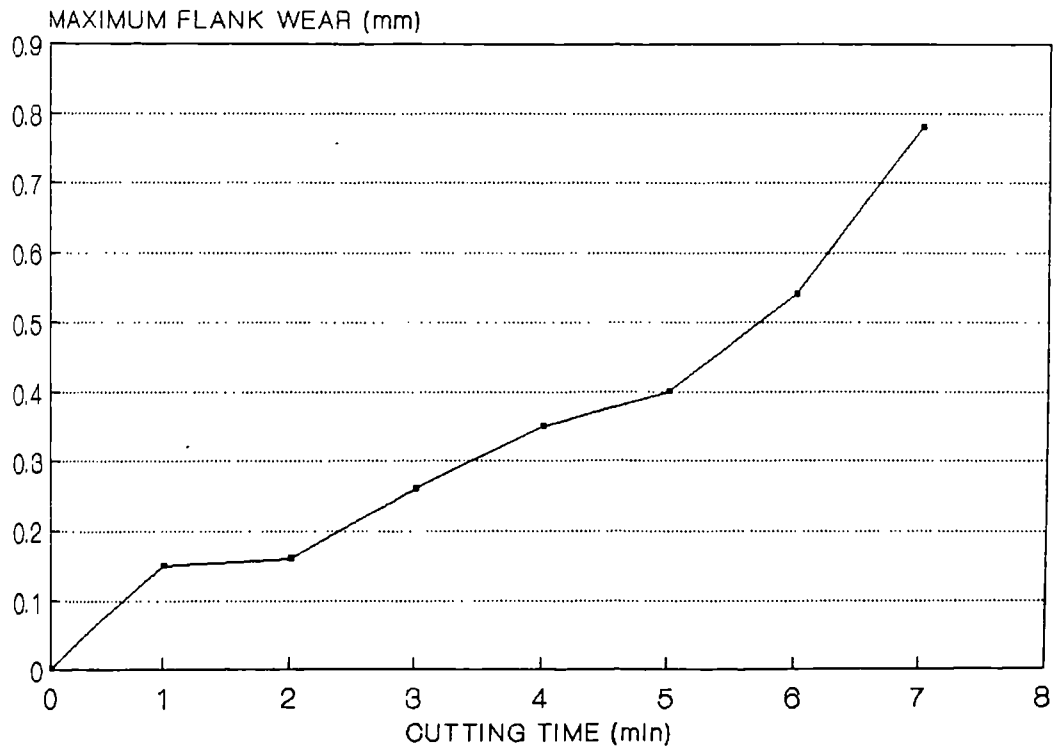


Figure 52

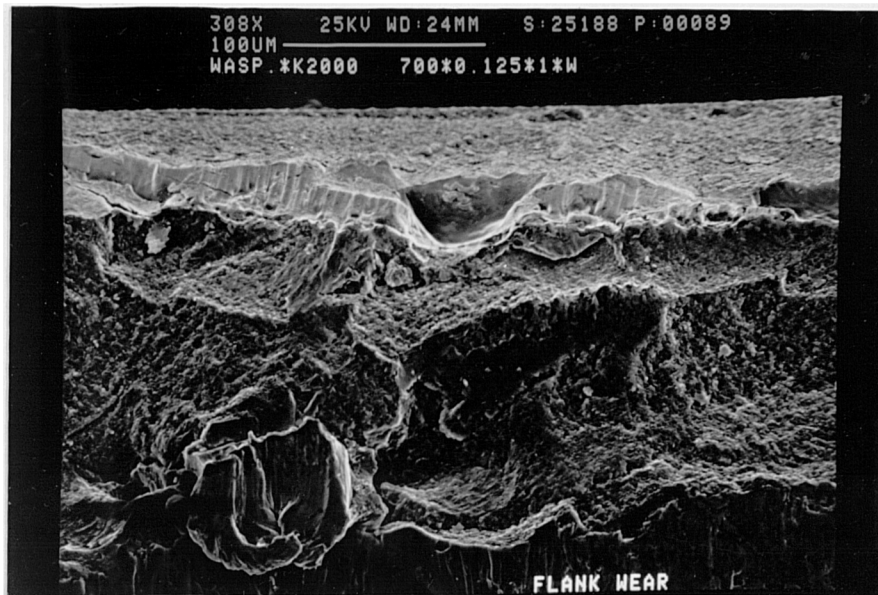


Figure 53: Crack on the honed area running parallel to the cutting edge of Kyon 2000 used to machine Waspaloy, (V=90m/min, F=0.18mm/rev, DOC=1mm)

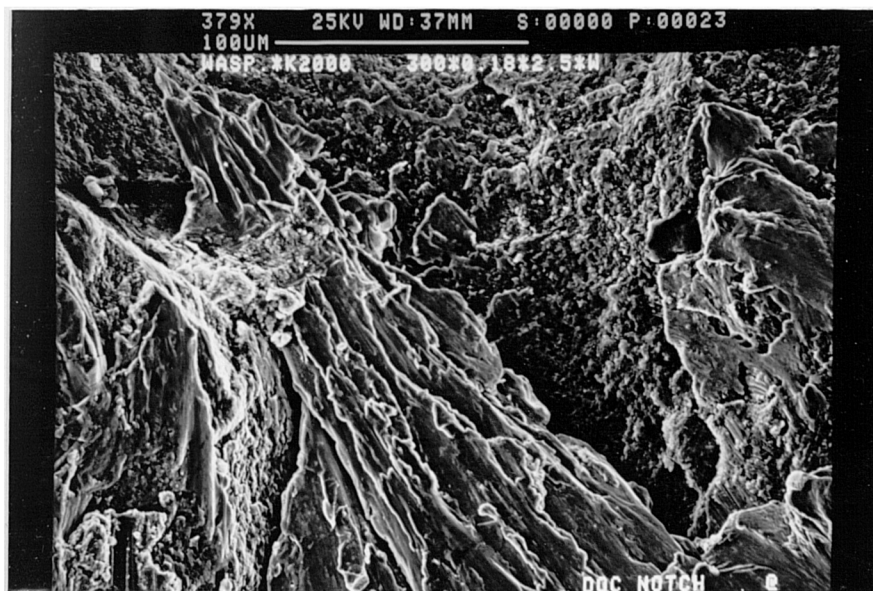


Figure 54: Adhered Waspaloy on DOC notch area of Kyon 2000 (V=90m/min, F=0.18mm/rev, DOC=2.5mm)





Figure 55: Generated cracks on the DOC notch area of Kyon 2000 used to machine Waspaloy, (V=90m/min, F=0.18mm/rev, DOC=2.5mm, Wet)

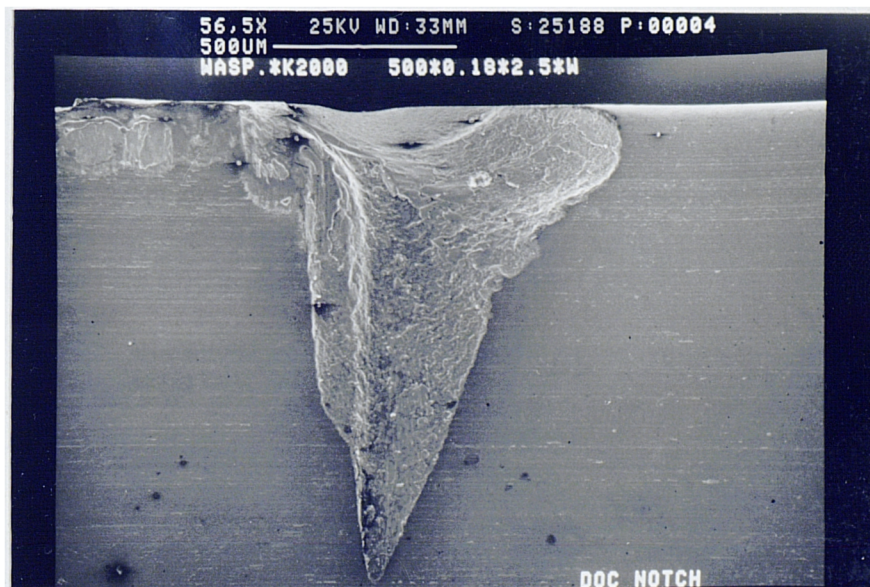


Figure 56: End of DOC notch on Kyon 2000 tool after wet machining of Waspaloy (V=150m/min, DOC=2.5mm, F=0.18mm/rev)

MACHINING OF WASPALOY WITH KYON 2000  
 $V=150\text{m/min}$ ,  $\text{DOC}=2.5\text{mm}$ ,  $F=0.18\text{mm/rev}$ , WET

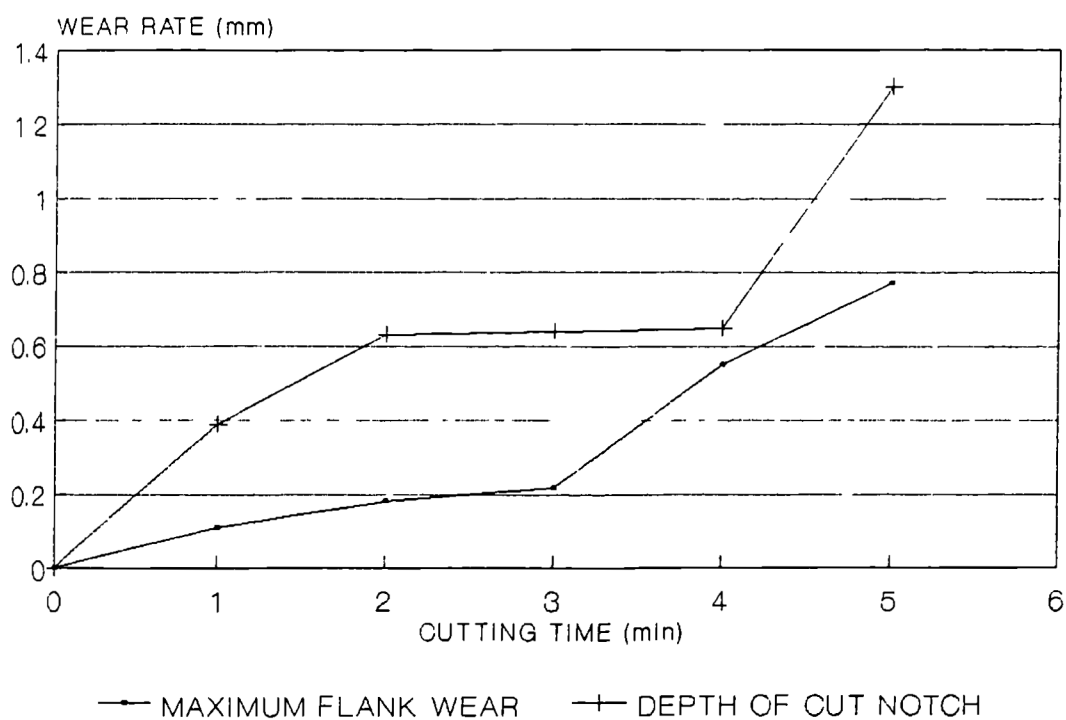


Figure 57

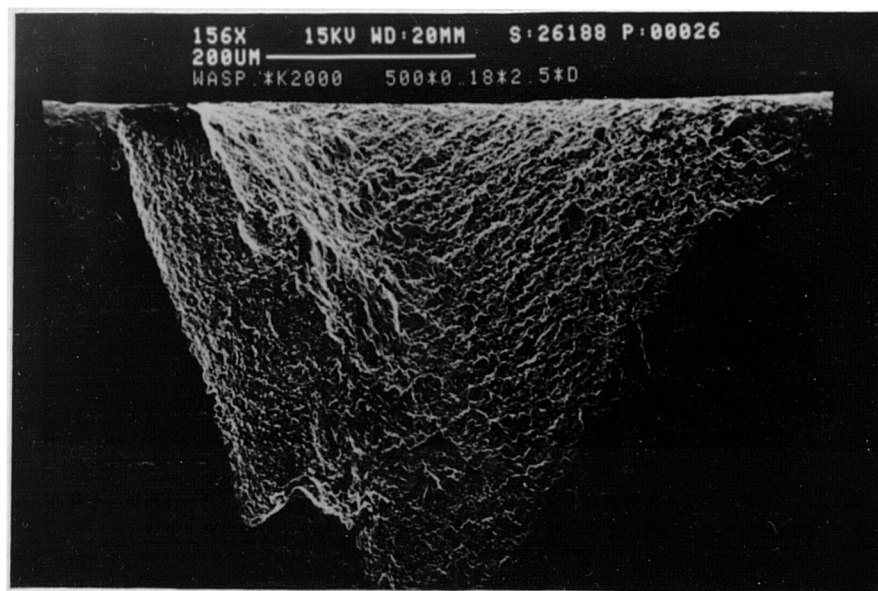


Figure 58: Notch wear of Kyon 2000 used to machine Waspaloy  
 $(V=150\text{m/min}$ ,  $F=0.18\text{mm/rev}$ ,  $\text{DOC}=2.5\text{mm}$ , Dry)

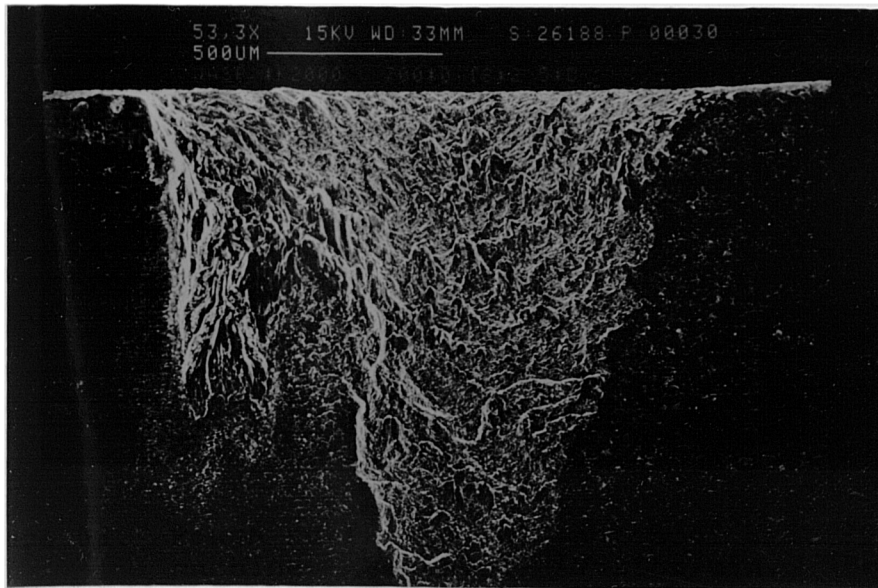


Figure 59: Rough surface of DOC notch of Kyon 2000 used to machine Waspaloy (V=215m/min, F=0.18mm/rev, DOC=2.5mm, Dry)

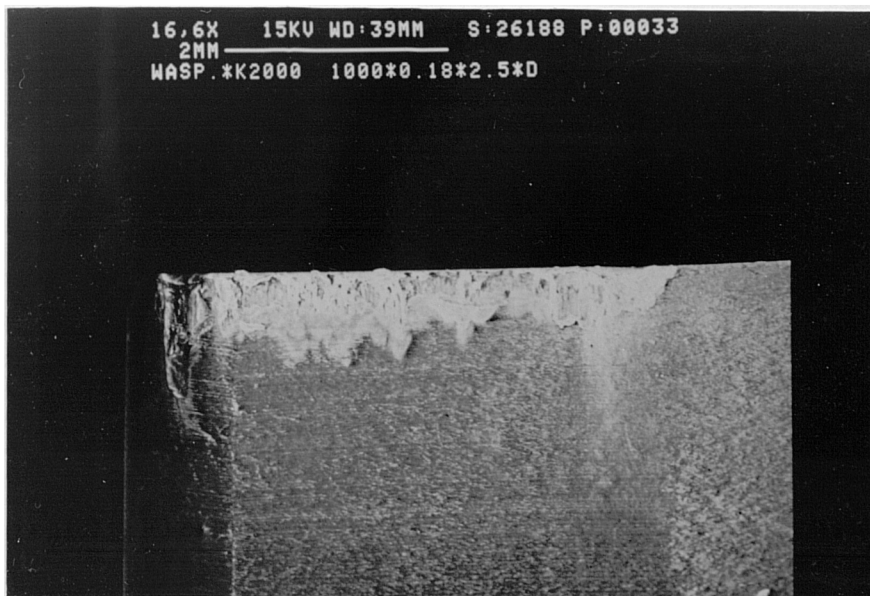


Figure 60: Flank wear of Kyon 2000 used to machine Waspaloy (V=300m/min, F=0.18mm/rev, DOC=2.5mm, Dry)



MACHINING OF WASPALOY WITH WG300  
DOC = 1mm

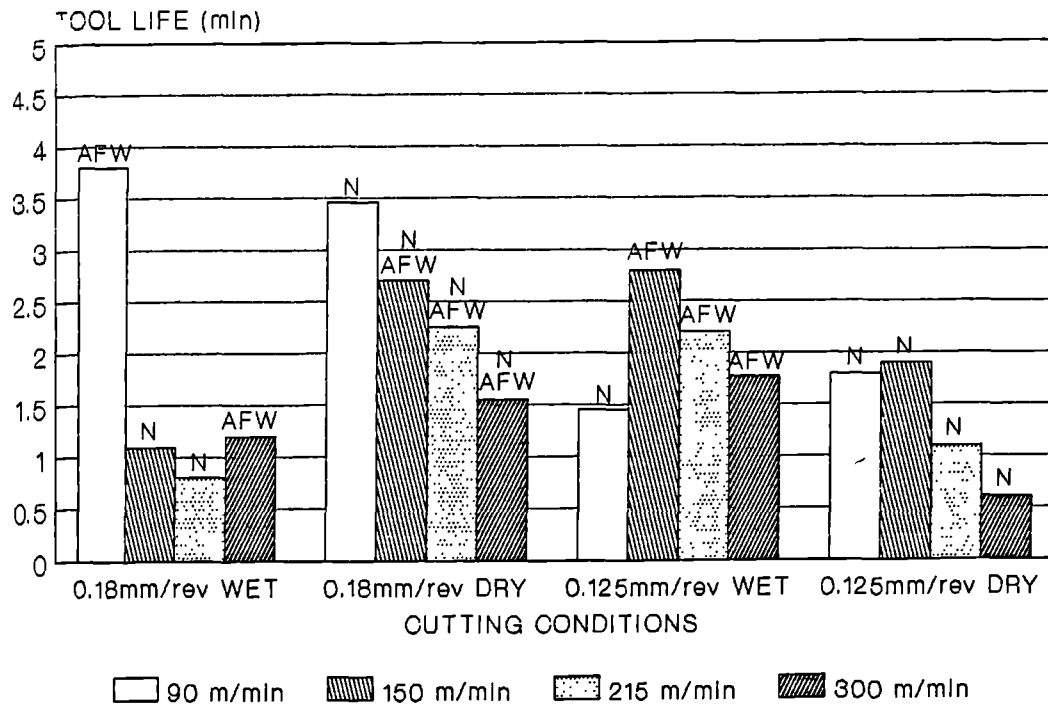


Figure 61

MACHINING OF WASPALOY WITH WG300  
DOC = 1mm

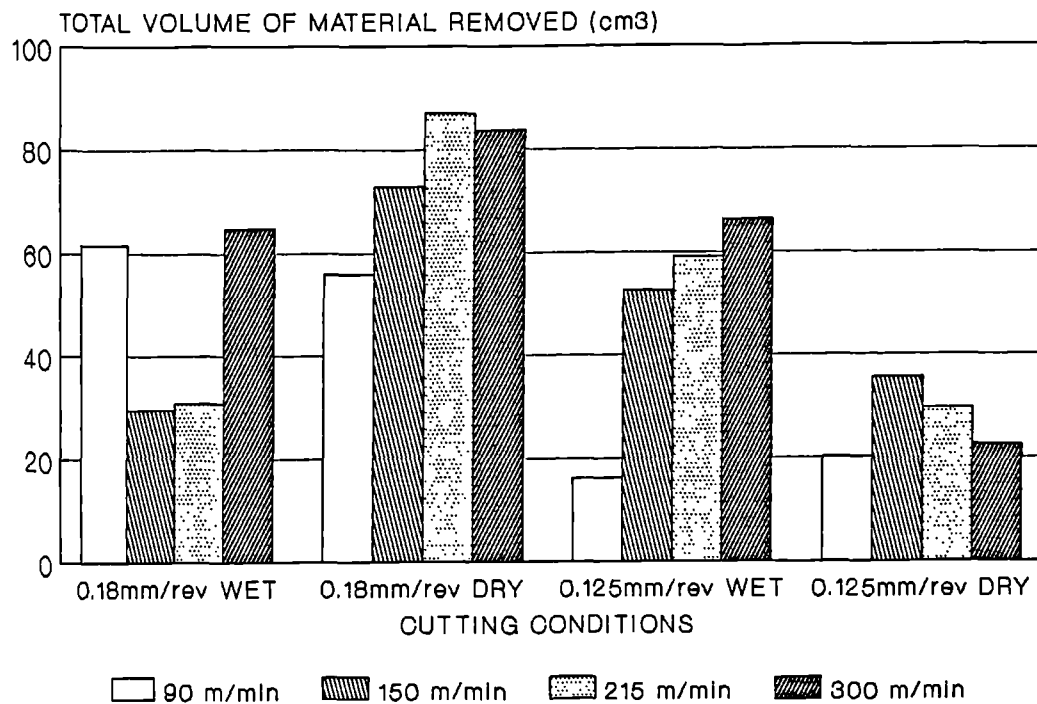


Figure 61a

MACHINING OF WSPALOY WITH WG300  
DOC = 2.5mm

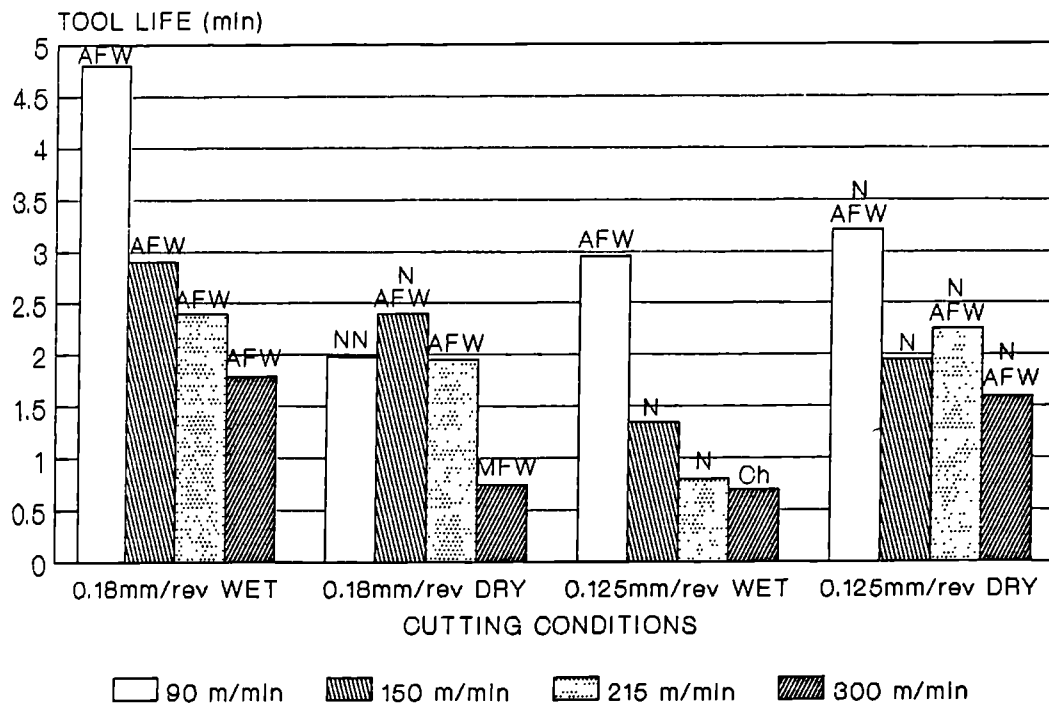


Figure 62

MACHINING OF WSPALOY WITH WG300  
DOC = 2.5mm

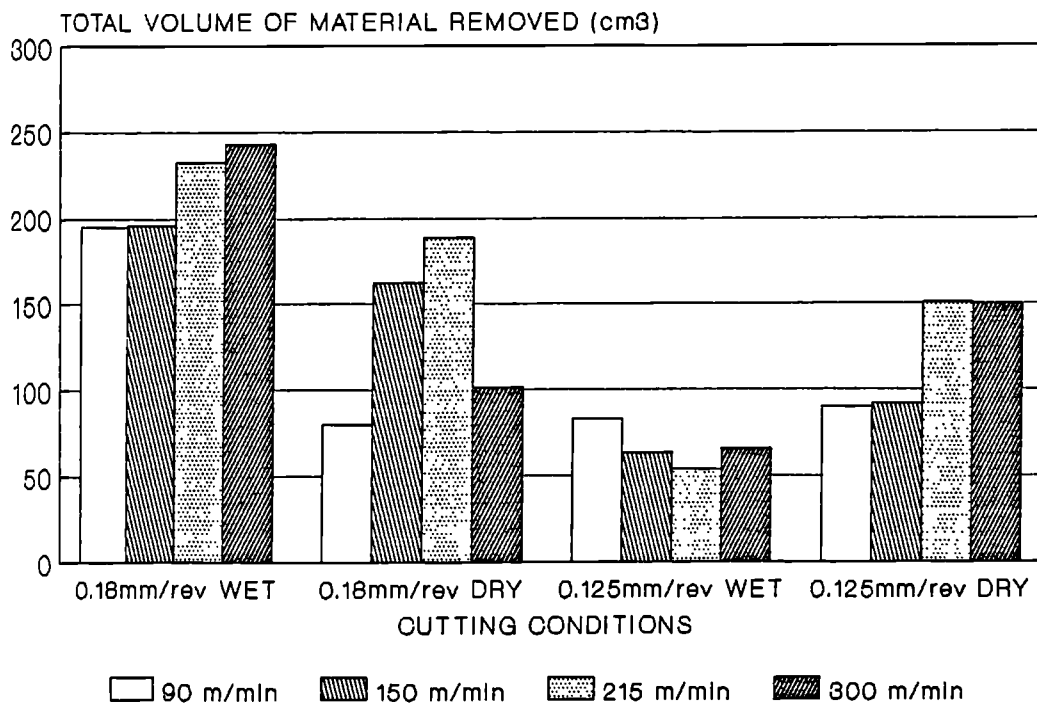


Figure 62a

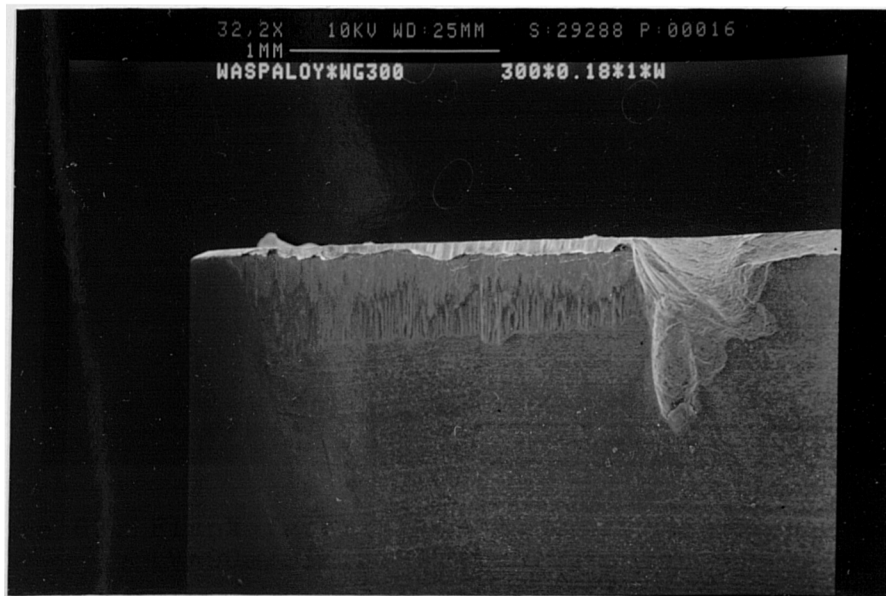


Figure 63: Flank face of WG-300 used to machine Waspaloy  
( $V=90\text{m/min}$ ,  $F=0.18\text{mm/rev}$ ,  $\text{DOC}=1\text{mm}$ , Wet)



Figure 64: View of the adhered Waspaloy on the DOC notched area of WG-300 tool which is ready to be removed (V=300m/min, F=0.18mm/rev, DOC=1mm)

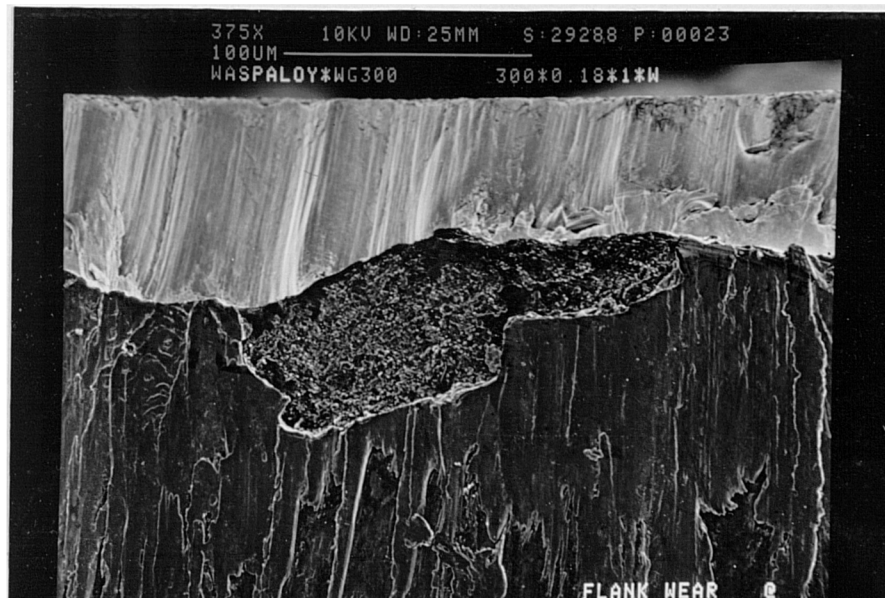


Figure 65: Attrition wear on the flank face of WG-300, same machining conditions as previous figure

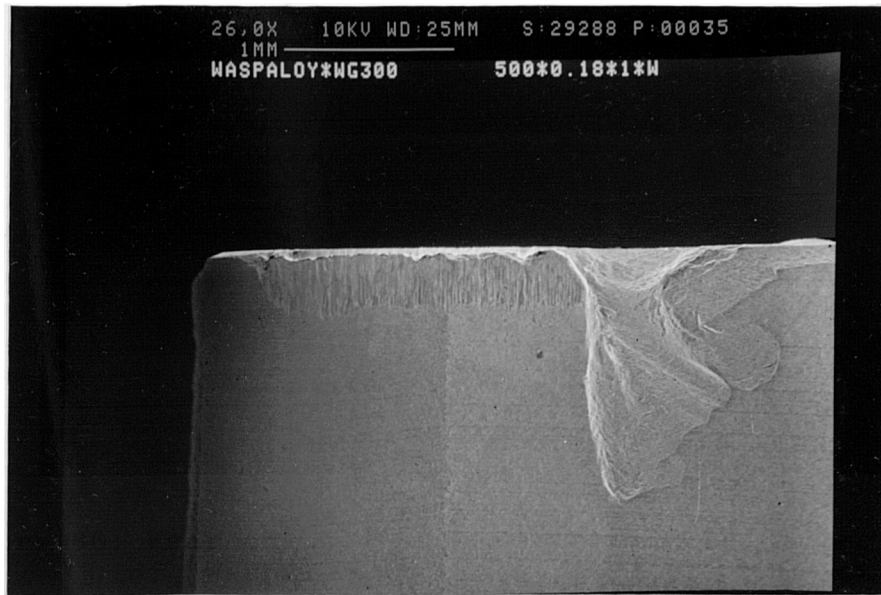


Figure 66: Wear on the flank face of WG-300 after machining of Waspaloy, (V=150m/min, F=0.18mm/rev, DOC=1mm, Wet)

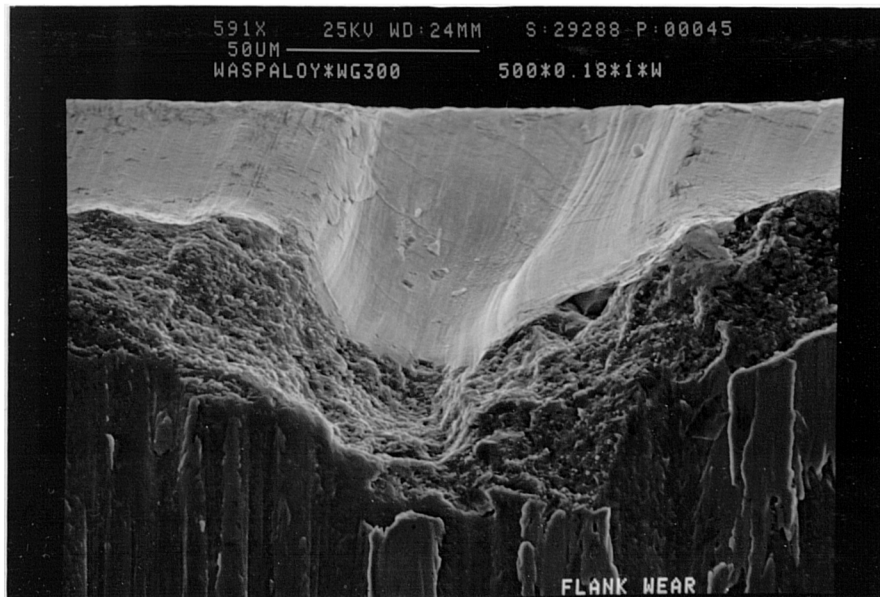


Figure 67: Magnified view of figure 66 showing the smooth and rough surfaces

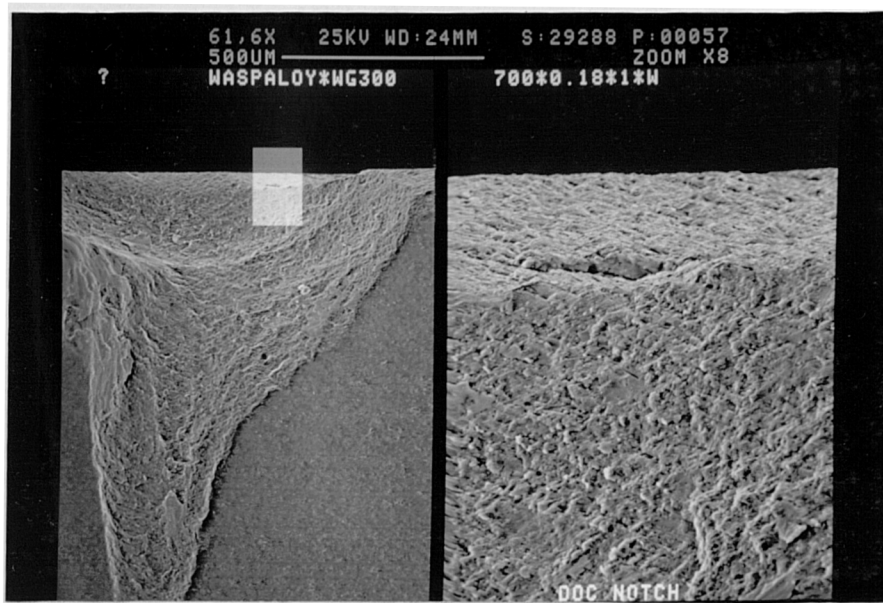


Figure 68: Crack running across the DOC notch area of WG-300 after machining of Waspaloy (V=215m/min, DOC=1mm, F=0.18mm/rev, Wet)

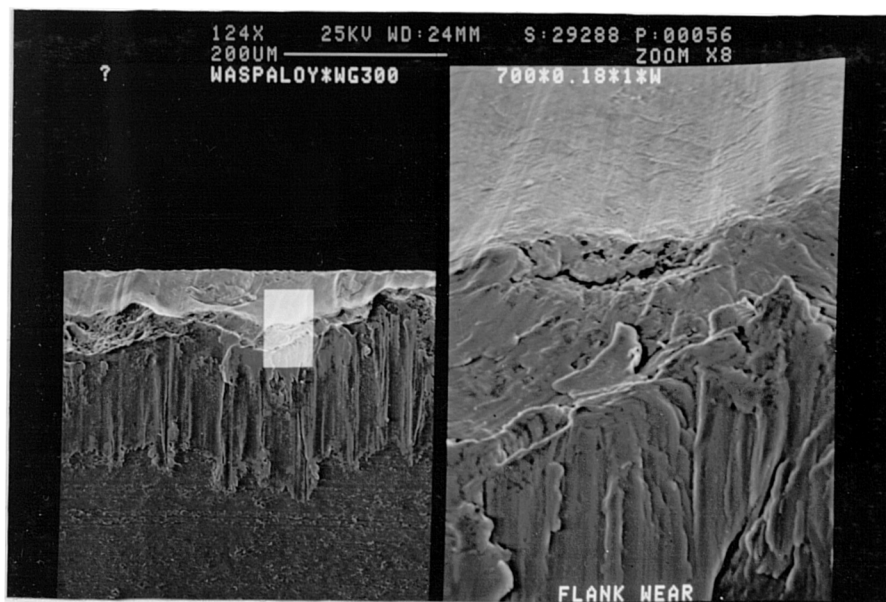


Figure 69: View of the flank face (of the above conditions)  
Crack running parallel to the cutting edge

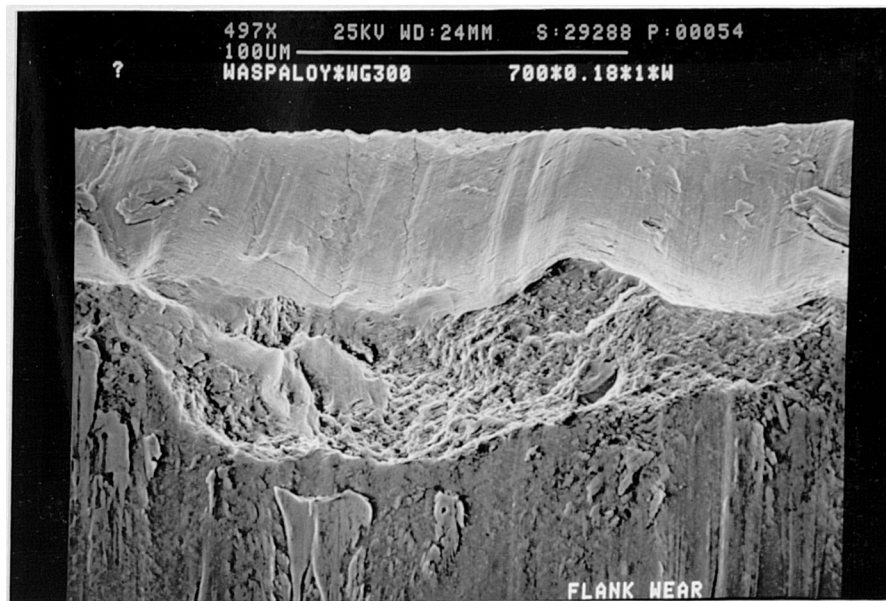


Figure 70: Different view of figure 68, showing smooth and rough area together with microcracks

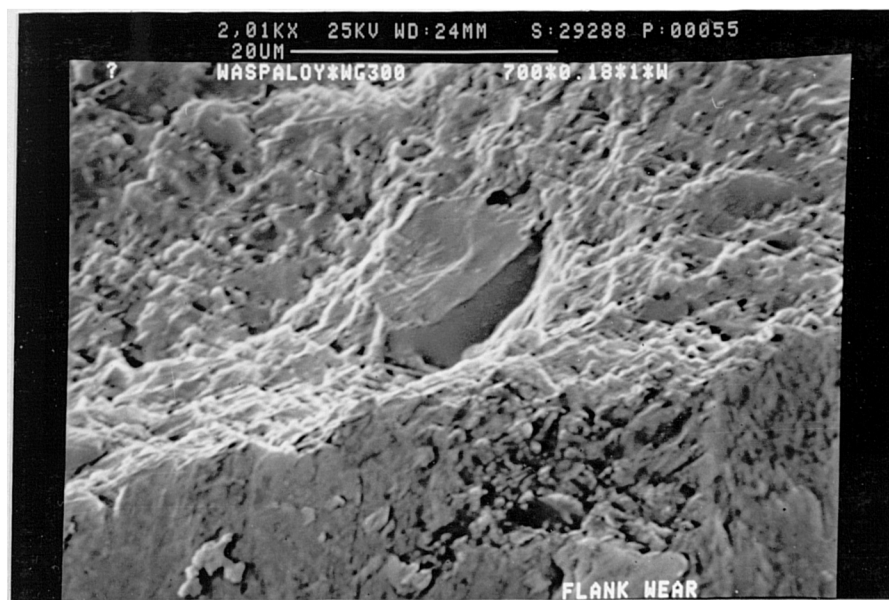


Figure 71: Enlarged view of figure 70

MACHINING OF WASPALOY WITH WG300  
 $V=300\text{m/min}$ ,  $\text{DOC}=1\text{mm}$ ,  $F=0.18\text{mm/rev}$ , WET

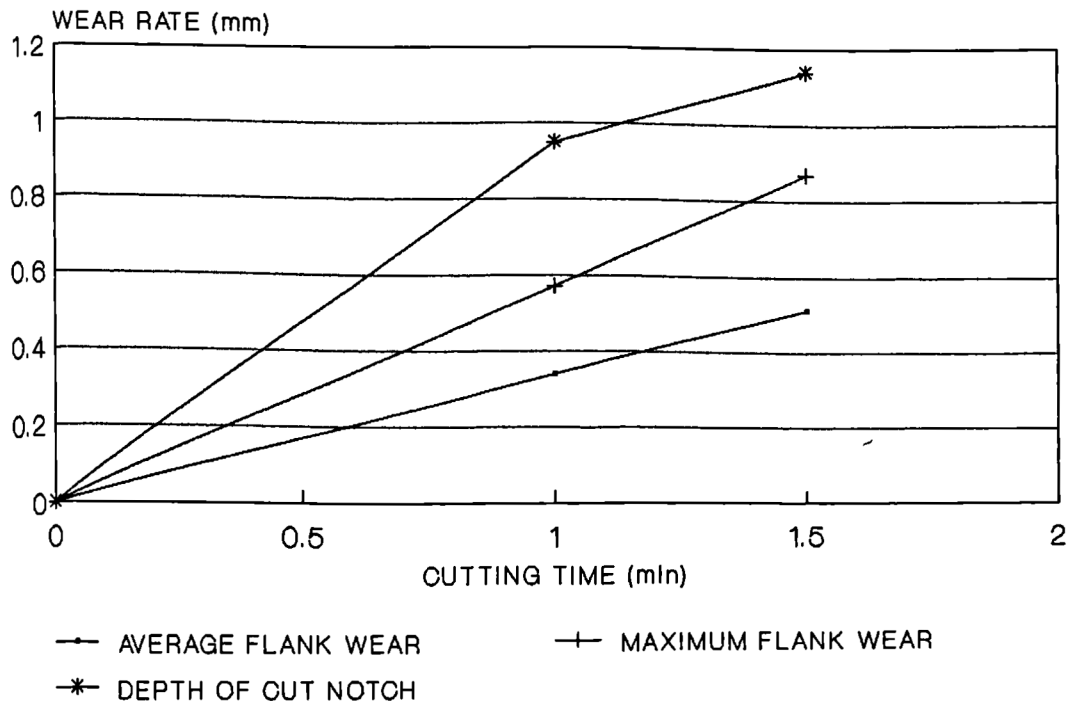


Figure 72

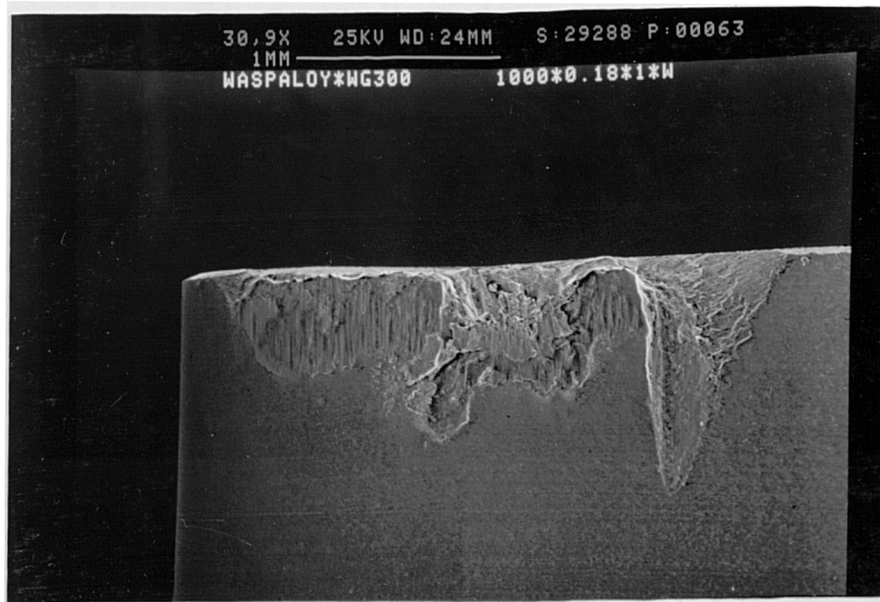


Figure 73: Wear pattern on the flank face of WG-300 after machining of Waspaloy ( $V=300\text{m/min}$ ,  $F=0.18\text{mm/rev}$ ,  $\text{DOC}=1\text{mm}$ , Wet)



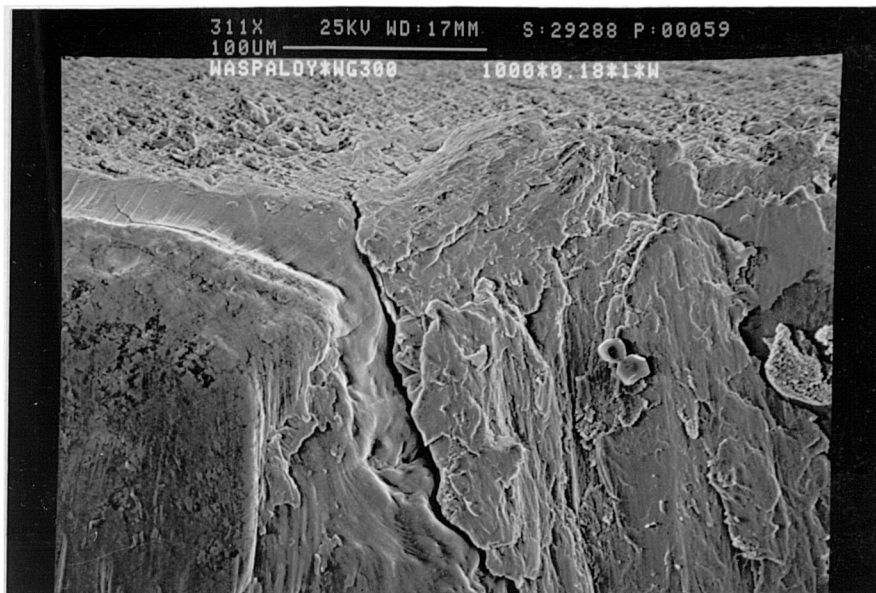


Figure 74: cracks on the vicinity of DOC notch of WG-300 used to machine Waspaloy, (V=300m/min, DOC=1mm, F=0.18mm/rev, Wet)

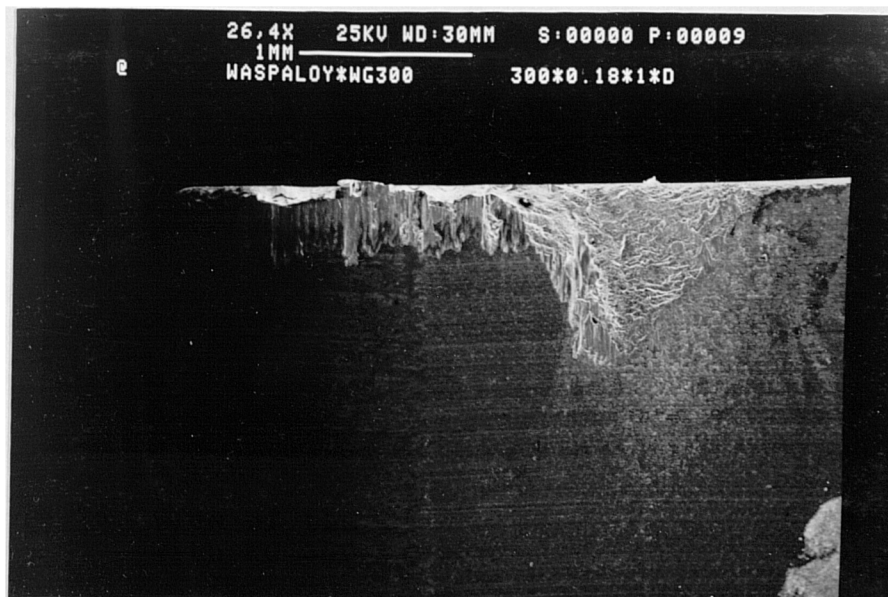


Figure 75: View of the flank wear, Dry machining of Waspaloy with WG-300 (V=90m/min, F=0.18mm/rev, DOC=1mm)

MACHINING OF WASPALLOY WITH WG300  
DOC=1mm, F=0.18mm/rev, DRY

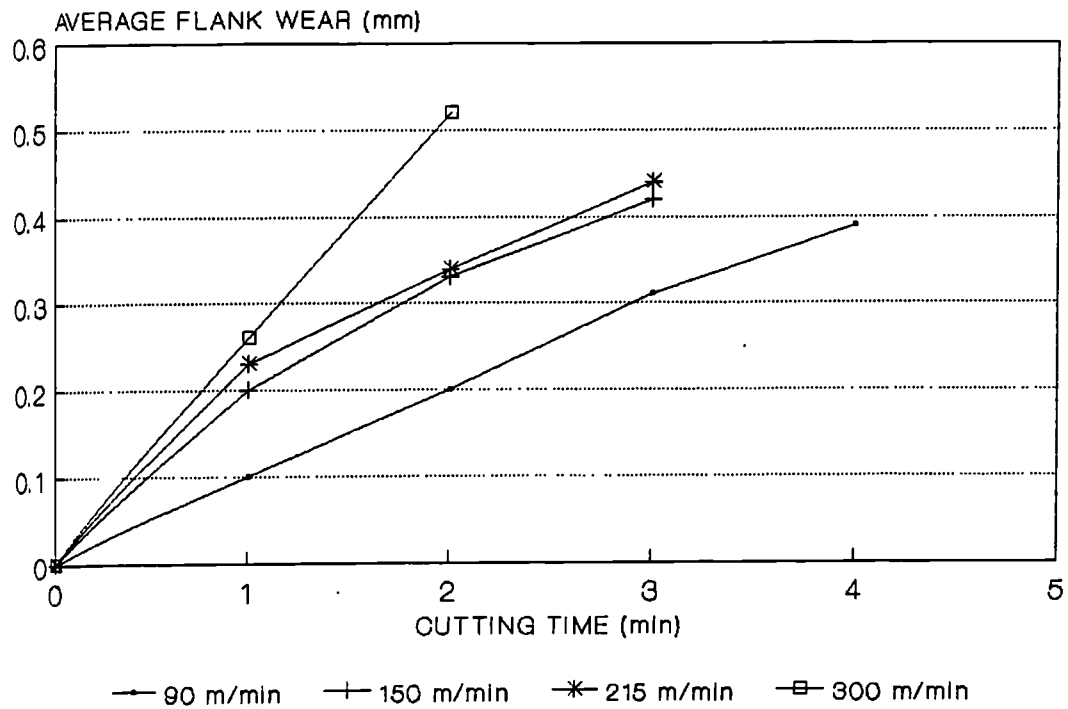
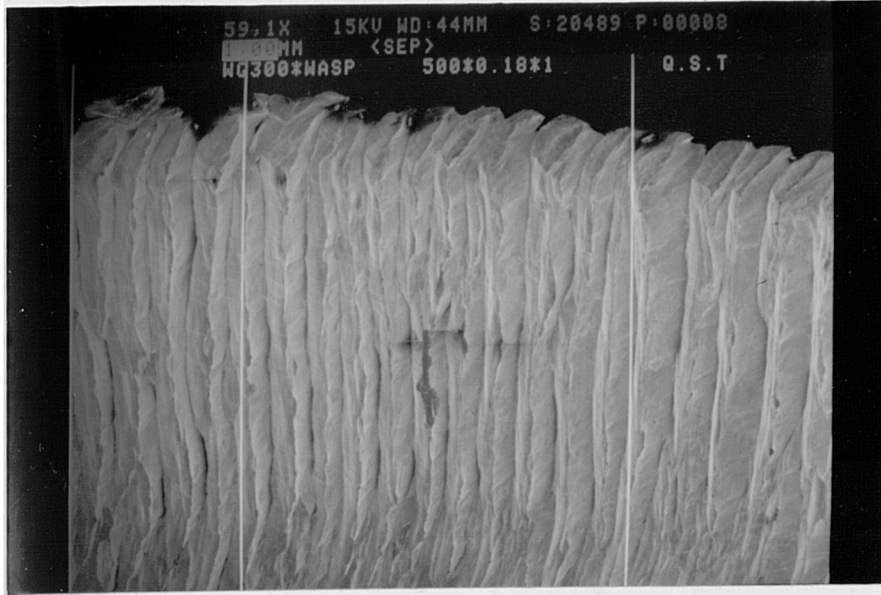
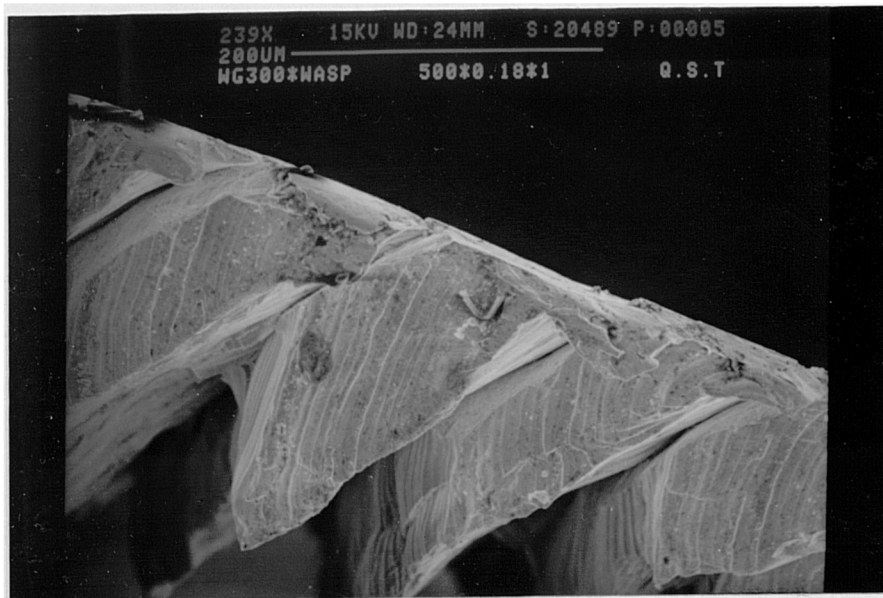


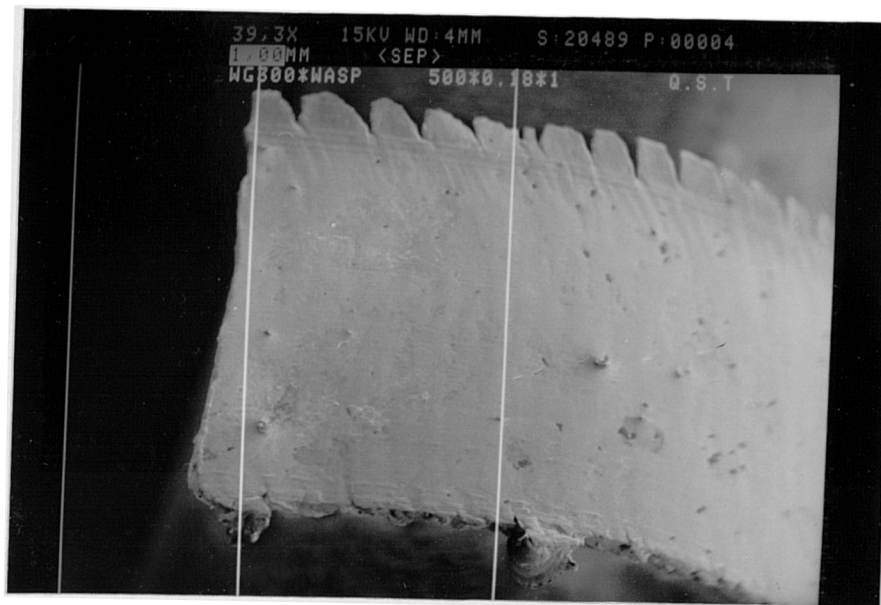
Figure 76



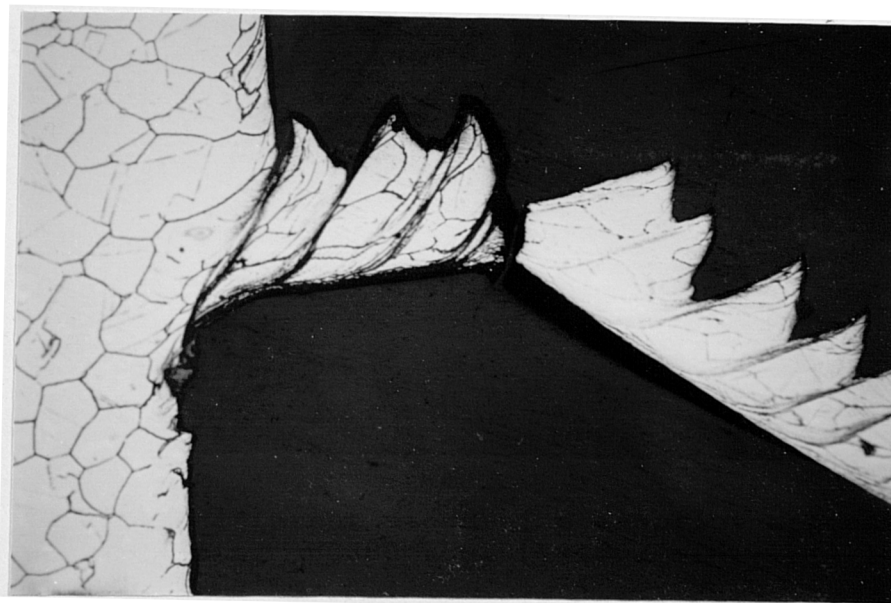
a.



b.



c.



d.

Figure 77(a-d): different views of a Waspaloy segmented chip using WG300 tool ( $V=150\text{m/min}$ ,  $F=0.18\text{mm/rev}$ ,  $\text{DOC}=1\text{mm}$ )

- |               |                            |
|---------------|----------------------------|
| a. top view   | b. side view               |
| c. underneath | d. quick stop wedge (x150) |

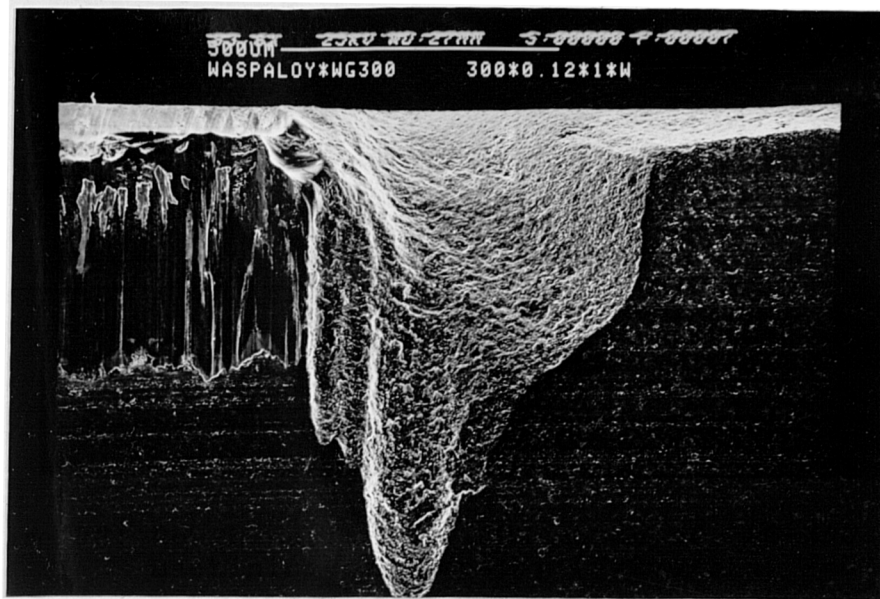


Figure 78: Rough surface of DOC notch of WG-300 after wet machining of Waspaloy (V=90m/min, F=0.125mm/rev, DOC=1mm)

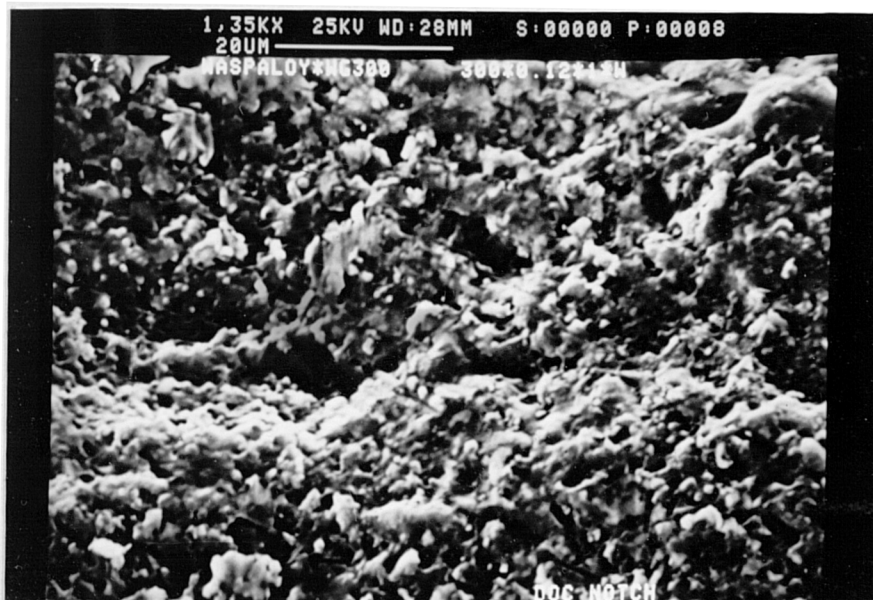


Figure 79: Magnified view of the above figure showing cracks running across the grains



Figure 80: Micro cracks on the honed area of WG-300 used to machine Waspaloy, ( $V=215\text{m/min}$ ,  $F=0.125\text{mm/rev}$ ,  $\text{DOC}=1\text{mm}$ , Wet)

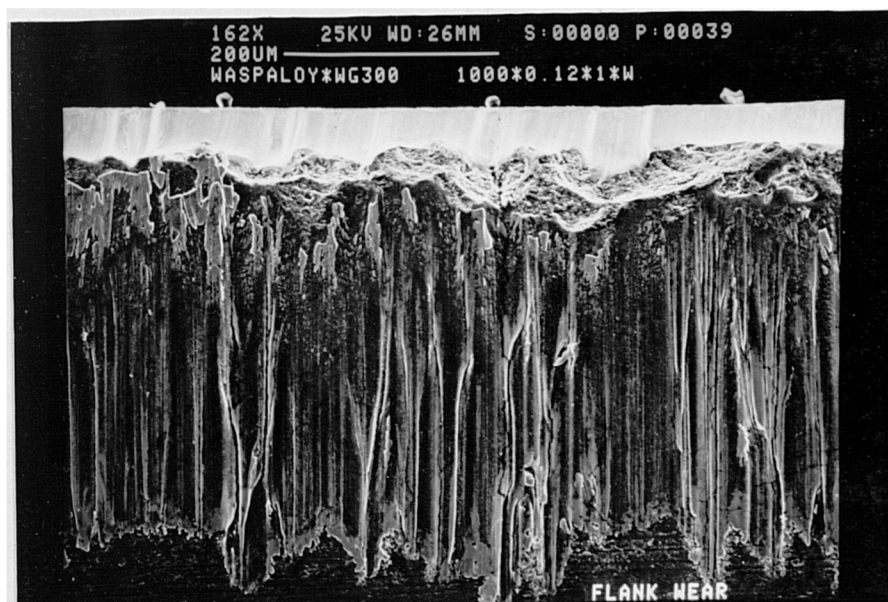


Figure 81: Wear on the flank face of WG-300 at  $V=300\text{m/min}$  (above conditions)

MACHINING OF WASPALOY WITH WG300  
DOC=1 mm, F=0.125mm/rev, DRY

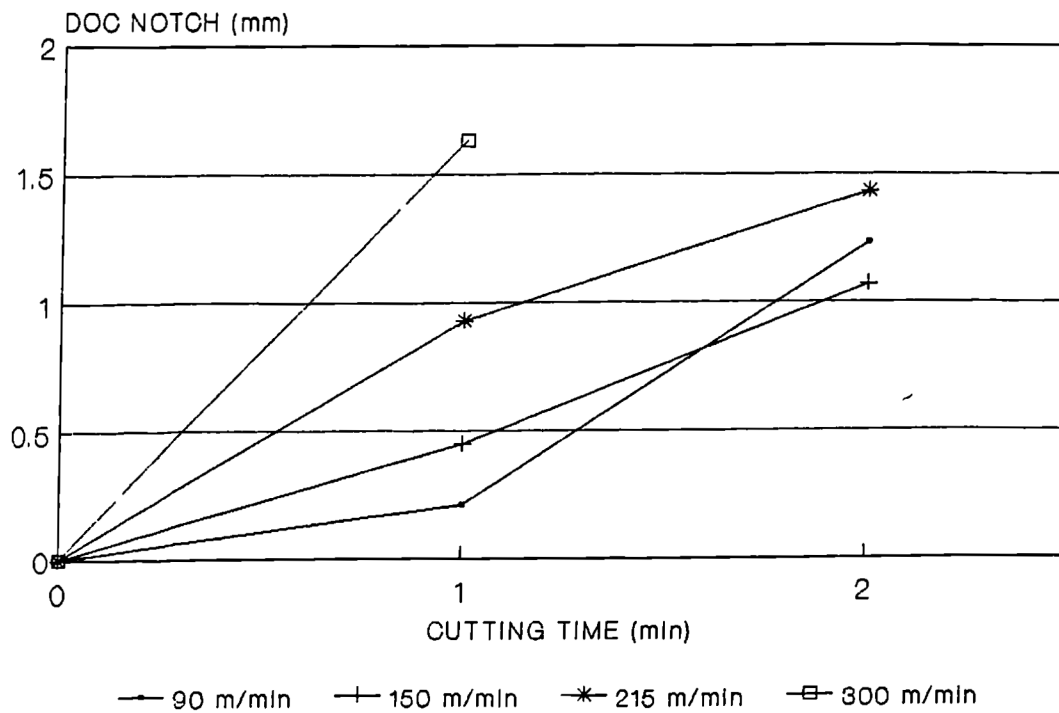


Figure 82

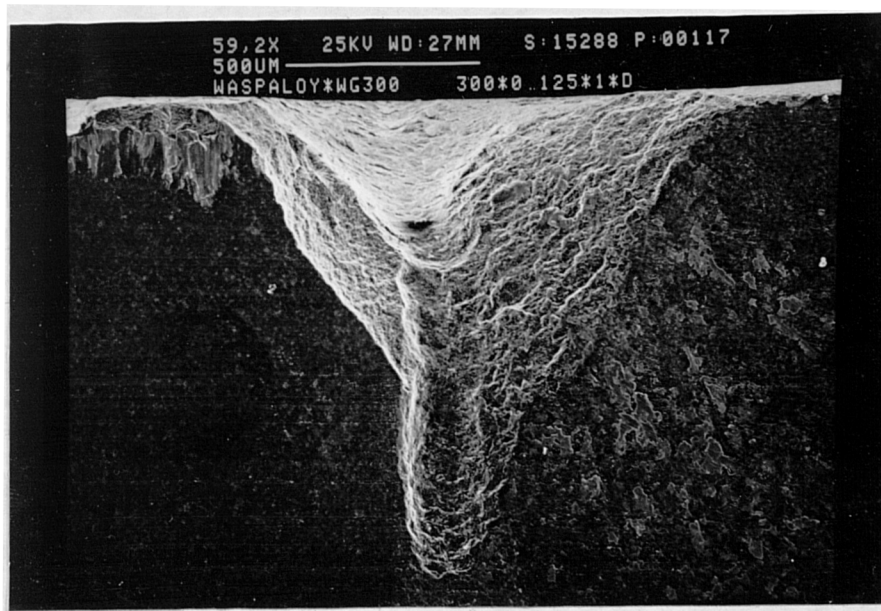


Figure 83: Rough surface on the DOCN area of WG-300 at the lowest cutting speed (above conditions)

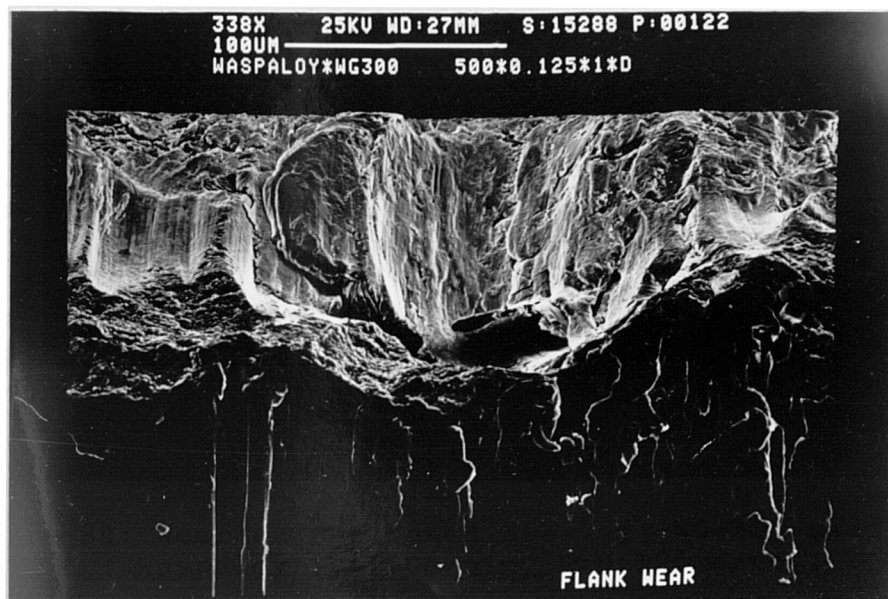


Figure 84: Wear on the honed area of WG-300 used to machine Waspaloy (V=150m/min, F=0.125mm/rev, DOC=1mm, Dry)

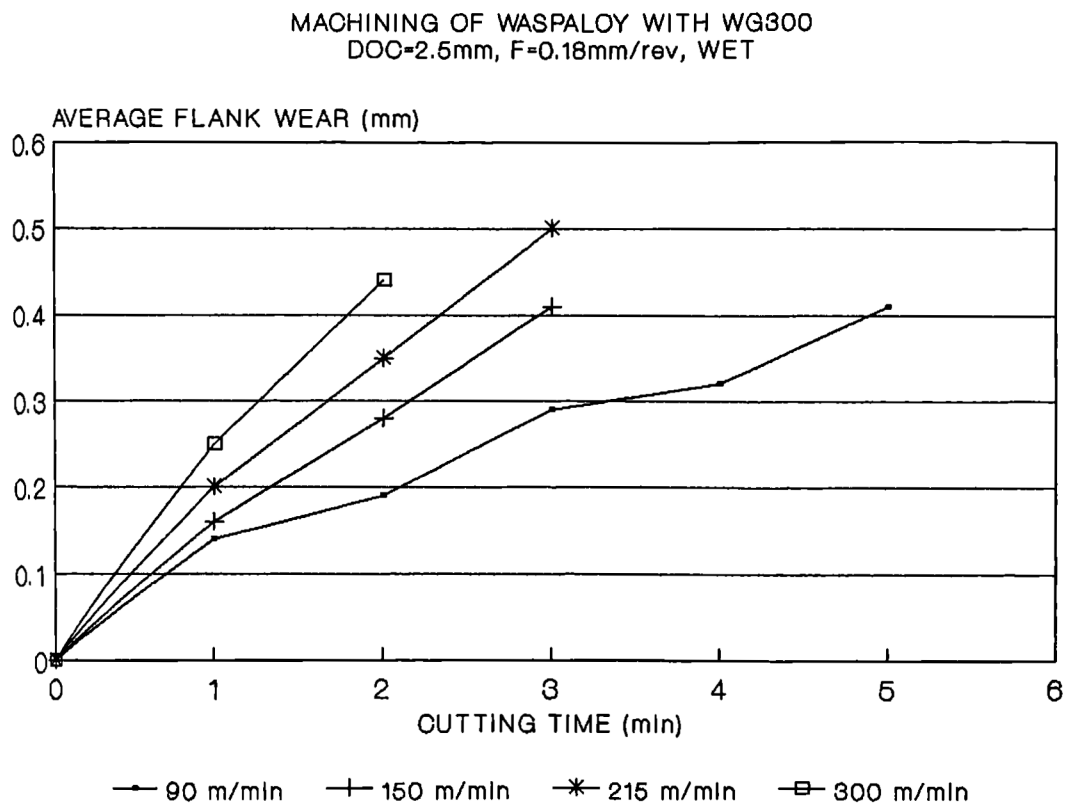


Figure 85



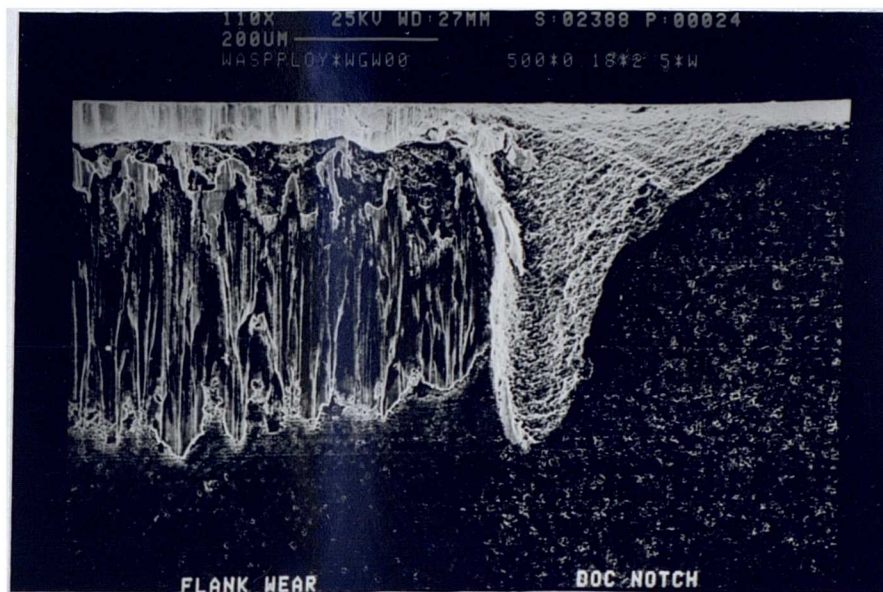


Figure 86: DOC notch and flank wear of WG300 used to machine Waspaloy (V=150m/min, F=0.18mm/rev, DOC=2.5mm, Wet)

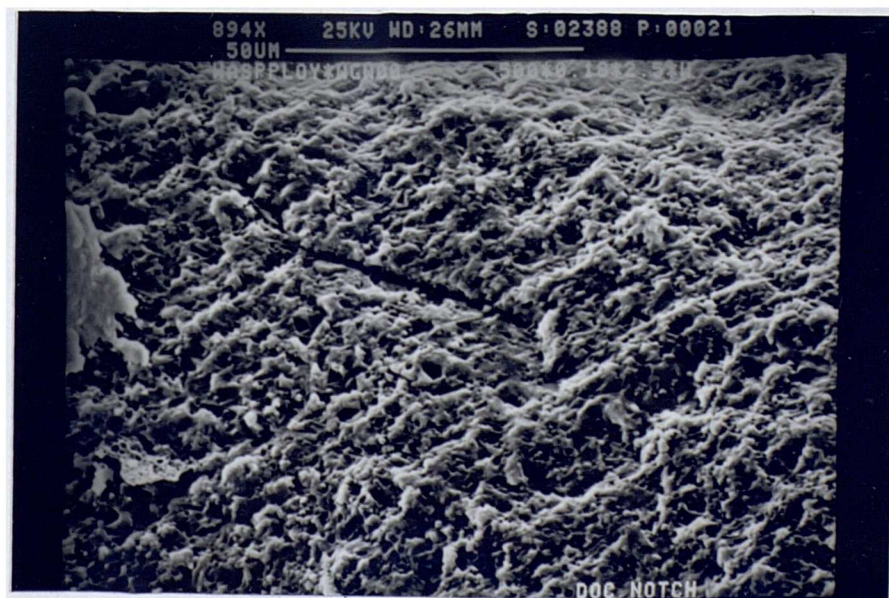


Figure 87: Magnified view of DOCN showing crack running across the grains

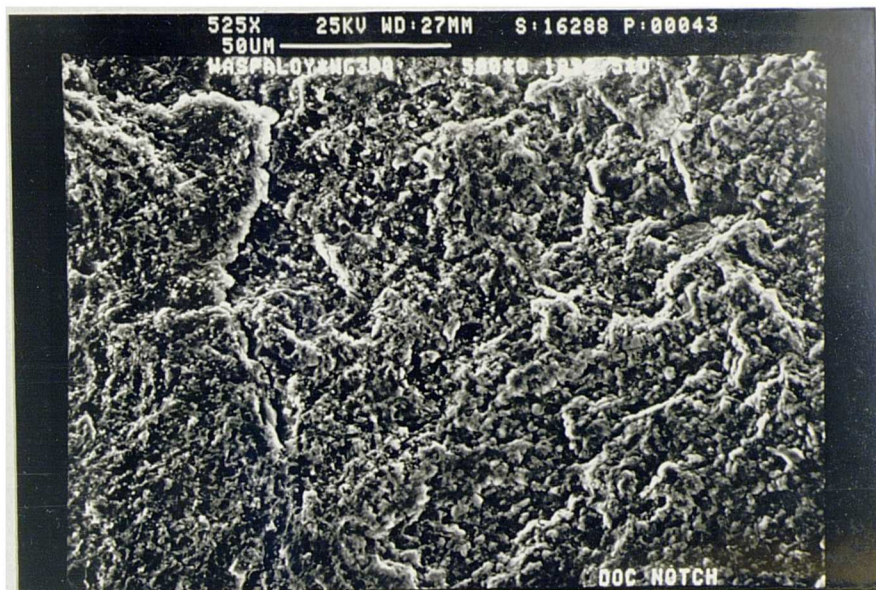


Figure 88: Different magnified view of figure 86 showing cracks

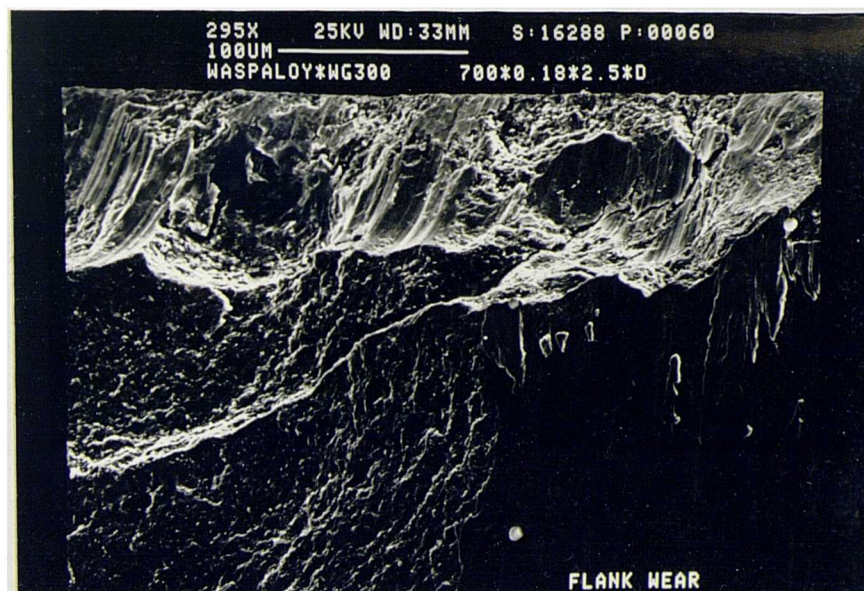


Figure 89: Cracks at the flank face of WG300 used to machine Waspaloy (V=215m/min, DOC=2.5mm, F=0.18mm/rev, Dry)





Figure 90: Crack at the flank face of WG300 used to machine Waspaloy ( $V=300\text{m/min}$ ,  $F=0.18\text{mm/rev}$ ,  $\text{DOC}=2.5\text{mm}$ , Dry)

MACHINING OF WSPALOY WITH WG300  
 $\text{DOC}=2.5\text{ mm}$ ,  $F=0.125\text{ mm/rev}$ , DRY

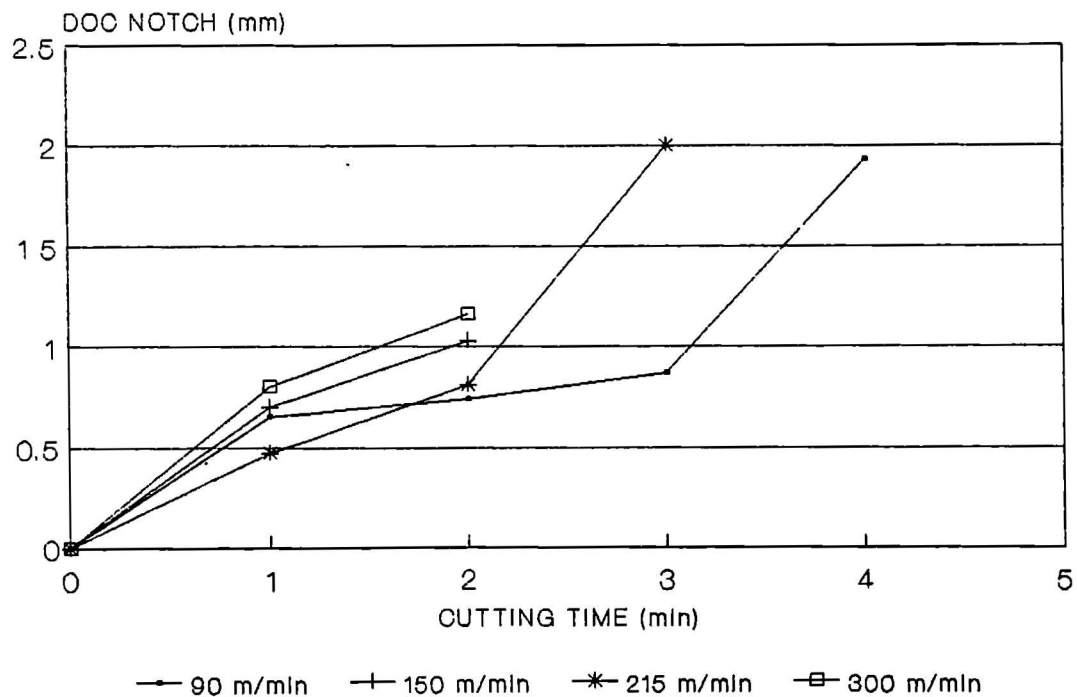


Figure 91

MACHINING OF WASPALOY WITH WG300  
DOC=2.5 mm, F=0.125 mm/rev, DRY

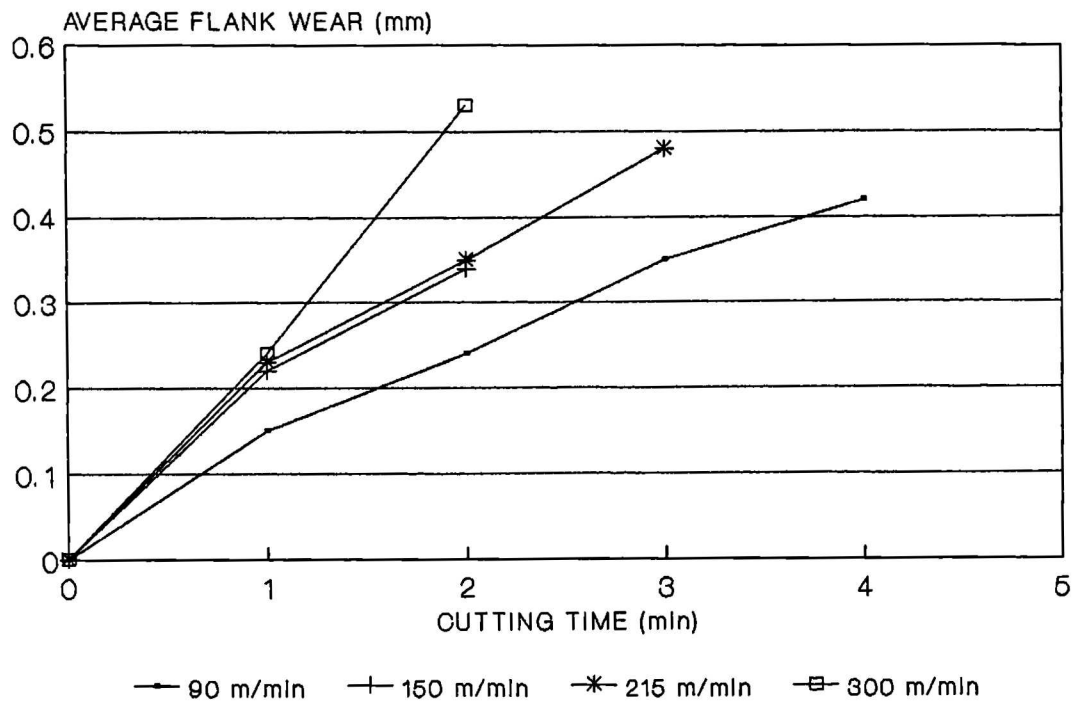


Figure 92

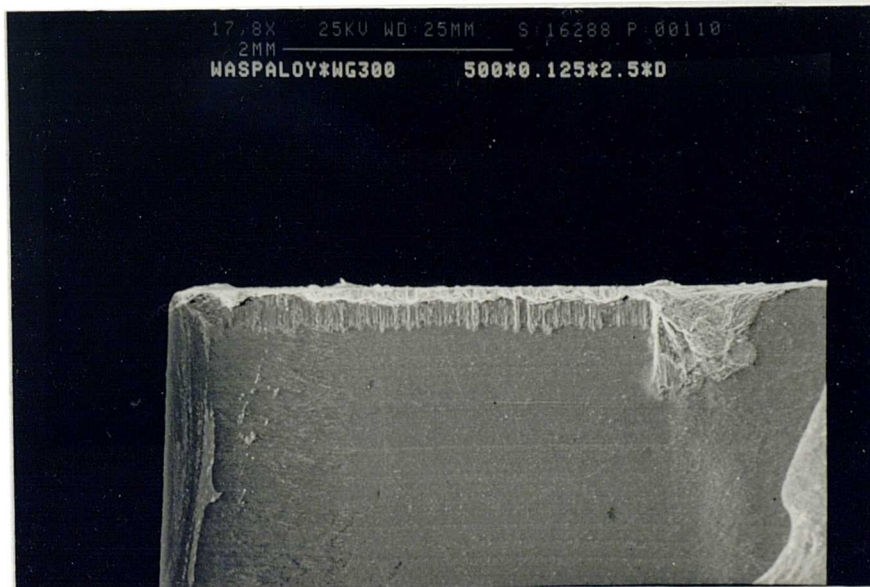


Figure 93: Wear of WG-300 at V=150m/min (above conditions)



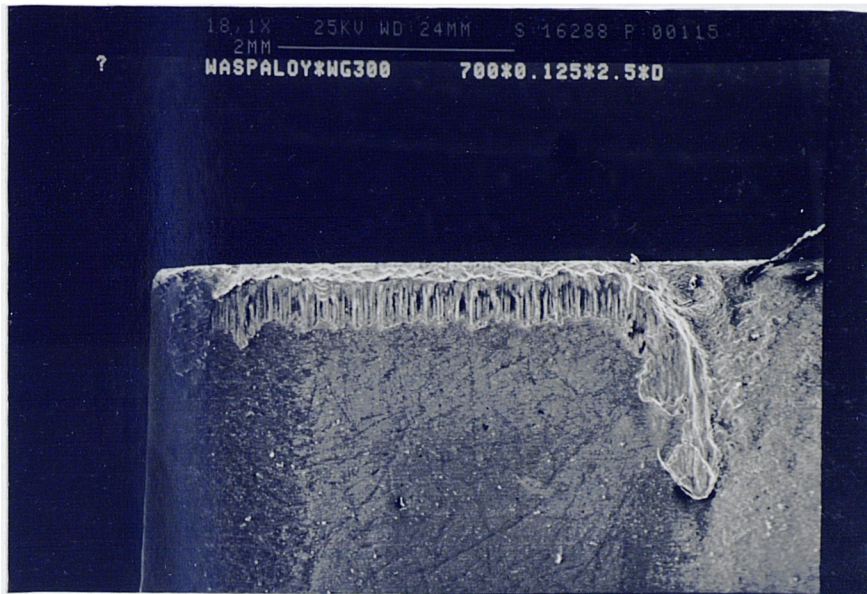


Figure 94: Overall wear of WG-300 used to machine Waspaloy  
(V=215m/min, F=0.125mm/rev, DOC=2.5mm, Dry)

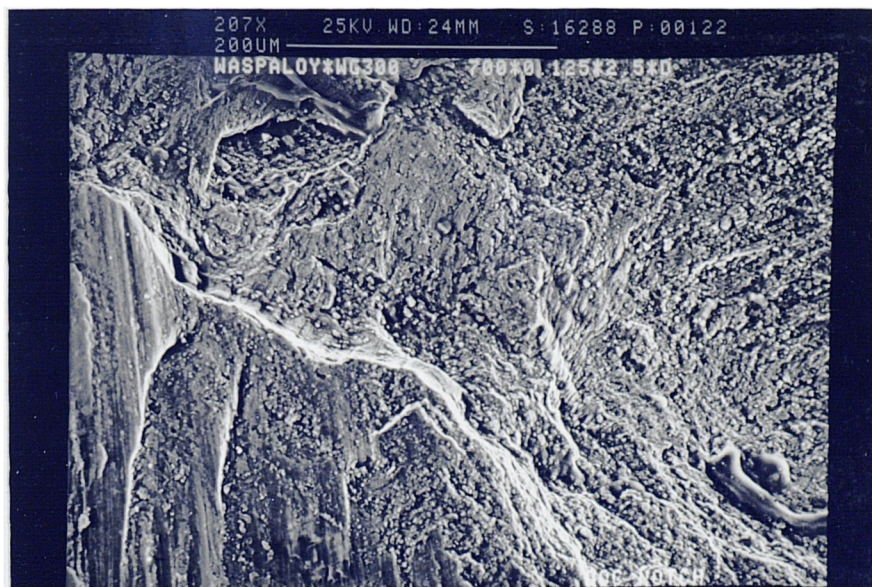


Figure 95: Magnified view of above showing rough surface of  
DOC notch

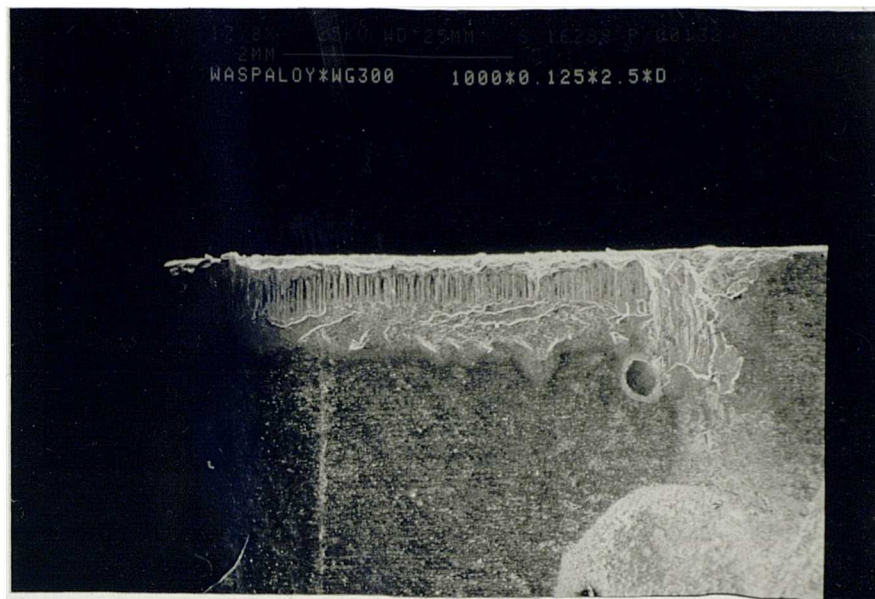


Figure 96: Overall view of the flank wear of WG-300 used to machine Waspaloy, ( $V=300\text{m/min}$ ,  $F=0.125\text{mm/rev}$ ,  $\text{DOC}=2.5\text{mm}$ , Dry)

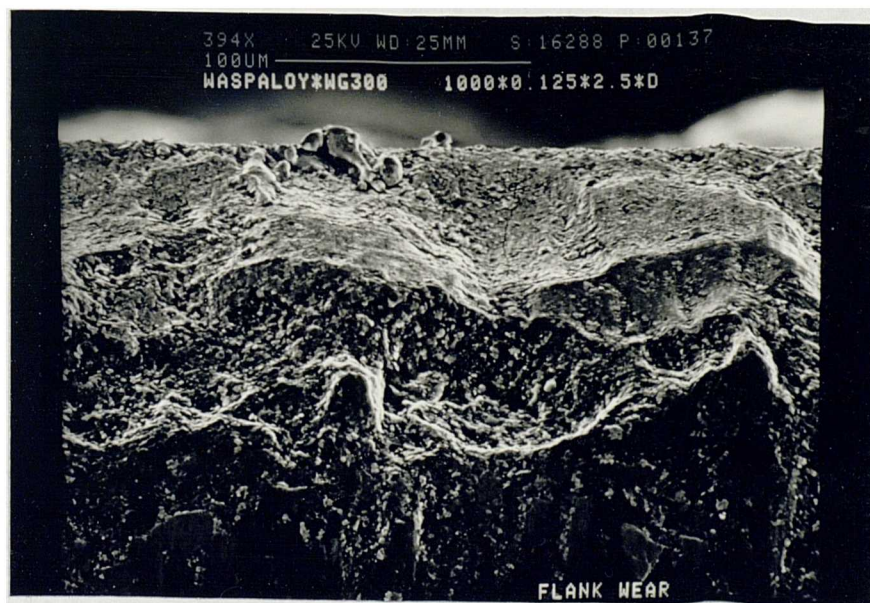


Figure 97: Magnified view of figure 96 showing microcracks on the honed area

MACHINING OF INCO 901 WITH OC650  
DOC = 1 mm

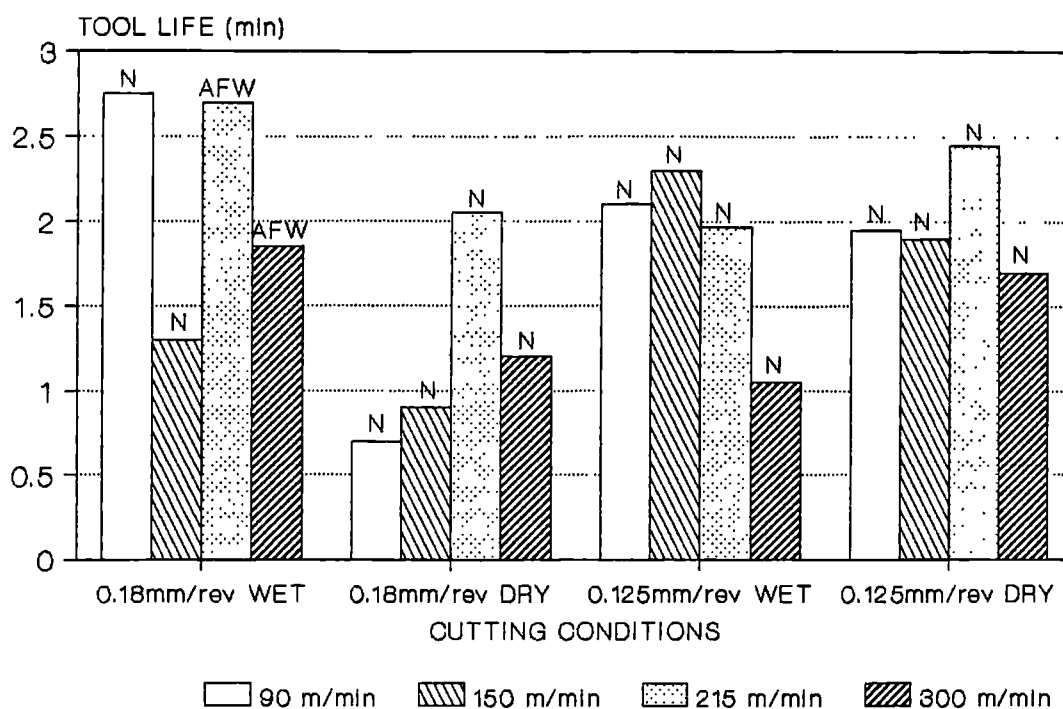


Figure 98

MACHINING OF INCO 901 WITH OC650  
DOC = 1 mm

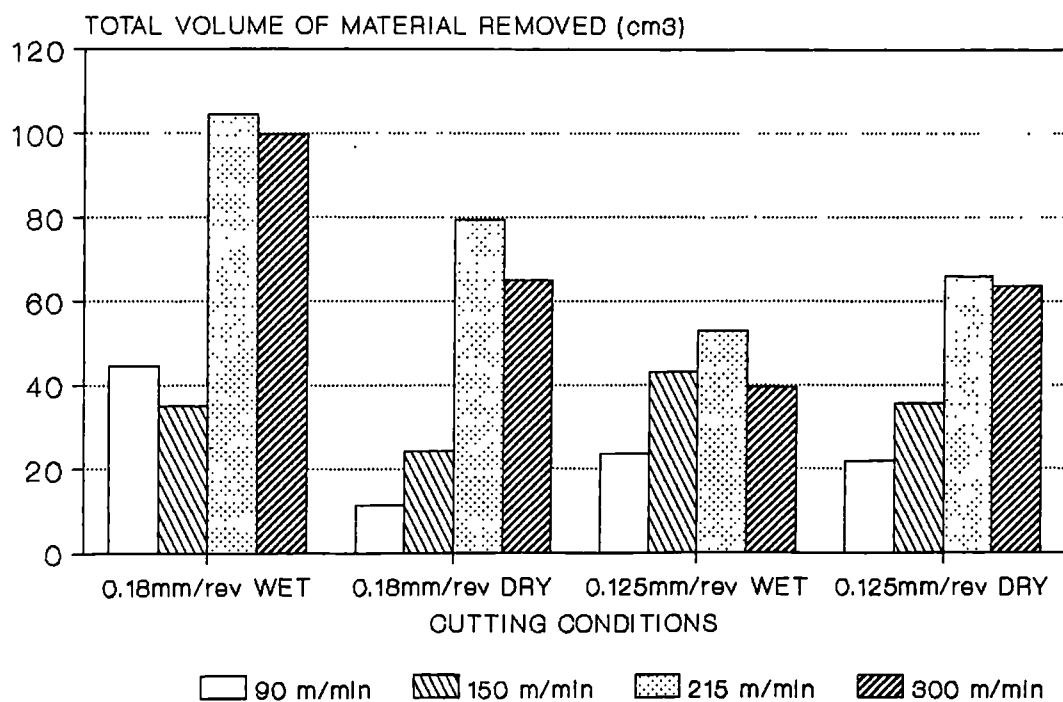


Figure 98a



MACHINING OF INCO 901 WITH CC650  
DOC = 2.5mm

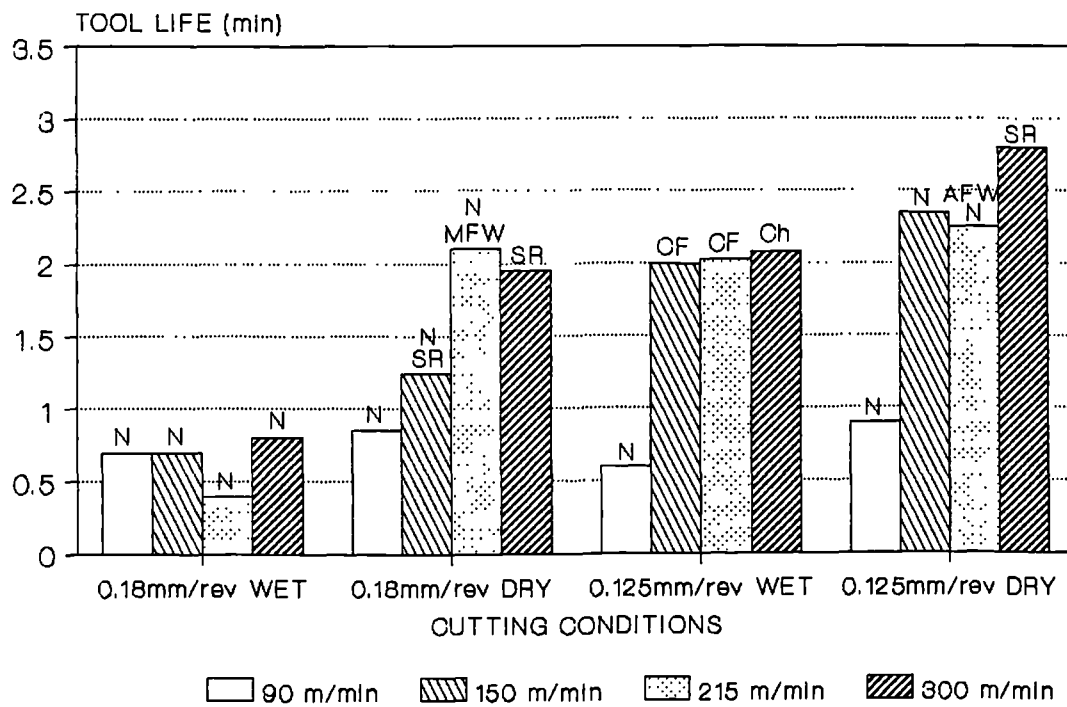


Figure 99

MACHINING OF INCO 901 WITH CC650  
DOC = 2.5mm

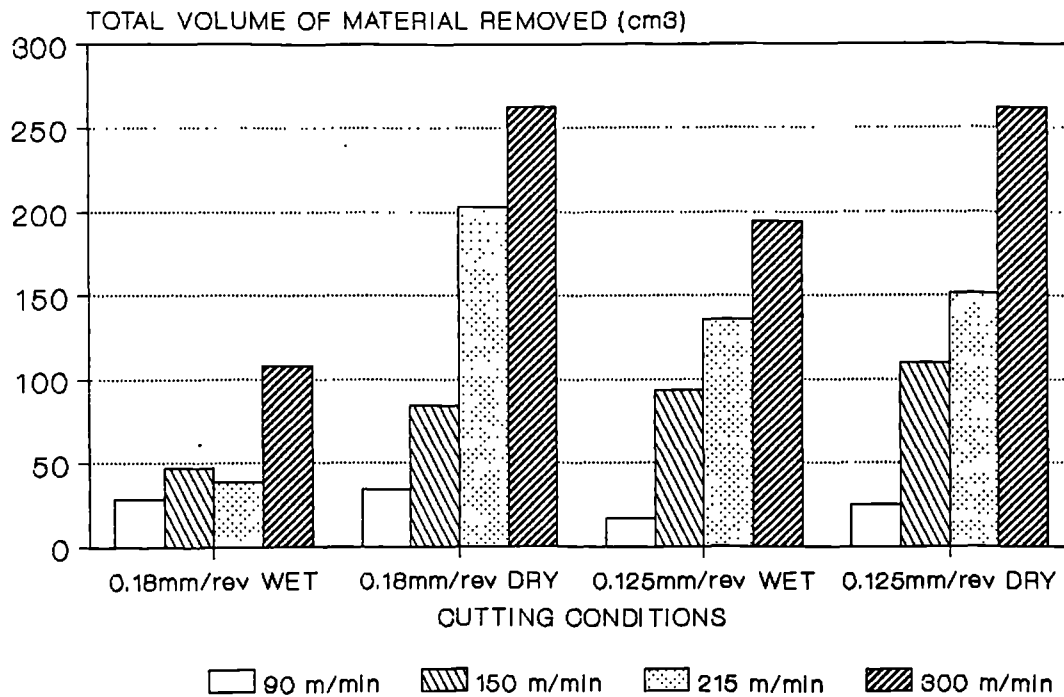


Figure 99a



MACHINING OF INCO 901 WITH CC650  
DOC=1 mm, F=0.18mm/rev, WET

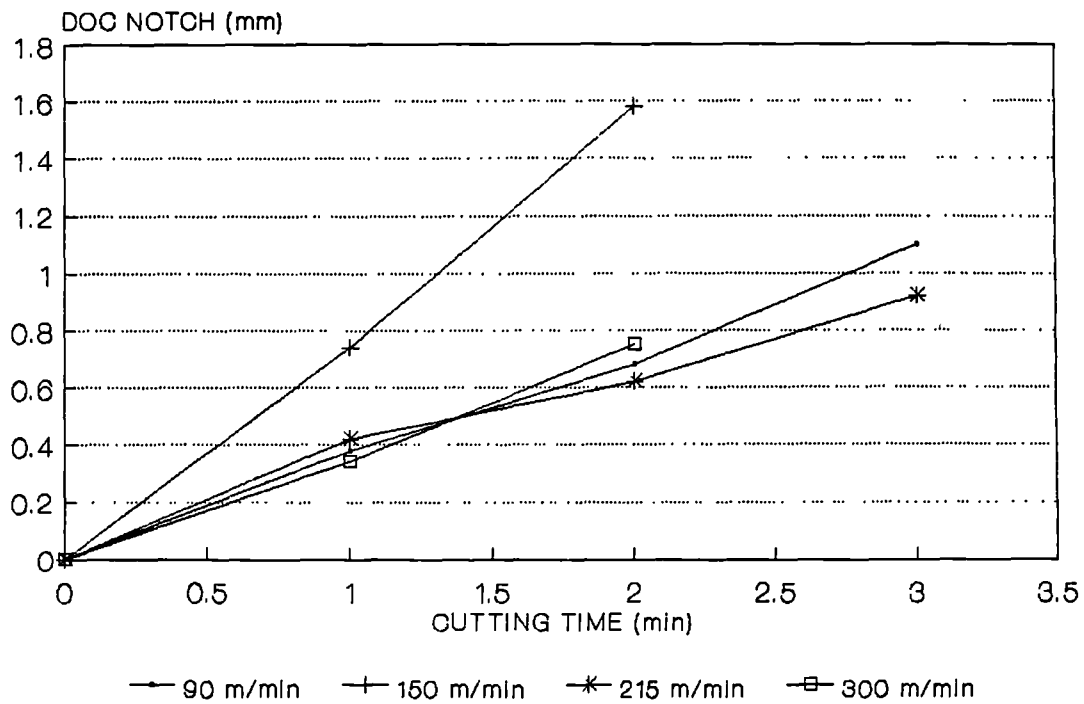


Figure 100

MACHINING OF INCO 901 WITH CC650  
DOC=1 mm, F=0.18mm/rev, WET

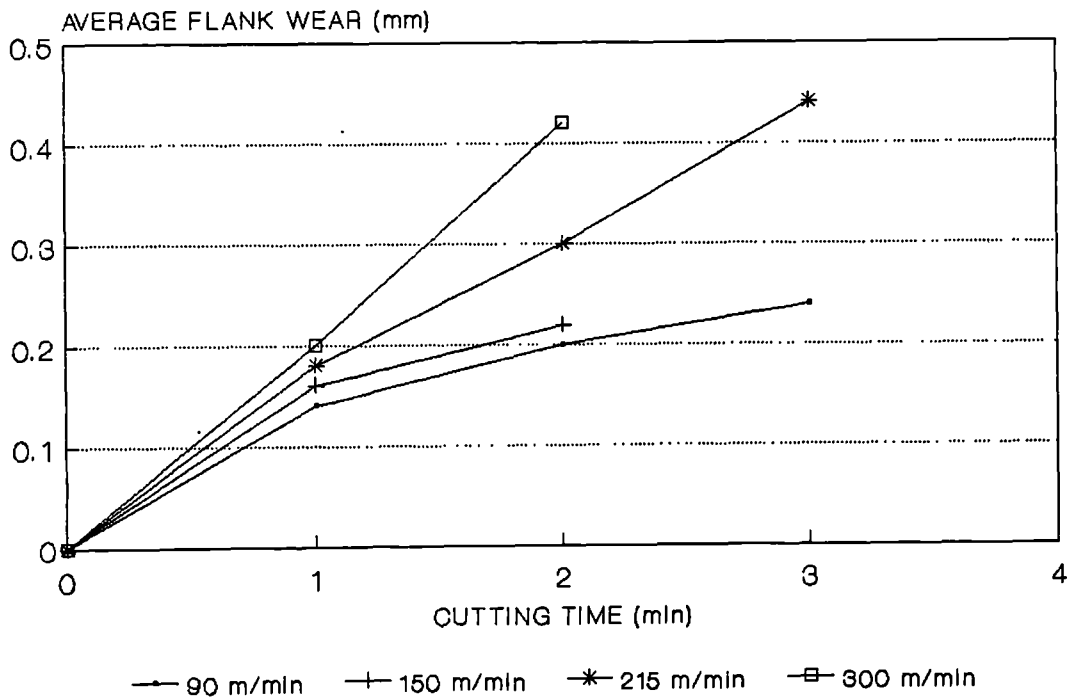


Figure 101

MACHINING OF INCO 901 WITH OC650  
DOC=1mm, F=0.125mm/rev, WET

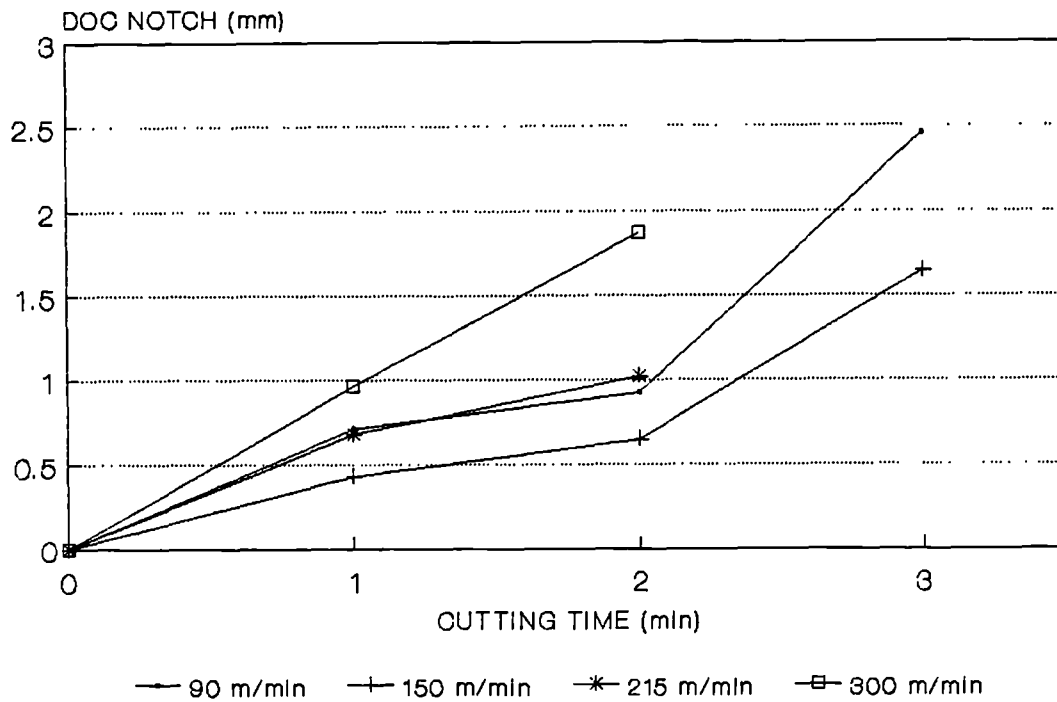


Figure 102

MACHINING OF INCO 901 WITH OC650  
DOC=1mm, F=0.125mm/rev, DRY

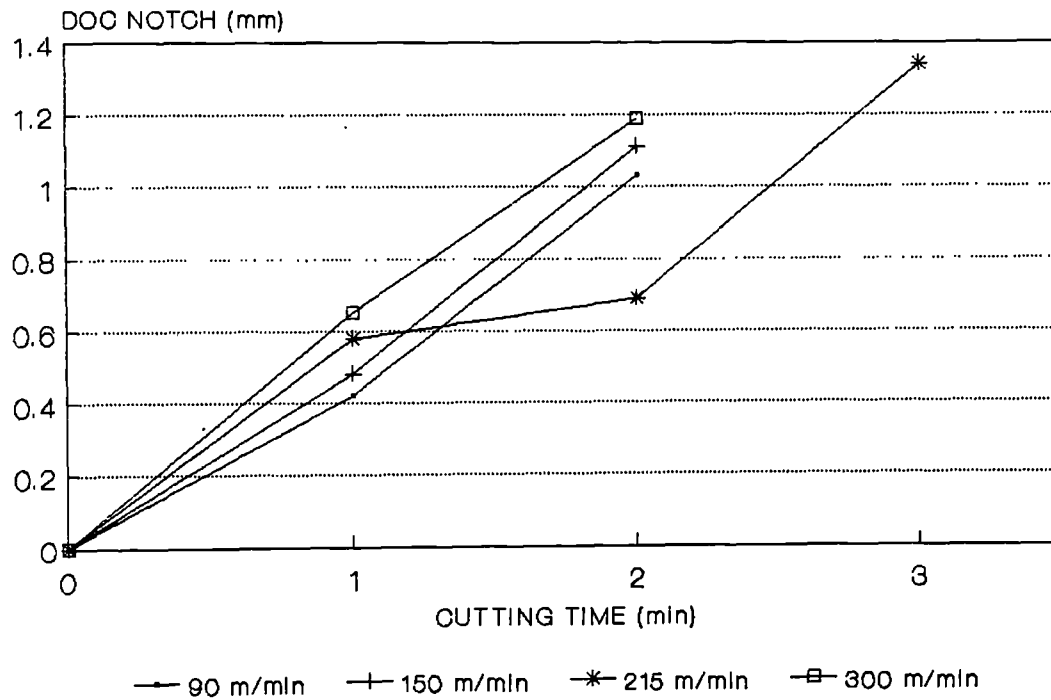


Figure 103

MACHINING OF INCO 901 WITH KYON 2000  
DOC = 1mm

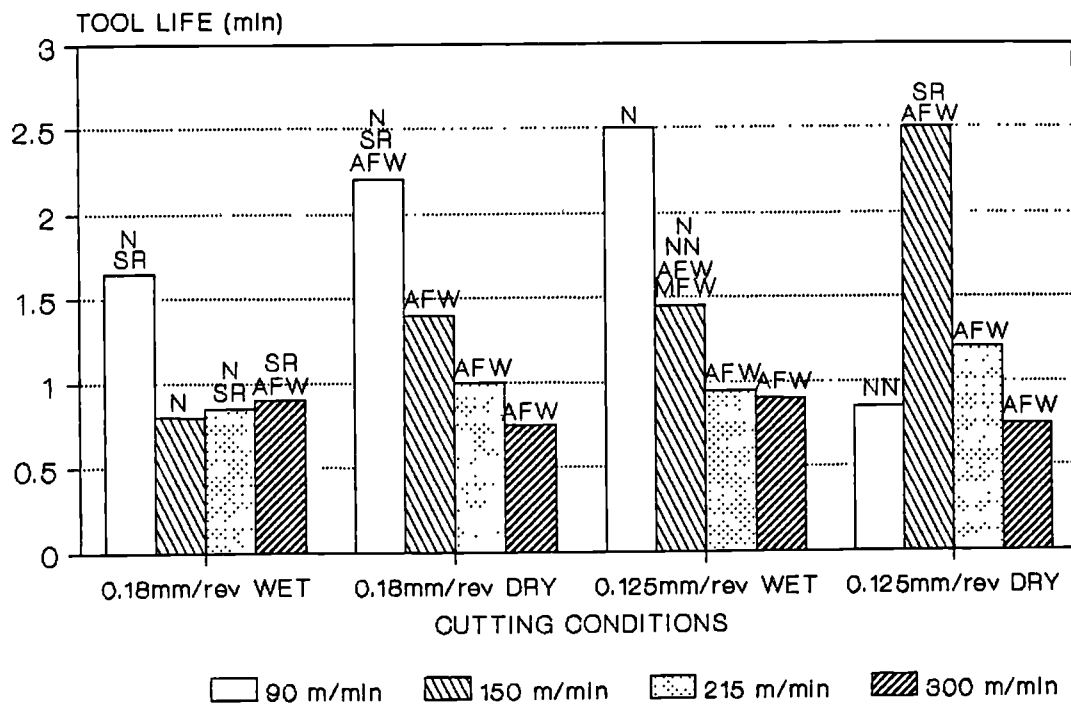


Figure 104

MACHINING OF INCO 901 WITH KYON 2000  
DOC = 1 mm

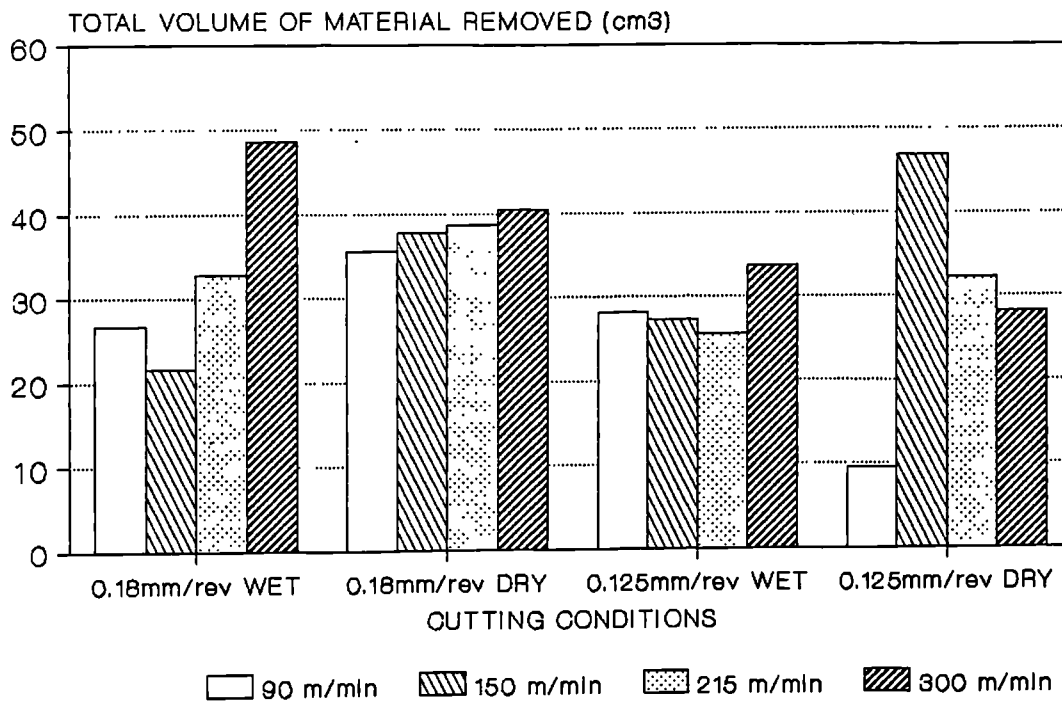


Figure 104a

MACHINING OF INCO 901 WITH KYON 2000  
DOC = 2.5mm

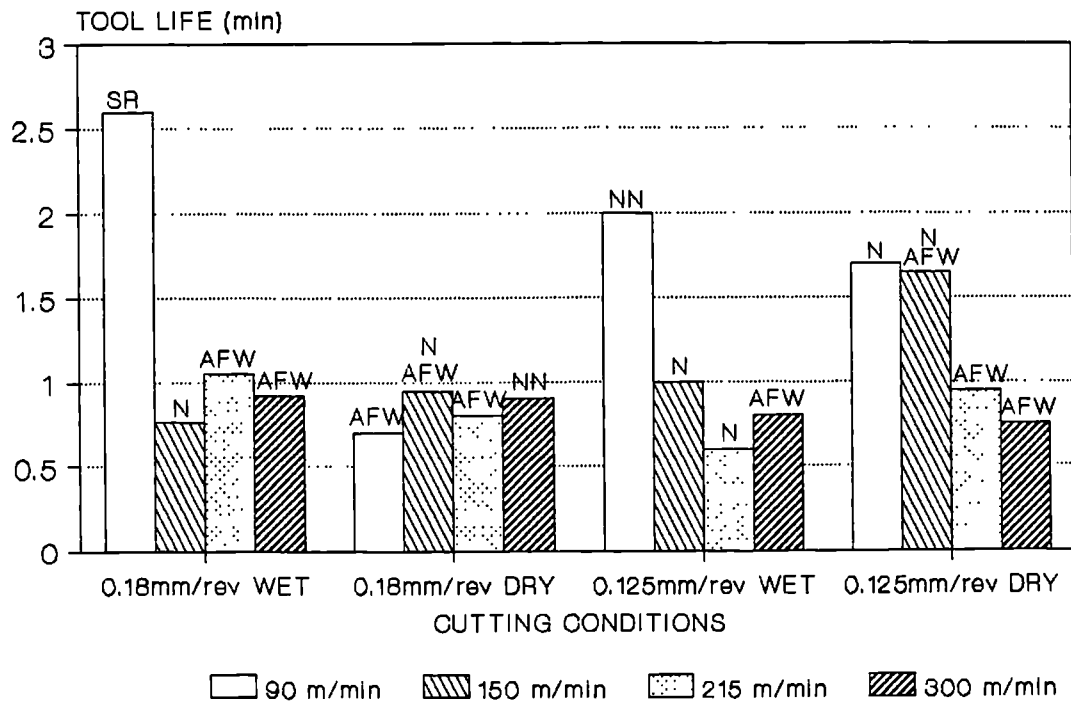


Figure 105

MACHINING OF INCO 901 WITH KYON 2000  
DOC = 2.5 mm

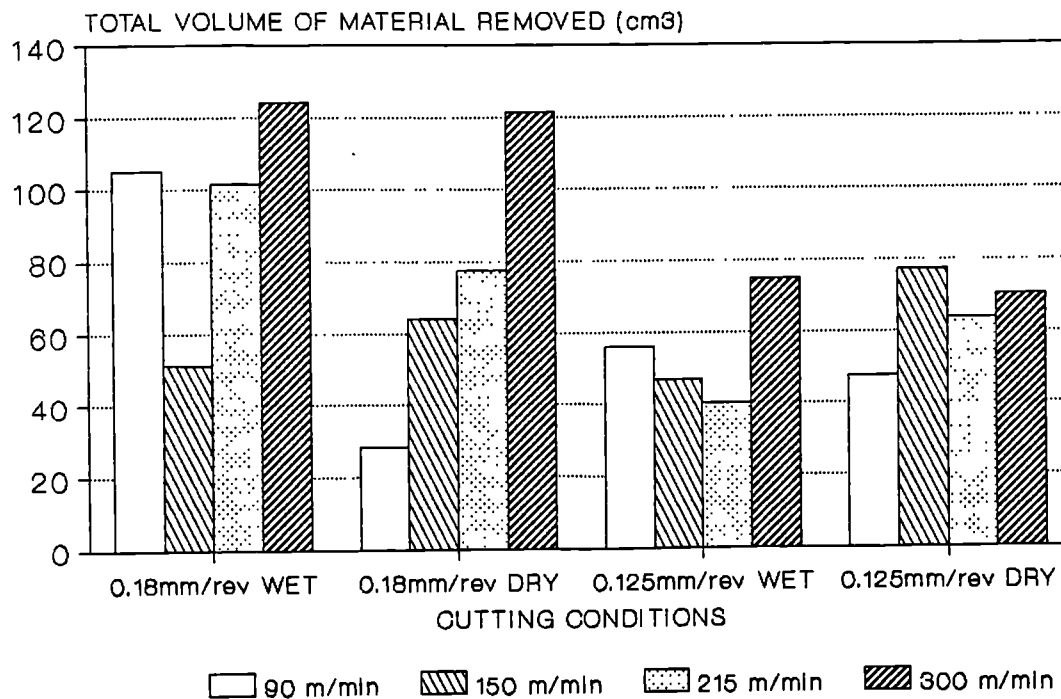


Figure 105a

MACHINING OF INCO 901 WITH KYON 2000  
DOC=1 mm, F=0.18 mm/rev, DRY

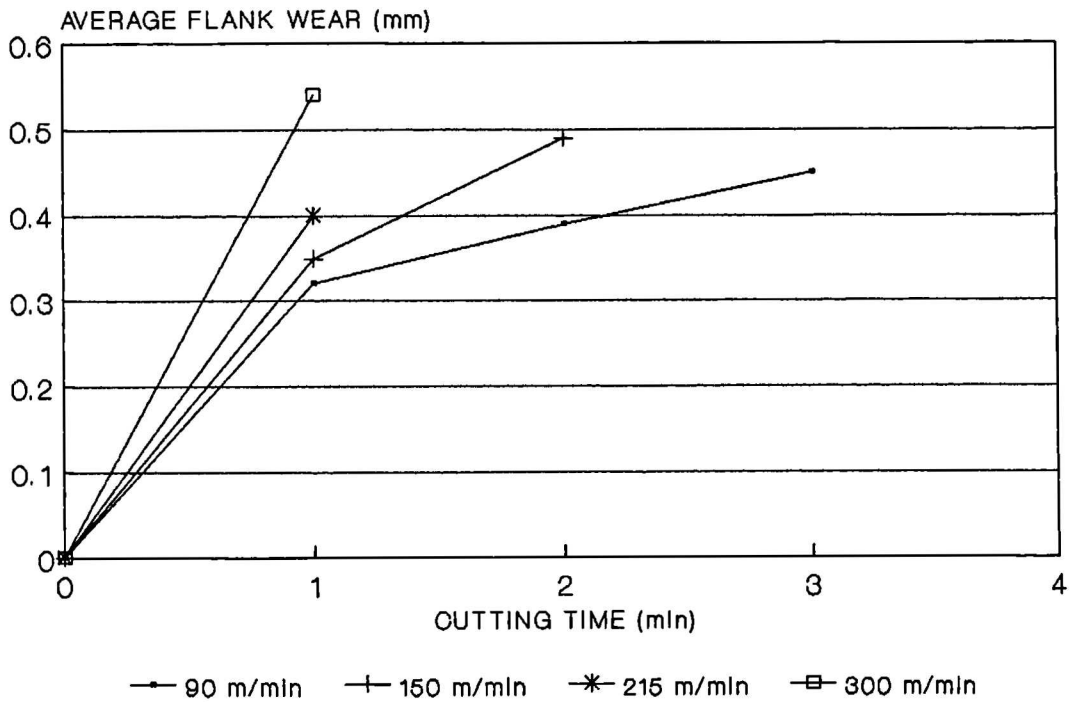


Figure 106

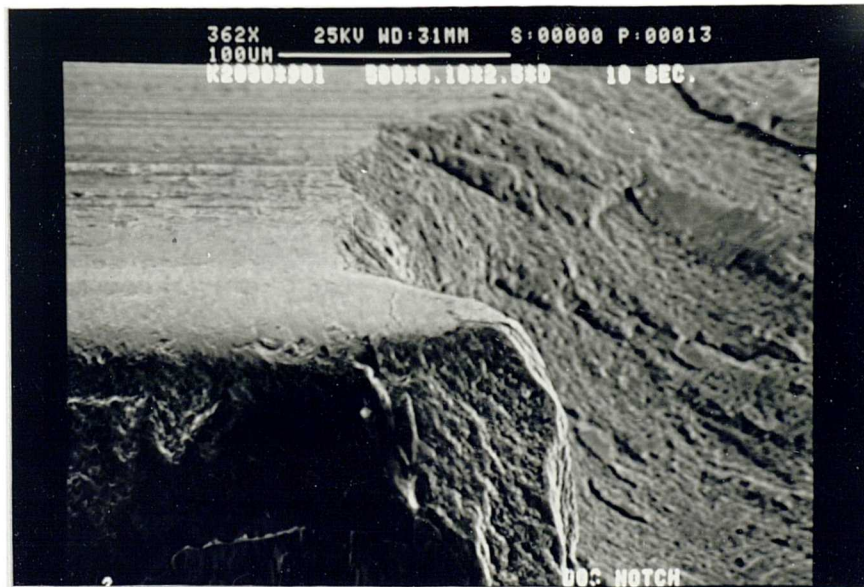


Figure 107: Crack at the beginning of DOCN of Kyon 2000 used to machine INCO 901 (V=150m/min, F=0.18mm/rev, DOC=2.5mm, Dry)

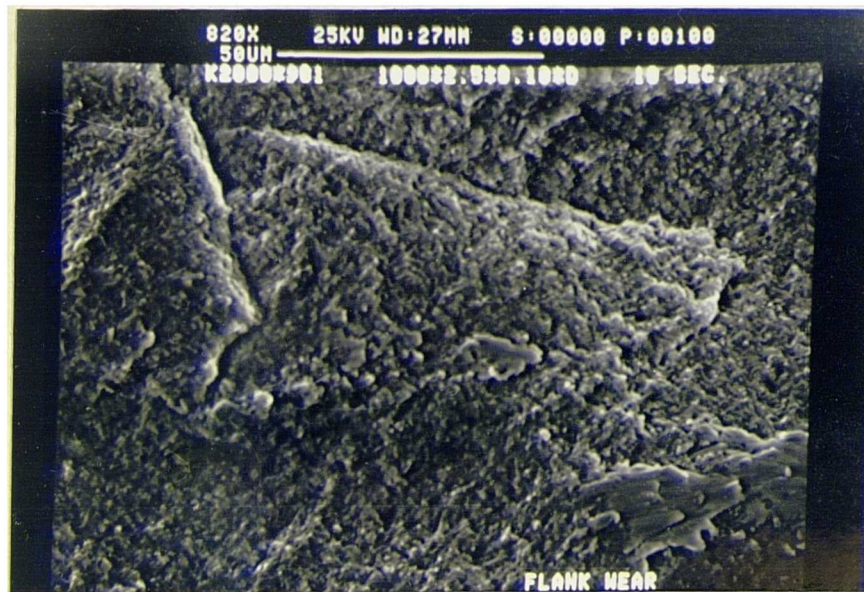


Figure 108: Cracks at the flank face of Kyon 2000 used to machine INCO 901 ( $V=300\text{m/min}$ ,  $F=0.18\text{mm/rev}$ ,  $\text{DOC}=2.5\text{mm}$ , Dry)

MACHINING OF INCO 901 WITH KYON 2000  
DOC = 2.5mm, DRY

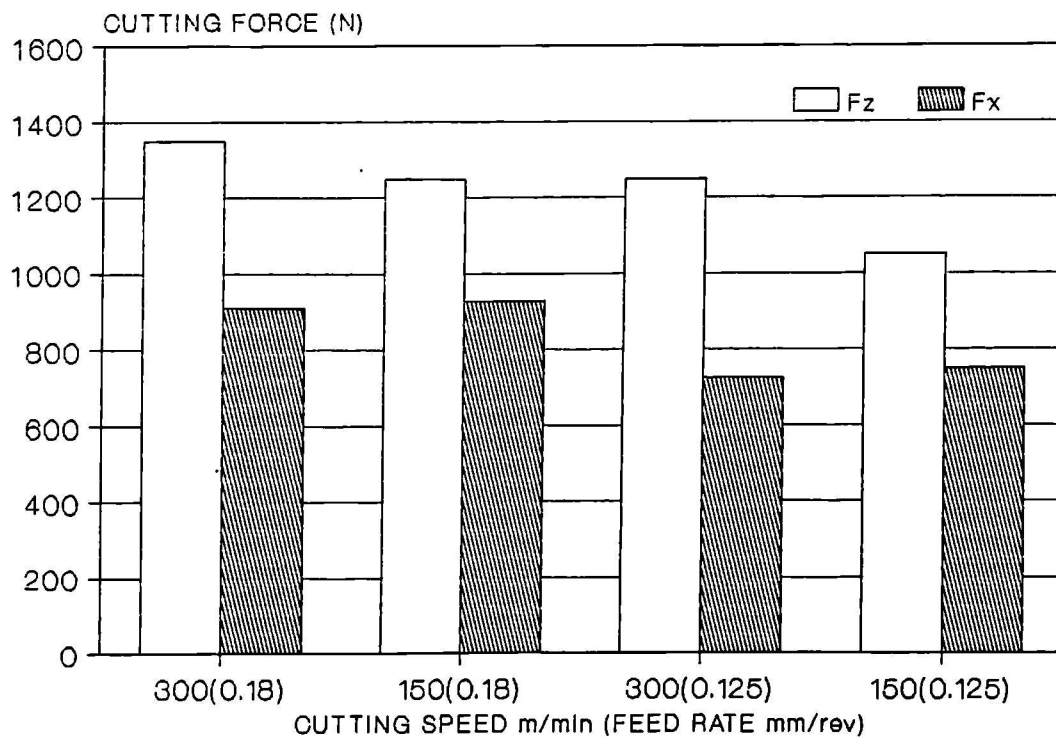
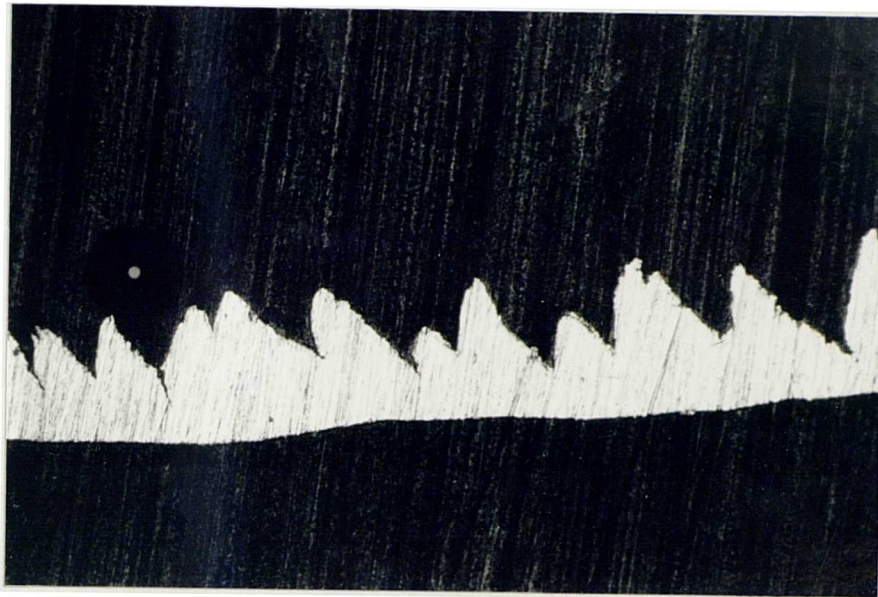
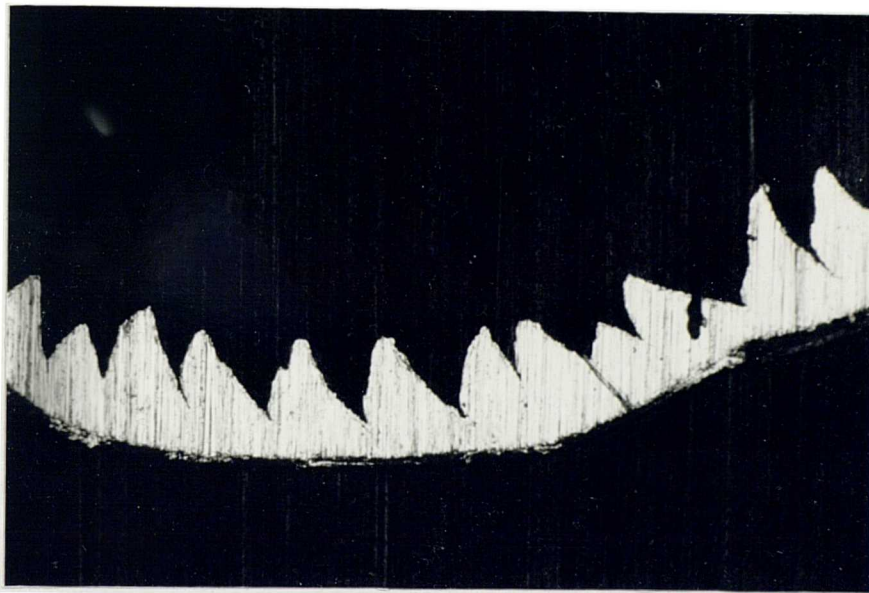


Figure 109





a. (V=150m/min)



b. (V=300m/min)

Figure 110: INCO 901 chips (F=0.18mm/rev, DOC=2.5mm, Dry)  
(x177)



**Figure 111: Crack running parallel to the cutting edge of Kyon 2000 used to machine INCO 901 (V=150m/min, F=0.125mm/rev, DOC=2.5mm, Dry)**



MACHINING OF INCO 901 WITH WG300  
DOC = 1mm

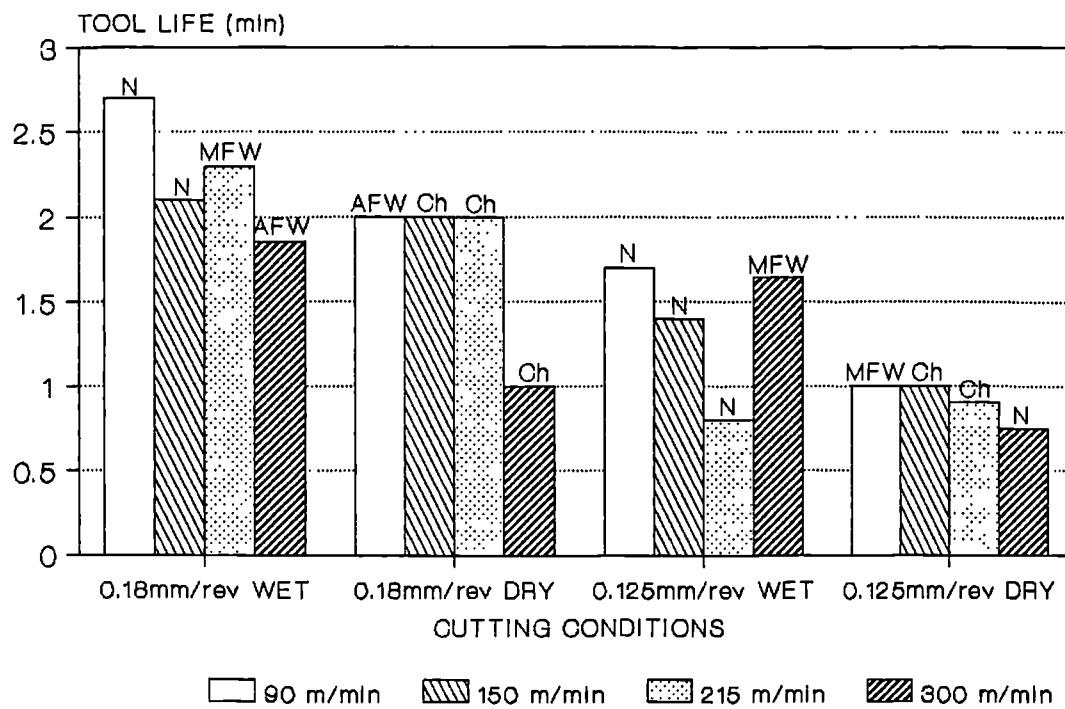


Figure 112

MACHINING OF INCO 901 WITH WG300  
DOC = 1mm

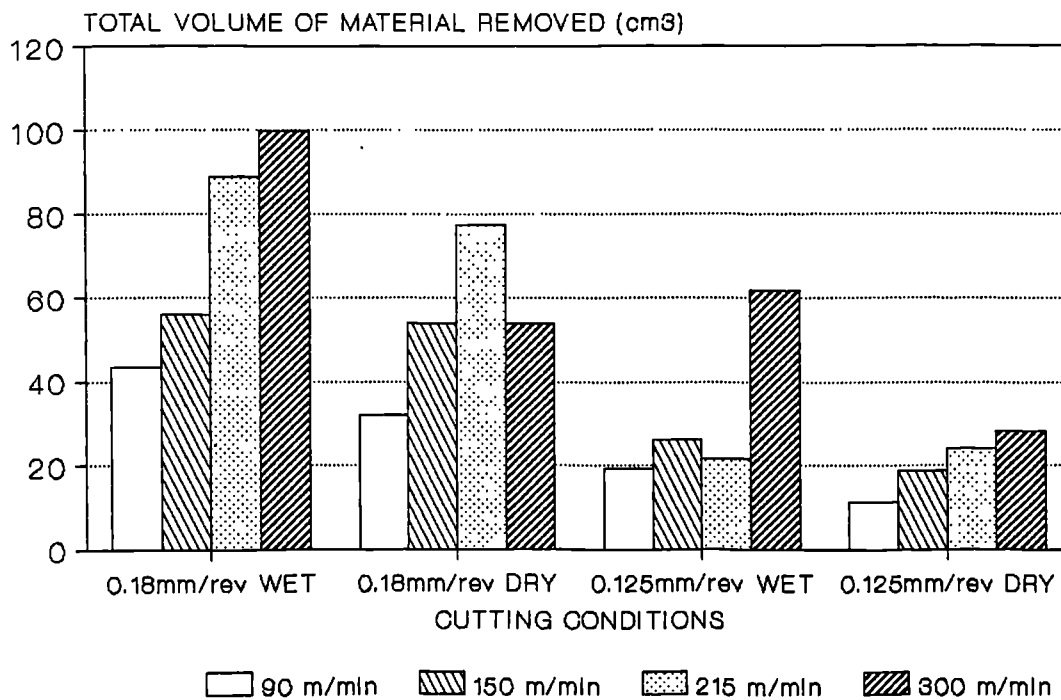


Figure 112a

MACHINING OF INCO 901 WITH WG300  
DOC = 2.5mm

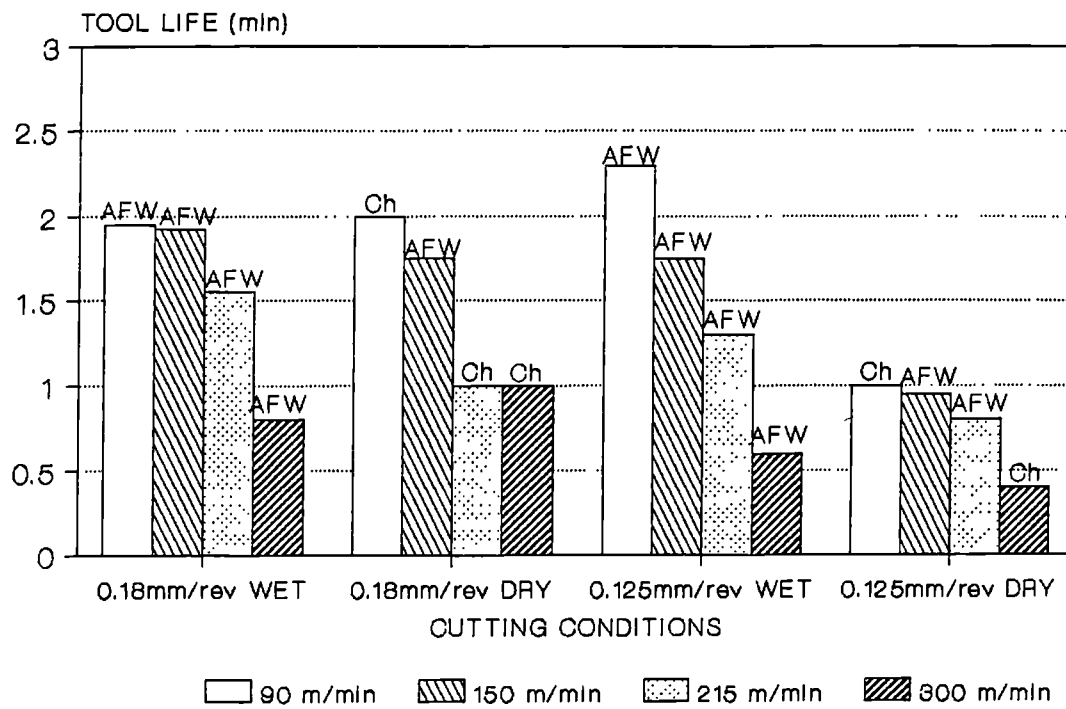


Figure 113

MACHINING OF INCO 901 WITH WG300  
DOC = 2.5mm

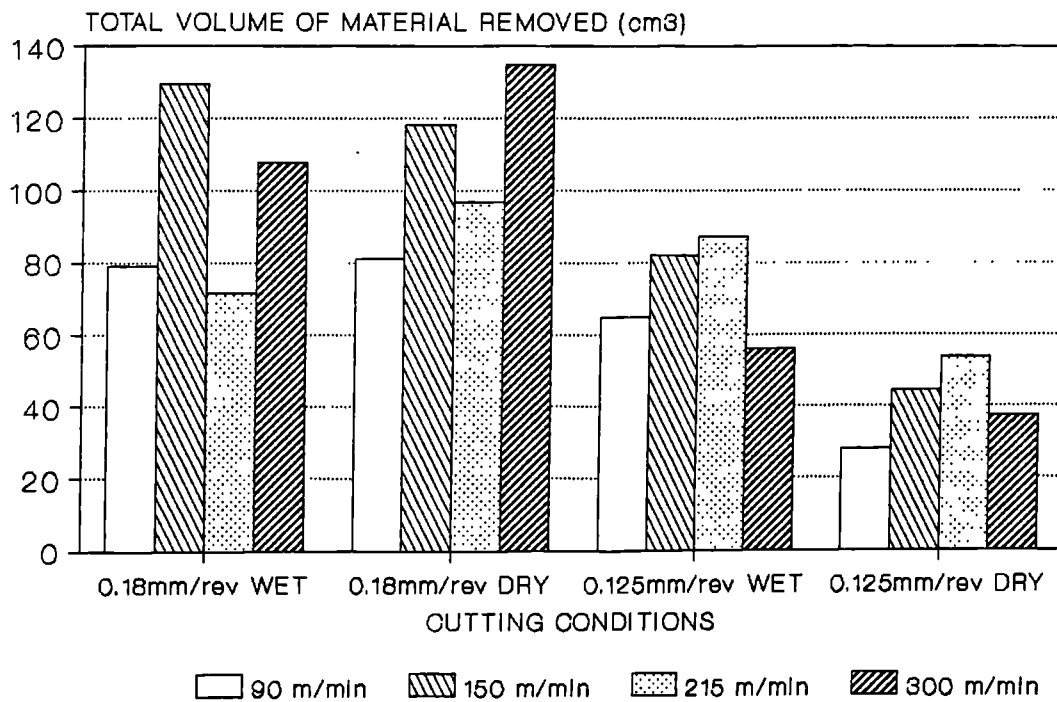


Figure 113a

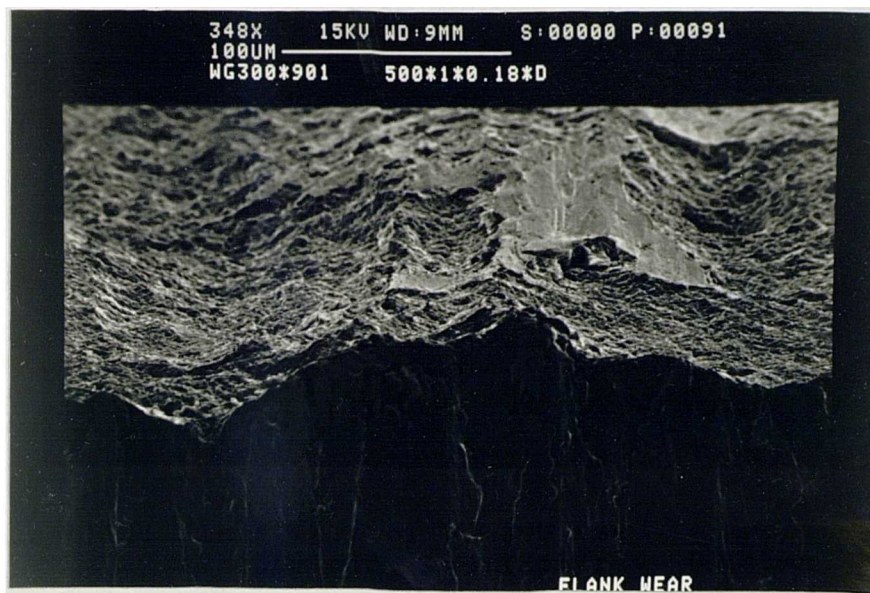


Figure 114: Flank wear of WG-300 used to machine INCO 901  
(V=150m/min, F=0.18mm/rev, DOC=1mm, Dry)

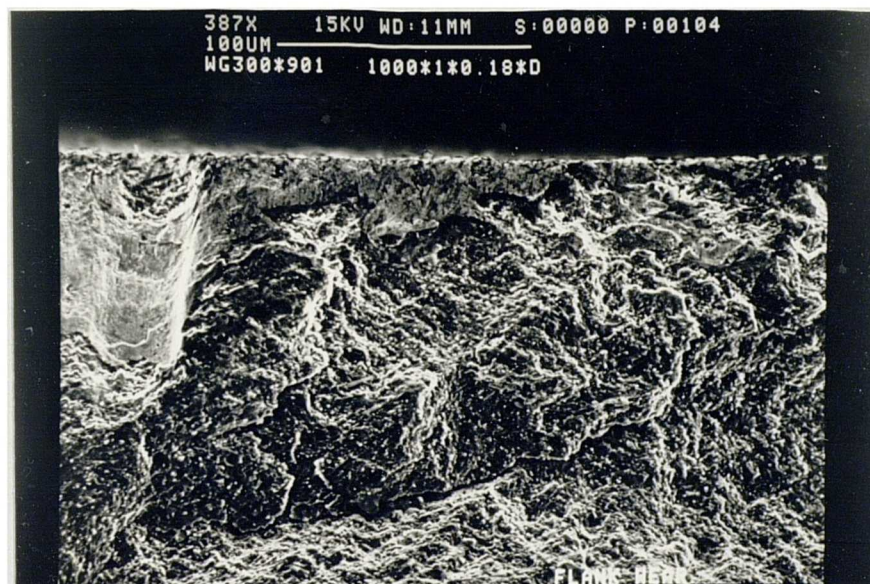


Figure 115: Cracks on the flank face of WG300 at V=300m/min  
(above conditions)



Figure 116: Quick-stop wedge of INCO 901 ( $V=90\text{m/min}$ ,  
 $F=0.18\text{mm/rev}$ ,  $\text{DOC}=1\text{mm}$ ) ( $\times 150$ )

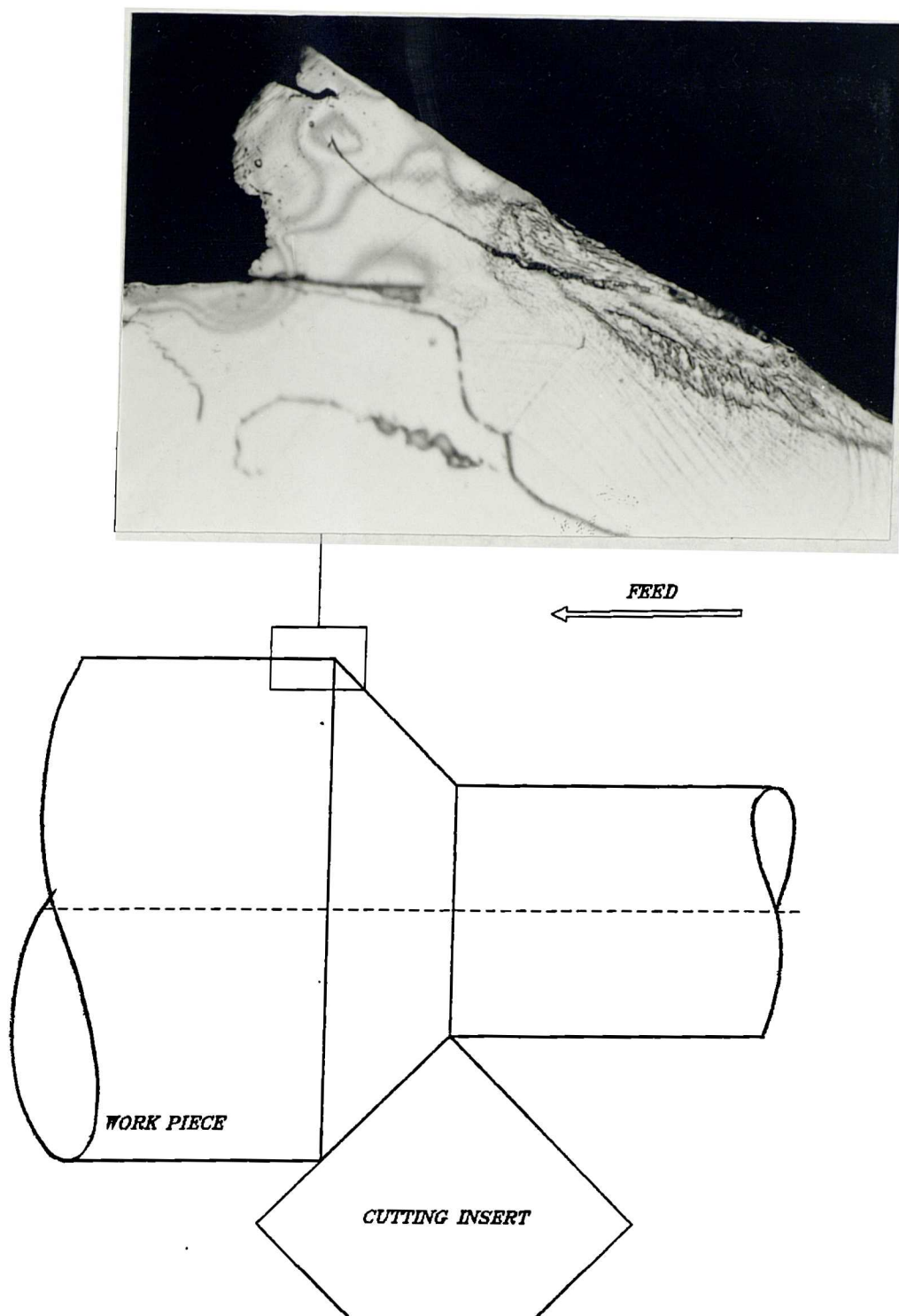


Figure 117: Formation of side flow when machining INCO 901  
( $v=150\text{m/min}$ ,  $F=0.18\text{mm/rev}$ ,  $\text{DOC}=1\text{mm}$ , Dry) (x340)





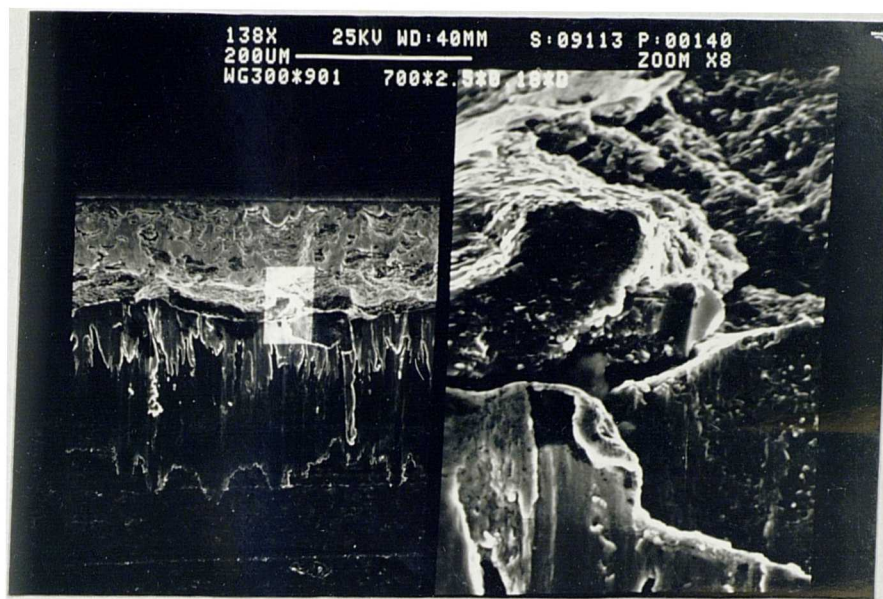
Figure 118: Quick-stop wedge of INCO 901 ( $V=90\text{m/min}$ ,  $F=0.18\text{mm/rev}$ ,  $\text{DOC}=1\text{mm}$ ) ( $\times 150$ )



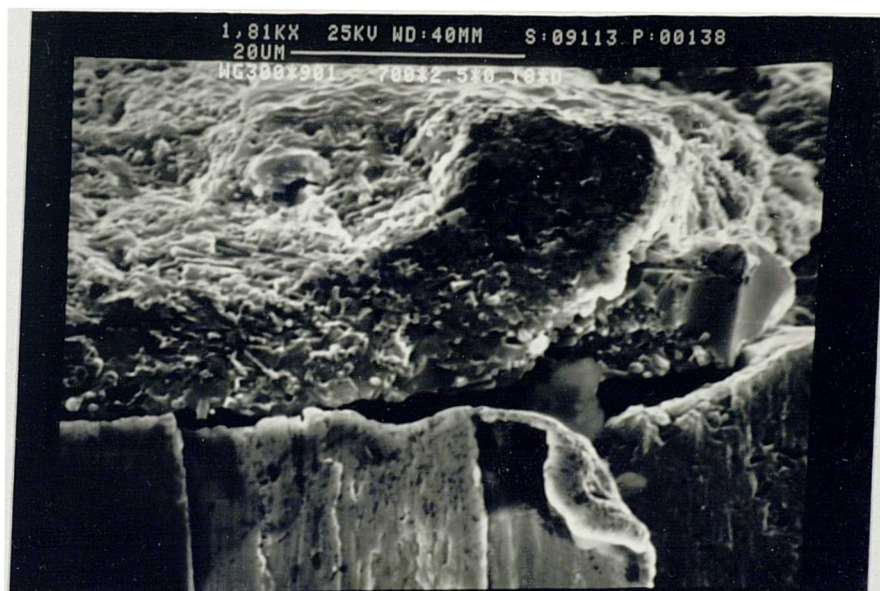
Figure 119: Crack on the honed area of WG300 used to machine INCO 901 ( $V=300\text{m/min}$ ,  $F=0.18\text{mm/rev}$ ,  $\text{DOC}=1\text{mm}$ , Dry)



Figure 120: Wear of WG-300 used to machine INCO 901  
(V=90m/min, F=0.18mm/rev, DOC=2.5mm, Dry)



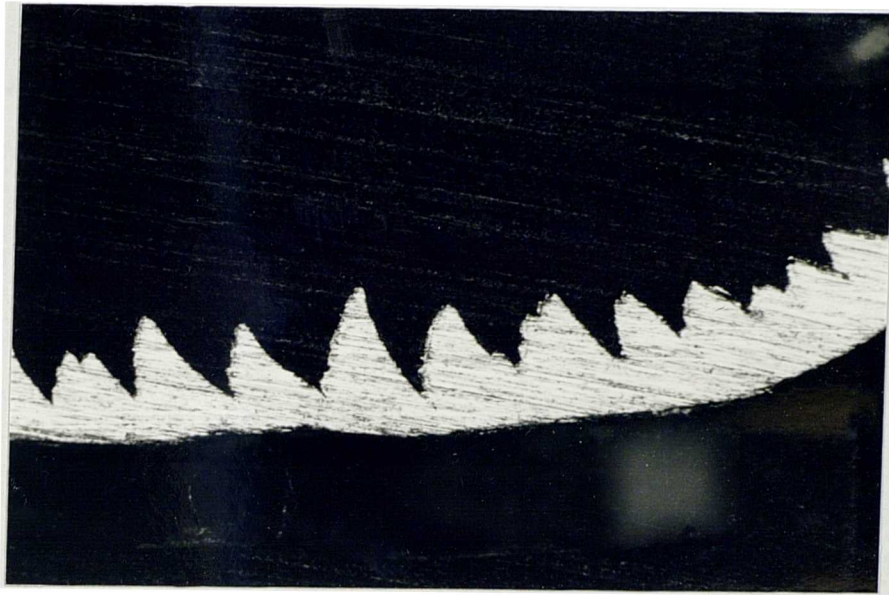
a.



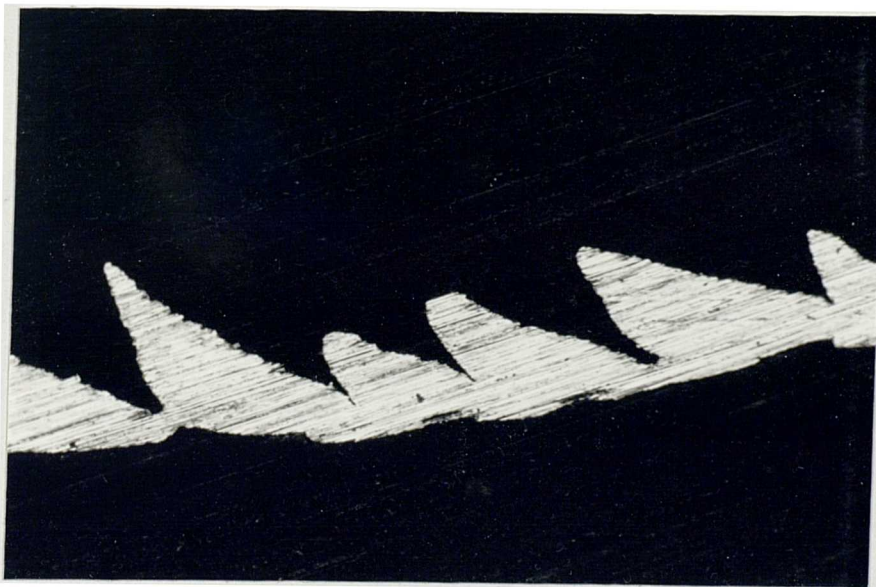
b.

Figure 121: Crack on the flank face of WG300 used to machine INCO 901 (V=215m/min, F=0.18mm/rev, DOC=2.5mm, Dry)





a. ( $V=150\text{m/min}$ )



b. ( $V=300\text{m/min}$ )

Figure 122: INCO 901 chips at different cutting speeds  
( $F=0.18\text{mm/rev}$ ,  $\text{DOC}=2.5\text{mm}$ , Dry) ( $\times 177$ )

MACHINING OF INCO 901 WITH WG300  
DOC=2.5mm, F=0.125mm/rev, WET

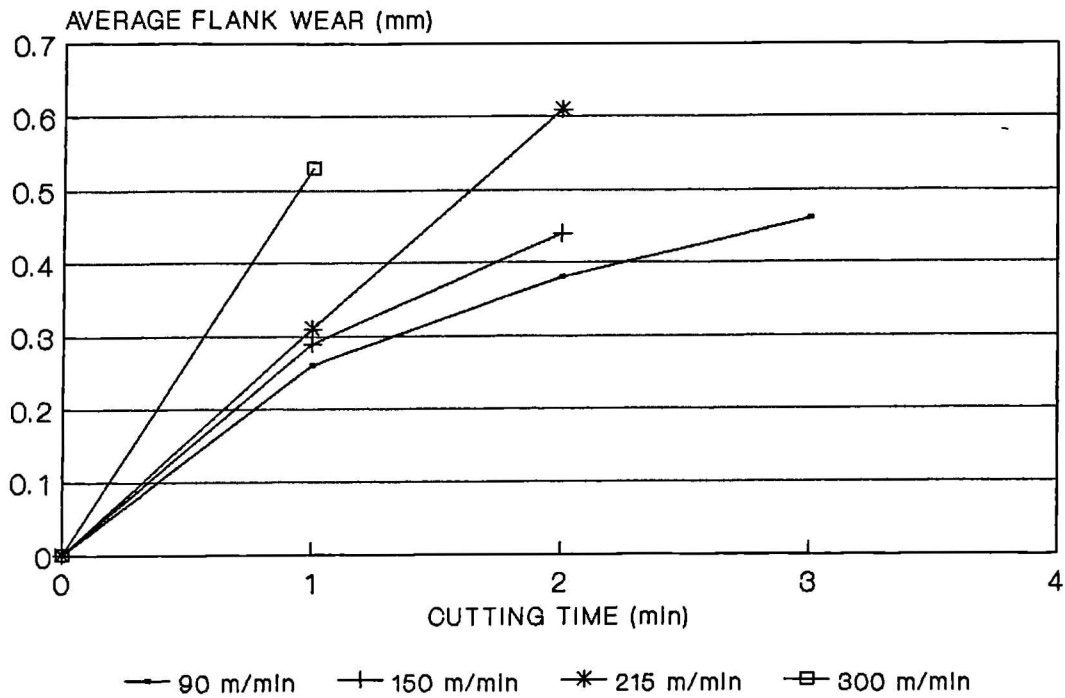


Figure 123



Figure 124: Flank wear of WG300 used to machine INCO 901  
(V=300m/min, F=0.18mm/rev, DOC=2.5mm, Wet)

MACHINING OF INCO 901 WITH WG-300  
DOC = 2.5mm, DRY

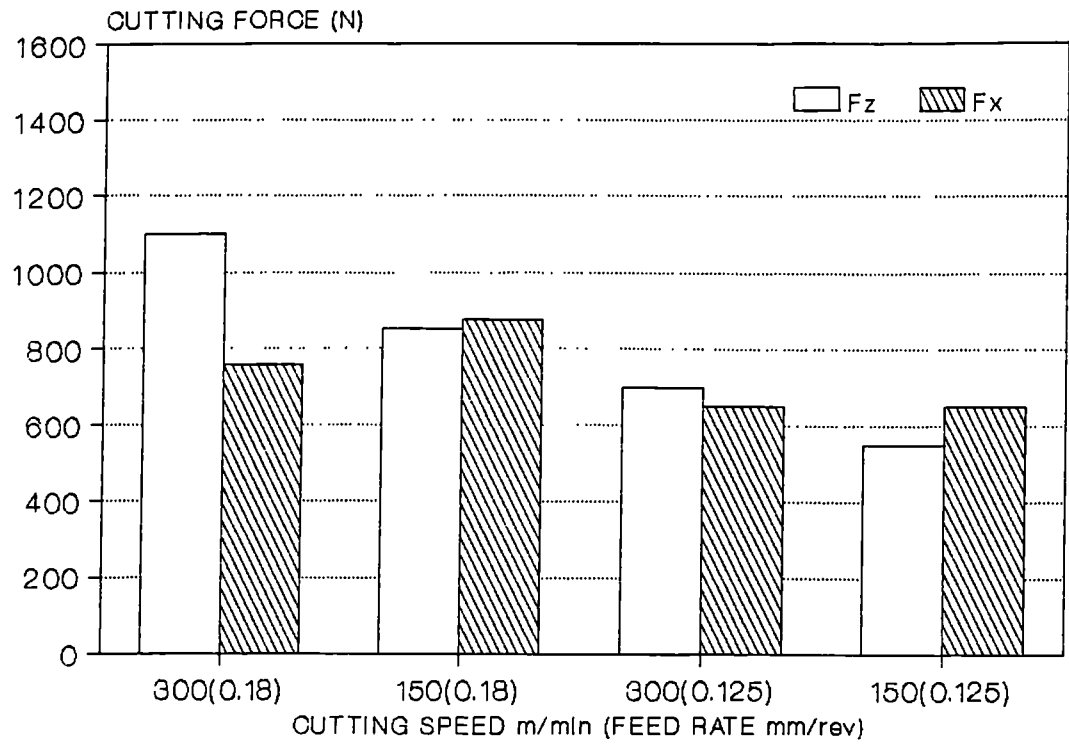


Figure 125

MACHINING OF INCO 901 WITH WG-300 TOOLS  
V=215m/min, F=0.125mm/rev, DOC=1mm

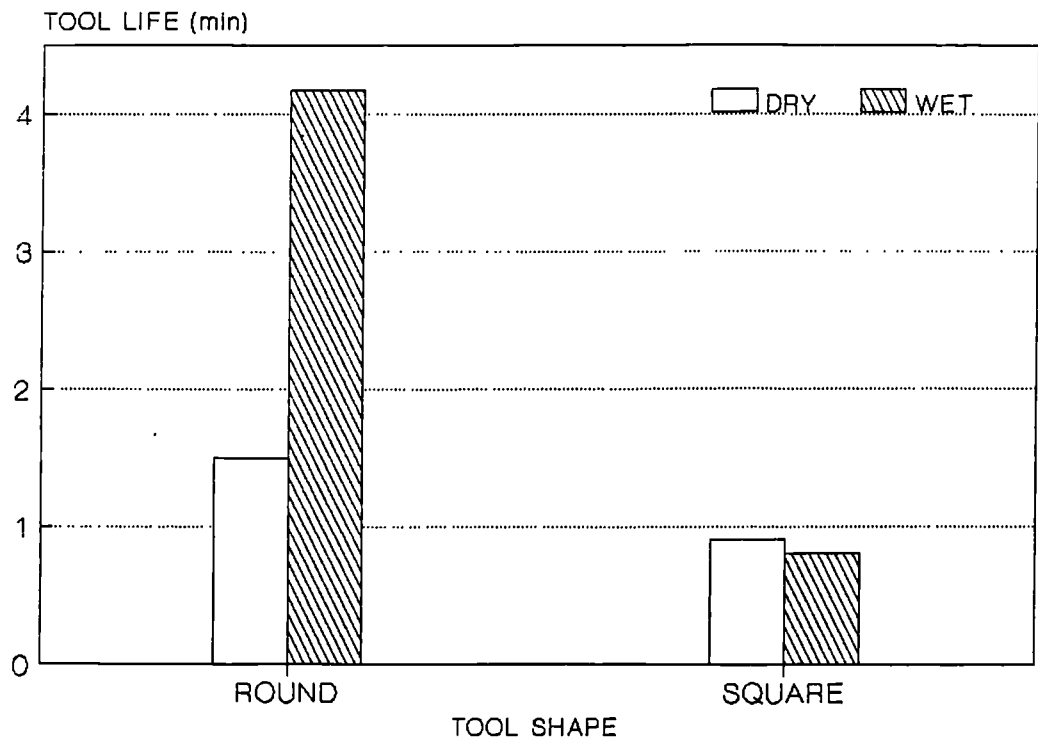


Figure 126

MACHINING OF INCO 718 WITH KYON 2000  
DOC = 1mm, DRY

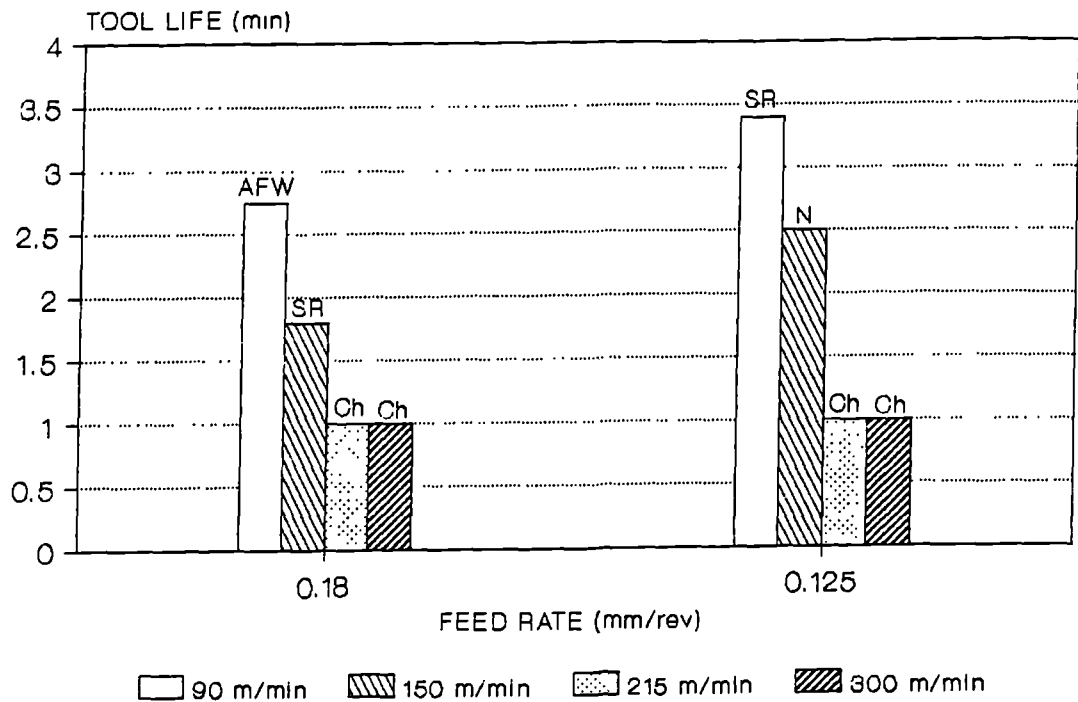


Figure 127

MACHINING OF INCO 718 WITH KYON 2000  
DOD = 1mm, DRY

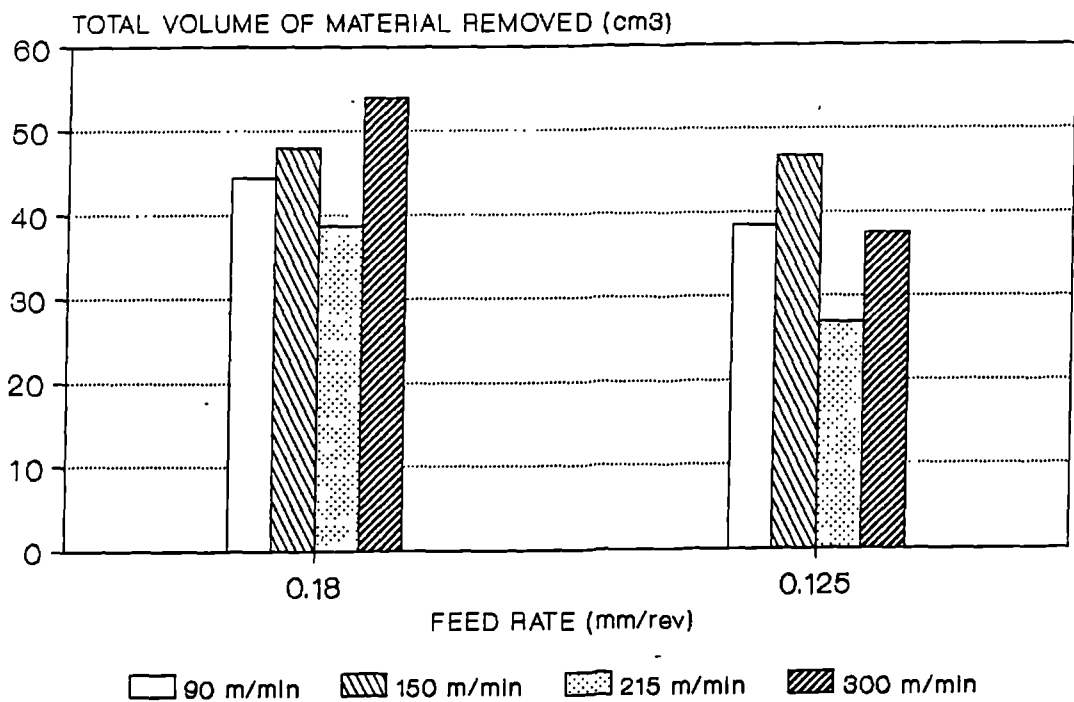


Figure 127a

MACHINING OF INCO 718 WITH KYON 2000  
DOC = 2.5mm, DRY

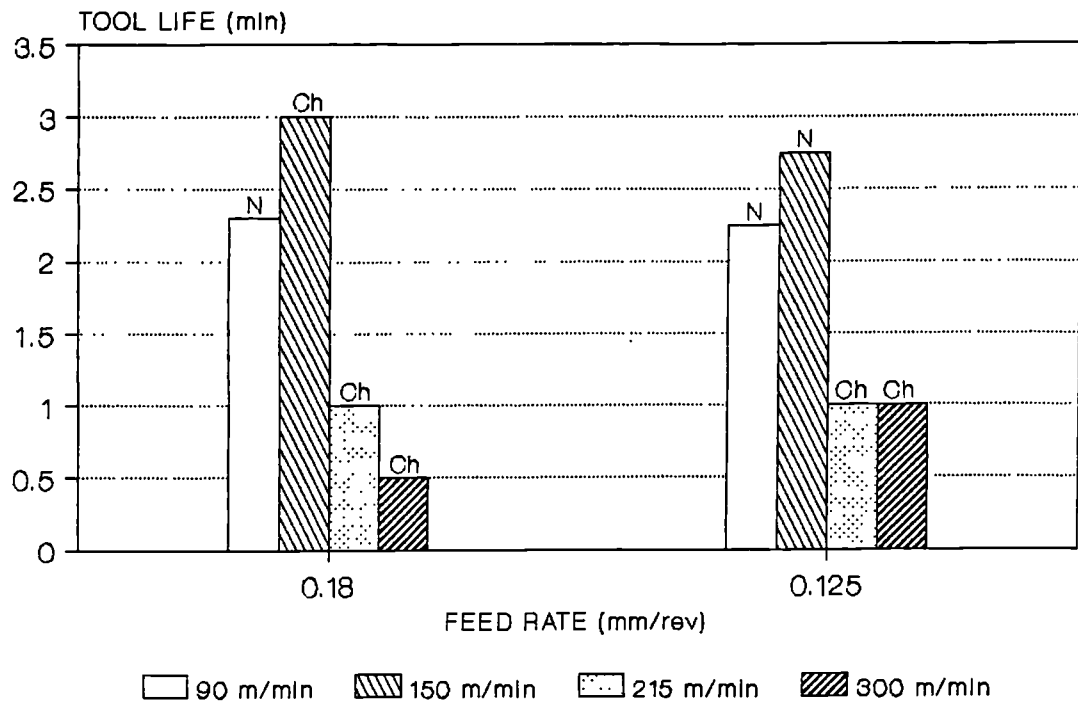


Figure 128

MACHINING OF INCO 718 WITH KYON 2000  
DOC = 2.5mm, DRY

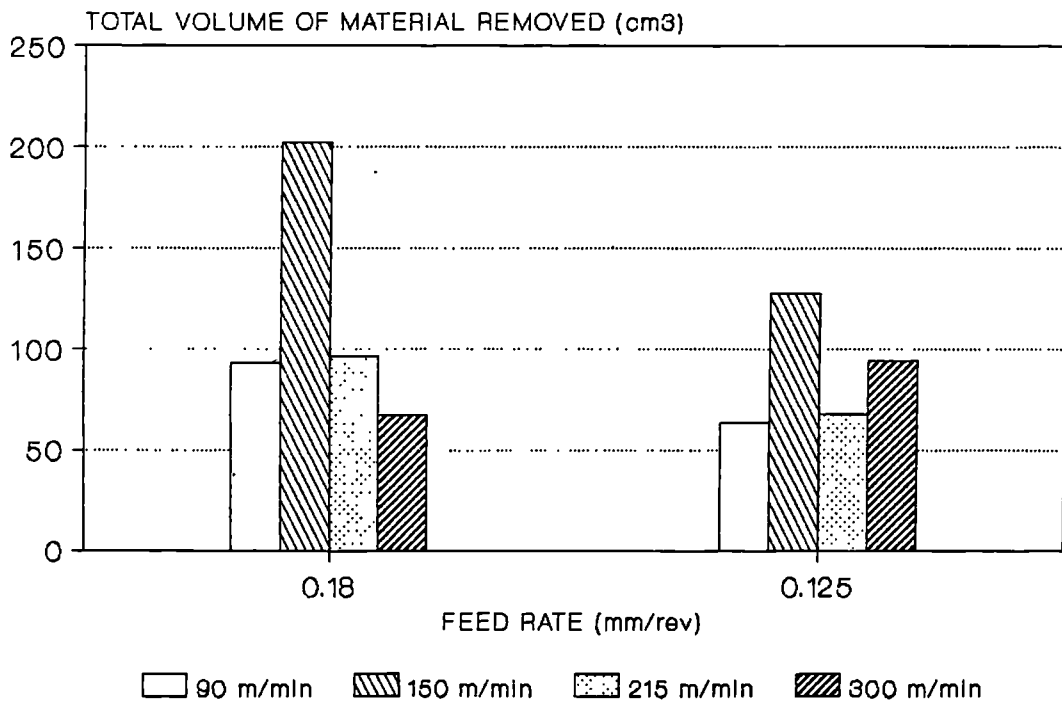


Figure 128a

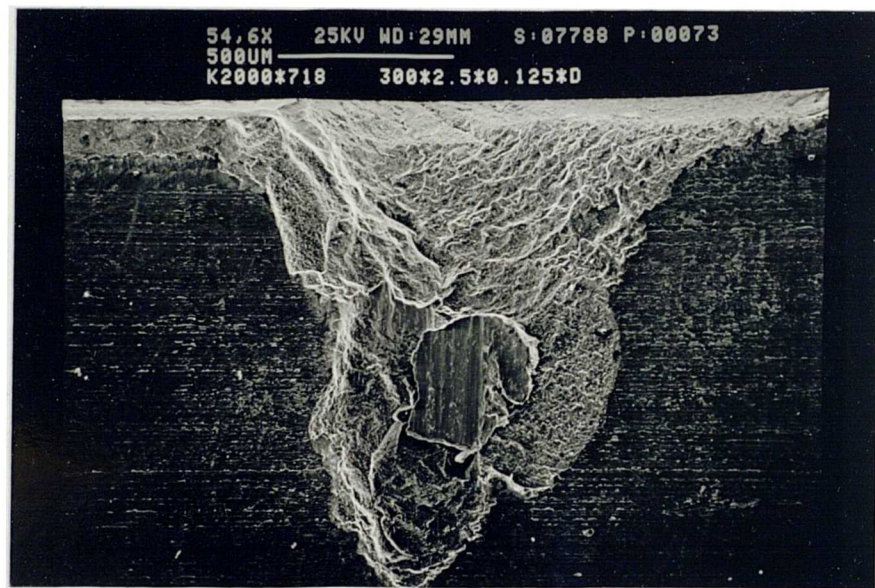


Figure 129: DOC notch on Kyon 2000 used to machine INCO 718  
(V=90m/min, F=0.125mm/rev, DOC=2.5mm, Dry)



MACHINING OF INCO 718 WITH WG300  
F=0.18 mm/rev, WET

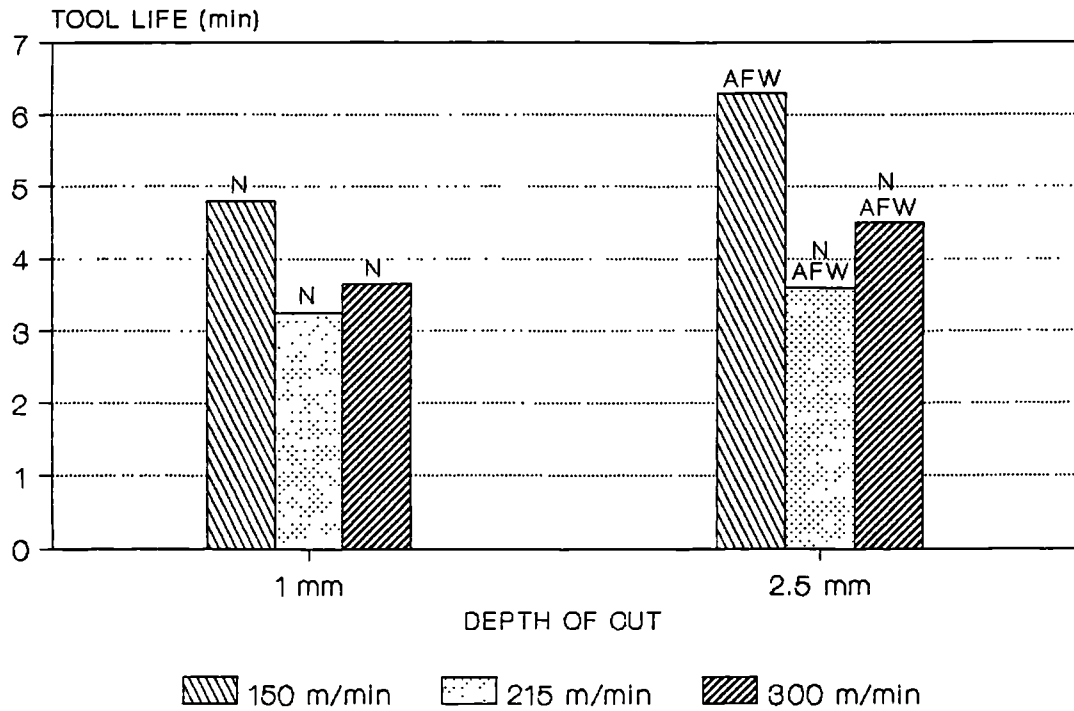


Figure 130

MACHINING OF INCO 718 WITH WG300  
F=0.18 mm/rev, WET

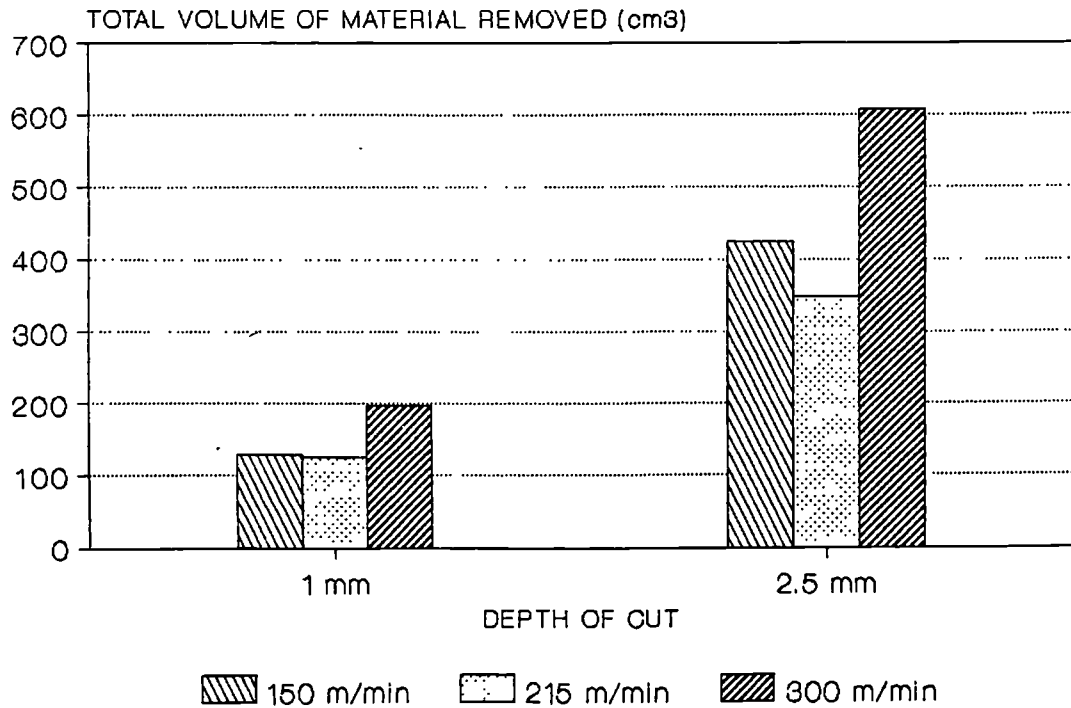


Figure 130a

MACHINING OF INCO 718 WITH WG-300  
 $V=300\text{m/min}$ ,  $F=0.18\text{mm/rev}$

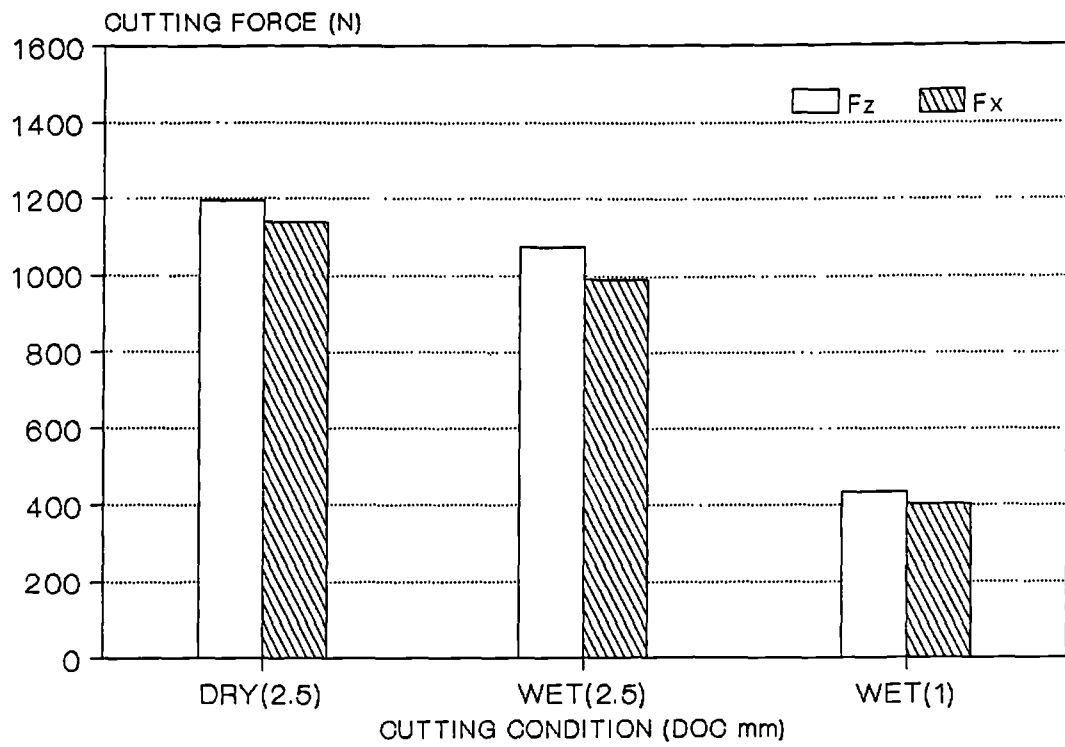


Figure 131

MACHINING OF INCO 718 WITH WG300  
 $V=150\text{m/min}$ ,  $\text{DOC}=2.5\text{mm}$ ,  $F=0.18\text{mm/rev}$ , WET

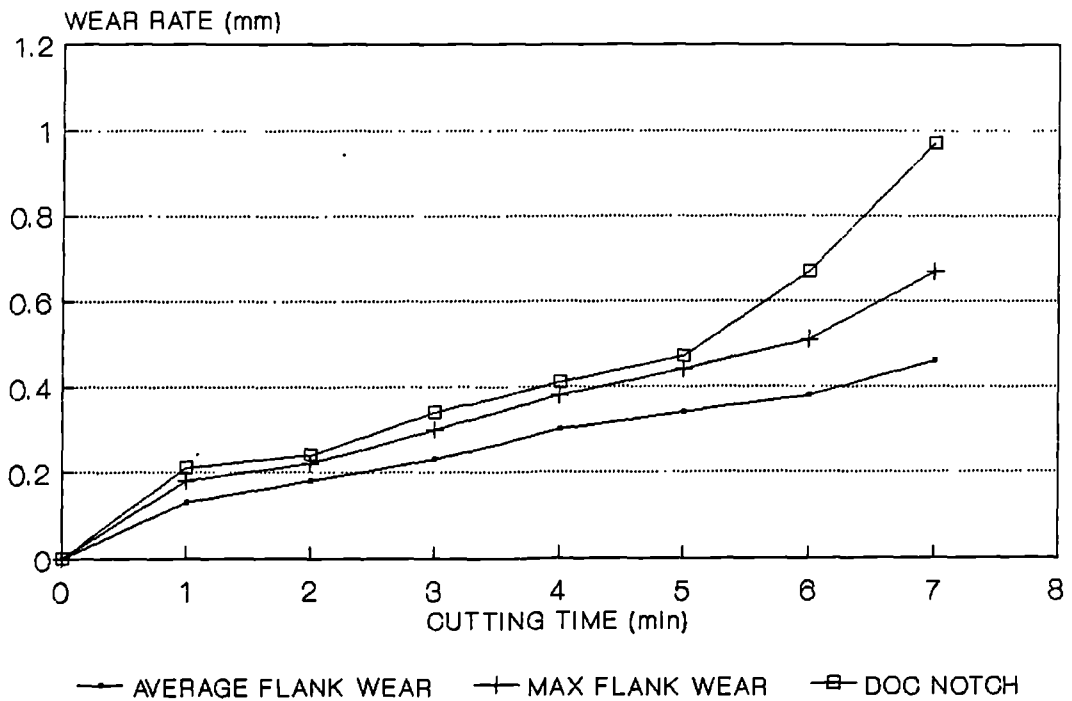


Figure 132



MACHINING OF INCO 718 WITH WG300  
F=0.18 mm/rev, DOC=2.5MM

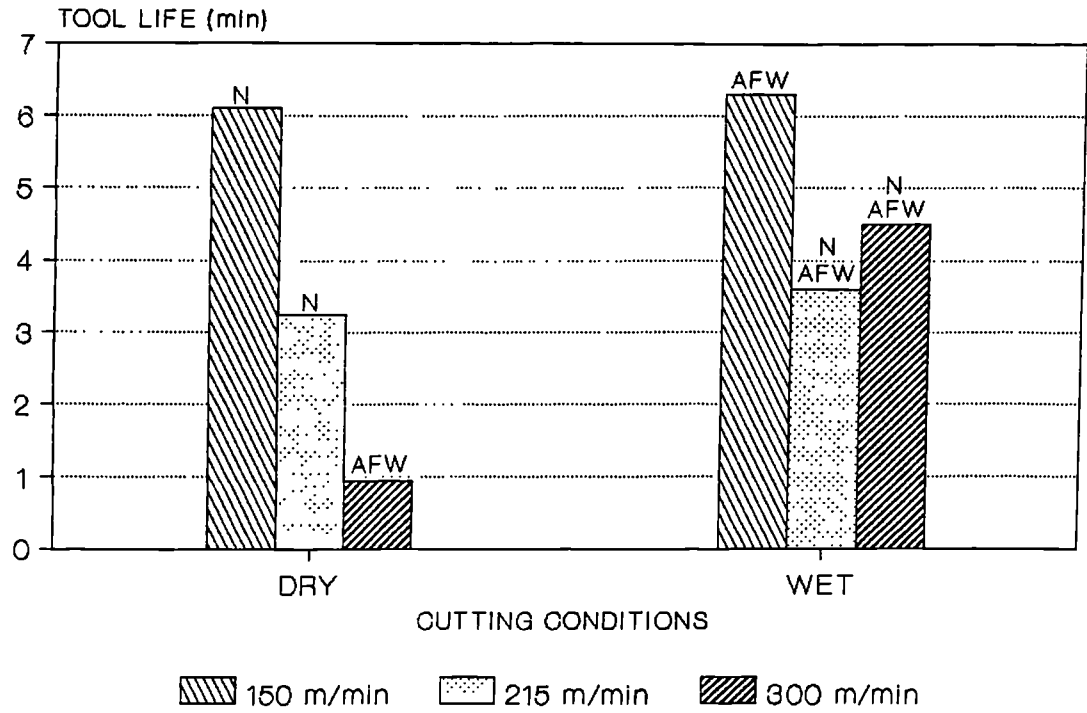


Figure 133

MACHINING OF INCO 718 WITH WG300  
DOC=2.5mm, F=0.18mm/rev

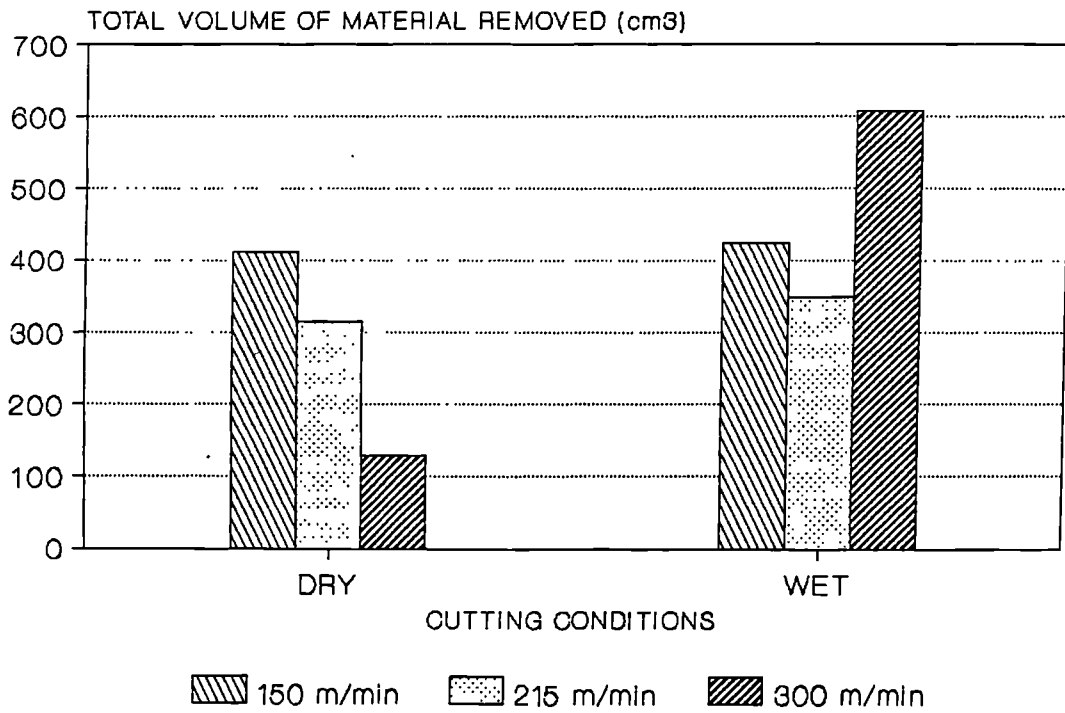


Figure 133a

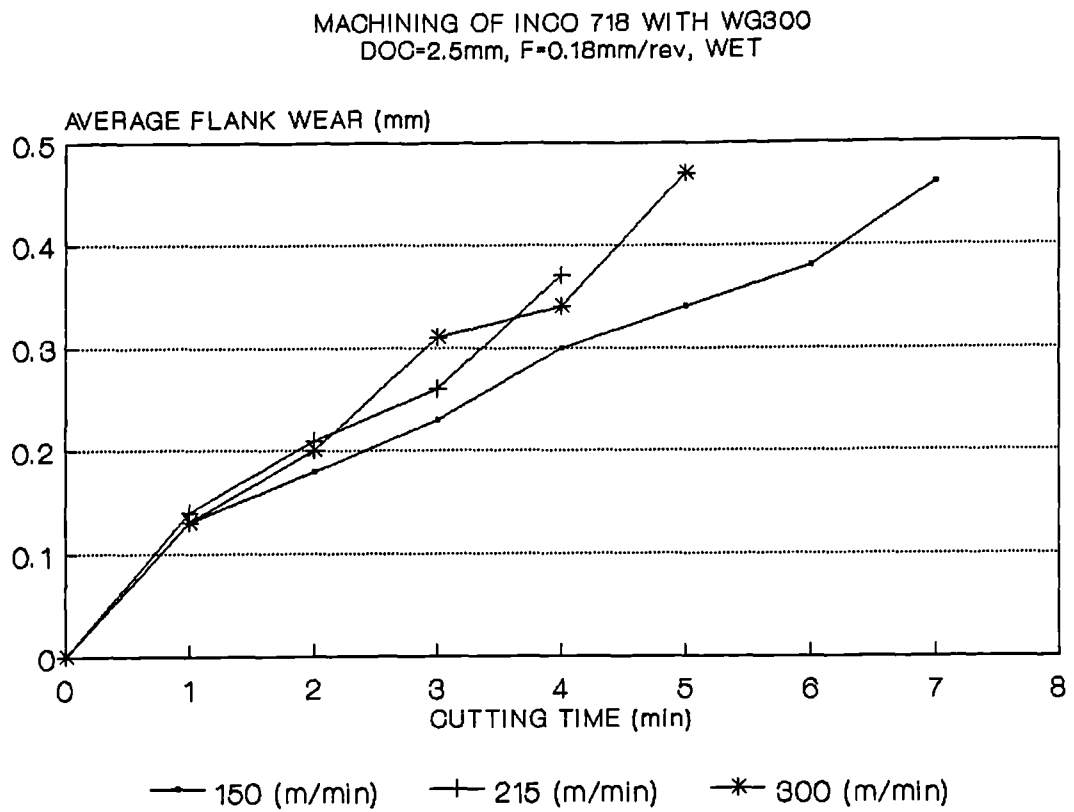


Figure 134

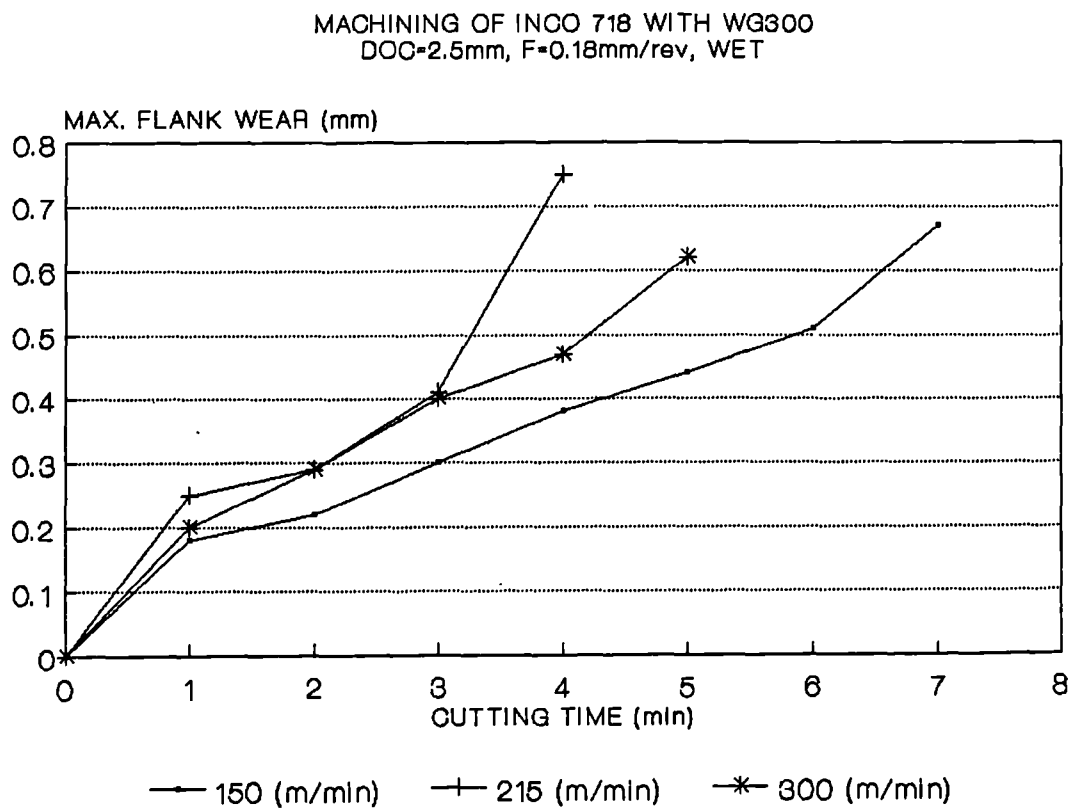


Figure 135

MACHINING OF INCO 718 WITH WG300  
DOC=2.5mm, F=0.18mm/rev, WET

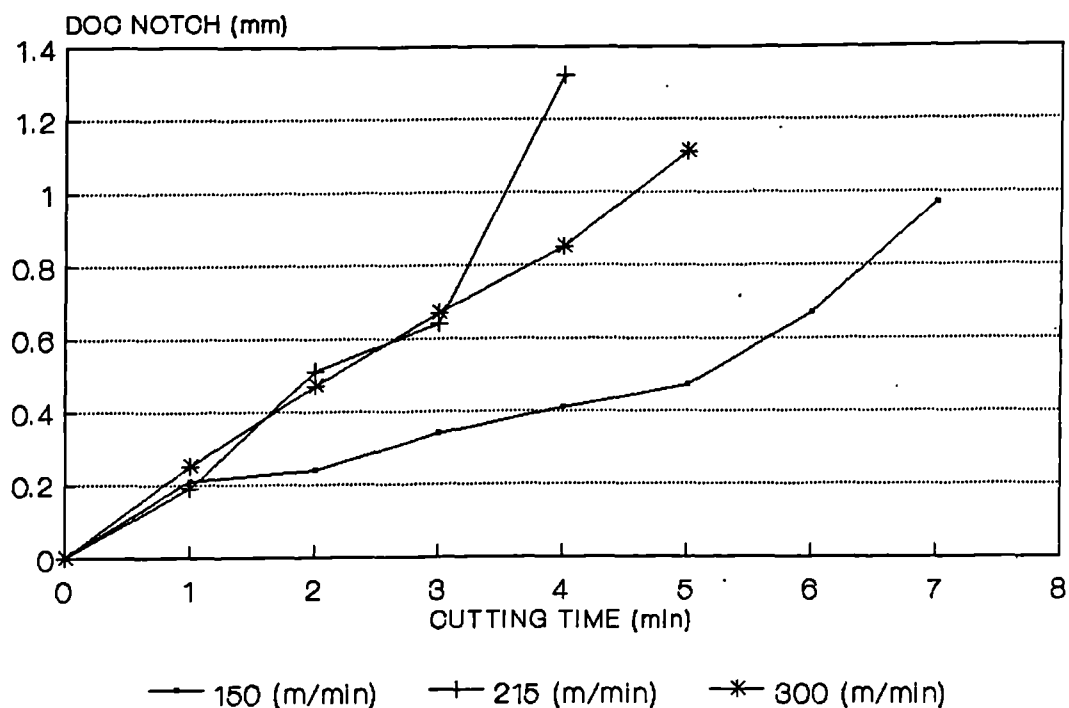


Figure 136

MACHINING OF INCO 718 WITH WG300  
DOC=2.5mm, F=0.18mm/rev, WET

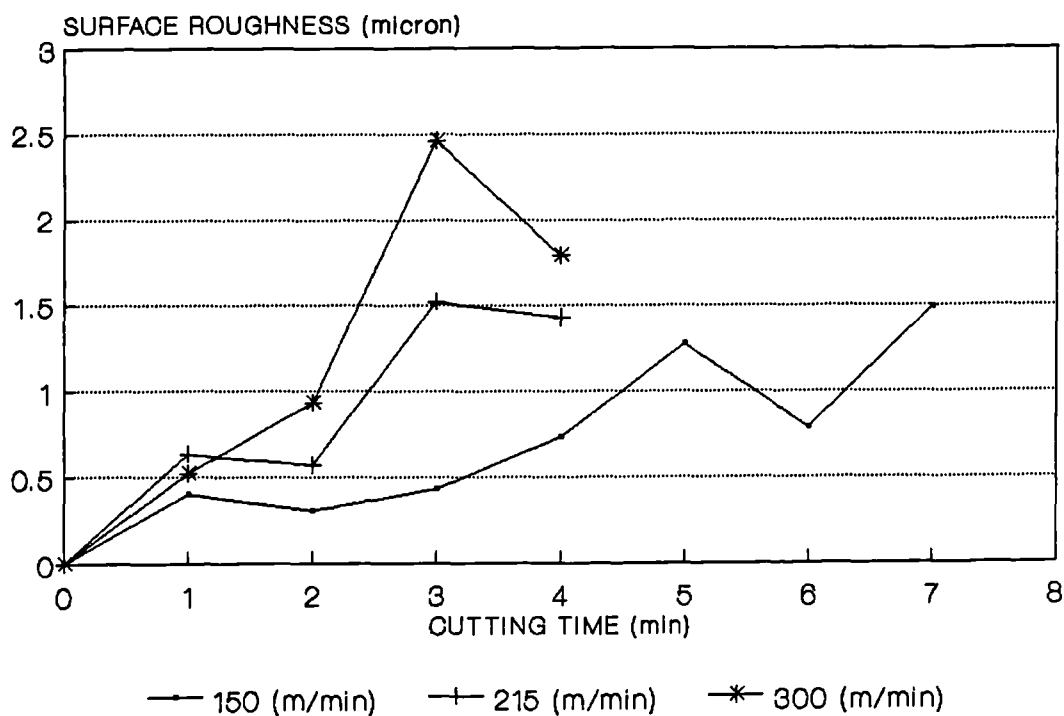
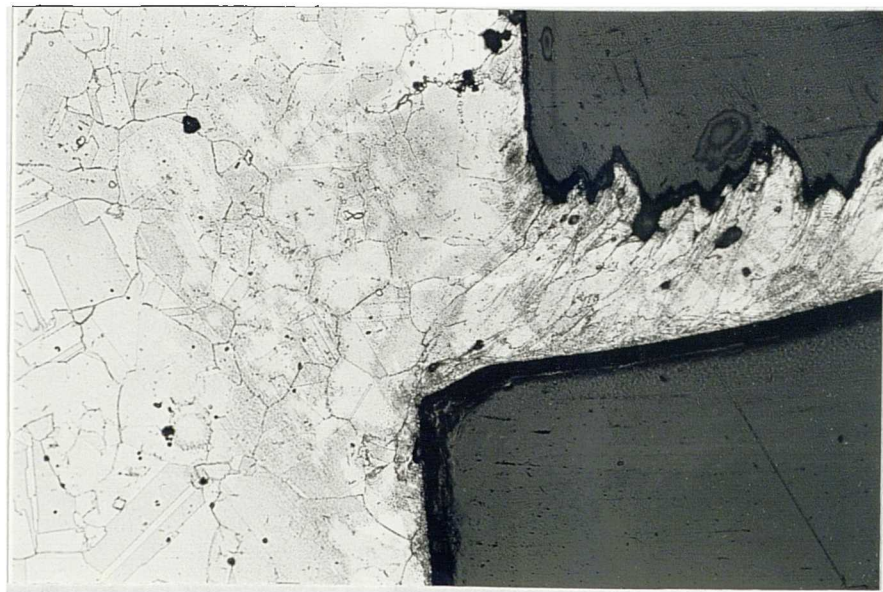


Figure 137



**Figure 138: Quick-stop wedge of INCO 718 ( $V=90\text{m/min}$ ,  $F=0.18\text{mm/rev}$ ,  $\text{DOC}=2.5\text{mm}$ ) ( $\times 150$ )**

MACHINING OF INCO 718 WITH WG-300 TOOLS  
 $V=215\text{m/min}$ ,  $F=0.125\text{mm/rev}$ ,  $\text{DOC}=1\text{mm}$

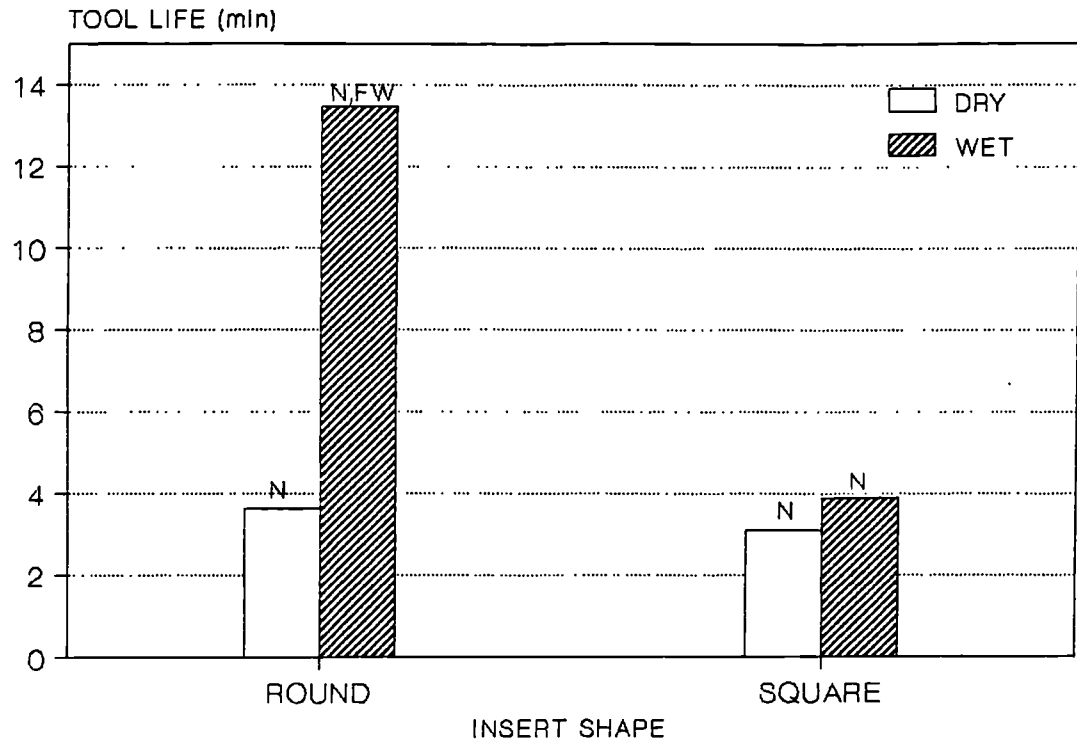


Figure 139

MACHINING OF INCO 718  
 WITH DIFFERENT WG300 TOOLS  
 $V=215\text{m/min}$ ,  $\text{DOC}=1\text{mm}$ ,  $F=0.125\text{mm/rev}$ , WET

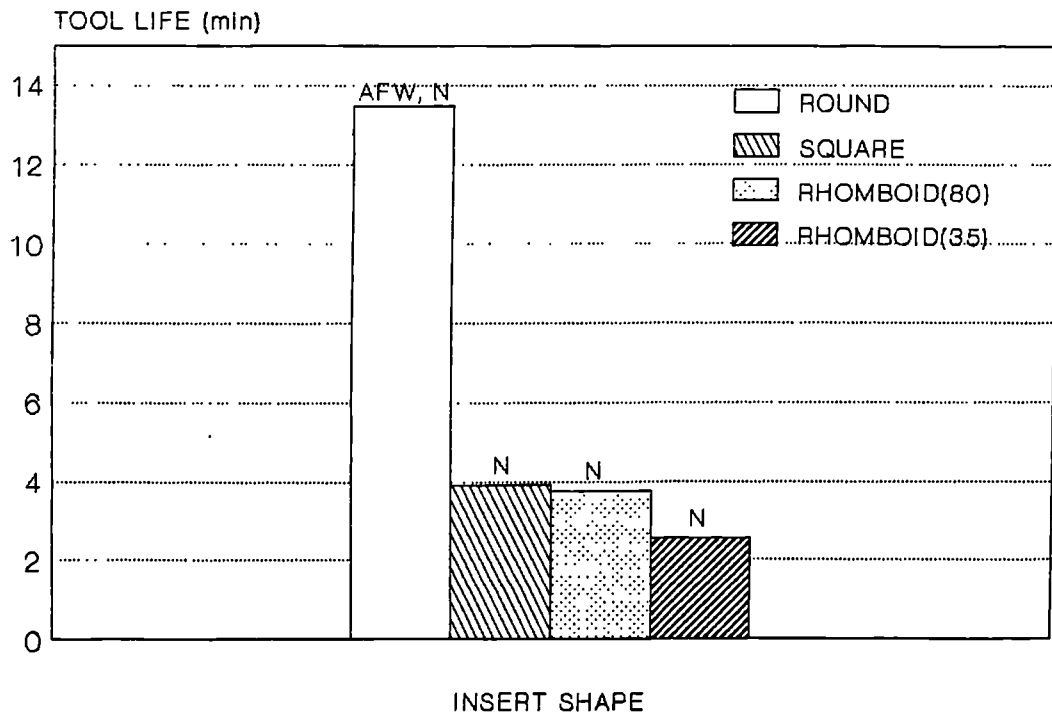
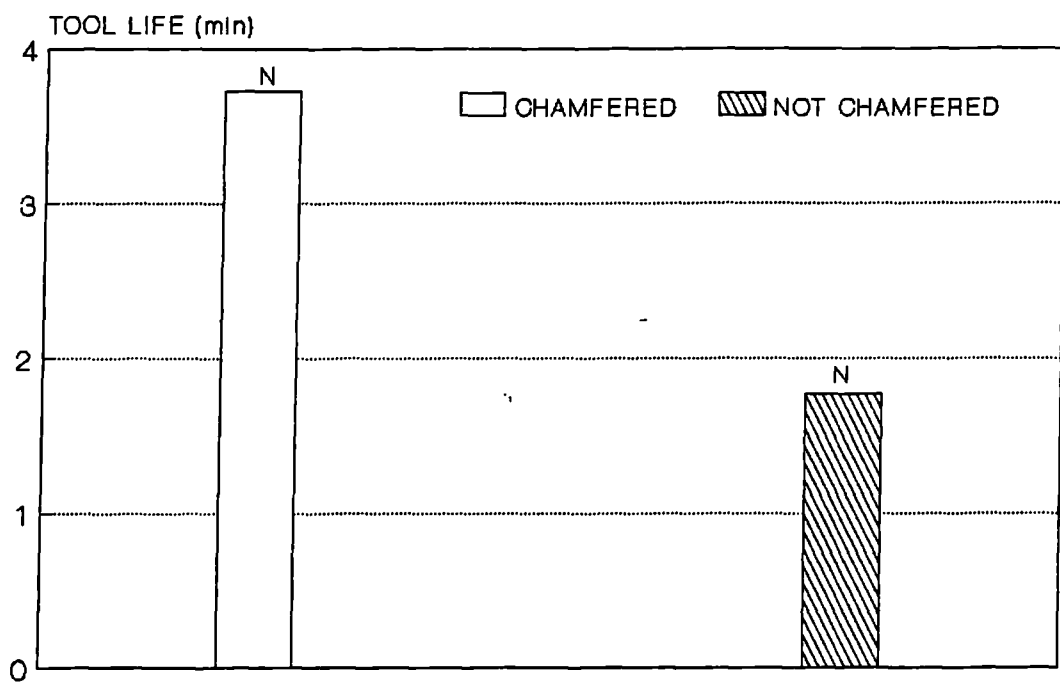


Figure 140

MACHINING OF INCO 718 WITH WG300  
V=215m/min, DOG=1mm, F=0.125mm/rev, WET



INFLUENCE OF CHAMFERE ON THE WORKPIECE

Figure 141

MACHINING OF INCO 718 WITH WG300  
IN THE PRESENCE OF DIFFERENT GASES  
V=215m/min, DOC=2.5mm, F=0.18mm/rev

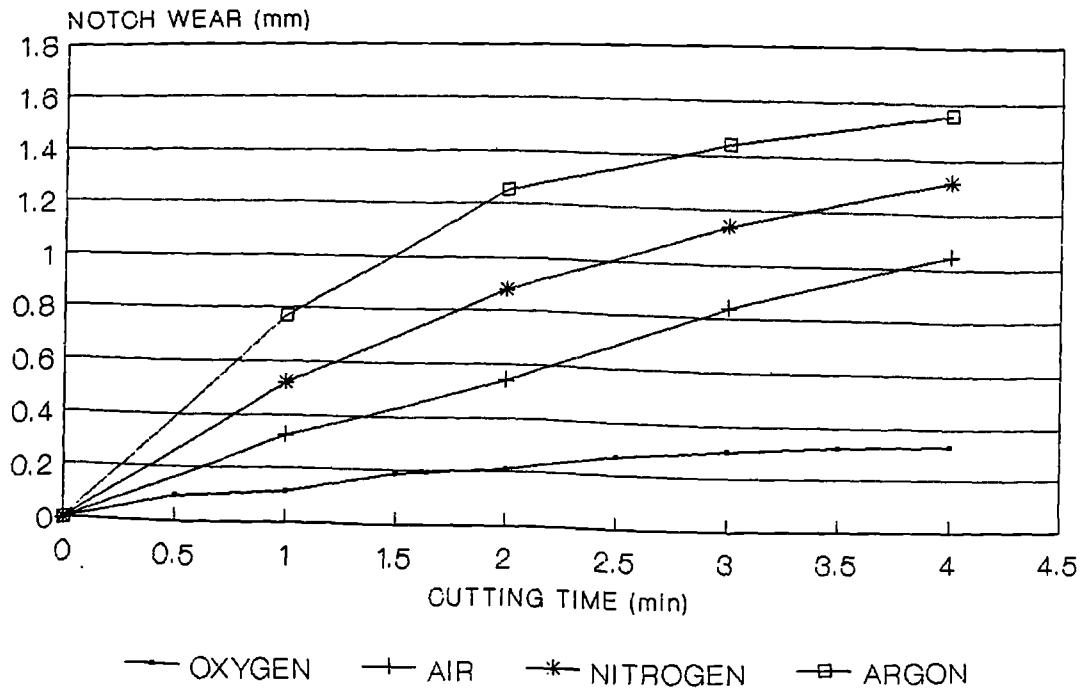


Figure 142

MACHINING OF 718 WITH WG300  
IN THE PRESENCE OF DIFFERENT GASES  
V=215m/min, DOC=2.5mm, F=0.18mm/rev

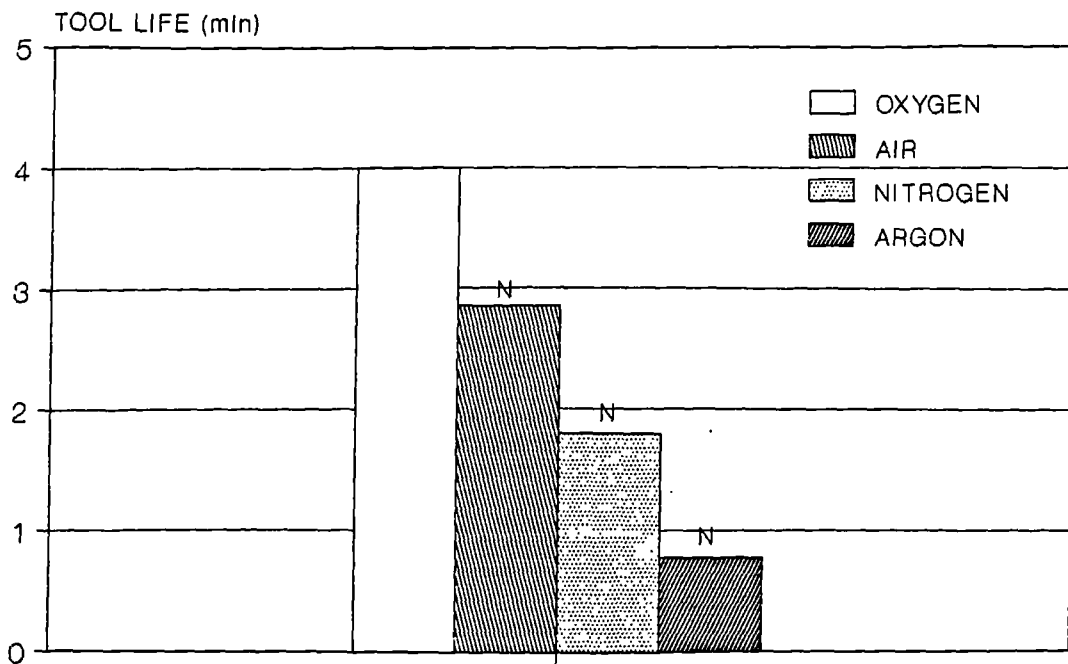


Figure 143

MACHINING OF INCO 718 WITH WG300  
IN THE PRESENCE OF DIFFERENT GASES  
V=150m/min, DOC=2.5mm, F=0.18mm/rev

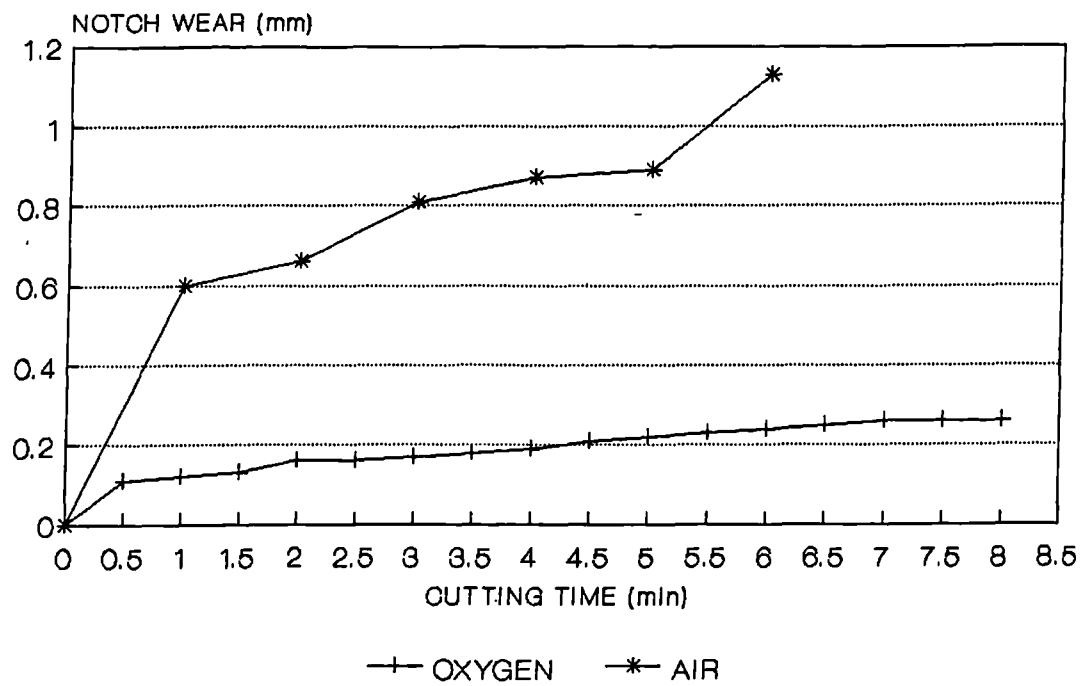


Figure 144



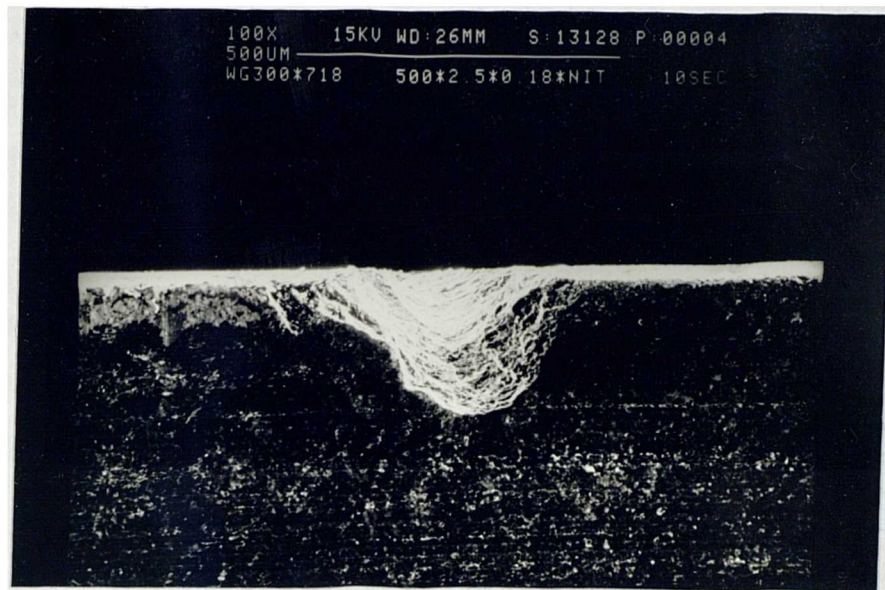


Figure 145: DOC notch after 10 seconds machining of INCO 718 with WG-300 in the presence of Nitrogen (V=150m/min, F=0.18mm/rev, DOC=2.5mm)

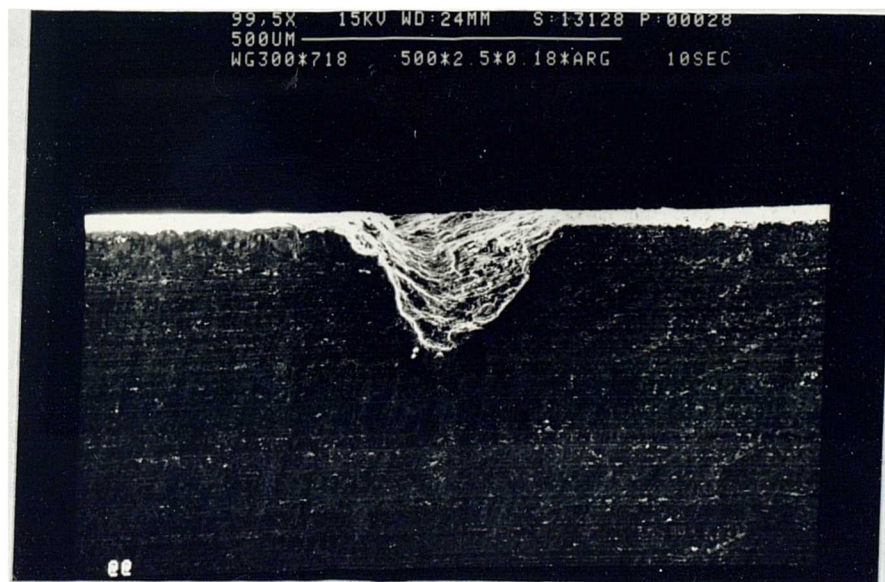


Figure 146: DOC notch in the presence of Argon (above conditions)

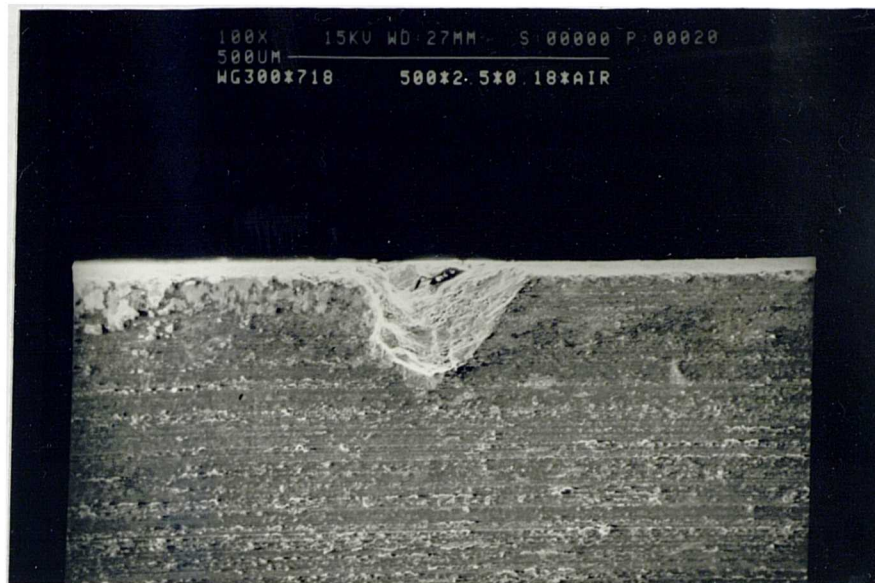


Figure 147: DOC notch in dry condition (above conditions)

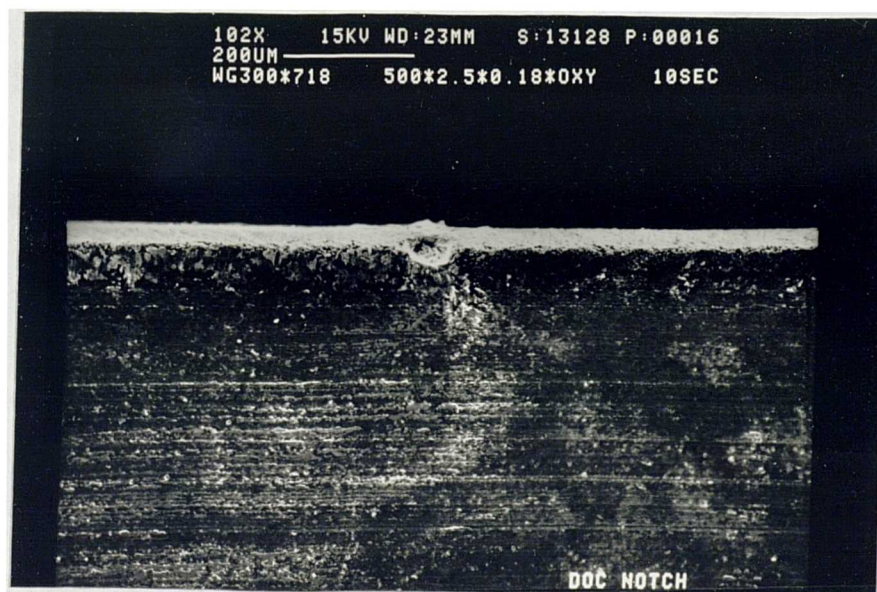


Figure 148: Reduced DOC notch in the presence of Oxygen  
(same conditions as figure 145)